HANTKENIANA

8 • 2013

A KÖTET MEGJELENÉSE
A TÁMOP – 4.2.2/B-10/1-2010-0030
„ÖNÁLLÓ LÉPÉSEK A TUDOMÁNY TERÜLETÉN” PROJEKT
TÁMOGATÁSÁBÓL VALÓSULT MEG

Nemzeti
Fejlesztési
Ügynökség

Nemzeti Fejlesztési Ügynökség
www.ujszechenyiterv.gov.hu
06 40 638 638

MAGYARORSZÁG MEGÚJUL

A projektek az Európai Unió
támogatásával valósulnak meg.

ÚJ SZÉCHENYI TERV

Pátria Nyomda Zrt.

HANTKENIANA

Contributions of the Department of Palaeontology
Eötvös University

8

Hantken Press
Budapest, 2013

Miklós KÁZMÉR
Editor

Available from

Department of Palaeontology,
Eötvös University
Pázmány Péter sétány 1/c
H-1117 Budapest
Hungary
http://paleo.elte.hu

ISSN 1219-3933

Hantkeniana 8, 1—169, Budapest, 2013

Contents

Hantkeniana 8, 7—23, Budapest, 2013

Middle Aalenian – Lower Bajocian (Middle Jurassic) ammonites from Büdöskút, an old locality in the Bakony Mts, Transdanubian Hungary

András GALÁCZ[1] & Zoltán KOVÁCS[2]

(with 2 figures, 1 table and 1 plate)

In one of the repositories of the Hungarian Geological and Geophysical Institute a collection of ammonites from the Bakony Mountains was discovered, which goes back to the field activities of J. NOSZKY in the 1930's. The material was collected at Büdöskút, in those times a farmhouse between Eplény and Lókút, near Zirc. The ammonites are Middle Aalenian and Lower Bajocian in age. These age intervals and faunas are known only in a few localities within the region. Although the well-preserved specimens were collected without special attention to fine stratigraphical information, thus their biostratigraphic value is very limited, the occurrences of certain species (e.g. *Erycites* (*Abbasitoides*) *modestus*, described in detail) give an addition to the knowledge of Middle Jurassic ammonite faunas of the Bakony Mts.

Introduction

J. NOSZKY jr., the geologist for the Hungarian Geological Institute made mapping in 1935 around Lókút, not far from the town of Zirc in the Bakony Mts. Here, at the foot of the Kávás-hegy Hill, near to a farm called Büdöskút (a name referring to a well) he discovered fossiliferous early Middle Jurassic rocks. He collected numerous fossils, mainly ammonites, but he never mentioned again this place or these fossils in his later works. The material went into the collections of the Geological Institute, NOSZKY prepared them and made some preliminary determinations, but the specimens remained unregistered. After his death in 1970 the specimens found their way to the repository of the Geological Institute and sank into oblivion.

In 2011 the material has been re-discovered in Rákóczi-telep, one of the repositories of the Institute. It became clear that it represents assemblages which may complement the knowledge about the Upper Aalenian and the Lower Bajocian ammonites of the Bakony Mts, thus it deserves studying. Unfortunately there are no information on the way of collecting, thus the stratigraphic background of the assemblages remains poor. However, the historic value of the collection and some faunistic data standing even without exact stratigraphic references make the investigations worth doing.

The locality and material

Büdöskút is a place where an old well and in the past a farmhouse situated by the now abandoned Eplény-Lókút road (Text-fig.1). The area is well-known as a locality of Lower Jurassic rocks and ammonites. Kávás-hegy, the hill north to the road, was the study area of L. KOVÁCS (e.g. 1942) and later of GÉCZY (e.g. 1971; 1976). These studies resulted in detailed presentation of Sinemurian and Pliensbachian ammonite faunas.

The track of the NW-SE road follows a prominent fault bringing higher Jurassic rocks onto the surface on the other, southwestern side of the valley (see map 1 in KONDA 1970), and probably here were those outcrops where Noszky collected his ammonites.

On the surviving original labels NOSZKY recorded four localities, each noted as 'mfh', i.e. 'megfigyelőhely = observation point'. This obviously refers to entry in his field notebook. Unfortunately neither field notebooks nor reconnaissance maps of NOSZKY are kept in the archives of the Geological Institute. On the other hand, maps edited by NOSZKY show smaller areas of exposed Middle Jurassic

[1] Eötvös University, Department of Palaeontology, H-1117 Budapest, Pázmány Péter sétány 1/C, Hungary. E-mail: galacz@ludens.elte.hu

[2] Department of Musicology and Music Theory, Liszt Academy of Music, H-1077 Budapest, Wesselényi u. 52, Hungary. E-mail: kzkovacszoltan@gmail.com

ammonite-bearing white *Bositra*-limestone. Most probably these exposures were at least partly artifical ones, because NOSZKY noted one as 'on the road leading to Lókút', possibly indicating a temporal situation due to road-maintenance or widening. Today, as Büdöskút being abandoned and ruined, and the road out of use, these outcops are unidentifiable.

The preservation of the specimens is uniform, i.e. there are no preservational differences between examples of Middle Aalenian and Lower Bajocian ones. All are internal casts with better, occasionally beautifully preserved lower sides. The matrix is white limestone with some clay content. The texture is dominated by thin *Bositra* shells as tiny filaments. This facies corresponds to the Bajocian clayey limestone known on the nearby Lókút Hill, which is ranged into the Eplény Limestone Formation (KNAUER in FŐZY 2012).

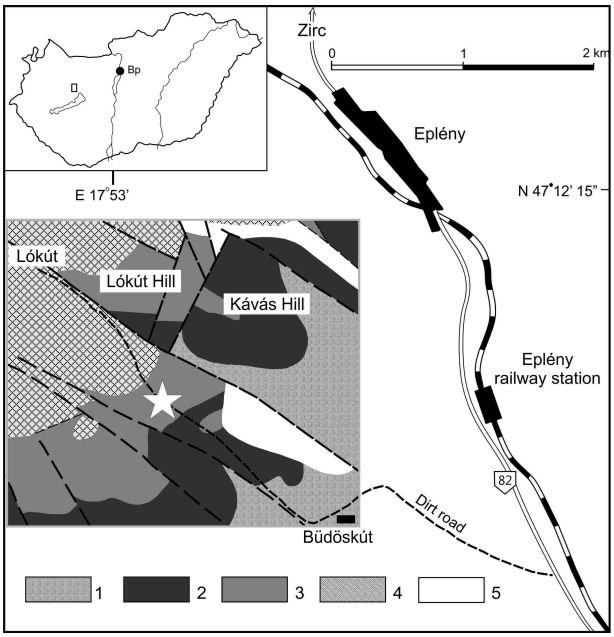

Text-fig. 1. The geographic situation of the Büdöskút locality with the geological build-up of the immediate surroundings (after KONDA 1970, fig.I). 1: Lowermost Jurassic limestone (Kardosrét Fm); 2: various Lower Jurassic carbonates; 3: Middle Jurassic limestones and radiolarite; 4: Upper Jurassic and lowermost Cretaceous carbonates; 5: Oligocene clastics. Asterisk indicates the most probable place of collecting.

The studied collection

The material consists of several hundred specimens, mainly ammonites. Other elements are extremely rare: only some belemnites and a few bivalves are in the collection. The majority of the ammonite specimens belongs to Phylloceratina and Lytoceratina, suborders usually represented with high proportions in Mediterranean, i.e. Bakony Mountains assemblages.

In our discussion we keep the notions of NOSZKY as he left as inscriptions on the specimens. All examples were labelled as „III", indicating the locality, and after a slash numbers 1 to 4, indicating the beds or the assemblages collected on different spots within the small locality area. Besides, each specimen bears a short combination of letters and numbers, referring probably to systematic affinity. For simplicity, we refer to the discussed specimens as belonging to „assemblages" III/1 to 4, however, these groups of individuals indicate very wide stratigraphic intervals (e.g. assemblage III/1 at least three Bajocian ammonite zones) or may indicate stratigraphic units in overlap (i.e. assemblages III/2 and 4, both indicating Middle Aalenian age). One point, corresponding to „assemblage" III/3, yielded extremely poor material: a few phylloceratids only.

The whole material belongs to the collections of the Hungarian Geological and Geophysical Institute (formerly Hungarian Geological Institute, MÁFI). The final cataloguing with inventory numbers will be given there, until then we refer to the specimens by their letters and numbers given by Noszky.

In the following sections we present the most interesting, important or significant ammonite species by subfamilies. We show here only those forms which contribute something new or additional to the Aalenian and Bajocian assemblages known previously from stratigraphically controlled sections. In the systematics, we follow the scheme recently published by HOWARTH (2013).

Systematic notes on the ammonites

Superfamily Hildoceratoidea HYATT, 1867
Family Hildoceratidae HYATT, 1936
Subfamily Tmetoceratinae SPATH, 1936

Tmetoceratinae show world-wide range and in the Mediterranean Province are characteristic in the Upper Toarcian—Aalenian. In Hungary, *Tmetoceras* was common in the Csernye and the Úrkút Sections, and a few specimens are known from the Gerecse Mts (KOVÁCS 2010). In the assemblages of Büdöskút, small to large specimens of *T. scissum* (BENECKE, 1865) (Tm 2 and Tm 6, Pl. 1, figs 1 and 2) agree well with those figured by GÉCZY (1967) from Csernye. A small complete adult specimen with subserpenticone coiling represents a rare species, *T. henriquesae* SANDOVAL, 2002 (Tm 7, Pl. 1, fig.3). It slightly differs from the type (Sandoval 2002, fig. 103) by being somewhat more evolute and by bearing more constrictions. It seems to agree with the *Tmetoceras* specimen figured by Callomon & Chandler (1994, pl. 6, fig. 3) that can be interpreted as *T. henriquesae* on the basis of morphological features. The species differs from *T. scissum* (Benecke), *T. regleyi* (Dumortier), and *T. difalense* (Gemmellaro) by very evolute coiling, smaller whorl expansion and blunter ribs. Two fragmentary specimens with subrectangular section and with dense, slightly sigmoid ribs are referred here to *T.* cf. *difalense* (Gemmellaro, 1886) (Tm 5, Pl. 1, fig.4). The species is known from Italy (Comptum—Haugi Subzones), and from Spain (Murchisonae Zone), and it clearly differs from *T. scissum* and *T. regleyi* by the section and by the specific shape of ribbing. A single specimen with more involute coiling, subcircular whorl-section, and dense, radiate ribs is identified as *T.* cf. *regleyi* (DUMORTIER, 1874) (Tm 3, Pl. 1, fig.5).

Family Graphoceratidae BUCKMAN, 1905
Subfamily Leioceratinae SPATH, 1936

Most taxa included in the family are zonal or horizon indices of the Aalenian, so the family has been widely discussed in the literature. Lately, genera *Leioceras*, *Canavarella*, *Cylicoceras*, *Costileioceras*, *Staufenia* were placed into Leioceratinae by HOWARTH (2013).

Genus *Leioceras* being absent, the Opalinum Zone cannot be documented. Genera *Costileioceras* and *Staufenia* with *Ludwigia haugi* DOUVILLÉ define the Haugi Subzone of the Murchisonae Zone. *Costileioceras opalinoides* (MAYER, 1864), as other species of the Graphoceratidae, shows moderate variability. From the well-preserved material of the Csernye Section, 6 morphotypes were described by GÉCZY (1967). The specimen figured here (Har. 316, Pl. 1, fig.7) with involute, platycone coiling, and with prorsiradiate, sigmoid, paired ribs is close to those forms which bear somewhat stronger ribs than the lectotype (refigured by SCHLEGELMILCH 1985, pl. 10, fig. 5). Similarly, *Staufenia sinon* (BAYLE, 1878) is also characterized by intraspecific variability. Three morphotypes occurred at Csernye. It is close to *Costileioceras* but differs in somewhat more evolute coiling (Har. 311, Har. 335, Pl. 1, figs 6, 8). The species is known from the Gerecse Mts as well (KOVÁCS & GÉCZY 2008).

Subfamily Graphoceratinae BUCKMAN, 1905

Graphoceratinae is represented at Büdöskút by Middle Aalenian genera *Ludwigia* and *Brasilia*. Due to lack of genus *Graphoceras*, the Concavum Zone cannot be recognized. All species mentioned below were recorded from the Csernye Section as well. Two species of *Ludwigia* are typical of the Haugi Subzone. *L. haugi* DOUVILLÉ, 1885 is a moderately evolute form with suboval section and strong, falcoid, simple or bifurcating ribs (Har. 305, Pl. 1, fig. 9). *L. crassa* HORN, 1909 is characterized by evolute coiling, subtrapezoid section, and by well-developed, slightly sigmoid, widely spaced ribs (Har. 343, Pl. 1, fig.10). *L. murchisonae* (SOWERBY, 1829) is the index of the Murchisonae Subzone. The species is a moderately evolute form with broad suboval section, and with simple or bifurcating, falcoid ribs (Har. 333, Har. 301, Pl. 2, figs 1 and 4). In Hungary, it is also known from the Mecsek Mts (VADÁSZ 1935), and from the Gerecse Mts (KOVÁCS & GÉCZY 2008). The morphology of a fragmentary specimen is close to *L. cosmia* (BUCKMAN, 1899), however, it differs by narrower section (Har. 350, Pl. 1, fig.12). Genus *Brasilia* is represented with three species. *B. bradfordensis* (BUCKMAN, 1881) is the zonal index of the Bradfordensis Zone/Subzone. It is a moderately evolute form with narrow suboval section, and fine, mostly bifurcating, prorsiradiate, falcoid ribs (Har 304, Har. 303, Pl. 2, figs 3, 4). *B. bradfordensis* was the most frequent taxon of the *Ludwigia—Brasilia* material of the Csernye Section, and occurred in the Mecsek Mts as well. *B. baylii* (BUCKMAN, 1887) with involute coiling, narrow suboval section, and dense, prorsiradiate, falcoid bifurcating ribs is considered as a transient form between *L. murchisonae* and *B. bradfordensis* (Har. 345, Pl. 1, fig.11). Three poorly preserved specimens with weakly developed, sigmoid, and bifurcating ribs are regarded as *B.* cf. *similis* (BUCKMAN, 1889) (Har. 332, Pl. 2 fig.2).

Family Hammatoceratidae BUCKMAN, 1887
Subfamily Hammatoceratinae BUCKMAN, 1887

A detailed taxonomic treatment of Hammatoceratidae was recently offered by RULLEAU (2009). The description of the Toarcian—Aalenian taxa of the Gerecse assemblages, as well as the revision of the hammatoceratid material of the Csernye Section was presented by KOVÁCS (2009).

Comparing the Büdöskút material with that from Csernye, its low number and diversity is noteworthy, because the subfamily is represented only by 7 specimens. Assemblage III/4 yielded a wholly septate and a fragmentary specimen of the rare *Hammatoceras spinosum* HANTKEN in PRINZ, 1904. Both agree with the holotype (PRINZ, pl. 18, figs 1-2, refigured by GÉCZY 1966, pl. 8, fig. 1) that is characterized by an evolute, compressed coiling, rounded flank, and high, carinate venter. The ornamentation consists of midflank tubercles on the inner whorls, which become elongated nodes on the last whorl of the phragmocone. The secondary ribs are dense and prorsiradiate (Ham. 305, Pl. 2, fig.6). At the Csernye Section, 13 specimens came from the Murchisonae Subzone. The species was also recorded without any description by BENSHILI (1989) from Morocco (Concavum Zone). *H. spinosum* was placed into genus *Accardia* by KOVÁCS (2009), however, the latter taxon is regarded as a synonym of *Hammatoceras* by HOWARTH (2013).

Genus *Planammatoceras* is represented by a poorly preserved *P. tenuinsigne* (VACEK, 1886) specimen. *Pseudaptetoceras klimakomphalum* (VACEK, 1886) (Har. 352, Pl. 3, fig.5) is known from the Bradfordensis Subzone—Concavum Zone at Csernye, and from the Murchisonae Subzone—?Concavum Zone in the Gerecse Mts. A single, poorly preserved specimen with evolute and very compressed coiling, high venter, fine ribs, and with a half whorl long preserved body chamber is referred to *Paviaites* sp. (Har 329, Pl. 3, fig.1). Its morphology is close to the lectotype of *P. iris* (CRESTA 2002, fig. 124/a), however, it differs by being slightly more involute. *P. iris* is known from Sicily (Aalenian) and Tunisia (Comptum Subzone).

Genus *Bredyia* is represented only by a poorly preserved specimen (Ham. 308, Pl. 3, fig.3). It is a wholly septate mold with moderately involute coiling, high, carinate venter, and wide-oval section. Strong, thin, radiate primaries bifurcate without any tubercles at the lower third of the flank, and intercalatory ribs appear regularly on the last whorl. The form differs from *B. subinsignis* (OPPEL, 1856) by bearing much finer and sharper ribs without any nodes, and from *B. alleoni* (DUMORTIER, 1874) in thinner and straight ribs.

Subfamily Erycitinae SPATH, 1928

Systematics and phylogeny of the subfamily, as well as the erycitid specimens of the Gerecse assemblages were recently treated by KOVÁCS & GÉCZY (2008). In his comprehensive book RULLEAU (2009) also offered a detailed taxonomic treatment of the subfamily.

The assemblages of Büdöskút yielded a rich erycitid material. *Erycites intermedius* HANTKEN in PRINZ, 1904 (Ham. 302, 303, Pl. 3, figs 4 and 7) is a moderately evolute form with slightly convex flanks, and with coarse, trifurcating ribs. The venter, which is divided by a smooth band, is low and broad on the phragmocone, while higher and narrower on the body chamber. The section is wide-oval in the inner whorls, but highly arched on the last whorl, and the body chamber is about one whorl in length. The species is known from the Murchisonae—Bradfordensis Subzones of Csernye, and from the Opalinum—Murchisonae Zones in the Gerecse Mts. *E. barodiscus* GEMMELLARO, 1886 is a moderately evolute form with subcircular whorl-section, and with coarse bi- or trifurcating ribs (Do. 102, Pl. 3, fig.2). It was not recorded from Csernye by GÉCZY (1966); however, the reinvestigation of the Csernye material (deposited in the collection of the Hungarian Geological and Geophysical Institute) proves its presence, as an *E.* cf. *subquadratus* GÉCZY (J5341), and 5 *Erycites* spp. (J4478, 4486, 4487, 4489, 4491) are emended here as *E. barodiscus*. In the Gerecse assemblages, *E. barodiscus* was the most abundant erycitid form in the Meneghinii—Opalinum Zones. Assemblage III/2 yielded some poorly preserved specimens of *E.* cf. *fallifax* ARKELL, 1958, *E.* cf. *baconicus* HANTKEN in PRINZ, 1904 and *E.* sp. aff. *partschi* Prinz, 1904 (Ham. 300, Pl. 3, fig.6).

Erycites (*Abbasitoides*) *modestus* (VACEK) is the most abundant species of the Erycitinae in the Büdöskút assemblages. As there is no such material of a respectable quantity discussed in the literature, we examine the taxon in detail.

Erycites (Abbasitoides) modestus (VACEK, 1886)
(Text-fig. 2 a-g)

1886 *Coeloceras modestum* n. sp. — VACEK, p. 100, pl. 17, figs 4-6

1923 *Coeloceras modestum* VACEK — RENZ, pl. 12, fig. 10

1966 *Erycites (Abbasitoides) modestus* (Vacek) — GÉCZY, p. 116-117, fig. 102, pl. 33, fig. 1, pl. 44, fig. 5 *(cum syn.)*

1970 *Erycites (Abbasitoides) modestus* (VACEK) — FISCHER, p. 602, pl. 4, figs 7-8

1988 *Abbasitoides modestum* (VACEK) — LINARES et al., pl. 2, fig. 4

1990 *Stephanoceras (Abbasitoides) modestum* (VACEK) — CALLOMON & CHANDLER, pl. 1, fig. 2

1990 *Stephanoceras (Abbasitoides)* aff. *modestum* (VACEK) — CALLOMON & CHANDLER, pl. 1, figs 3-4

2007 *Abbasitoides modestus* (VACEK) — RULLEAU, p. 110, pl. 86, fig. 3, pl. 103, fig. 8

2008 *Abbasitoides modestus* (VACEK) — KOVÁCS & Géczy, p. 83, pl. 9, figs 2-3, pl. 13, fig. 2

2009 *Abbasitoides modestus* (VACEK) — RULLEAU, p. 82, fig. 19/6, pl. 85, figs 3, 13

2011 *Abbasitoides modestus* (VACEK) — SANDOVAL et al., fig. 11/6

Material: 15 specimens with subserpenticone, gradually growing coiling; wide, shallow umbilicus; convex flanks; broad, rounded venter, and subcircular section. The body chamber is 3/4 whorl in length; the peristome is simple and slightly projected. Fine, sigmoid ribs persist throughout the whorls. Radiate primaries bifurcate under the mid-flank, the secondaries bend slightly backward first, then curve forward on the venter, and fade out in the middle. They alternate with a narrow smooth band between them. Simple erycitid suture-line with short E, longer, ramified L, and divided, oblique U.

Measurements:

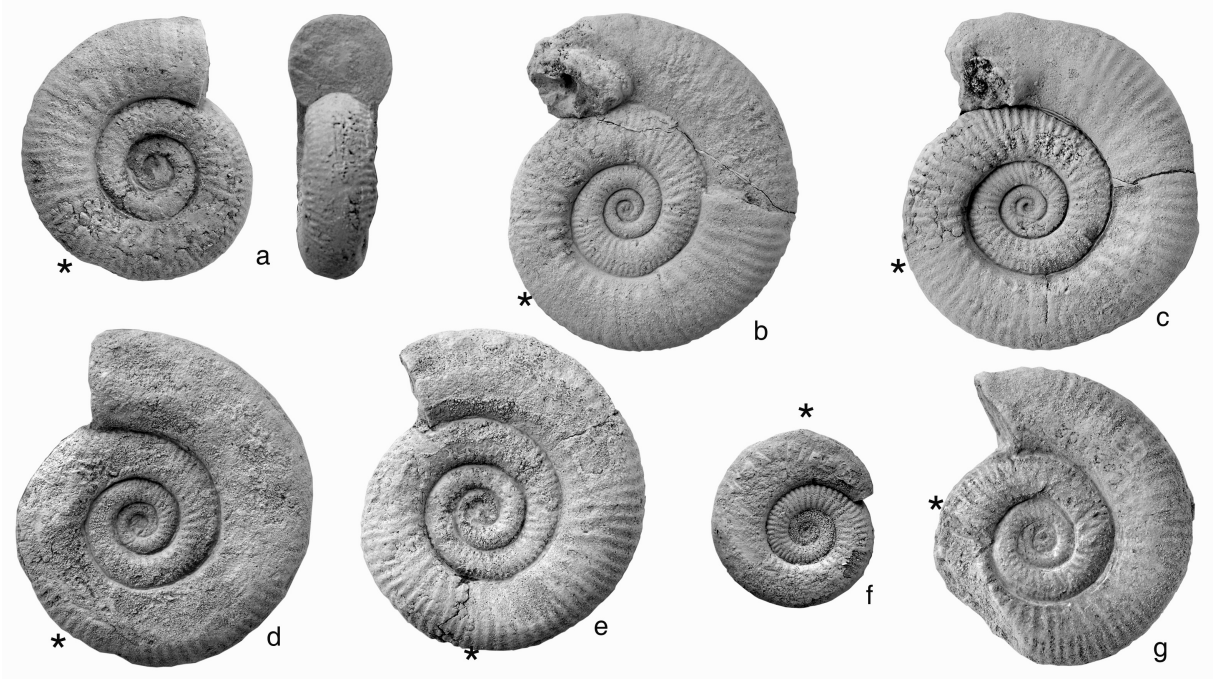

Text-fig. 2. *Abbasitoides modestus* (VACEK, 1886). All from Büdöskút, assemblages III/2 or III/4. a: Coe 111, III/4; b: Coe 105, III/2; c: Coe 108, III/4; d: Coe 104, III/2; e: Coe 103, III/2; f: Coe 100, III/2; g: Coe 102, III/2. All figures natural size, asterisk indicates end of phragmocone.

specimen	Diameter	Height	H/D%	Width	W/D%	Umbilical width	U/D%	Ribs on the last whorl
Coe 105	44.5	14	31.5	13.5	30.5	22	49.5	38
Coe 104	44	13,5	30.5	13	29.5	21	47.5	?
Coe 108	44	13	29.5	13	29.5	21	47.5	36
Do 103	43.5	14	32	16	36.5	20	46	?
Coe 103	43	13	30	13.5	31.5	21	49	37
Coe 107	42	12.5	29.5	13.5	32	20.5	49	37
Coe 102	40	12	30	13	32.5	20	50	?
Coe 111	35.5	12	34	13	36.5	17	48	33
Coe 109	32	10	31	10	31	15.5	48.5	?
Coe 112	29..5	10	34	10	34	14.5	49	?
Coe 100	23	8	34.5	7	30.5	10	43.5	?

Remarks: Subgenus *Abbasitoides* was created by GÉCZY (1966) with type species *Coeloceras modestum* (VACEK). The lectotype (VACEK, 1886, p. 100, pl. 17, fig. 4-6) was designated and refigured by WESTERMANN (1964, pl. 6, fig. 8). The taxon is regarded as a synonym of genus *Erycites* by HOWARTH (2013), however, considering the small size of the species included into the subgenus, the separation of the group by the conservation of the subgenus name seems to be established.

The interpretation of *A. modestus* is controversial. It was regarded as the earliest representative of the Otoitidae, included in genus *Stephanoceras* by PAGE (1993); and as the microconch of „*Stephanoceras" longalvum* (VACEK) by CALLOMON & CHANDLER (1990). On the other hand, — based on the erycitid suture-line, the ventral interruption and the simple aperture — WESTERMANN (1964, 1995) considered it as a small erycitid macroconch. The latter interpretation was confirmed by DIETZE et al. (2001), and RULLEAU (2009). *Coeloceras placidum* VACEK (= *Ammonites blampis*, GREGORIO 1886, pl. 11, fig. 5) which is a similar form in morphology, was regarded as a synonym of *A. modestus* by GREGORIO (l.c.) and RULLEAU (2009), however, it differs in suture construction with more developed external lobe (see VACEK l.c., pl. 17, fig. 8; GREGORIO l.c., pl. 11, fig. 5/c-d) that is not typical of the Erycitinae (GÉCZY 1966).

In the literature, the shape of ribbing and the proportion of involution of *A. modestus* show moderate variability. The type is characterized by prorsiradiate ribs, and its U/D is app. 43%. The example of RENZ (1923) resembles in the involution (U/D: app. 42%), while differs in fine, but almost radiate ribs. The specimens of FISCHER (1970, fig. 7), and of SANDOVAL et al. (2011) also bear less prorsiradiate ribs, and their style of coiling is more evolute (U/D: 50%). Three specimens were figured by CALLOMON & CHANDLER (1990, pl. 1, figs 2-4). Both the involution and the ornamentation of the example on their fig. 2 are closer to those of *Abbasites gardincola* (GREGORIO), — this specimen can be regarded as a transient form. The ribs of both *S.* (*A.*) aff. *modestum* (l.c., figs 3-4), — like the specimen of Rulleau (2007, pl. 103, fig. 8) — differ from the type by crossing the venter. A phylogenetic change might be manifested by these examples: the ventral interruption that was typical of the Erycitinae disappeared gradually in the last period of the subfamily (Bradfordensis—Concavum Zones: *Abbasites—Ambersites* group). This change can be connected with the Aalenian—Bajocian migration of ammonites between the Mediterranean and NW European regions of Europe when some Mediterranean taxa (e.g. *Erycites*, *Abbasitoides*, *Riccardiceras*, *Tmetoceras*) migrated northward to England where they became relatively common (SANDOVAL & CHANDLER 2000).

Three taxa were described from the Csernye assemblage: *Erycites* (*Abbasitoides*) *modestus* (VACEK) (10 specimens), *E.* (*A.*) *modestus crassornatus* GÉCZY (12 specimens), *E.* (*A.*) *modestus compressus* (PRINZ) (7 specimens). Both subspecies are larger forms with radiate and strong ribs. At Csernye, most specimens came from a horizon of 10 cm in the Opalinoides Subzone, but the genus ranged up to the Bradfordensis Zone. From the Gerecse Mts two *A. modestus* specimens were recorded from the Opalinum—Murchisonae Zones.

More than 30 specimens are known from different Italian localities (see VACEK 1886, BOTTO-MICCA 1893, BONARELLI 1893, RENZ 1923, WENDT 1971, KÄLIN & URETA 1987, CALLOMON et al. 1995, CRESTA 1996, PALLINI et al. 2005), but only a few were figured with different morphology (VACEK 1886, pl. 17, figs 4-5; WESTERMANN 1964; RENZ 1923, pl. 12, fig. 10). The *A. modestus* material of complete adults of the Csernye—Gerecse assemblages also shows moderate variability in size, involution and whorl-width. Some of them are close to that figured by RENZ (1923); on the other hand, each specimen from Büdöskút belongs to the same evolute morphotype. Most specimens of the mentioned Hungarian sections differ from the type by somewhat more evolute coiling, and by less prorsiradiate ribs. The species is abundant in the Betic Cordillera (SANDOVAL et al. 2011), where also the evolute form seems to be characteristic. Based on available data, the slightly more evolute style of coiling (U/D: 48-50%) can be regarded as specific form of the taxon.

A. modestus is known from Italy (Opalinum—Murchisonae Zones), Spain (Comptum Subzone—Concavum Zone), France (Bradfordensis Zone), Portugal (Bradfordensis Subzone), Austria (Murchisonae Zone), Morocco (Murchisonae—Concavum Zones), Greece and (?)Albania (Aalenian), England (Murchisonae Subzone—[?]Lower Discites Zone).

Family Sonniniidae BUCKMAN, 1892
Subfamily Witchelliinae CALLOMON & CHANDLER, 2006

Sonniniidae are represented in the nearby Lókút Section and in the Gerecse Mountains, the northeastern part of the Transdanubian Range (GALÁCZ 1991; CRESTA & GALÁCZ 1990), however their detailed documentation is still lacking. In Csernye the respective levels are very poor in ammonites, thus only some specimens were documented by GÉCZY (1967). The family was discussed recently in detail by DIETZE et al. (2005), and additional information was also published in

SANDOVAL & CHANDLER (2000), DIETZE et al. (2003) and OHMERT (2004). The limited material gives less than few new data on the representation of this family in the Bakony Mts. There are a few specimens from Assemblage 1 which belong to Sonniniidae, most of them are very poorly preserved. One *Witchellia* (Am 103, Pl. 4, fig.1) could be ranged into *W. pavimentaria* (BUCKMAN, 1927) with its size, dimensions and ribbing. Buckman's type (1903-33, pl. 751) came from the upper part (Romanoides faunal horizon) of the Laeviuscula Zone (see DIETZE et al. 2007, p. 13). Microconchiate forms also occur. One slightly worn internal cast is referred here to *Pelekodites spatians* (BUCKMAN, 1928). This specimen (Har 330, Pl. 4, fig. 3) is slightly bigger than the type (BUCKMAN 1903-33, pl. 399), but its ribbing matches well the holotype and the later figured topotypes (CHANDLER et al. 2006, fig. 4(5); DIETZE et al. 2007, figs 4a-b, d-g).

Superfamily Stephanocerataceae NEUMAYR, 1875
Family Stephanoceratidae NEUMAYR, 1875
Subfamily Stephanoceratinae NEUMAYR, 1875

Assemblage III/1 yielded some stephanoceratids indicating the Humphriesianum Zone. A medium-sized *Stephanoceras* (Am 102, Pl. 4, fig. 7) with its compressed and more overlapping whorls and lower and rounded tubercles can be ranged into *S. plicatum* (QUENSTEDT, 1858). Accidentally, a microconch, identified as *Itinsaites latansatus* (BUCKMAN, 1920) also appears in the same assemblage (Cad 111, Pl. 4, fig.8). These two forms were suggested by PAVIA (1983, p. 132) as a dimorphic pair. Similarly, a fragment of a densely ribbed *Lokuticeras* (Cad 104, Pl. 4, fig. 5), reminding the species *L. rossbrunnense*, described originally from the Lókút locality nearby, occurs together with the better preserved thus closer determinable *Masckeites densus* BUCKMAN, 1920 (Cad 109, Pl. 4, fig. 6), suggested also as a corresponding dimorphic pair (GALÁCZ 1994, p. 168). The *Lokuticeras/Masckeites* dimorph pair, as well as *Itinsaites latansatus* indicate the upper part of the Humphriesianum Zone. The same is suggested by an indeterminable *Teloceras* fragment, while a poorly-preserved, incomplete *Skirroceras* is similar to the Sauzei Zone forms of this genus.

Family Otoitidae MASCKE, 1907

This family is represented in assemblage III/1 with a few *Emileia* and *Otoites* specimens (macroconchs and microconchs respectively). The single *Emileia* is very poorly preserved, while one of the two *Otoites* is only a partially preserved specimen (Cad 107, Pl. 4, fig.4), but the other one is determinable as *O. compressus* WESTERMANN, 1954. This form (Cad 122, Pl. 4, fig.2) with its slender body chamber represents a comparatively rare species which is known only by the type and paratype specimens from Gerzen (NW Germany, WESTERMANN 1954, p.109) and one more specimen recorded recently from the Schwäbische Alb, SW Germany (DIETZE et al. 2008, p.144). At both localities the species came from the Otoites sauzei Zone.

Family Sphaeroceratidae BUCKMAN, 1920
Subfamily Sphaeroceratinae BUCKMAN, 1920

The early members of this subfamily is represented in assemblage III/1 by *Labyrinthoceras* and its microconch pair *Manselites*. The big size of the macroconchiate specimen indicates *L. meniscum* (WAAGEN, 1868) (Em 100 and Em 104, Text-fig.3 a and b) and the microconch could be identified as *L.* (*Manselites*) *manselii* (J. BUCKMAN, 1881) (Am 110, Text-fig. 3c). The appearance of these Sauzei Zone forms in the material is not surprising, because the locality is very near to the Lókút Section, where these genera occur commonly (see GALÁCZ 1990). Humphriesianum Zone sphaeroceratids are represented also in assemblage III/1 by some poorly preserved *Chondroceras*.

Conclusions

The above discussed ammonite fauna represents Aalenian and Bajocian levels, however significant hiati appear, (see Table I). The Aalenian is indicated by ammonites characteristic to the Middle Aalenian Ludwigia murchisonae and Brasilia bradfordensis Zones (including the two zonal indices) in assemblages III/ 2 and 4, while the Upper Aalenian Graphoceras concavum Zone seems missing. Similarly, the Lower Bajocian Hyperlioceras discites and Fissilobiceras ovale Zones are not represented, then at least three higher Bajocian zones, the Witchellia laeviuscula, Otoites sauzei and Stephanoceras humphriesianum Zones are indicated in the single assemblage III/1. However, these representations do not mean total covering of the zones in question. Probably the beds which yielded the specimens might belong to different horizons, but to reconstructing the original situation would need more information on the circumstances in the time of the collecting, or good exposures in recent times for a revision.

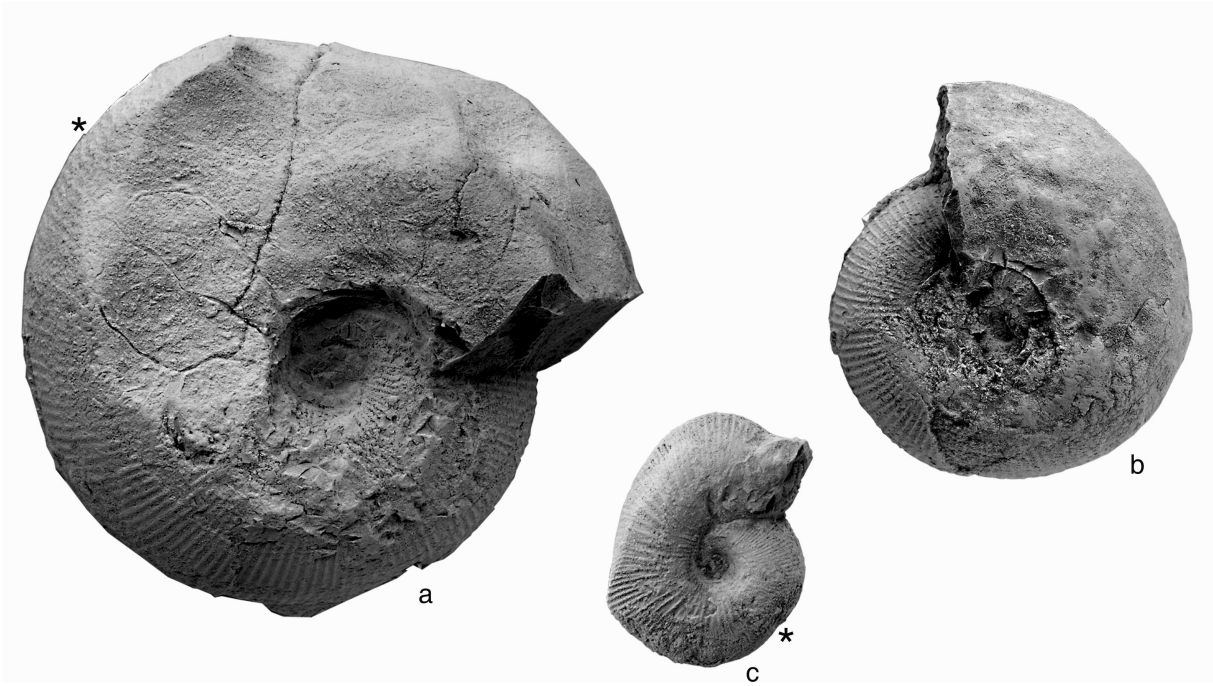

Text-fig. 3. *Labyrinthoceras.* Macro- and microconch specimens from Büdöskút, assemblage III/1. a and b: *Labyrinthoceras* (*Labyrinthoceras*) *meniscum* (WAAGEN, 1868), Em 100 and Em 101; c:, corresponding microconch, *Labyrinthoceras* (*Manselites*) *manselii* (J. BUCKMAN), Am 110. All figures natural size, asterisk indicates end of phragmocone.

Table I. Biostratigraphic representation of Middle Aalenian to Lower Bajocian ammonite zones in the Büdöskút material (shaded cells) with the identified diagnostic ammonites.

Stages	Substages	Zones	Zones indicated by diagnostic ammonites in the here described Büdöskút material
BAJOCIAN	Lower	Humphriesianum	*Stephanoceras* (*S.*) *plicatum* (QUENSTEDT); *Stephanoceras* (*Itinsaites*) *latansatus* (BUCKMAN); *Lokuticeras rossbrunnense* GALÁCZ; *Masckeites densus* Buckman
		Sauzei	*Labyrinthoceras* (*L.*) *meniscum* (WAAGEN); *Labyrinthoceras* (*Manselites*) *manselii* (J.BUCKMAN); *Otoites compressus* WESTERMANN
		Laeviuscula	*Witchellia pavimentaria* (BUCKMAN); *Pelekodites spatians* (BUCKMAN)
		Ovale	
		Discites	
AALENIAN	Upper	Concavum	
	Middle	Bradfordensis	*Brasilia bradfordensis* (BUCKMAN); *Brasilia baylii* (BUCKMAN); *Brasilia* cf. *similis* (BUCKMAN)
		Murchisonae	*Ludwigia haugi* DOUVILLÉ; *Ludwigia* cf. *haugi* DOUVILLÉ; *Ludwigia crassa* HORN; *Staufenia sinon* (BAYLE); *Costileioceras opalinoides* (MAYER); *Ancolioceras* sp.; *Staufenia* sp.

Acknowledgements

The authors are indebted to Dr Bálint PÉTERDI from the Collections of the Hungarian Geological and Geophysical Institute for helping to save this material. Prof. L. KORDOS, formerly head of the Collections, is thanked for making available this material for study. We acknowledge the help of Zoltán SZENTESI and Emőke TÓTH who constructed the map on Fig.1.

References

BENSHILI, K. (1989): Lias–Dogger du Moyen-Atlas Plissé (Maroc), sédimentologie, biostratigraphie et évolution paléogéographique. — *Documents des Laboratoires de Géologie de la Faculté des Sciences de Lyon*, 106: 1-285, Lyon.

BONARELLI, G. (1893): Osservazioni sul Toarciano e l'Aleniano dell'Appennino Centrale. — *Bollettino della Societá Geologica Italiana*, 12(2): 195–254, Roma.

BOTTO-MICCA, L. (1893): Fossili degli "Strati a *Lioceras opalinum* Rein. e *Ludwigia Murchisonae* Sow. della Croce di Valpore (M. Grapa) provincia di Treviso. — *Bollettino della Societá Geologica Italiana*, 12(2): 143–193, Roma.

BUCKMAN, S.S. (1909-1930): (Yorkshire) Type Ammonites, Vols 1-7, Wesley & Son, London and the Author, Thame, 790 pls.

CALLOMON, J.H. & CHANDLER, R.B. (1990): A review of the ammonite horizons of the Aalenian–Lower Bajocien Stages in the Middle Jurassic of southern England. — *Memorie Descrittive della Carta Geologica d'Italia*, 40: 85–112, Roma.

CALLOMON, J.H. & CHANDLER, R.B. (1994): Some early Middle Jurassic ammonites of Tethyan affinities from the Aalenian of southern England. — *Palaeopelagos, Special Publication* 1: 17–40, Roma.

CALLOMON, J.H. & CHANDLER, R.B. (2006): Notes on the ammonite faunas. In: CHANDLER, R.B., CALLOMON, J.H., KING, A., JEFFREYS, K., VARAH, M. & BENTLEY, A.: The stratigraphy of the Inferior Oolite at South Main Road Quarry, Dundry, Somerset. – *Proceedings of the Geologists' Association*, 117: 365-372, London.

CALLOMON, J.H., CRESTA, S. & PAVIA, G. (1995): A revision of the classical Aalenian succession in the Middle Jurassic of San Vigilio, Lake Garda, Northern Italy. — *Geobios*, 17: 103–110, Lyon.

CRESTA, S. (1996): Aalenian Ammonite Biostratigraphy in Northern Apennines (Italy). — *GeoResearch Forum*, 1–2: 135–138.

CRESTA, S. (2002): *Paviaites iris* (GEMMELLARO 1886). — *In*: Revision of Jurassic ammonites of the Gemmellaro collections, *Quaderni del Museo Geologico "G. G. Gemmellaro*", n.6 (coord. Pavia, G. & Cresta, S.): 190-191, Palermo.

CRESTA, S. & GALÁCZ, A. (1990): Mediterranean basal Bajocian ammonite faunas. Examples from Hungary and Italy. - *Memorie Descrtive della Carta Geologica d'Italia*, 40: 165-198. Roma.

DIETZE, V., CHANDLER, R.B. & SCHWEIGERT, G. (2003): *Witchellia pseudoromanoides* n. sp. (Ammonoidea, Sonniniidae) aus der Laeviuscula-Zone (Mittlerer Jura, Unter-Bajocium) der östlichen Schwäbischen Alb (Südwestdeutschland). – *Stuttgarter Beiträge der Naurkunde*, B, Nr.337: 1-25, Stuttgart.

DIETZE, V., CHANDLER R. B., SCHWEIGERT, G. & AUER, W. (2001): New Stephanoceratids (Ammonitina) from the Lower Bajocian of Bruton (Somerset, S England) and Achdorf (Wutach area, SW Germany). — *Stuttgarter Beiträge zur Naturkunde*, B, 312: 1–21, Stuttgart.

DIETZE, V., SCHWEIGERT, G., CALLOMON, J.H. & CHANDLER, R.B. (2005): The ammonite fauna and biostratigraphy of the Lower Bajocian (Ovale and Laeviuscula zones) of E Swabia (S. Germany).- *Stuttgarter Beiträge der Naturkunde*, B, Nr.353: 1-82 Stuttgart.

DIETZE, V., STAPPENBECK, G., WANNENMACHER, N. & SCHWEIGERT, G. (2008): Stratigraphie und Ammoniten-Faunenhorizonte im Grenzbereich Sauzei-/Humphriesianum Zone (Unter-Bajocium, Mitteljura) der westlichen Schwäbischen Alb (SW-Deutschland). – *Palaeodiversity*, 1: 141-165, Stuttgart.

FISCHER, R. (1970): Ammoniten aus dem Aalenium der nördlichen Kalkalpen. — *Neues Jahrbuch für Geologie und Paläontologie*, 10: 585–604, Stuttgart.

GALÁCZ, A. (1990): Taxonomy, dimorphism and phylogenetic significance of the Bajocian (Middle Jurassic) ammonite *Labyrinthoceras*. In: PALLINI, G., CECCA, F., CRESTA, S. & SANTANTONIO, M. (Eds): Fossili, Evoluzione, Ambiente. Atti del secondo convegno internazionale, Pergola, 25-30 ottobre 1987: 341-348, Roma.

GALÁCZ, A. (1991): Lower Bajocian Sonniniid ammonites from the Gerecse Mountains, Hungary. - Conference on Aalenian and Bajocian Stratigraphy. Isle of Skye, April 1991. *Abstracts*: 109-111. London.

GALÁCZ, A. (1994): *Lokuticeras* nov. gen. – a new genus for a Mediterranean Bajocian (Middle Jurassic) stephanoceratid ammonite group. – *Miscellanea del Servizio Geologico Nazionale*, 5: 161-175, Roma.

GÉCZY, B. (1966): Ammonoides Jurassiques de Csernye, Montagne Bakony, Hongrie, Part I. (Hammatoceratidae). — *Geologica Hungarica, Series Palaeontologica*, 34: 1-276, Budapest.

GÉCZY, B. (1967): Ammonoides Jurassiques de Csernye, Montagne Bakony, Hongrie, Part II. (excl. Hammatoceratidae). — *Geologica Hungarica, Series Palaeontologica*, 35: 1-413, Budapest.

GÉCZY, B. (1971): Pliensbachian of the Bakony Mountains. – *Acta Geologica Academiae Scientiarum Hungaricae,* 15: 115-125, Budapest.

GÉCZY, B. (1976): Les ammonites du Carixien de la Montagne du Bakony. Akadémiai Kiadó: 223 p., Budapest.

GREGORIO, A. (1886): Monographie des fossiles de San Vigilio. — *Annales de Géologie et de Paléontologie*, 5: 3–34, Palermo.

HOWARTH, M.K. (2013): Treatise Online Nr.57, Part L, Revised, Volume 3B, Chapter 4: Psiloceratoidea,

Eoderoceratoidea, Hildoceratoidea. University of Kansas, Paleontological Institute, 1-139, Lawrence, Kansas, USA.

KÄLIN, O. & URETA, S. (1987): El Lias superior y el Dogger inferior en Gorgo a Cerbara (Apenino Central): Aspectos bioestratigráficos y sedimentológicos. — *Estudios Geologicos*, 43: 489–511, Madrid.

KNAUER J. (2012): Eplényi Mészkő Formáció. In: Főzy I. (Szerk.): Magyarország litosztratigráfiai alapegységei. Jura. Magyarhoni Földtani Társulat: 65-68, Budapest.

KONDA, J. (1970): Lithologische und Fazies-Untersuching der Jura-Ablagerungen des Bakony-Gebirges. - *Annales Instituti Geologici Publici Hungarici*, 50(2), 155-260, Budapest.

KOVÁCS, L (1942): Monographie der liassischen Ammoniten des nördlichen Bakony. – *Geologica Hungarica, Series Palaeontologica*, 17, 1-220, Budapest.

KOVÁCS, Z. (2009): Toarcian–Aalenian Hammatoceratinae (Ammonitina) from the Gerecse Mts (NE Transdanubian Range, Hungary) — *Fragmenta Palaeontologica Hungarica*, 27: 1-72, Budapest.

KOVÁCS, Z. (2010): Tmetoceratidae (Ammonitina) fauna from the Gerecse Mts (Hungary) – *Central European Geology*, 53(4), 343-376, Budapest.

KOVÁCS, Z. & GÉCZY, B. (2008): Upper Toarcian–Middle Aalenian (Jurassic) Erycitinae Spath (Ammonitina) from the Gerecse Mts, Hungary. — *Hantkeniana*, 6: 57–108, Budapest.

LINARES, A., URETA, M.S. & SANDOVAL, J. (1988): Comparison between the Aalenian Ammonite associations from the Betic and Iberian Cordilleras: elements of correlation. — *In*: 2nd International Symposium on Jurassic Stratigraphy, 193–208, Lisboa.

NOSZKY, J. jun. (1935): Beiträge zur Frage der Wasserversorgung der Ortschaft Lókút.─ *Hidrológiai Közlöny*, 14, 83-104, Budapest.

OHMERT, W. (2004): Ammoniten-Faunen im Tiefen Unter-Bajocium des Reutlinger Gebiets (mittlere Schwäbische Alb). – *Jahreshefte des Landesamts für Geologie, Rohstoffe und Bergbau Baden-Württemberg*, 40, 9-141, Freiburg.

PAGE, K.N. (1993): Mollusca: Cephalopoda (Ammonoidea: Phylloceratina, Lytoceratina, Ammonitina and Ancyloceratina) — *In*: The Fossil Record 2, (ed. Benton M. J.), 213-227, London.

PALLINI, G., ELMI, S. & GASPARINI, F. (2005): Late Toarcian – Late Aalenian Ammonites Assemblage from Mt. Magaggiaro (Western Sicily, Italy). — *Geologica Romana*, 37 (2003–2004): 1–66, Roma.

PAVIA, G. (1983): Ammoniti e biostratigrafia del Baiociano inferiore di Digne (Francia SE, Dip. Alpes-Haute-Provence). – *Museo Regionale di Scienze Naturali, Monografie*, II, 1-354, Torino.

PRINZ, Gy. (1904): Die Fauna der älteren Jurabildungen im nordöstlichen Bakony. — *Mitteilungen aus dem Jahrbuche der kgl. Ungarischen Geologischen Reichsanstalt*, 15: 1–142, Budapest.

RENZ, C. (1923): Vergleiche zwischen dem südschweizerischen, apenninischen, und westgriechischen Jura. — *Verhandlungen der Naturforschenden Gesellschaft*, 34: 264–296, Basel.

RULLEAU, L. (2007): Biostratigraphie et Paleontologie du Lias superieur et du Dogger de la region lyonnaise, Tome 1, 1-382, Lozanne.

RULLEAU, L. (2009): Les Hammatoceratidae et les Erycitidae NW Européens et Tethysiens du Lias et du Dogger. 1-285, Lozanne.

SANDOVAL, J. (2002): *Tmetoceras difalense* (Gemmellaro 1886); *Tmetoceras henriquesae* n. sp. — *In*: Revision of Jurassic ammonites of the Gemmellaro collections, *Quaderni del Museo Geologico "G. G. Gemmellaro",* n.6 (coord. PAVIA, G. & CRESTA, S.), 161-162, 165-166, Palermo.

SANDOVAL, J. & CHANDLER, R.B. (2000): The Sonniniid Ammonite *Euhoploceras* from the Middle Jurassic of South-West England and Southern Spain. — *Palaeontology*, 43(3): 495–532, London.

SANDOVAL, J., MARTÍNEZ, G., & URETA, S. (2011): Upper Toarcian — Lower Bajocian (Jurassic) Hammatoceratoidea (Ammonitina) of the Betic Cordillera (southern Spain): biostratigraphy and zonal correlations. — *Bulletin de la Société Géologique de France*, 182(3): 241-254, Paris.

SCHLEGELMILCH, R. (1985): Die Ammoniten des süddeutschen Doggers. — G. Fischer Verlag, 1-284, Stuttgart – New York.

VACEK, M. (1886): Über die Fauna der Oolithe von Cap San Vigilio. — *Abhandlungen der k.k. geologischen Reichsanstalt*, 12: 57–212, Wien.

VADÁSZ E. (1935): A Mecsekhegység. — *Magyar tájak földtani leírása* 1, 1-148, Magyar Királyi Földtani Intézet, Budapest.

WENDT, J. (1971): Geologia del Monte Erice (provincia di Trapani, Sicilia occidentale). — *Geologica Romana*, 10: 53–76, Roma.

WESTERMANN, G. (1954): Monographie der Otoitidae (Ammonoidea). – *Beihefte zum Geologischen Jahrbuch*, 15, 1-364, Hannover.

WESTERMANN, G.E. (1964): Sexual-dimorphismus bei Ammonoideen und seine Bedeutung für die Taxonomie der Otoitidae. — *Palaeontographica*, Abt. A, 124/1–3: 33–73, Stuttgart.

WESTERMANN, G.E. (1995): Mid-Jurassic Ammonitina from the Central Ranges of Irian Jaya and the origin of stephanoceratids. — *Hantkeniana* 1: 105-118, Budapest.

Plate I. Figs 1 and 2: *Tmetoceras scissum* (BENECKE, 1865), Tm 2, from assemblage III/2, Tm 6, III/2; Fig. 3: *Tmetoceras henriquesae* SANDOVAL, 2002, Tm 7, III/2; Fig. 4: *Tmetoceras* cf. *difalense* (GEMMELLARO, 1886), Tm 5, III/2; Fig. 5: *Tmetoceras* cf. *regleyi* (DUMORTIER, 1874), Tm 3, III/2; Figs 6 and 8: *Staufenia sinon* (BAYLE, 1878), Har 311, III/2 and Har 335, III/4; Fig. 7: *Costileioceras opalinoides* (MAYER, 1864), Har 316, III/2; Fig. 9: *Ludwigia haugi* DOUVILLÉ, 1885, Har 305, III/2; Fig. 10: *Ludwigia crassa* HORN 1910, Har 343, III4; Fig. 11: *Brasilia baylii* (BUCKMAN, 1887), Har 345, III/4; Fig. 12: *Ludwigia* cf. *crassa* (BUCKMAN, 1899), Har 350, III/4. All figures natural size, asterisk indicates end of phragmocone.

Plate 1

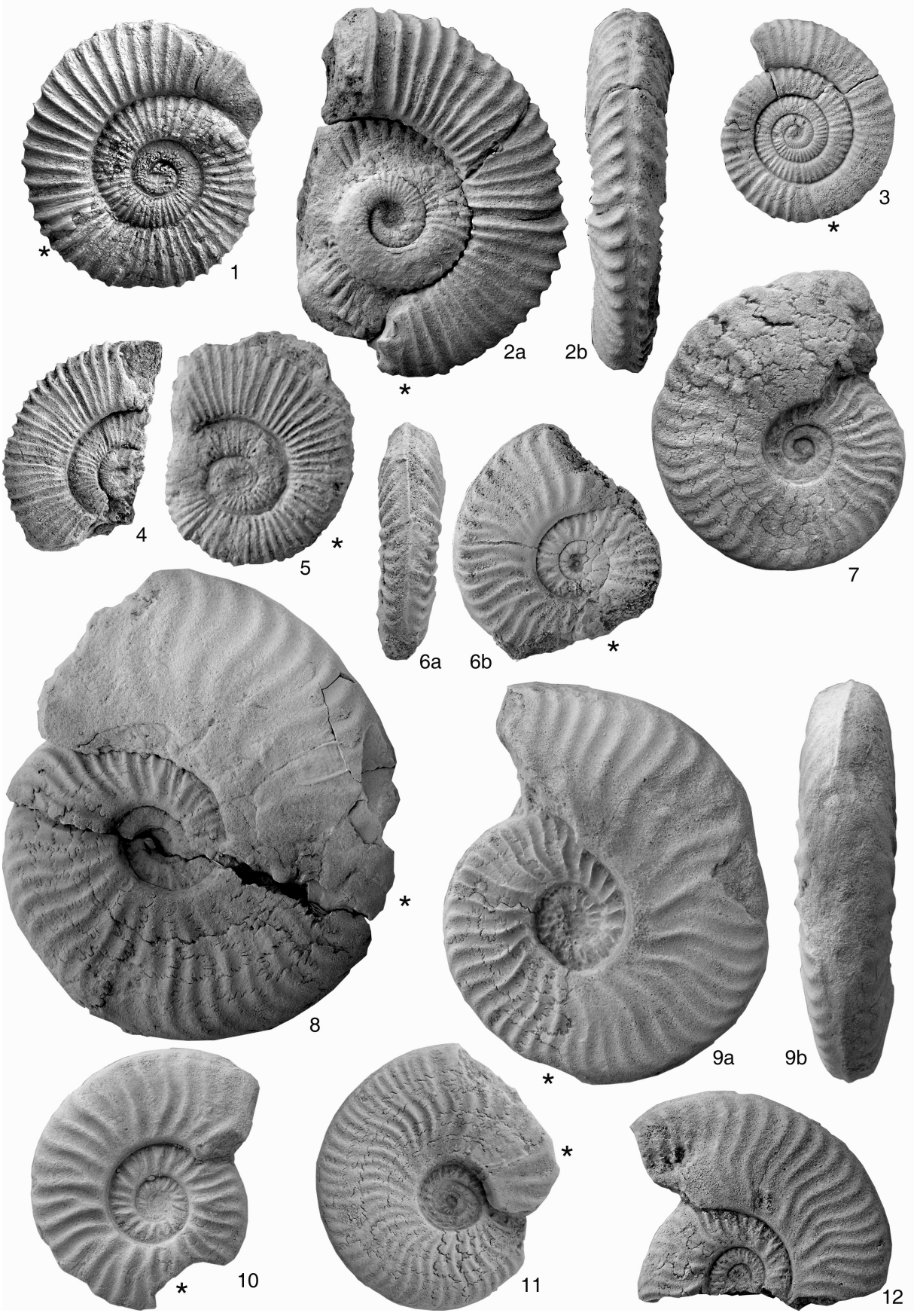

Plate 2

Figs 1 and 5: *Ludwigia murchisonae* (SOWERBY, 1829), Har 333, from assemblage III/4; Har 301, III/2;

Fig. 2: *Brasilia* cf. *similis* (BUCKMAN, 1889), Har 332, III/4;

Figs 3 and 4: *Brasilia bradfordensis* (BUCKMAN, 1881) Har 314, Har 303, both III/2;

Fig. 6: *Hammatoceras spinosum* HANTKEN in PRINZ, 1904, Ham 305, III/4.

All figures natural size, asterisk indicates end of phragmocone.

Plate 2

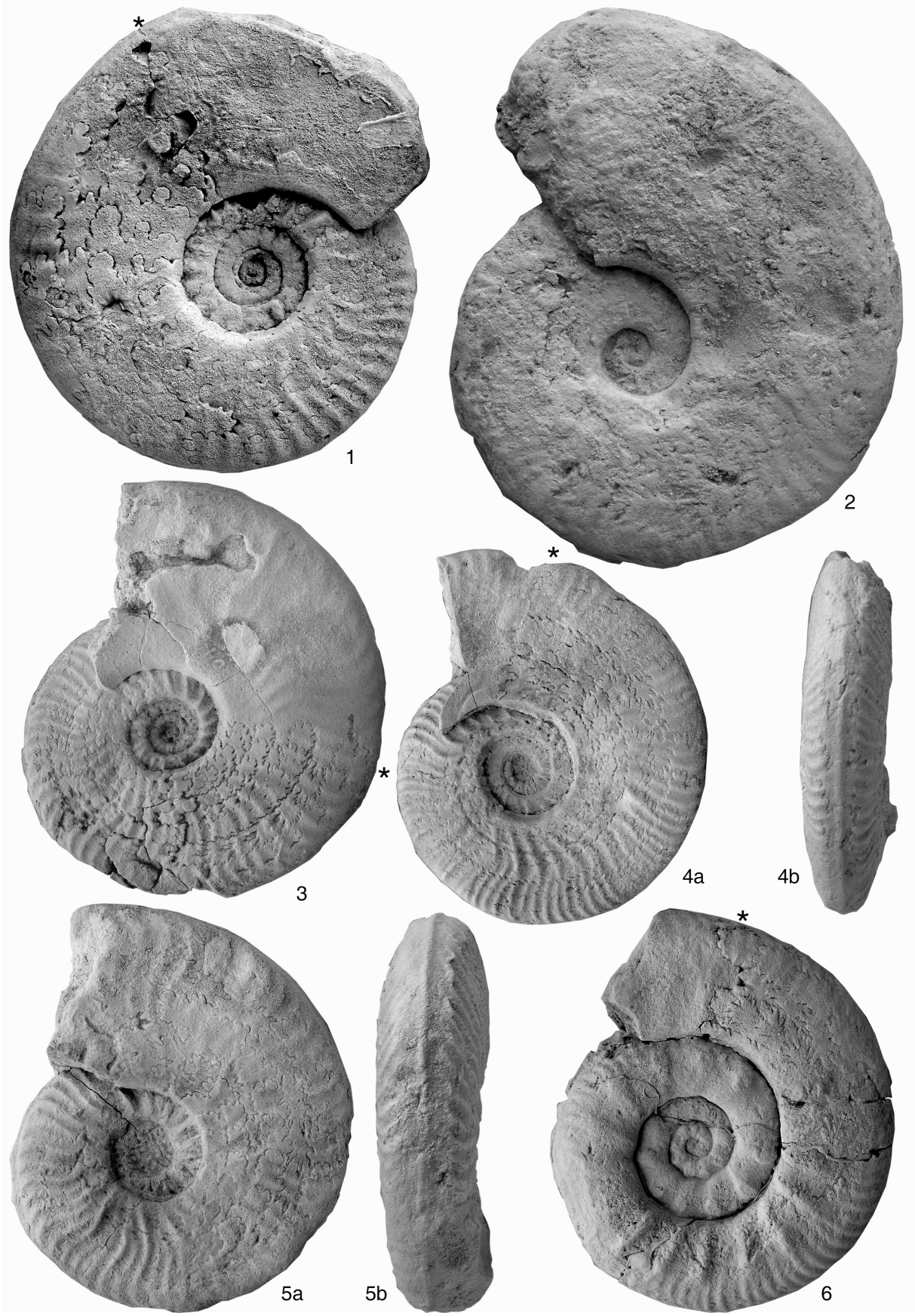

Plate 3

Fig. 1: *Paviaites* sp., Har 329, from assemblage III/2;

Fig. 2: *Erycites barodiscus* GEMMELLARO, 1886, Do 102, III/2; *Bredyia* sp., Ham 308, III/4;

Figs 4 and 7: *Erycites intermedius* HANTKEN in PRINZ, 1904, Ham 302 and Ham 302, both III/2;

Fig. 5: *Pseudaptetoceras klimakomphalum* (VACEK, 1886), Har 352, III/4; *Erycites* sp. aff. *partschi* PRINZ, 1904, Ham 300, III/2.

All figures natural size, asterisk indicates end of phragmocone.

Plate 3

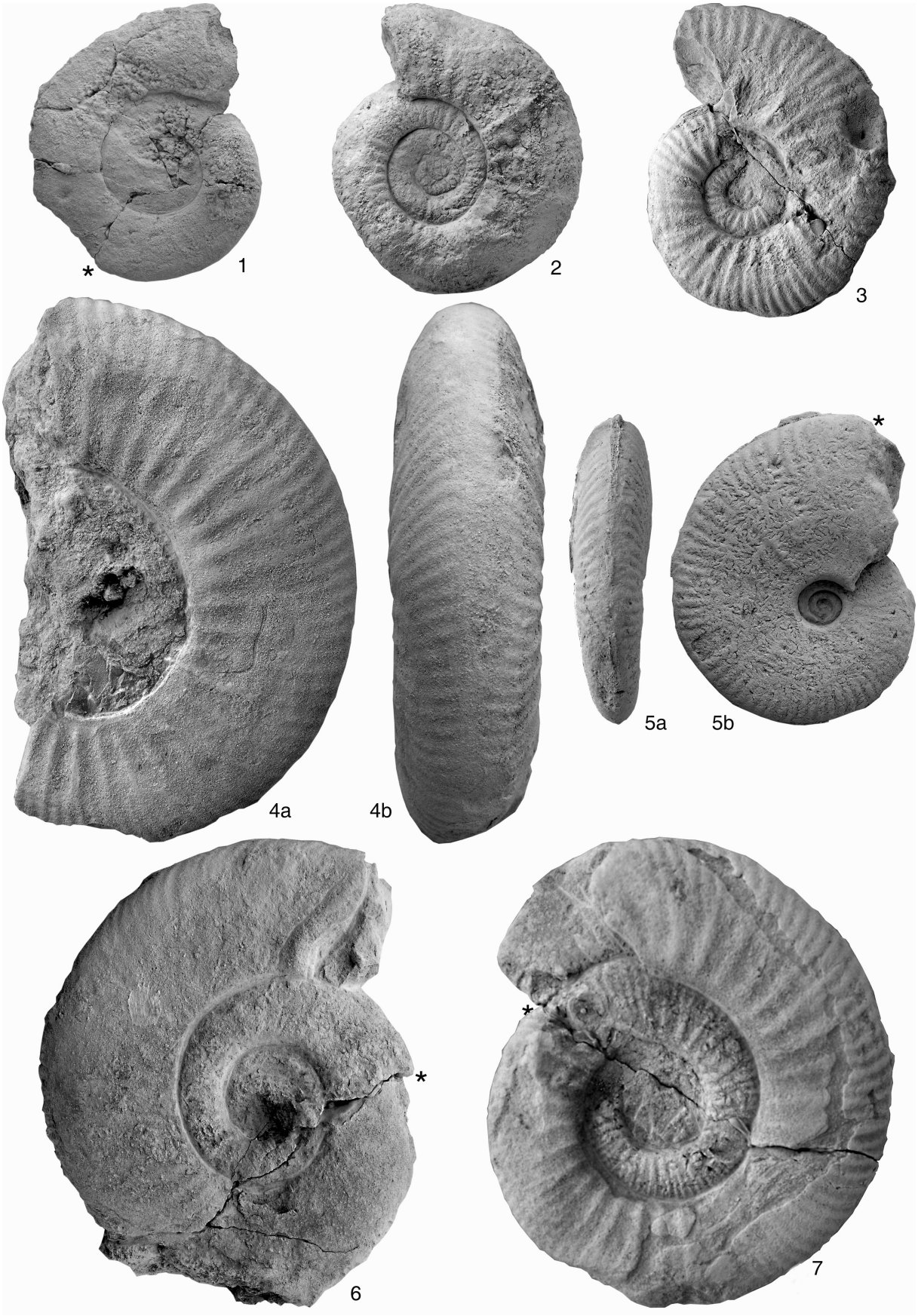

Plate 4

Fig. 1: *Witchellia pavimentaria* (BUCKMAN, 1927), Am 103, from assemblage III/1;

Fig. 2: *Otoites compressus* WESTERMANN, 1954, Cad 122, III/1; *Pelekodites spatians* (BUCKMAN, 1928), Har 330, III/1;

Fig. 4: *Otoites* sp., Cad 107, III/1;

Fig. 5: *Lokuticeras* cf. *rossbrunnense* GALÁCZ, 1994, Cad 104, III/1; *Masckeites densus* Buckman, 1920, Cad 109, III/1;

Fig. 7: *Stephanoceras plicatum* (QUENSTEDT, 1858), Am 102, III/1; *Itinsaites latansatus* (BUCKMAN, 1920), Cad 111, III/1.

All figures natural size, asterisk indicates end of phragmocone.

.

Plate 4

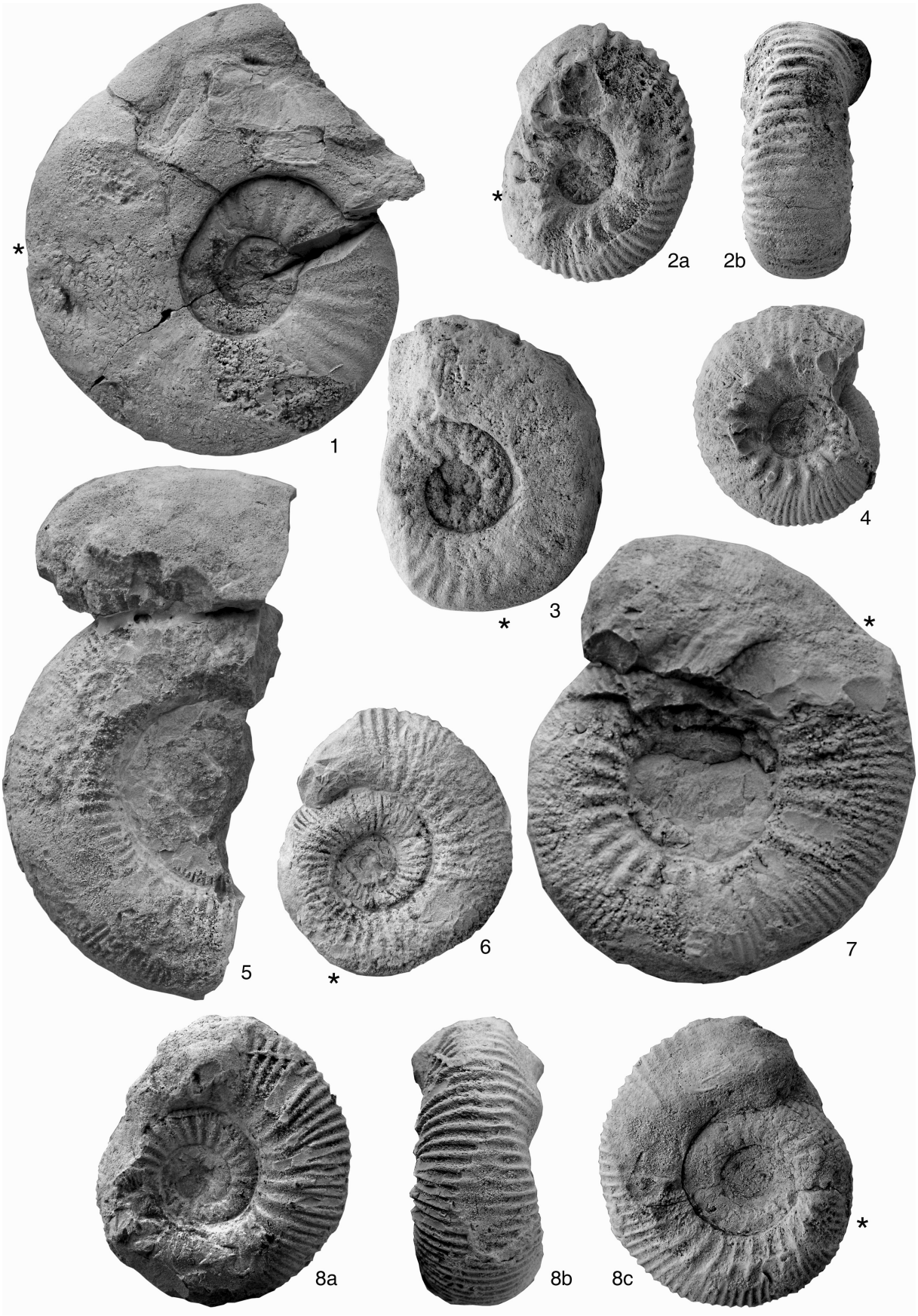

Hantkeniana 8, 25—35, Budapest, 2013

Rare myodocopid ostracods from the Lower Cretaceous (Albian) strata of Vértes Foreland (NW-Hungary)

Tünde CSÉFÁN[1] & Emőke Tóth[1]

(with 6 figures and 1 plate)

Occurrences of myodocopid ostracods in fossil record particularly in Mesozoic sequences are very scarce because of preservation potential of their carapaces, despite that Recent forms occur worldwide in various water depths of marine environments as benthic, nektobenthic or planktonic organisms. Two myodocopid ostracod genera ("*Conchoecia"* and *Polycope*) belonging to two families Halocyprididae and Polycopidae were identified from the studied Lower to Middle Albian successions of the boreholes Agt-2 and Vst-8. These occurrences from Vértes Foreland of Hungary are one of the earliest representatives of halocyprid ostracods. These data completed the palaeobiogeographical distribution of the described genera during the Albian in the Tethys Ocean. The previous paleoenvironmental reconstructions based on planktonic and benthic foraminifera faunas in the studied boreholes confirmed the same ecological requirement of Cretaceous halocyprid forms as that of their living relatives. The depositional environment of Vértessomló Siltstone is shallow bathyal semi-enclosed basin with high organic matter input and dysoxic conditions allowing the preservation of these rare forms.

Introduction

Myodocopid ostracods are very poor in fossil record because of the preservation potential of their weakly calcified carapaces. Recent forms occur worldwide in various water depths of marine pelagic environments as benthic, nektobenthic or planktonic organisms. The modern myodocopid ostracods may have originated from late Palaeozoic forms belonging to the "Superfamily nov. A" via the cypridinacean lineage (Permian to Recent) (BECKER 2003; VANNIER & ABE 1992). Mesozoic record is sporadic compared to the knowledge about Palaeozoic ancestors. Mesozoic myodocopids can be classified into modern superfamilies such as Cyprinidoidea, Thaumatocypridoidea, Polycopoidea and Halocypridoidea. The main aim of the present work is to give a detailed systematic description of myodocopid ostracods from Albian successions of boreholes Agt-2 and Vst-8 in the Vértes Foreland. Documentation, palaeobiogegraphical and palaeoecological interpretations of these forms can provide new data about halocyprid and polycopid lineage of Myodocopida and about the palaeoenvironmental conditions in this region of Tethys during the Early and Middle Albian.

Geological settings

The studied boreholes (Vst-8 and Agt-2) are located in the Vértes Foreland, in the eastern zone of the Transdanubian Central Range, north-western Hungary (Fig 1). The studied strata belong to the Vértessomló Siltstone Formation deposited in the mid-Cretaceous sedimentary cycle, in a shallow bathyal basin environment with low oxygen levels and normal salinity. It interfingers with the Környe Limestone Formation (a platform carbonate, urgon facies) which is a heteropic facies of the Vértessomló Siltstone (GÖRÖG 1993; CSÁSZÁR 2002; SZINGER 2008).

In the borehole Vst-8 the Környe Limestone, an allodapic limestone bed is intercalated in the Vértessomló Siltstone which is transported with a turbidity current from the platform margin into the basin. Beneath the Környe Mészkő bed the strata are rich in glauconitic grains which are derived from nearshore environment (CSÁSZÁR 2002).

[1] Eötvös University, Department of Palaeontology, H-1117 Budapest, Pázmány Péter sétány 1/C, Hungary. E-mail: cs.tunde88@gmail.com & tothemoke.pal@gmail.com

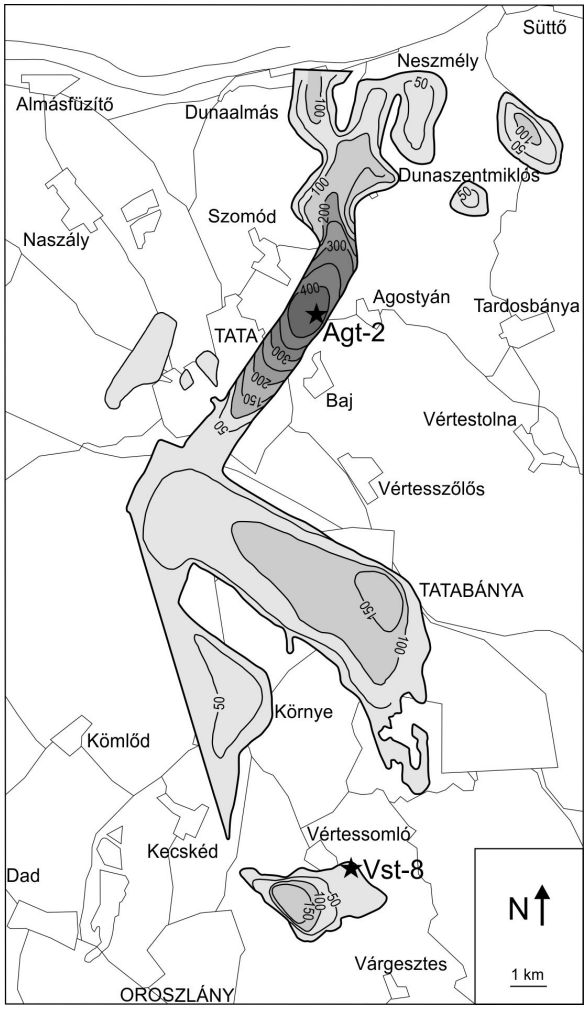

Fig. 1. Geographical locations of the boreholes Vst-8 and Agt-2 and recent extent and thickness distribution of the Vértessomló Siltstone Formation (modified after CSÁSZÁR, 2002)

The Vértessomló Siltstone is underlain by the Tata Limestone which is reappeared above the siltstone caused by reverse fault movement. The lithology of the studied succession is varied because it gradually develops from the Tata Limestone Formation as limestone and marly limestone. The upper part of the Vértessomló Siltstone consists of silty marls (CSÁSZÁR 2002, 1991).

In the borehole Agt-2 the Vértessomló Siltstone is unconformably overlain by Pannonian strata and underlain by Jurassic strata. The succession reaches the maximum thickness (410 m) in this borehole (JÁMBOR et al. 1973).

The upper part of the section – which produced the studied ostracod fauna – consists of silty marls, argillaceous marls and a thin layer of limestone breccia and marly limestone. The lower part bears sandstone and breccia layers, alternating with argillaceous marls and glauconitic sandstone (JÁMBOR et al. 1973; CSÁSZÁR 2002) (Fig. 2.).

The age of the investigated formation according to various biostratigraphical studies is Early to Middle Albian. The planktonic foraminifera and ammonite data indicate Early Albian age, but orbitolinids from the upper part of the section indicate that the deposition continued in the Middle Albian too (FÜLÖP 1975; GÖRÖG 1993; CSÁSZÁR 1998). The borehole Vst-8 penetrated only the Lower Albian strata of Vértessomló Siltstone based on large foraminiferal studies (GÖRÖG 1996). The studied succession in the borehole Agt-2 represent Lower to Middle Albian age according to planktonic foraminiferal studies. Three planktonic foraminiferal zones can be distinguished: *Ticinella bejauensis – Hedbergella gorbachikae* Interval Zone (338 to 421 m, lowermost Albian), *Hedbergella planispira – Hedbergella retroflexa* Interval Zone (162 to 338 m, upper Lower Albian), *Ticinella primula* Interval Zone (20 to 162 m, lower Middle Albian) (BODROGI 1992).

In the borehole Vst-8, SZINGER (2008) divided the studied series into three parts based on the changes of foraminiferal fauna and microfacies. In the lower part of the succession (153 to 135 m) the assemblage indicated a slightly dysoxic, open marine environment. The middle strata (135 to 112 m) which are rich in planktonic foraminifera could be deposited in an offshore, low oxygenated and nutrient poor environment. In the upper part (112 to 100 m) the depositional environment was poor in oxygen and rich in nutrients.

Material and methods

The studied Albian sections produced valuable planktonic ostracod material with 62 specimens of the borehole Vst-8 (interval 104 m to 168 m) and significantly fewer specimens (n=9) from the borehole Agt-2 (interval 235 m to 363 m). All pelagic forms are restricted to the Lower Albian part of the section. About 200 g of the air-dried silty sediments has been soaked in a dilute solution of hydrogen peroxide. From hard limestones the microfauna was extracted by using pure acetic acid. The planktonic ostracods mainly came from the silty marl layers which may be the result of preservation potential. The preservation of studied specimens is good in most cases and there are strongly compressed carapaces in the studied material. Ostracods were separated under stereomicroscope. For the taxonomic work photos were made by scanning electron microscope. The samples are housed in the Department of Palaeontology, Eötvös Loránd University, Budapest.

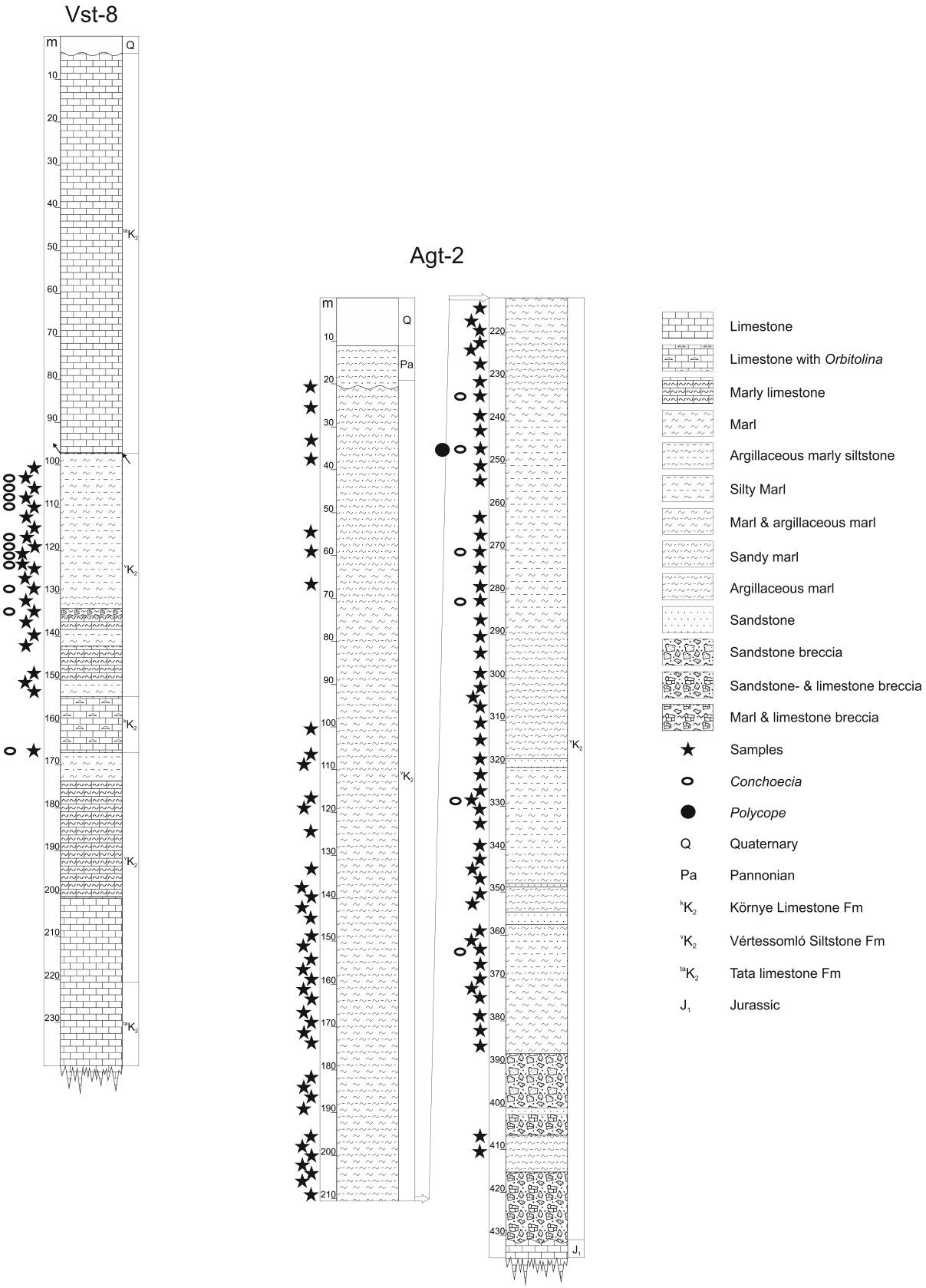

Fig. 2. Litostratigraphical sections of the boreholes Vst-8 and Agt-2

Previous studies about Cretaceous halocyprid and polycopid ostracods

First fossil halocyprid ostracod was described by POKORNÝ (1964), from the Coniacian strata from the former Czechoslovakia as *Conchoecia cretacea*. Previously the *Conchoecia* genus was known only from recent material. Later other scientists also found specimens assumed belonging to this genus in Cretaceous sequences (e.g., COLIN & ANDREU 1990), however they have an uncertain taxonomic place due to the hiatus in the fossil record and slight differences in morphological characters of the carapaces such as the lack of rostrum and rostral incisure (genus aff. "*Conchoecia*"). Moreover, the taxonomy of Recent ostracods mainly based on the number and features of their limbs and other unfossilized characteristics of the soft body which possess difficulties in classification of fossil taxa.

The described Cretaceous specimens occurred mainly in Albian to Cenomanian fine-grained sediments in Atlantic as well as in Tethyan realm. For example, they were extracted from argillaceous marls and marls from the Joux Valley in Switzerland and from Israel (CHAROLLAIS et al. 1977; ROSENFELD & RAAB 1984), from calcareous shales and mudstones in England (KAYE 1965), from organic-rich calcareous shales, mudstones, siltstones of Potiguar and Sergipe basins in Brazil (VIVIERS et al. 2000). Further occurrences of genera *Conchoecia* and aff. "*Conchoecia*" in Cretaceous sequences summarized in Fig. 3.

Although the first representatives of undoubtedly polycopid ostracods have already been described from Carboniferous strata (e.g., NEALE 1983; KORNICKER & SOHN 2000), the fossil record is very poor in Mesozoic as well as in Cenozoic era (NEALE 1983). This phenomenon is also characteristic of Cretaceous faunas. The representatives of the genus *Polycope* have been described only from Berriasian to Albian fine grained sediments such as calcareous clays from southeastern Czech Republic (POKORNÝ 1973), gray shales from Algoa Basin in South Africa (BRENNER & OERTLI 1976), marls from Bauges and Chartreuse Mountains in France and North Tunisia (DONZE 1964, 1971; DONZE et al. 1975) and gray marls from Israel (ROSENFELD & RAAB 1984). Moreover Cenomanian to Maastrichtian soft, unstratified, pale grayish-white chalk sediments also produced specimens of *Polycope* genus: from Rügen Island in North Germany (HERRIG 1963, 1964, 1994; HERRIG et al. 1997), from Wrotham in England (KAYE 1965) and from southeastern England (WEAVER 1982) (Fig. 4.). Detailed stratigraphic distributions are shown in Fig. 5.

The genus *Polycopsis* is less common than *Polycope* and published only from Maastrichtian chalk sediments (Rügen Island in North Germany (HERRIG 1963, 1966) and Mont Aimé in France (MARGERIE 1967)).

The detailed discussion about Cretaceous halocyprid ostracods (genera *Conchoecia* and aff. "*Conchoecia*") is published by COLIN & ANDREU (1990) and about polycopid ostracods by NEALE (1983).

Systematic descriptions

Classification of the ostracods follows that of HARTMANN & PURI (1974) and MARTIN & DAVIS (2001). The specimens are deposited in the Department of Palaeontology of Eötvös University. Abbreviations: L=length and H=height.

Subclass Ostracoda LATREILLE, 1806
Order Myodocopida SARS, 1866
Suborder Halocypriformes SKOGSBERG, 1920
Superfamily Halocypridoidea DANA, 1853
Family Halocyprididae DANA, 1852
Genus *Conchoecia* Dana, 1849
„*Conchoecia*" sp.
Pl. 1, figs 1-3, 5-7.

1965. ?*Conchoecia* sp. B; KAYE p. 230-231, pl. 1, figs 1-2; pl. 2, figs 2,7.
1977. *Conchoecia*? sp.; OERTLI (in CHAROLLAIS et al.), pl. 1, fig. 8.
1979. '*Conchoecia*' GA D 31; GROSDIDIER (in COLIN & ANDREU 1990), pl. 1, fig. 5.
1984. Genus aff. „*Conchoecia*" sp. 215; ROSENFELD & RAAB, p. 113, pl. 7, figs 8-9.
1984. Genus aff. „*Conchoecia*" sp. 150; ROSENFELD & RAAB, p. 113, pl. 7, fig. 10.
1992. *Conchoecia* sp.; ANDREU, pl. 1, fig.1.
1995. *Conchoecia*(?) sp.; DAMOTTE, p. 577, pl. 3, figs 11-12.
2000. *Conchoecia*? sp.; VIVIERS et al., pl. 24, figs 9-17.

Material. Borehole Vst-8: 104 m: 1 carapace, 106 m: 1 carapaces, 108 m: 2 carapaces, 110 m: 7 carapaces, 117 m: 3 carapaces, 119 m: 38 carapaces, 121 m: 5 carapaces, 123 m: 1 carapace, 129 m: 2 carapaces, 135 m: 1 carapace, 168 m: 1 carapace. Borehole Agt-2: 235 m: 1 carapace, 247 m: 1 carapace, 271 m: 1 carapace, 279 m: 3 carapaces, 283 m: 1 carapace, 329 m: 1 carapace, 363 m: 1 carapace.

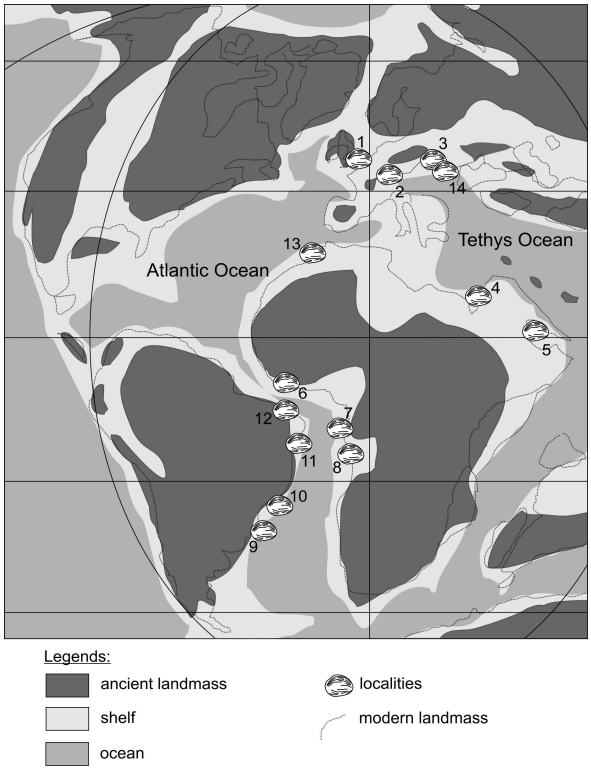

Fig. 3. Palaeogeographic map of Early Cretaceous *Conchoecia* (modified after Atlantic Geoscience Society & Geological Survey of Canada)**1**: ?*Conchoecia* sp. A & B Wrotham, England (KAYE 1965); **2**: *Conchoecia*? sp. Switzerland, Joux Valley in the Vaudois Jura (CHAROLLAIS et al. 1977); **3**: *Conchoecia cretacea* POKORNÝ 1964, Czech Republic (COLIN & ANDREU 1990); **4**: Genus aff. „*Conchoecia*" sp. 215 & 150 Israel (ROSENFELD & RAAB 1984); **5**: '*Conchoecia*' IR O 27 Persian Gulf, Iran (COLIN & ANDREU 1990); **6**: Ivory Coast (COLIN & ANDREU 1990) unpublished; **7**: '*Conchoecia*' GA D 31 & GA E 1 Gabon (COLIN & ANDREU 1990); **8**: Congo (COLIN & ANDREU 1990) unpublished; **9, 10**: Santos and Campos basins (COLIN & ANDREU 1990); **11, 12**: *Conchoecia*? sp. Potiguar and Sergipe basins, NE Brazil (COLIN & ANDREU 1990, VIVIERS et al. 2000); **13**: *Conchoecia* sp. Agadir-Nador, Morocco (ANDREU 1992).

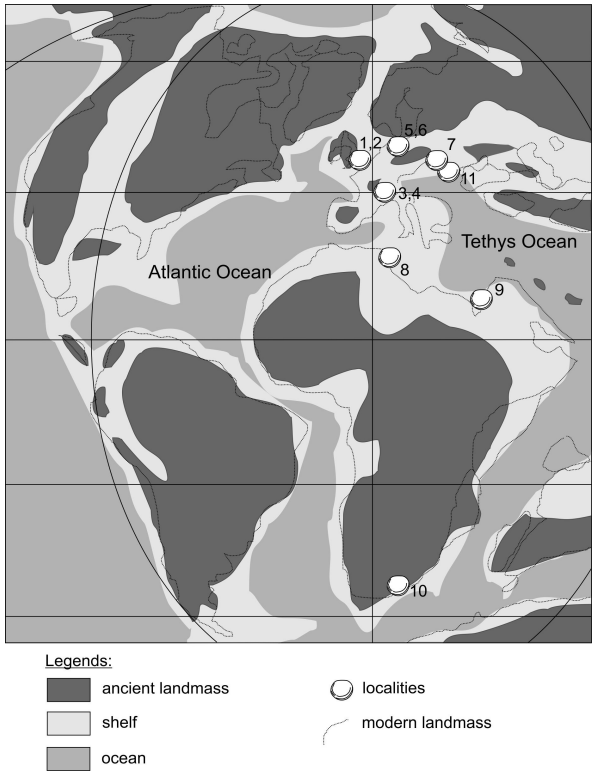

Fig. 4. Palaeogeographic map of Cretaceous *Polycope* (modified after Atlantic Geoscience Society & Geological Survey of Canada)- **1**: *Polycope nuda* KAYE, 1965 *P. oweni* KAYE, 1965 Wrotham, England (KAYE 1965); **2**: *P. bluebellensis* WEAVER, 1982, *P. delicate* WEAVER, 1982, *P. nuda* KAYE, 1965, *P. oweni* Kaye, 1965 SE England (WEAVER, 1982); **3**: *Polycope* sp. Bauges and Chartreuse Mountains, France (DONZE 1964); **4**: *Polycope* sp. SE France (DONZE,1971); **5**: *P. avicularia* HERRIG et al., 1997 *P. bonnemai* HERRIG, 1963, *P. luxuriosa* HERRIG, 1964 Rügen Island, N Germany (HERRIG 1963, 1964, HERRIG et al. 1997); **6**: *P. bonnemai* HERRIG 1963, *P. dorsispinata* HERRIG 1994, *P. krauseae* HERRIG 1994, *P. luxuriosa* HERRIG 1964, *P. nuda* KAYE 1965, *P. proboscidea* HERRIG, 1994, near Malchow, NE Germany (HERRIG 1994); **7**: *Polycope* sp. South-eastern part of Czech Republic (POKORNÝ 1973); **8**: *Polycope* sp. N Tunisia (DONZE et al 1975); **9**: *Polycope* spp., Israel (ROSENFELD & RAAB 1984); **10**: *Polycope* sp. Algoa Basin, S Africa (BRENNER & OERTLI 1976); **11**: *Polycope* sp. Hungary.

Dimensions: L: 0.43-1.30 mm
H: 0.22-1.05 mm
L/H: 1.1-1.9

Description. Form #1 (figs 6-7.): Carapace rounded. Anterior margin straight to convex; dorsal margin strongly arched; posterior margin slightly pointed; ventral margin convex. Valves ornamented by narrow longitudinal ribs, slightly arched by following the shape of the outline. Internal features not observed. Eye spot absent.

Form #2 (fig. 2.): Carapace suboval, elongated. Anterior margin concave; dorsal margin convex; posterior margin pointed, below 2/3 height; ventral margin convex. Valves ornamented by narrow longitudinal ribs, slightly arched by following the shape of the outline, but more pronounced than Form #1. Internal features not observed. Eye spot absent.

Form #3 (figs 1, 3, 5.): Carapace subcircular. Anterior, dorsal and ventral margins convex; posterior margin slightly pointed. Ornamentation of the valve surface is longitudinal ribs similarly to the Form #2. Most of these specimens are flat and deformed. Internal features not observed. Eye spot absent.

Remarks. The classification in genus level is

questionable because of the lack of the rostrum and rostral incisure. The specimens can be split into three different groups based on their shapes and their sizes. Form #1 is mainly distributed in the group 0.5-0.7 mm, but two specimens are smaller than 0.5 mm. Forms #2 and #3 are larger than 0.7 mm.

Occurences and stratigraphic ranges. Czech Republic: Coniacian (POKORNÝ 1964) Wrotham, Kent, England: Upper Albian (KAYE 1965), Switzerland, Joux Valley in the Vaudois Jura: Middle Albian (CHAROLLAIS et al. 1977), Israel, Coastal Plain: Albian, Albian to Lower Cenomanian (ROSENFELD & RAAB 1984), Agadir-Nador, Morocco: Upper Albian (ANDREU 1992), Iran: Albian (GROSDIDIER 1973); Gabon: Lower Albian (GROSDIDIER 1979); Mid-Pacific Mountains: Albian (DAMOTTE 1995), Florianopolis and Santos basins, Brazil: Lower to Middle Albian (KOUTSOUKOS & DIAS-BRITO 1987); Potiguar and Sergipe basins, northeastern Brazil: Albian (VIVIERS et al. 2000).

Suborder Cladocopa SARS, 1866
Superfamily Polycopoidea SARS, 1865
Family Polycopidae SARS, 1866
Genus *Polycope* Sars, 1866

Polycope sp.
Pl. 1, Fig. 4.

Material. Borehole Agt-2: 247 m: 1 specimen.
Dimensions: L: 0.40 mm
H: 0.37 mm
L/H: 1.1

Description. . Carapace subcircular. Dorsal margin straight to convex; anterior, posterior and ventral margins rounded. Along the margin strongly depressed. Valve weakly reticulated with small tubercles, ornamentation confined to the margins. Internal features not observed. Eye spot absent.

Remarks. The described specimen is similar in its ornamentation to the *Polycope* sp. described by ROSENFELD & RAAB (1984, Pl. 1, fig. 1.) but their shape is very different.

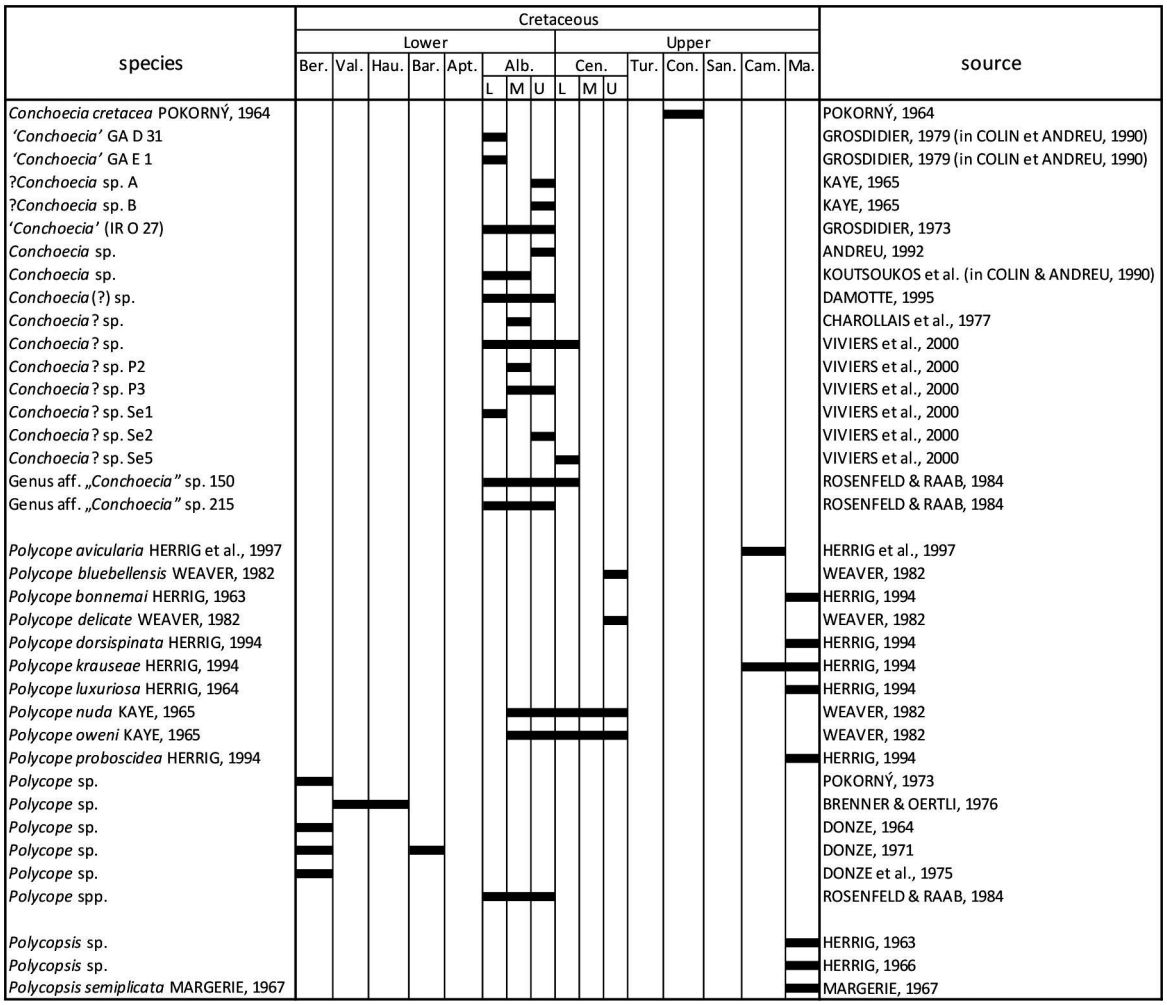

Fig. 5. Stratigraphical distribution of Cretaceous halocyprid and polycopid ostracods Ber.: Berriasian, Val.: Valanginian, Hau.: Hauterivian, Apt.: Aptian, Alb.: Albian, Cen.: Cenomanian, Tur.: Turonian, Con.: Coniacian, San.: Santonian, Cam.: Campanian, Ma.: Maastrichtian

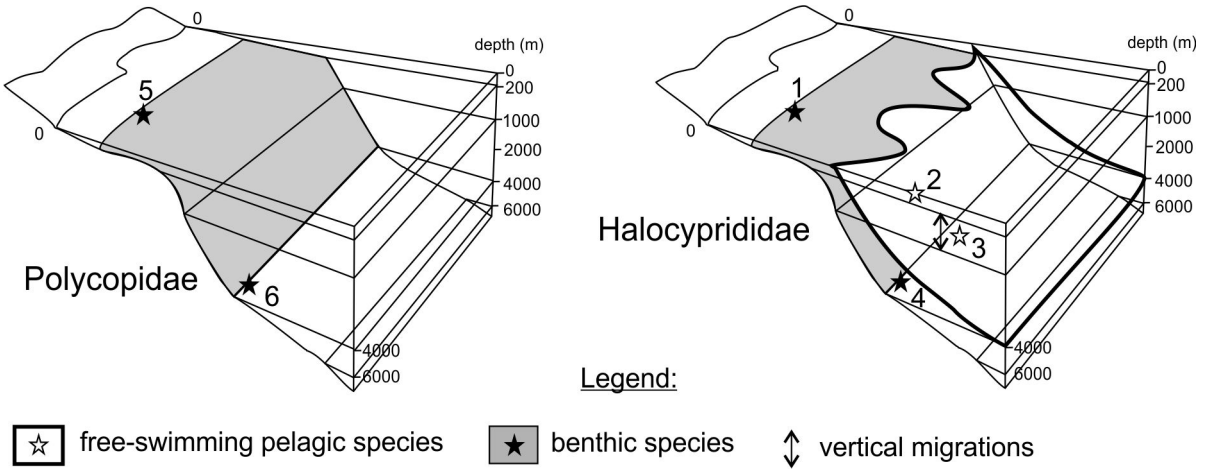

Fig. 6. Depth range of recent podocopid and halocyprid ostracods (modified after VANNIER & ABE, 1992). **1**: non spinous *Bathyconchoecia* (130 to 3165 m); **2**: neustonic halocyprids (= the surface 10 cm of the water column); **3**: planktonic halocyprids; **4**: *Bathyconchoecia septemspinosa* (271 to 3600 m); **5**: *Polycope japonica* (0 to 0.3 m); **6**: *Polycope ovalis* (335 to 3105 m).

Discussion

Myodocopid ostracods have a very rare occurrence compared to the other podocopid and platycopid ostracods in Cretaceous sequences due to their poor preservation potential. In most cases they occur in fine-grained sediments such as organic-rich clays, siltstones and marls of Lower Cretaceous sequences and Upper Cretaceous chalk sediments. The halocyprid forms mostly derived from Albian to Cenomanian organic-rich sediments (Fig. 5). They have fragile, weakly calcified carapaces which mainly consist of organic matter, so their preservation requires low oxygenated bottom water conditions. These conditions often result in pyrite-filled moulds of the carapace. The partly organic carapace is capable of plastic deformation which results strongly depressed and compressed carapaces. These phenomena can be very well recognized on the studied specimens from Vértessomló Siltstone Formation, also.

However the carapace of *Polycope* genus is more calcified than halocyprid ostracods, their occurrence in Cretaceous sediments is very similar as that of the genera *Conchoecia* and aff. „*Conchoecia*".

Palaeogeographical distribution of the above mentioned halocyprid ostracod seems to be worldwide during the Albian to Cenomanian, but they mainly occur in the Tethyan and Atlantic regions which can be explained by the human factor (Fig. 3). A single record was published from Albian sequences of Mid-Pacific Mountains (DAMOTTE 1995). The cause of the widespread occurrence of the genera *Conchoecia* and aff. „*Conchoecia*" during the Albian to Cenomanian is their lifestyle. Probably in the Late Cretaceous the situation is similar, but the fossil record is more incomplete. During the Cretaceous spatial distribution of *Polycope* genus is more restricted compared to the *Conchoecia* and aff. „*Conchoecia*" and moreover the specimens from different localities belong to different species in most cases. More than 10 species were described (Fig. 4). In contrast of this fact the *Conchoecia* genus subdivided only maximum two species. These phenomena can be explained by the different mode of life between the two taxa. The lifestyle of Recent *Polycope* is benthic and capable of swimming only short distances limiting wide distribution. Moreover benthic or nektobenthic myodocopid forms biogeographic regions can be recognized based on recent studies (KORNICKER 1975). The palaeoecological value of the genus is low in palaeoenvironmental reconstruction because its habitat range is very wide. Recently they live in water depth from 0 to 3000 m.

The *Conchoecia* is a free-swimming pelagic ostracod whom vertical migration depends on nutrient supply. Recent forms live in 0 m (neuston) to 3900 m (surface water to abyssopelagic region), with a maximum abundance of 200 to 400 m and with a maximum diversity of 1000 to 1500 m in the water column (VANNIER & ABE 1992). Planktonic mode of life of Cretaceous *Conchoecia* is confirmed by the wide distribution (Atlantic, Pacific and Tethyan realm) (Fig. 6). Presumably the Cretaceous representatives of the genus lived in an environment with similar conditions.

SZINGER (2008) and BODROGI (1992) estimated shallow bathyal water depth (180 to 350 m) with normal marine and dysoxic conditions as depositional environment of the Vértessomló Siltstone based on

the palaeoecological interpretation of the benthic and planktonic foraminifera faunas from the studied borehole Vst-8 and Agt-2. This interpretation well fits to the maximum abundance of the Recent planktonic halocyprids.

Conclusions

Two myodocopid ostracod genera were identified from the Lower Albian Vértessomló Siltstone Formation (of boreholes Vst-8 and Agt-2), namely „*Conchoecia*" and *Polycope*. The *Polycope* genus is presented by only one well-preserved carapace and halocyprid forms by numerous strongly deformed carapaces. ítheir ratios compared to the podocopids and platycopids are low in the studied samples. The specimens from the genus „*Conchoecia*" can be divided into three forms based on size and shapes but their taxonomic value is questionable. During the Albian to Cenomanian the worldwide distribution of halocyprid form can be explained by their free-swimming pelagic lifestyle based on recent analogies. Recent forms live with a maximum abundance in 200 to 400 m in water column. The described Albian specimens from Vértessomló Siltstone may live at similar water depth. This interpretation is supported by the previous benthic and planktonic foraminiferal results suggesting 180 to 350 m water depth as the depositional environment of the studied strata.

Acknowledgements

The authors are grateful to Miklós MONOSTORI, Ágnes GÖRÖG and András GALÁCZ (Eötvös Univ. Budapest) for providing the material and helpful discussions during the preparation of this paper. The authors thank Zsolt BENDŐ for the technical assistance during the SEM photography. This work was supported by the Hantken Foundation.

References

ANDREU, B. 1992. Associations d'ostracodes et paléoécologie du Crétacé (Barrémien à Turonien) le long d'une transversale Agadir-Nador (Maroc). *Palaeogeography, Palaeoclimatology, Palaeoecology* 99:291-319.

BECKER, G. 2003. A new "cypridinid"-like ostracod (Myodocopida) from the Lower Frasnian of Bergisch Gladbach (Upper Devonian; Rheinisches Schiefergebirge). *N. Jb. Geol. Paläont. Abh.* 227 (2):233-258.

BODROGI, I. 1992. Az Agostyán, Agt. 2. jelű alapfúrás mikrofaunája felülvizsgálatáról, biozonációjáról és ökológiai viszonyairól. Unpublished report of the Geological Institute of Hungary, data warehouse of Geophisics and Mining.

BRENNER, & OERTLI, H. J. 1976. Lower Cretaceous ostracodes (Valanginian to Hauterivian) from the Sundays River Formation, Algoa Basin, South Africa. *Bull. Centre Rech. Pau – SNPA 10* 2:471-533.

CHAROLLAIS, J., et al. 1977. Découverte de microfaunes de l'Albien Moyen et supérieur dans la vallée de Joux (Jura vaudois, Suisse). *Géobios* 10 (5):683-695.

COLIN, J.-P., & ANDREU, B. 1990. Cretaceous halocyprid Ostracoda. In *Ostracoda and Global Events*: 515-526., edited by R. Whatley and C. Maybury. Cambridge: Chapman and Hall.

CSÁSZÁR, G. 1991. Vértessomló Vst-8. Unpublished report of the Geological Institute of Hungary, data warehouse of Geophisics and Mining.

CSÁSZÁR, G. 2002. Urgon formations in Hungary. *Geologica Hungarica Series Geologica* 25:209.

CSÁSZÁR, G., ed. 1998. *Dunántúli-középhegység alsó- és középső-kréta képződményeinek rétegtana*: 46-56., Edited by I. Bérczi and Á. Jámbor, *Magyarország geológiai képződményeinek rétegtana*. Budapest: publication of MOL Rt. and MÁFI.

DAMOTTE, R. 1995. 35. data report: Cretaceous ostracodes from holes 865A and 866A (Mid-Pacific Mountains). In *Proceedings of the Ocean Drilling Program, Scientific Results 143*: 575-580., edited by E. L. WINTERER, et al.

DONZE , P. 1964. Ostracodes berriasiens des Massifs Subalpins Septentrionaux (Bauges et Chartreuse). *Trav. Lab. Geol. Fac. Sc. Lyon. N. S.* 11:103-158.

DONZE , P. 1971. Rapports entre les faciès et la répartition générique des ostracodes dans quatre gisements-types deux à deux synchroniques du Berriasien et du Barrémien du Sud-Est de la France. In *Paléoécologie des Ostracodes*: 651-661., edited by H. J. Oertli: *Bulletin du Centre de Recherches Pau-SNPA*.

DONZE , P., LE HEGARAT, G., & MEMMI, L. 1975. Les formations de la limite Jurassique-Crétacé en Tunisie septentrionale (Djebel Oust). Série lithologique; résultats biostratigraphiques et paléogéographiques d'après les Ammonites, les Calpionelles et les Ostracodes. *Géobios* 8 (2):147-151.

FÜLÖP, J. 1975. Tatai mezozoós alaphegységrögök. *Geologica Hungarica Series Geologica* 16:225.

GÖRÖG, Á. 1993. Orbitolina -félék (nagyforaminiferák) megjelenése magyarországi alsó- és középső- kréta képződményekben. *Őslénytani viták, Budapest* 39:51-72.

GÖRÖG, Á. 1996. Magyarországi kréta Orbitolina-félék vizsgálata, sztratigráfiai és ökológiai értékelése. Unpublished PhD Thesis.

GROSDIDIER, E. 1973. Associations d'ostracodes du Crétacé d'Iran. *Rev. Inst. fr. Pétrole, Paris* 28 (2):131-168.

GROSDIDIER, E. 1979. Principaux ostracodes marins de l'intervalle Aptien-Turonien du Gabon (Afrique occidentale). *Bull. Centres Rech. Explor.-Prod., Elf-Aquitaine, Pau* 3 (1):1-35.

HARTMANN, G., & PURI, H. S. 1974. Summary Of Neontological And Paleontological Classification Of Ostracoda. *Mitt. Hamburg. Zool. Mus. Inst.* 70:7-73.

HERRIG, E. 1963. Neue Ostracoden-Arten aus der Weißen Schreibkreide der Insel Rügen (Unter-Maastricht). *Wissenschaftliche Zeitschrift der Ernst-Moritz-Arndt-Universität Greifswald, Math.-nat. Reihe* 12 (3/4):289-325.

HERRIG, E. 1964. Polycope luxuriosa. In *Catalogue of Ostracoda, supplement, no. 10 (1969)*, edited by Ellis and Messina.

HERRIG, E. 1966. Ostracoden aus der Weißen Schreibkreide (Unter-Maastricht) der lnsel Rügen. . *Palaontologische Abhandlungen (A:Palaozoologie)* 2 (4):693-1024.

HERRIG, E. 1994. Polycopidae (Crustacea, Ostracoda) aus der borealen Oberkreide des mittleren und südlichen Ostseeraumes. *Paläont. Z.* 68 (3/4):351-359.

HERRIG, E., FRENZEL, P., & REICH, M. 1997. Zur Mikrofauna einer Ober-Campan-Scholle von der Halbinsel Wittow (NW Rügen/Ostsee). *Freiberger Forschungsheft* 468:129-169.

JÁMBOR, Á., HERNÁDY, L., & CSÁSZÁR, G. 1973. Az Agt-2 sz. fúrás földtani adatai. Unpublished report of the Geological Institute of Hungary, data warehouse of Geophisics and Mining.

KAYE, P. 1965. Some new British Albian Ostracoda. *Bull. Br. Mus. Nat. Hist. (Geol.) London* 11:215-254.

KORNICKER, L. S. 1975. Antarctic Ostracoda (Myodocopina) Part 1. *Smithsonian Contributions to Zoology* 163:1-368.

KORNICKER, L. S., & SOHN, I. G. 2000. Myodocopid Ostracoda from the Late Permian of Greece and a Basic Classification for Paleozoic and Mesozoic Myodocopida. *Smithsonian Contributions to Paleobiology* 91 (1-33).

KOUTSOUKOS, E. M. & DIAS-BRITO, D. 1987. Paleobatimetria da margem continental do Brasil durante o Albiano. Revista Brasileira de Geociências 17 (2):86-91.

MARGERIE, P. 1967. Inventaire des ostracodes conservés dans les couches inférieures des formations post-campaniennes du Mont-Aimé (Marne) France. *Mémoires de la Société d'Agriculture, Commerce, Sciences et Arts du Département de la Marne* 82:7-29.

MARTIN, J. W., & DAVIS, G. E. 2001. An Updated Classification of the Recent Crustacea. *Natural History Museum of Los Angeles County, Science Series* 39:1-124.

NEALE, J. W. 1983. Geological history of the Cladocopina. In *Applications of ostracoda*: 612-626., edited by R. F. Maddocks. Houston: Univ. Houston Geosc.

POKORNÝ, V. 1964. *Conchoecia* ? *cretacea* n. sp., first fossil species of the family Halocyprididae (Ostracoda, Crustacea). *Acta Univ. Carol., Geol., Praha* (2):176-179.

POKORNÝ, V. 1973. The Ostracoda of the Klentnice Formation (Tithonian?) Czechoslovakia. *Vydal Ústřední ústav geologický, Praha*:5-107.

ROSENFELD, A., & RAAB, M. 1984. Lower Cretaceous Ostracodes from Israel and Sinai. *Israel Journal of Earth Sciences* 33 (3):85-134.

SZINGER, B. 2008. Albian Foraminifera from Vértessomló Vst-8 borehole, Vértes Mountains (Hungary). *Geologica Pannonica* 36:153-185.

VANNIER, J., & ABE, K. 1992. Recent and early palaeozoic myodocope ostracodes: functional morphology, phylogeny, distribution and lifestyles. *Palaeontology* 35 (3):485-517.

VIVIERS, M. C., et al. 2000. Stratigraphy and biogeographic affinities of the late Aptian–Campanian ostracods of the Potiguar and Sergipe basins in northeastern Brazil. *Cretaceous Research* 21:407-455.

WEAVER, P. P. E. 1982. Ostracoda from the British Lower Chalk and Plenus Marls. *Monograph of the Palaeontographical Society* 135 (562):1-127.

Plate 1

Figs 1-3., 5-7. *Conchoecia* sp.

Fig. 1. borehole Vst-8, 119 m

Fig. 2. borehole Agt-2, 329 m

Fig. 3. borehole Vst-8, 110 m

Fig. 5. borehole Vst-8, 106 m

Fig. 6. borehole Vst-8, 108 m

Fig. 7. borehole Vst-8, 110 m

Fig. 4. *Polycope* sp. borehole Agt-2, 247 m

.

Plate 1

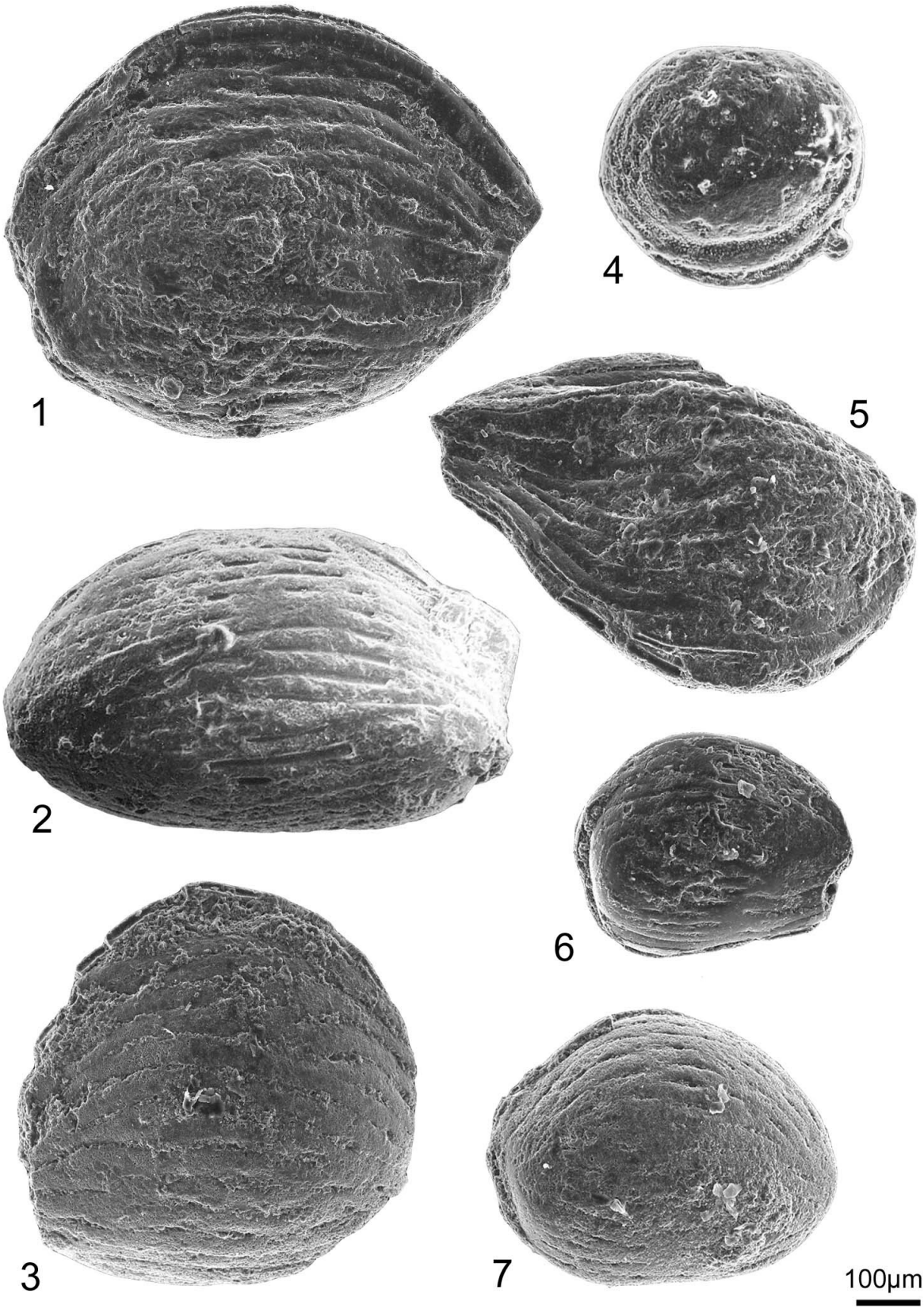

Hantkeniana 8, 37—149, Budapest, 2013

Neogene songbirds (Aves, Passeriformes) from Hungary

Eugen KESSLER[1]

(with 1 figure and 26 plates)

The author has studied and identified an exceptionally rich fossil songbird material (385 identified bones) from West Hungary (Polgárdi localities, Fejér County, Upper Miocene, MN 13) and from Southwest Hungary (Csarnóta and Beremend localities, Baranya County, Pliocene, MN 15-16). These are presented with rich figures (247) and with necessary biometrical data. All indentified taxa (98) represent a new species. These are following:

Alauda tivadari n. sp.; *Lullula minor* n. sp.; *Calandrella gali* n. sp.; *Hirundo gracilis* n. sp.; *Delichon polgardiensis* n. sp.; *Riparia minor* n. sp.; *Aegithalos gaspariki* n. sp.; *Sitta gracilis* n. sp.; *Tichodroma capeki* n. sp.; *Muscicapa miklosi* n. sp.; *Luscinia denesi* n. sp.; *Saxicola lambrechti* n. sp.; *Oenanthe kormosi* n. sp.; *Turdicus pannonicus* n. sp.; *Turdus miocaenicus* n. sp.; *Turdus polgardiensis* n. sp.; *Cettia janossyi* n. sp.; *Acrocephalus major* n. sp.; *Acrocephalus minor* n. sp.; *Hippolais veterior* n. sp.; *Sylvia intermedia* n. sp.; *Locustella kordosi* n. sp.; *Phylloscopus venczeli* n. sp.; *Anthus híri* n. sp.; *Motacilla intermedia* n. sp.; *Bombycilla brevia* n. sp.; *Troglodytes robustus* n. sp.; *Cinclus gaspariki* n. sp.; *Prunella freudenthali* n. sp.; *Lanius capeki* n. sp.; *Sturnus brevis* n. sp.; *Passer híri* n. sp.; *Carduelis kretzoii* n. sp.; *Carduelis lambrechti* n. sp.; *Pyrrhula gali* n. sp.; *Fringilla kormosi* n. sp.; *Emberiza pannonica* n. sp.; *Emberiza polgardiensis* n. sp.; *Plectrophenax veterior* n. sp. (from Polgárdi);

Galerida pannonica n. sp.; *Lullula parva* n. sp.; *Hirundo major* n. sp.; *Delichon pusillus* n. sp.; *Aegithalos congruis* n. sp.; *Parus robustus* n. sp.; *Parus parvulus* n. sp.; *Sitta pussila* n. sp.; *Certhia immensa* n. sp.; *Saxicola baranensis* n. sp.; *Saxicola parva* n. sp.; *Phoenicurus erikai* n. sp.; *Oenanthe pongraczi* n. sp.; *Turdus major* n. sp.; *Turdus medius* n. sp.; *Turdus minor* n. sp.; *Cettia kalmani* n. sp.; *Acrocephalus kretzoii* n. sp.; *Acrocephalus kordosi* n. sp.; *Sylvia pussila* n. sp.; *Locustella janossyi* n. sp.; *Phylloscopus pliocaenicus* n. sp.; *Anthus baranensis* n. sp.; *Cinclus minor* n. sp.; *Prunella kormosi* n. sp.; *Lanius hungaricus* n. sp.; *Passer minusculus* n. sp.; *Carduelis parvulus* n. sp.; *Carduelis medius* n. sp.; *Pyrrhula minor* n. sp.; *Fringilla petényii* n. sp.; *Loxia csarnotanus* n. sp.; *Pinicola kubinyii* n. sp.; *Emberiza media* n. sp.; *Emberiza parva* n. sp (from Csarnóta 2);

Melanocorypha minor n. sp.; *Galerida pannonica* n. sp. *Lullula parva* n. sp.; *Lullula minuscula* n. sp.; *Delichon major* n. sp.; n. sp.; *Parus robostus* n. sp.; *Parus medius* n. sp.; *Sitta villanyensis* n. sp.; *Muscicapa petényii* n. sp.; *Erithacus minor* n. sp.; *Luscinia pliocaenica* n. sp.; *Saxicola baranensis* n. sp.; *Saxicola magna* n. sp.; *Monticola pongraczi* n. sp.; *Phoenicurus baranensis* n. sp.; *Oenanthe pongraczi* n. sp.; *Turdus major* n. sp.; *Turdus medius* n. sp.; *Turdus minor* n. sp.; *Oriolus beremendensis* n. sp.; *Acrocephalus kretzoii* n. sp.; *Sylvia pussila* n. sp.; *Locustella magna* n. sp.; *Locustella janossyi* n. sp.; *Regulus pliocaenicus* n. sp.; *Motacilla minor* n. sp.; *Motacilla robusta* n. sp.; *Bombycilla kubinyii* n. sp.; *Prunella kormosi* n. sp.; *Lanius major* n. sp.; *Lanius intermedius* n. sp.; *Sturnus pliocaenicus* n. sp.; *Sturnus baranensis* n. sp.; *Passer pannonicus* n. sp.; *Coccothraustes major* n. sp.; *Loxia csarnotanus* n. sp.; *Emberiza gaspariki* n. sp. (from Beremend 26).

[1] Dr. Eugen Kessler, Ősz utca 14, 2310 Szigetszentmiklós, Hungary. E-mail: kessler_jeno@yahoo.com

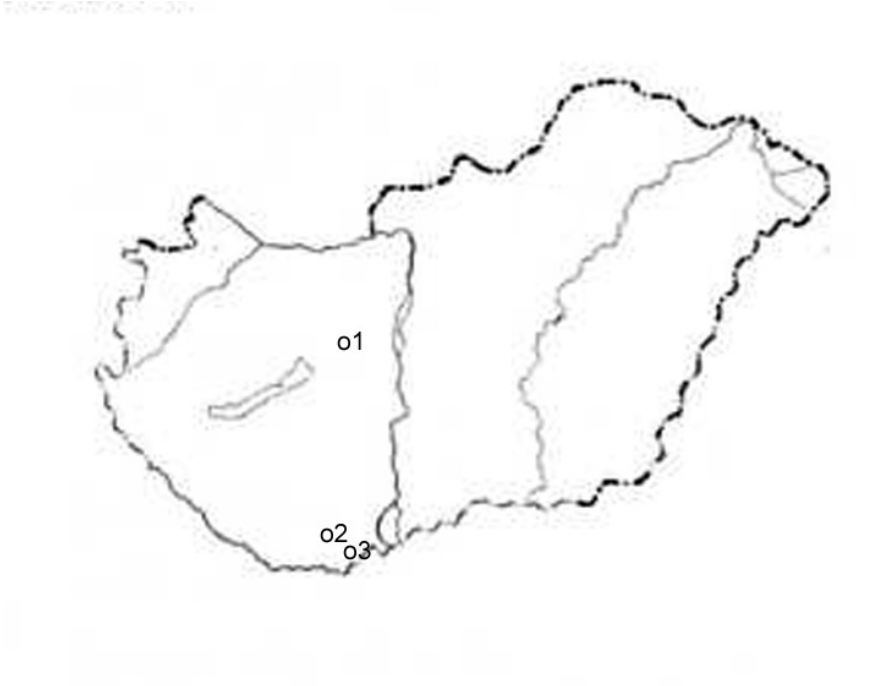

Fig. 1. Map with fossiliferous localities from Hungary. 1. Polgárdi; 2. Csarnóta; 3. Beremend.

Introduction

In this paper the author presents the remains of songbird fauna from Hungarian Neogene localities. First the paper presents the rich fossil bird material indicating the environmental conditions at the end of the sedimentation of the Pannonian Lake through the passerine bird fauna of Polgárdi in Fejér county in Hungary. In the continuation presents the environmental conditions 2 million years after the sedimentation of the Pannonian Lake through the passerine bird fauna of Csarnóta and Beremend in Baranya County in Hungary.

In the vicinity of the town Polgárdi the limestone quarries of Somlyó Hill and Kőszár Hill (226 m alt.) contained several karst fissures with vertebrate remains. Among them the Polgárdi 2, 4 and 5 localities furnished birds bones.

Polgárdi 2 had been quarried in two excavation campaigns in 1910 by Tivadar KORMOS. The bird remains were identified by Waclav ČAPEK and were published by Kálmán LAMBRECHT in 1912 and 1933 (LAMBRECHT 1912, 1933) as: *Mergus* sp.?; *Gallus* sp.?; cf. *Coturnix* sive *Perdix* sp., cf. *Lanius minor* and Aves indet. Miklós KRETZOI also announced this list in his paper, published in 1957 (KRETZOI 1957)

Polgárdi 4 was discovered in 1984-1985 (KORDOS 1991a). This locality yielded a rich mammal and bird assemblage. The mammal fauna was published by Mathias FREUDENTHAL and László KORDOS in 1989 (FREUDENTHAL & KORDOS 1989) and the bird fauna was identified and published by Dénes JÁNOSSY in 1991 (JÁNOSSY 1991)

Polgárdi 5 was discovered in the NE part of the quarry system in 1988 (KORDOS 1991a) and the bird fauna was published by Dénes JÁNOSSY in 1991 (JÁNOSSY 1991)

Previously JÁNOSSY reidentified from Locality 2 the carpometacarpus of *Gallus* sp.? as *Gallus aesculapi* GAUDRY, 1862 (JÁNOSSY 1976) and the complete carpometacarpusus of *Mergus* sp. ? as *Anas albae* JÁNOSSY, 1979 (JÁNOSSY 1979)

The list of the bird fauna from Polgárdi 4 and Polgárdi 5 (JÁNOSSY 1991, 1995) includes the following taxa: *Paleocryptonix hungaricus* JÁNOSSY, 1991; *Pavo aesculapi phasianoides* JÁNOSSY, 1991; *Porzana estramosi veterior* JÁNOSSY, 1991; *Rallicrex polgardiensis* JÁNOSSY, 1991; *Otis* aff. *khosiatzkyi* BOCHENSKI ET KUROCHKIN, 1987; *Capella* sp, ?*Cursorius* sp., *Tringa* sp, *Tyto campiterrae* JÁNOSSY, 1991; *Chaetura* aff. *baconica* JÁNOSSY, 1977; *Motacilla* sp., *Acrocephalus* sp. I. *(„arundinaceus"), Acrocephalus* sp .II., *Cettia* sp., *Sylvia* sp., *Turdus* sp. *(„iliacus"), Luscinia* sp., Fringillidarum gen et sp. indet., *Corvus* sp. (JÁNOSSY 1991, 1995**).**

From the unidentified material the author identified and published the following taxa in 2009 and 2010: *Egretta polgardiensis* KESSLER, 2009 (P4),

Anas. clypeata L. 1758; (P4, 5), Anatidae indet. (P4, 5), *Buteo* sp. (P4), *Falco* cf. *cherrug* GRAY, 1834 (P4), *Falco tinnunculus atavus* JÁNOSSY, 1972 (P5), *Palaeortyx gallica* MILNE-EDWARDS, 1869 (P4, 5), *P. brevipes* MILNE-EDWARDS 1869 (P4, 5), *Palaeortyx phasianoides* MILNE-EDWARDS, 1869 (from *Pavo aesculapi phasianoides*) (P4, 5), *Galliformes* indet. (P4, 5), *Porzana estramosi* JÁNOSSY, 1979 (P4, 5), *Porzana kretzoii* KESSLER, 2009 (P4), *Rallicrex polgardensis* KESSLER, 2009 (P4, 5), *Otis kalmani* JÁNOSSY, 1972 (P4), *Calidris janossyi* KESSLER, 2009 (P5), *Gallinago veterior* JÁNOSSY, 1979 (P4), *Charadrius lambrechti* KESSLER, 2009 (P4), *Limosa* sp. (P5), *Tringa* sp. (P4), *Tyto campiterrea* JÁNOSSY, 1991 (P4), *Athene noctua veta* JÁNOSSY, 1992 (P4), *Surnia robusta* JÁNOSSY, 1977 (P4, 5), *Cuculus pannonicus* KESSLER, 2010 (P4), *Apus baranensis* JÁNOSSY, 1977 (P4), *Chaetura baconica* JÁNOSSY, 1977 (P4), *Anthus* sp. (P4), *Motacilla* sp. (P5), *Parus* sp.1, 2, (P4), Muscicapidae gen et sp. indet. (P5), *Luscinia* sp. (P4), *Turdus sp.* (P4, 5), *Bombycilla* sp. (P4, 5), *Acrocephalus* sp. (P4), *Prunella sp.* (P4), *Troglodytes* sp. (P4), *Certhia* sp, (P4), *Sitta* sp. (P5), *Lanius* sp. 1, 2. (P5), *Corvus pliocaenus* (P5), *Corvus* sp. indet. (P4), *Miocorvus larteti* (MILNE-EDWARDS, 1871) (P4), *Sturnus* sp. (P4), *Fringillidae* sp. (P5), Emberizidae sp. indet. (P5), Passeriformes indet. (P4), Aves indet**.** (P4, 5) (KESSLER 2009a,b, 2010).

From this material the following extinct new species have been identified and are described here:

Alauda tivadari n. sp.; *Lullula minor* n. sp.; *Calandrella gali* n. sp.; *Hirundo gracilis* n. sp.; *Delichon polgardiensis* n. sp.; *Riparia minor* n. sp.; *Aegithalos gaspariki* n. sp.; *Sitta gracilis* n. sp.; *Tichodroma capeki* n. sp.; *Muscicapa miklosi* n. sp.; *Luscinia denesi* n. sp.; *Saxicola lambrechti* n. sp.; *Oenanthe kormosi* n. sp.; *Turdicus pannonicus* n. sp.; *Turdus miocaenicus* n. sp.; *Turdus polgardiensis* n. sp.; *Cettia janossyi* n. sp.; *Acrocephalus major* n. sp.; *Acrocephalus minor* n. sp.; *Hippolais veterior* n. sp.; *Sylvia intermedia* n. sp.; *Locustella kordosi* n. sp.; *Phylloscopus venczeli* n. sp.; *Anthus híri* n. sp.; *Motacilla intermedia* n. sp.; *Bombycilla brevia* n. sp.; *Troglodytes robustus* n. sp.; *Cinclus gaspariki* n. sp.; *Prunella freudenthali* n. sp.; *Lanius capeki* n. sp.; *Sturnus brevis* n. sp.; *Passer híri* n. sp.; *Carduelis kretzoii* n. sp.; *Carduelis lambrechti* n. sp.; *Pyrrhula gali* n. sp.; *Fringilla kormosi* n. sp.; *Emberiza pannonica* n. sp.; *Emberiza polgardiensis* n. sp.; *Plectrophenax veterior* n. sp.

According to information provided by M. PÁLFY, Tivadar KORMOS began collecting bone material from the red clay deposited in the clefts of the disused stone quarry on the flat top of Cserhegy hill near the village of Csarnóta in the western part of the Villány Mountains between 1910 and 1930 (marking the site as the "upper quarries"). Between 1954–1959 Miklós KRETZOI and Dénes JÁNOSSY regularly collected material there.

The site age has caused much contraversy.

In absolute chronology the age of sites is follow: Csarnóta 2: 3.7 my (MN 15b) - Lower Pliocene- ; Csarnóta 3: 3.5 my; Csarnóta 1: 3.3 my and Csarnóta 4: 3.2 my (MN 15-16) - Middle - Upper Pliocene). Cronostratigraphically belong to Romanian stage. Biostratigraphically belongs to: Csarnótanum (Middle Pliocene) - after KRETZOI (1956, 1962, 1969), Uppermost Pliocene after JÁNOSSY (1976, 1979) and Upper Pliocene (MN16a) after KORDOS (1991b). From the absolute chronology to be classified in Lower Cserhegy, *Mimomys occitanus* Zone.

We do not want to decide the dispute on Pliocene stratigraphy, mainly in the Carpathian Basin special substages were definied: Ruscinian, Csarnótanum, Beremendium, for with the Lower, Middle and Upper Pliocene, repectively.

Of the four sites, Sites 2 and 4 yielded bird material.

Site 1 was destroyed during the road construction and from its material and from site 3 KORMOS did not report birds remains (KRETZOI 1962).

The bird remains were determined by Dénes JÁNOSSY and Eugen KESSLER.

The Csarnóta 2 list of species is as follows: *Tetrao macropus* JÁNOSSY, 1976 (=*Tetrao praeurogallus* JÁNOSSY, 1969), *Francolinus capeki* LAMBRECHT, 1933; *Rallus aquaticus* (=*Rallicrex polgardensis* KESSLER 2009); *Gallinago veterior* JÁNOSSY, 1979; *Cuculus csarnotanus* JÁNOSSY, 1979; *Bubo bubo, Aegolius* sp., *Hirundo* sp. *(=Hirundo major* n. sp.); *Garrulus glandarius, Pyrrhocorax graculus vetus* KRETZOI, 1962; *Sitta* sp. (=*Sitta pusilla* n. sp.), *Turdus viscivorus* (= *Turdus major* n.sp.), *Turdoides borealis* JÁNOSSY 1979 (KRETZOI 1962, JÁNOSSY 1976a,b, 1977, 1979a,b).

Over recent years the author has identified and defined the species below from the surviving unclassified material: *Podiceps Csarnótanus* KESSLER, 2009; *Anas albae* JÁNOSSY, 1979; *Falco tinnunculus atavus* JÁNOSSY, 1972; *Palaeortyx brevipes* MILNE-EDWARDS, 1869; *Gallus beremendensis* JÁNOSSY, 1976; *Otis kalmani* JÁNOSSY, 1972; *Rallicrex polgardensis* JÁNOSSY, 1991; *Porzana kretzoii* KESSLER, 2009; *Glaucidium baranensis* KESSLER, 2009; *Athene noctua veta* JÁNOSSY, 1992; *Apus baranensis* JÁNOSSY, 1992; *Motacilla sp., Hirundo* sp., (=*Hirundo major* n. sp.); *Sylvia* sp. (=*Sylvia pussila* n. sp.), *Turdus* sp. (= *Turdus major* n. sp.), Muscicapidae sp. indet. (= *Saxicola, Phoenicuros, Oenanthe* n. sp.), *Bombycilla sp., Cinclus sp.*(= *Cinclus minor* n. sp.), *Lanius sp.* (=*Lanius hungaricus* n. sp.), *Certhia sp.* (= *Certhia immensa* n. sp.), *Sitta sp.*(= *Sitta pusilla* n. sp.), *Prunella sp.*(= *Prunella kormosi* n. sp.), *Corvus harkanyensis* KESSLER, 2010; *Miocorvus larteti* (MILNE-EDWARDS), 1871; *Pica pica major* JÁNOSSY, 1979; Fringillidae gen. et sp. indet. (=*Carduelis parvulus* n. sp.; *Carduelis medius* n. sp.; *Pyrrhula*

minor n. sp.; *Fringilla petényii* n. sp.; *Loxia Csarnótanus* n. sp.; *Pinicola kubinyii* n. sp.), Emberizidae gen. et sp.indet. (=*Emberiza media* n. sp.; *Emberiza parva* n. sp.), Passeriformes , Aves indet (KESSLER 2009a, 2009b, 2010), in last year from Csarnóta 4 (PONGRÁCZ L. collection) was collected bones of *Tetrao partium* KRETZOI, 1962.

Based on the latest classifications the following extinct new species have been identified and described: *Galerida pannonica* n. sp. *Lullula parva* n. sp.; *Hirundo major* n. sp.; *Delichon pusillus* n. sp.; *Aegithalos congruis* n. sp.; *Parus robustus* n. sp.; *Parus parvulus* n. sp.; *Sitta pussila* n. sp.; *Certhia immensa* n. sp.; *Saxicola baranensis* n. sp.; *Saxicola parva* n. sp.; *Phoenicurus erikai* n. sp.; *Oenanthe pongraczi* n. sp.; *Turdus major* n. sp.; *Turdus medius* n. sp.; *Turdus minor* n. sp.; *Cettia kalmani* n. sp.; *Acrocephalus kretzoii* n. sp.; *Acrocephalus kordosi* n. sp.; *Sylvia pussila* n. sp.; *Locustella janossyi* n. sp.; *Phylloscopus pliocaenicus* n. sp.; *Anthus baranensis* n. sp.; *Cinclus minor* n. sp.; *Prunella kormosi* n. sp.; *Lanius hungaricus* n. sp.; *Passer minusculus* n. sp.; *Carduelis parvulus* n. sp.; *Carduelis medius* n. sp.; *Pyrrhula minor* n. sp.; *Fringilla petényii* n. sp.; *Loxia ssarnotanus* n. sp.; *Pinicola kubinyii* n. sp.; *Emberiza media* n. sp.; *Emberiza parva* n. sp.

The Beremend 26 site age is almost identical with Csarnóta 2, but the latter's age definition caused much controversy.

The Szőlő Hill from Beremend (174 m altitude) is located aproximative 9 km south around of Villány village. It made up the flat and loess covered Lower Cretaceous limestone (Nagyharsány Limestone Formation). The limestone has been quarried over hundred years and each year more and more karstic kavities and fissures containing bones were discovered.

Already in 1847 Salamon János PETÉNYI and Ferenc KUBINYI collected in the sites No. 1-3. In 1910, 1916 and in the 1930s Tivadar KORMOS collected in the sites No. 4-10. In 1953 Miklós KRETZOI and Dénes JÁNOSSY continued the collect in the mine. Later JÁNOSSY and Endre KROLOPP ply the research and excavation since 1973 (sites No. 11-17) and with László KORDOS (JÁNOSSY 1979; KORDOS 2001).

From 1993 László PONGRÁCZ found new sites (No. 18-39) and collected the fossil remains for as long as possible (PONGRÁCZ 1999).

The age of sites covers a large interval from 3.7 my to 1.3 my (Lower-Upper Pliocene , MN 15-17) belong the Csarnótanum to Biharium biochronological units in the following sequence: 26 – 5 – 11 – 15 etc. (KORDOS 1991, 2001, 2004).

The Beremend 26 is in 100 m (deepest) level in the quarry. It was an about 30 m wide and 20-25 m high red clay fissure filling. In this site the Hungarian Geological Institute carried out a detailed geological investigation in 2001 and the mammal fauna was determined by László KORDOS (2001). The site was blown down, but László PONGRÁCZ saved the significant part of the fossil remains. The birds bones from this material was identified and described by author in previous years and in this paper.

In 2009 and 2010 the author presented the following fauna list:

Podiceps sp. (*ruficollis* size)., *Egretta* sp. (*garzetta* size), *Accipiter* sp**.** **(***nisus* size*), Falco tinnunculus atavus, Falco* sp**.** (*peregrinus* size) *Tetrao praeurogallus, Tetrao partium, Gallus beremendensis, Francolinus capeki, Palaeocryptonix hungaricus, Perdix perdix jurcsaki, Rallus polgardensis, Miorallus major, Porzana* sp., (*Porzana porzana* size)*, Otis kalmani, O. lambrechti, Chlidonias* sp., *Tringa* sp. (*glareola-ochropus* size)*, Columba* sp., *Glaucidium baranensis, Athene noctua veta, Strix intermedia, Picus* sp., *Dendrocopus* sp 1, 2, 3 **(***medius, minor* and *major* size*) ,Alaudidae* sp. 1, 2, *Melanocorypha* sp, *Motacilla* sp, *Hirundo* sp. 1, 2, *Turdus* sp., *Muscicapidae* sp.1, 2, *Sylvia* sp, *Acrocephalus* sp., *Parus* sp. 1, 2, *Bombycilla* sp.1, 2, *Lanius* sp, *Sitta* sp., *Certhia* sp., *Pica pica major, Corvus pliocaenus, Miocorvus larteti, Corvus* sp., *Nucifraga* sp. (as *N. caryocatactes*), *Coccothraustes* sp. (as *C. coccothraustes*)*, Pyrrhula* sp. (as *P. pyrrhula*)*,* Fringillidae sp., *Emberiza* sp., Passeriformes indet., Aves indet. (KESSLER 2009 a,b, 2010).

The taxa definied only genus level - except song birds - are or very fragmented, or are represented by claws and therefore they can not be identified at species level.

Based on the latest classifications the following extinct species have been identified and described: *Picus pliocaenicus* KESSLER, 2012; *Dendrocopos praemedius* JÁNOSSY, 1974 (KESSLER 2012-2013).

Recently, the author identified the very rich songbird material at species level, described in the current paper. These are:

Melanocorypha minor n. sp.; *Galerida pannonica* n. sp. *Lullula parva* n. sp.; *Lullula minuscula* n. sp.; *Delichon major* n. sp.; *Parus robostus* n. sp.; *Parus medius* n. sp.; *Sitta villanyensis* n. sp.; *Muscicapa petényii* n. sp.; *Erithacus minor* n. sp.; *Luscinia pliocaenica* n. sp.; *Saxicola baranensis* n. sp.; *Saxicola magna* n. sp.; *Monticola pongraczi* n. sp.; *Phoenicurus baranensis* n. sp.; *Oenanthe pongraczi* n. sp.; *Turdus major* n. sp.; *Turdus medius* n. sp.; *Turdus minor* n. sp.; *Oriolus beremendensis* n. sp.; *Acrocephalus kretzoii* n. sp.; *Sylvia pussila* n. sp.; *Locustella magna* n. sp.; *Locustella janossyi* n. sp.; *Regulus pliocaenicus* n. sp.; *Motacilla minor* n. sp.; *Motacilla robusta* n. sp.; *Bombycilla kubinyii* n. sp.; *Prunella kormosi* n. sp.; *Lanius major* n. sp.; *Lanius intermedius* n. sp.; *Sturnus pliocaenicus* n. sp.; *Sturnus baranensis* n. sp.; *Passer pannonicus* n. sp.; *Coccothraustes major* n. sp.; *Loxia Csarnótanus* n. sp.; *Emberiza gaspariki* n. sp.

Material and methods

The osteological and biometrical comparison of the fossil bird material was made by using recent and fossil comparative collections of the Hungarian Natural History Museum. The anatomical terminology follows BAUMEL et al. (1979) and GILBERT, MARTIN & SAVAGE (1981) and for the measurements follows Angela von den DRIESCH (1976)

The identification of song bird remains was based on the characteristics found on the contours of epiphyses. Out of the total of 63 characteristics found on the nine skeletal types (coracoid, scapula, humerus, ulna, carpometacarpus, phalanga alae 1. dig.II., femur, tibiotarsus, tarsometatarsus), 54 is connected to the contour. Only nine characteristics are to be found on the surface of bones (one on the scapula, two on the proximal epiphysis of the humerus, two on the proximal epiphysis of the ulna, and four on the distal epiphysis of the tibiotarsus). This method makes possible the identification of rather small and fragmented bones at species level, in spite of the often damaged surface of the epiphysis, or the occasional mineral sediment attached to the bone remain. In this paper, the diagnoses of the 39 new species have been made according to the aforementioned characteristics, and they are illustrated on the Plates as well. The contour is essential, not the condition of the surface of the bone.

Institutional abbreviations

MÁFI = Geological Institute of Hungary (recently renamed as Geological and Geophysical Institute of Hungary: GGIH), Budapest, Hungary; MTM = Department of Paleontology and Geology of the Hungarian Natural History Museum, Budapest, Hungary.

BKA = Foundation „Beszélő kövek" (private collection, established by László PONGRÁCZ in Villány).

P2, P4, P5 = Polgárdi site 2, 4 and 5.

MTM n=1 = number of recent specimen from osteological collection.

Measurement abbreviations

A (GL) = greatest length,
B (Lm) = medial length,
C (Bp) = breadth of the proximal length,
C1 = thickness of the proximal end,
D (Dp) = depth of the proximal end,
E (Sc) = smallest breadth of the corpus,
E1 = thickness of the corpus (in the case of carpometacarpus = the breadth of metacarpus II.),
F (Bd) = breadth of the distal end,
G (Dd) = depth of the distal end.

Systematic description

Order Passeriformes (LINNAEUS, 1758)
Family Alaudidae (VIGORS, 1825)
Genus *Alauda* LINNAEUS, 1758
Alauda † *tivadari* nova sp.
(Plate I. Figure 1 A-B)

Type locality and age: Polgárdi 4, Late Miocene (MN 13).

Holotype: Coracoideum dext. (damaged sternal), (Polgárdi 4, MÁFI V.11.63.1; V.29138).

Paratype: Distal fragment of the tibiotarsus sin. (Polgárdi 4, MÁFI V.11.801; V.29155).

Measurements: 1. coracoid B=15.11 mm; C=2.36 mm; D=2.96 mm; E=1.04 mm; 2. tibiotarsus F= 2.71 mm; G=2.63 mm.

Comparative material: Alauda arvensis (MTM n=1: 1. coracoid D=3.69 mm; E=1.15 mm; 2. tibiotarsus F=2.72 mm; G=2.64 mm); *Galerida cristata* (MTM n=1: 1. coracoid D=4.02 mm; E=1.27 mm; 2. tibiotarsus F=3.17 mm);, *Calandrella brachydactyla* (MTM n=1: 1.coracoid B=17.27 mm; C=2.46 mm; D= 3.01 mm; E=1.08 mm; 2. tibiotarsus F=2,44 mm); *Lullula arborea* (MTM n=1: 1. coracoid B=18.06 mm; D=3.92 mm; E=1,17 mm; 2. tibiotarsus F=2.64 mm); *Eremophilla alpestris* (MTM n=1: tibiotarsus F=2.94 mm).

Diagnosis: Small species of lark. On the cranial part of coracoid (Fig. 1A), the *processus acrocoracoidalis* (a) has blunted symmetric conical shape, and its cranial edge forms a straight line. *Processus accesorius* (b) is short and broadly hook-shaped. Edge of *sulcus musculi supracoracoidei* (c) has one flattened concave shape. Lateral edge of *facies articularis humeralis* (d) is rounded. *Processus procoracoidalis* (e) is pointed and well developed, exceeds the medial edge of bones.

On tibiotarsus in cranial view (Fig. 1B), there is a *tuberositas retinaculi m. fibularis* (a) which is pointed and weakly grown. Distal end of *sulcus extensorius* (b) is narrowing in V-shape and pointed. *Pons supratendineus* (c) is wide and oblique. *Condylus lateralis* (d) has flattened and pointed oval shape. *Incisura intercondylaris* (e) forms asymmetrical concave line. *Condylus medialis* (f) has flattened egg shape.

Name: Was named after the Hungarian paleontologist Tivadar KORMOS,

Description: The coracoid is somewhat smaller than in recent species, while the distal fragment of the tibiotarsus is equal to it in the size. The extinct species from Felsőtárkány (MN 7/8: *Praealauda hevesensis* KESSLER et HÍR, 2012 differs in its age, sizes and morphological characteristics (KESSLER & HÍR 2012).

Distribution: In the Carpathian Basin the recent genus and species are also known from the Early Pleistocene in Hungary (Beremend 16), Romania (Betfia 9) (JÁNOSSY 1992; GÁL 2002). The genus was reported recently outside the Carpathian Basin in Bulgaria (Upper Pliocene, MN 17, Varshets) as *Alauda xerarvensis* BOEV, 2012 (but from other types of skeletal fragments: ulna, sternum, mandibula) (BOEV 1996, 2012) and is also known with recent species from the Early Pleistocene from Valerots (France) and Stránská skála (Czech Republic) (TYRBERG 1998).

Alauda gypsorum PORTIS, 1887 and *Alauda major* PORTIS, 1887 (PORTIS 1887) from the Late Miocene (MN 13) of Seniglia and Gabbro (Italy) were reported in slab as fossil species, but MLÍKOVSKÝ (2002) put them into *„Family incertae sedis"*.

Genus *Galerida* BOIE, 1828
Galerida †*pannonica* nova sp.
(Plate I. Figure 2 A-D)

Type locality and age: Csarnóta 2, Pliocene (MN 15-16).

Holotype: Distal fragment of the tibiotarsus sin. (MÁFI V .11.13.1; V.29088).

Paratypes: Distal fragment of the humerus sin; carpometacarpus sin.; distal fragment of the tarsometatarsus sin. (Beremend 26, BKA).

Measurements: 1. humerus E=2,57 mm; F=5,75 mm;G=3,39 mm; 2. carpometa-carpus A=17,42 mm; B=14,10 mm; C=4,28 mm; E=3,08 mm; F=3,95 mm; 3. tibiotarsus F =2.85 mm; G=2.45 mm; 4. tarsometatarsus E=1,25 mm; F=2,65 mm; G=1,83 mm.

Comparative material: Galerida cristata (MTM n=1-2: humerus E=2,40-2,46 mm; F=6,08-6,21 mm; G=3,44 mm; carpometacarpus A=17,41-18,56 mm; B=14,87 mm; C=3,85-4,12 mm; E=2,11 mm; F=3,67 mm; tarsometatarsus E=1,25-1,29 mm; F=2,70-2,79 mm; G=1,67 mm; tibiotarsus: F=3.17 mm; G=3.04 mm); *Alauda arvensis* (MTM n=1: carpometacarpus A=17,26 mm; C=3,85 mm; tibiotarsus: F=2.72 mm; G=2.88 mm; tarsometatarsus E=1,26mm; F=2,76 mm); *Lullula arborea* (MTM n=1: humerus E=2,28; F=4,88 mm; carpometacarpus A=16,39 mm; C=3,73 mm; tibiotarsus: F=2.64 mm; G=2.48 mm; tarsometatarsus E=1,24 mm; F=2,52 mm); *Calandrella brachydactila* (MTM n=1: carpometacarpus A=14,61 mm; C=3,54 mm; tibiotarsus: F=2.44 mm; tarsometatarsus E= 1,29 mm; F=2,20 mm); *Melanocorypha calandra* (MTM n=1: humerus E=2,46 mm; F=6,65 mm; tibiotarsus: F=3.71 mm; tarsometatarsus E=1,43 mm; F=3,53 mm); *Eremophila alpestris* (MTM n=1: carpometacarpus A=17,05 mm; C=4,24 mm; tibiotarsus: F=2.94 mm; tarsometatarsus E=1,10 mm, F=2,77).

Diagnosis: On distal epiphysis in cranial view of humerus (Fig. 2A), the *tuberculum ventrale* (a) is weakly developed. The *epicondylus ventralis* (b) is rounded. *Condylus ventralis* (c) has lying oval shaped and distally more protruding. *Incisura intercondylaris* (d) is wider but slightly deeper than in the recent genus. The *condylus dorsalis* (e) has mildly oblique oval shape. *Epicondylus dorsalis* (f) is less rounded. *Processus supracondylaris dorsalis* (g) is short and wide with with two unequal branches.

On proximal epiphysis of carpometacarpus in ventral view (Fig. 2B), the *trochlea carpalis* (a) has semicircular-like shape. *Proc. extensorius* (b) has short and pointed oblique conical shape. *Processus alularis* (c) is less developed and the *fovea subalularis* (d) has weakly developed acute angle shape. *Protuberantia metacarpalis* (e) is in the external edge of the *os metacarpale majus* and forms wider and oblique triangular bulgle. *Facies arrticularis digiti major* (f) in medial part has tooth-like protrusions.

On tibiotarsus of distal epiphysis in cranial view (Figure 2C), the *tuberositas retinaculi m. fibularis* (a) is flattened. The distal end of *sulcus extensorius* (b) is wide and arched. *Pons supratendineus* (c) is middling wide and straight. The lower slot of the *canalis extensorius* (d) is wide and has regularly eye-like shape. *Incisura intercondylaris* (e) has concave shape. *Condylus medialis* (f) has regular egg shape.

On distal epiphysis of tarsometatarsus in dorsal view (Fig. 2D), the *trochlea metatarsi* II. (a) has laterally protruding conical shape, with cut-off end. *Incisura intertrochlearis lateralis* (b) is pointed, wide and deep. *Trochlea metatarsi tertii* (c) is wide and bellow average with concave end. *Incisura intertrochlearis medialis* (d) is pointed, deep and wide. *Trochlea metatarsi* IV. (e) is injured.

Name: Was named after the name of the Pannonia region.

Description: It corresponds in characters and sizes with recent species of the genus. The cranial part of the *condylus lateralis* is missing partly and in the *condylus medialis* it is missing totally. The *incisura intercondylaris* is damaged partly. Its characters corresponds with *Galerida cserhatensis* KESSLER et HÍR, 2012 from Litke 2 – Hungary (Lower Miocene, MN 5), but the *tuberositas retinaculi m.fibularis* narrower and more pointed than in the Csarnótian specimen, also the sizes is smaller (KESSLER et HÍR 2012).

Distribution: The genus is known from Beremend 17 – Hungary (Lower Pleistocene, MQ1), (JÁNOSSY 1992) as *Galerida* sp. and from Betfia 2, 9 - Romania (Lower Pleistocene, MQ1) (ČAPEK 1917; LAMBRECHT

1933; JÁNOSSY 1979a; KESSLER, 1975; GÁL, 2002); and Somssich-Hill 2 – Hungary (Lower Pleistocene, MQ2) (JÁNOSSY 1979a, 1980) as recent species *Galerida cristata* (LINNAEUS, 1758).

The genus was reported outside the Carpathian Basin in Bulgaria from Varshets (Late Pliocene, MN 17) as *Galerida bulgarica* BOEV, 2012 (BOEV 2012). It is also known with recent species only from Middle Pleistocene in Europa's fossil localities (TYRBERG 1998).

Genus *Lullula* KAUP, 1829

Lullula †*minor* nova sp.

(Plate I. Figure 3 A-D)

Type locality and age: Polgárdi 4, 5; Late Miocene (MN 13).

Holotype: Ulna sin. (Polgárdi 5, MÁFI V.11.93.1; V.29168).

Paratypes: Distal fragment of the humerus sin. (Polgárdi 4, MÁFI V.11.81.2; V.29156/1); distal fragment of the tarsometatarsus sin. (Polgárdi 4, MÁFI V.11.81.2; V.29156/2).

Measurements: 1. ulna A=24.23 mm; C=3.57 mm; E=1.79 mm; F=3.25 mm; G=2.42 mm; 2. humerus E=1.43 mm; F=3.14 mm; G=2.02 mm; 3. tarsometatarsus E=1.09 mm; F=2.58 mm; G=1.58 mm.

Comparative material: Lullula arborea (MTM n=1: 1. ulna A=28.64 mm; C=3.94 mm; E=1.76 mm; F=3.39 mm; G=2.49 mm; 2. humerus E=2.15 mm; F=5.02 mm; G=2.87 mm; 3. tarsometatarsus E=1.25 mm; F=2.52 mm; G=1.51 mm); *Alauda arvensis* (MTM n=1: 1. ulna A=29.68 mm; C=3.96 mm; E=1.92 mm; F=3.32 mm; 2. tarsometatarsus E=1.26 mm; F=2.76 mm); *Galerida cristata* (MTM n=1: 1. ulna A=34.46 mm; C=3.92 mm; E=2.25 mm; F=3.68 mm; 2. humerus E=2.46 mm; F=6.01 mm; 3. tarsometatarsus E=1.29 mm; F=2.79 mm); *Calandrella brachydactyla* (MTM n=1: ulna A=25.73 mm; C=3.38 mm; E=1.51 mm; F=2.88 mm; 2. tarsometatarsus E=1.25 mm; F=2.20 mm).

Diagnosis: Small species of skylark. On distal epiphysis of humerus in cranial view (Fig. 3A), the *tuberculum ventrale* (a) is weakly developed. *Epicondylus ventralis* (b) is strongly arched. *Processus flexorius* (c) is distally projecting and has symmetrical blunted conical shaped. *Condylus ventralis* (d) has extended oval shaped. *Incisura intercondylaris* (e) is slightly deeper than in the recent genus. *Condylus dorsalis* (f) has curved oval shape. *Epicondylus dorsalis* (g) is more rounded than in the recent genus. *Processus supracondylaris dorsalis* (g) is small, wide with less pointed end.

On proximal epiphysis of ulna in cranial view (Fig. 3B), the *oleocranon* (a) has average length, with blunted conical shape. *Cotyla dorsalis* (b) is asymmetrical conical shaped, with rounded end. *Cotyla ventralis* (c) has circular shape. *Tuberculum lig. colat. ventralis* (d) is less well discernible than in recent genus. *Depressio m. brachialis* (e) is well developed. On distal epiphysis in medial view (Fig. 3C), *condylus dorsalis* (f) has blunted claw-like shape. *Sulcus intercondylaris* (g) is slightly concave. *Condylus ventralis* (h) is wide and has less convex shape. *Tuberculum carpale* (i) has asymmetrically blunted conical shape.

On distal epiphysis of tarsometatarsus in dorsal view (Fig. 3D), the *trochlea metatarsi* II. (a) has laterally protruding conical shape, with cut-off end. *Incisura intertrochlearis lateralis* (b) is weakly wide and deep. *Trochlea metatarsi tertii* (c) is wide and bellow average with concave end. *Incisura intertrochlearis medialis* (d) is much deeper and wider than in recent genus. *Trochlea metatarsi* IV. (e) is beak-like and more pointed than in recent genus.

Name: It was dubbed based on its dimensions.

Description: The fossil species differs from recent with its smaller sizes and in some morphological characters. The fossil species *Lullula neogradensis* KESSLER et HÍR, 2012 from Mátraszőlős 1 was described based on tibiotarsus and its age is much older (KESSLER & HÍR 2012).

Lullula † *parva* nova sp.

(Plate II. Figure 4 A-C)

Type locality and age: Csarnóta 2, Pliocene (MN 15-16).

Other locality: Beremend 26, Pliocene (MN 15-16).

Holotype: Distal fragment of tibiotarsus sin. (Csarnóta 2, MÁFI V.11.20.1; V.29095).

Paratype: Humerus dext. (Beremend 26, BKA).

Measurements: 1. humerus A=21,15 mm; B=9,04 mm; C=6,70 mm; D=5,66 mm; E=1,95 mm; F= 5,06 mm; G=2,76 mm. 2. tibiotarsus F=2.40 mm; G=2.30 mm.

Comparative material: Galerida cristata (MTM n=1; 1.humerus A= 28,00 mm; C=8,25 mm; E=2,45 mm; F=6,34; 2. tibiotarsus: F=3.17 mm; G=3.04 mm); *Alauda arvensis* (MTM n=1; tibiotarsus: F=2,72 mm; G=2.68 mm); *Lullula arborea* (MTM n=1; 1. humerus: A=22,00-23,02 mm; B=10,06 mm; C=6,33-6,80 mm; D=5,90 mm; E=2,10-2,28 mm; F=4,60-4,88 mm; G=2,73 mm; 2. tibiotarsus: F=2.64 mm; G=2.51 mm); *Calandrella brachydactila* (MTM n=1; tibiotarsus: F=2.44 mm); *Melanocorypha calandra* (MTM n=1; 1. humerus A=27,75 mm; C= 8,33 mm; E=2,46 mm; F=6,65 mm; 2. tibiotarsus: F=3.71 mm); *Eremophila alpestris* (MTM n=1; tibiotarsus: F=2.94 mm).

Diagnosis: On proximal epiphysis of humerus in caudal view (Fig. 4A), the *tuberculum dorsale* (a) is rounded. *Caput humeri* (b) is wide and convex, but not too outstanding. *Tuberculum ventrale* (c) forms one protruding oval-like spur. *Crista bicipitalis* (d) is strongly protruding and rounded. *Crus fossae* (e) can

be seen but it is blurred, the *fossae pneumotricipitalis* (f) is divided into two part. On distal epiphysis in cranial view (Fig. 4B), the *tuberculum supracondylare ventrale* (g) is less developed; the *epicondylus ventralis* (h) is less rounded. *Processus flexorius* (i) is protruding and rounded. *Condylus ventralis* (j) has wide lying oval shape. *Incisura intercondylaris* (k) is wide but it is less deep. *Condylus dorsalis* (l) is crooked oval shaped. *Epicondylus dorsalis* (m) is less rounded. *Processus supracondylaris dorsalis* (n) is short, bent and has two unequal branches.

On distal epiphysis of tibiotarsus in cranial view (Figure 4C), the distal end of *sulcus extensorius* (b) is narrowing. *Pons supratendineus* (c) is wide and slightly oblique. *Condylus lateralis* (d) has oval shape. *Incisura intercondylaris* (e) forms oblique line. *Condylus medialis* (f) has wide egg shape.

Name: The name refers to its dimensions.

Description: It corresponds in characters to the recent genus. The fossil species *Lullula neogradensis* KESSLER et HIR, 2012 (KESSLER & HIR, 2012) from Mátraszőlős 1 – Hungary (Middle Miocene, MN 7/8) and *Lullula † minor* from Polgardi differ in its age and sizes to Csarnótian specimen.

Lullula † minuscula nova sp.
(Plate II. Figure 5 A-B)

Type locality and age: Beremend 26, Pliocene (MN 15-16).

Holotype: Humerus dext. (BKA)

Measurements: humerus A=14,62 mm; B=6,07 mm; C=4,45 mm; D=4,15 mm; E=1,41 mm; F=3,89 mm; G=1,95 mm.

Comparative material: Lullula arborea (MTM n=3: humerus: A=22,00-23,02 mm; B=10,06 mm; C=6,33-6,80 mm; D=5,90 mm; E=2,10-2,28 mm; F=4,60-4,88 mm; G=2,73 mm).

Diagnosis: On proximal epiphysis of humerus in caudal view (Fig. 5A), the c*aput humeri* (a) is wide and convex, but not too outstanding. *Tuberculum ventrale* (b) forms rounded ovalic spur. *Crista bicipitalis* (c) is strongly protruding and distally pointed. *Crus fossae* (d) is well developed, the *fossae pneumotricipitalis* (e) is divided into two part. On distal epiphysis in cranial view (Fig. 5B), the *tuberculum supracondylare ventrale* (f) is less developed; the *epicondylus ventralis* (g) is rounded. *Processus flexorius* (h) is strongly protruding, is wider than in recent species and rounded. *Condylus ventralis* (i) has lying oval shape. *Incisura intercondylaris* (j) is deep and has angle shape. *Condylus dorsalis* (k) has crooked oval shape. *Epicondylus dorsalis* (l) is rounded. *Processus supracondylaris dorsalis* (m) is short, bent and has two unequal branches.

Name: The name refers to very small dimensions of the species.

Description: In size corresponds with *Lullula minor* KESSLER, 2012 from Polgárdi - Hungary (Upper Miocene, MN 13) but is younger. It is different in size and in characters to *Lullula parva*. The *tuberculum dorsale* is missing.

Distribution: The genus was reported outside the Carpathian Basin in Bulgaria from the Late Miocene Chrabarsko as *Lullula* sp. (BOEV 2000), and from the Late Pliocene - Early Pleistocene as *Lullula slivnicensis* BOEV, 2012 (Slivnica, MN 17) and *L. balcanica* BOEV, 2012 (Varshets, MN 18) based on other skeletal types (coracoid, sternum and phalanga alae) (BOEV 1996, 2012).

The recent species *Lullula arborea* (LINNAEUS), 1758 is known from Betfia 2, 9 – Romania (Lower Pleistocene, MQ1**)** (ČAPEK 1917; LAMBRECHT 1933; JÁNOSSY 1979; KESSLER 1975; GÁL 2002) and was reported from the Late Pliocene and the Early Pleistocene (MN 18) in Mallorca (Spain) (SONDAAR et al. 1995).

Genus *Calandrella* KAUP, 1829
Calandrella † gali nova sp.
(Plate II. Figure 6 A-D)

Type locality and age: Polgárdi 4, 5; Late Miocene (MN 13).

Holotype: Humerus sin. (Polgárdi 4, MÁFI V.11.65.1; V.29140).

Paratypes: Coracoideum dext. (Polgárdi 4, MÁFI V.11.109.1; V.29184), distal fragment of tibiotarsus dext. (Polgárdi 5, MÁFI V.11.127.1; V.29202).

Measurements: 1. humerus A=21.04 mm; B=5.91 mm; C=6.24 mm; D=4.81 mm; E=1.82 mm; F=5.23 mm; G=2.45 mm; 2. coracoid A=15.75 mm; B=14.68 mm; C=2.19 mm; D= 2.81 mm; E=1.05 mm; G=3.53 mm; 3. tibiotarsus F=2.51 mm; G=2.52 mm.

Comparative material: Calandrella brachydactyla (MTM n=1: 1. humerus: A=20.00 mm; C=6.00 mm; E= 1.80 mm; F=4.5 mm; 2. coracoid A=18.08 mm; B=17.27 mm; C=2.46 mm; D= 3.01 mm; E=1.08 mm; G=4.31 mm; 3. tibiotarsus F=2.44 mm); *Alauda arvensis* (MTM n=1: 1. humerus: A=26.4 mm; B=8.45 mm; C=7.67 mm; E=2.26 mm; F=5.91 mm; G=3.08 mm; 2**.** coracoid A=17.74 mm; D=3.69 mm; E=1.15 mm; F=2.72 mm; G=2,64 mm; 3.tibiotarsus F=2,72 mm G=mm); *Galerida cristata* (MTM n=1: 1.humerus: A=28,08 mm; B=9.71 mm; C=8,24 mm; D=5,79 mm; E=2,45 mm; F=6.09 mm; G=3.24 mm; 2. coracoid A=22,84 mm; D=4,02 mm; E=1.27 mm; tibiotarsus F=3.17 mm; G= G=3.04 mm**);** *Melanocorypha calandra* (MTM n=1: 1. humerus: A=27.75 mm; C=8,63 mm; E=2,46 mm; F=6.65 mm; 2. tibiotarsus: F=3.71 mm); *Lullula arborea* (MTM n=3: 1. humerus: A=22.00-23.02 mm; B=18.06 mm; C=6.33-6.80 mm; D=5.90 mm; E=2.10-2.28 mm; F=4.60-4.88 mm; G=2.73 mm; 2. coracoid A=18.53 mm; D=3,92 mm; E=1.17 mm; 3. tibiotarsus F=2.64 mm; G=2.48 mm).

Diagnosis: Middle sized species of lark. On coracoid in dorsal view (Fig. 6A), the *acrocoracoid*

(a) has asymmetrical blunted conical shape, blunter than in the recent genus. *Processus accesorius* (b) is short and hook-like with rounded edge, but longer than in recent genera of this family. Edge of *sulcus m. supracoracoidei* (c) has flattened concave shape. *Facies aricularis humeralis* (d) has rounded protruding cranial end. Point of *processus procoracoidei* (e) exceeds the medial edge of corpus.

On proximal epiphysis of humerus in caudal view (Fig. 6B), the *tuberculum dorsale* (a) is rounded. *Caput humeri* (b) is wide and convex, but not too protruding. *Tuberculum ventrale* (c) forms oval-like spur. *Crista bicipitalis* (d) is rounded. *Crus fossae* (e) can be seen, because *fossae pneumotricipitalis* (f) is divided into two part. On distal epiphysis in cranial view (Fig. 6C), the *epicondylus ventralis* (g) is rounded. *Processus flexorius* (h) is protruding and with rounded end. *Condylus ventralis* (i) has lying oval shape. *Incisura intercondylaris* (j) is in angle hollow. *Condylus dorsalis* (k) is mildly lopsided and oval. *Epicondylus dorsalis* (l) is rounded. *Processus supracondylaris dorsalis* (m) is short, bent and has pointed end.

On tibiotarsus of distal epiphysis in cranial view (Fig. 6D), the *tuberositas retinaculi m. fibularis* (a) is flattened, but more developed than in recent genus. *Sulcus extensorius* (b) is relatively shallow. *Pons supratendineus* (c) is no too wide, lopsided. *Condylus lateralis* (d) is flattened and distally rounded. *Incisura intercondylaris* (e) has concave shape. C*ondylus medialis* (f) is distally rounded and regularly oval.

Name: after the Hungarian paleornithologist Erika GÁL.

Description: It corresponds in its characters to recent species, but its size is somewhat differ.

Distribution: The genus was reported only from the Late Pleistocene of Tarchankut, Ukraine with recent species *Calandrella brachydactyla* (LEISLER, 1814), (VOJINSTVENS'KYJ 1967).

Genus *Melanocrypha* BOIE, 1826
Melanocorypha † minor nova sp.
(Plate III. Figure 7 A-B)

Type locality and age: Beremend 26, Pliocene (MN 15-16).

Holotype: Humerus sin. (BKA),

Measurements: Humerus A=17,1-17,7 mm, C=4,8-5,5 mm, F=3,9-4,4 mm.

Comparative material: Melanocorypha calandra (MTM n=1: humerus: A=27,75 mm; C= 8,63 mm; E=2,46 mm; F=6,65 mm; G=3,28 mm); *Calandrella brachydactyla* (MTM n=1: humerus: A=20,00 mm; C=6,00 mm; E= 1,80 mm; F=4,5 mm); *Alauda arvensis* (MTM n=1: humerus: A=26,4 mm; B=8,45 mm; C=7,67 mm; E=2,26 mm; F=5,91 mm; G=3,08 mm); *Galerida cristata* (MTM n=1:.humerus: A=28,08 mm; B=9.71 mm; C=8,24 mm; D=5,79 mm; E=2,45 mm; F=6,09 mm; G=3,24 mm**);** *Lullula arborea* (MTM n=3: humerus: A=22,00-23,02 mm; B=18,06 mm; C=6,33-6,80 mm; D=5,90 mm; E=2,10-2,28 mm; F=4,60-4,88 mm; G=2,73 mm;).

Diagnosis: On proximal epiphysis of humerus in caudal view (Fig. 1A), the *tuberculum dorsale* (a) is rounded. *Caput humeri* (b) is wide and convex, but not too outstanding. *Tuberculum ventrale* (c) forms ovale-like spur. *Crista bicipitalis* (d) is strongly protruding and rounded. *Crus fossae* (e) can be seen, because the *fossae pneumotricipitalis* (f) is divided into two parts. On distal epiphysis in cranial view (Fig. 1B), the *tuberculum supracondylare ventrale* (g) is well developed; the *epicondylus ventralis* (h) is flattened. *Processus flexorius* (i) is protruding and wider than in recent species. *Condylus ventralis* (j) has wide lying oval shape. *Incisura intercondylaris* (k) is wide but it is less deeper than in recent species. *Condylus dorsalis* (l) is mildly oblique and oval shaped. *Epicondylus dorsalis* (m) is rounded. *Processus supracondylaris dorsalis* (n) is short, bent and has two unequal branches.

Name: after the small size.

Description: It corresponds to the recent genus, but dimensions are smaller.

Distribution: The genus was reported from Bulgaria: *Melanocorypha serdicensis* BOEV, 2012 (Upper Miocene, Hrabarsko); and *Melanocorypha donchevi* BOEV, 2012; (Upper Pliocene, Varshets), (BOEV 2012). One fossil species of larks have been described from the Pleistocene deposits in Israel: *Melanocorypha gracilis* TCHERNOV, 1968 (TYRBERG 1998).

The other genera were reported from Bulgaria: *Eremarida xerophila* BOEV, 2012 (Upper Miocene, Hrabarsko); *Eremophila prealpestris* BOEV, 2012 (Upper Pliocene, Varshets), (BOEV 1996, 2012). The recent species *Eremophila alpestris* (LINNAEUS, 1758) was described from the Late Pliocene of Mas Ramboult (France) (MOURER-CHAUVIRÉ 1975). Finally, ZELENKOV (2011) reported the *Eremophila* aff. *E. alpestris* in the Late Pliocene (MN 16) of Beregovaya (Bichursky District, Republic of Buryatia, Russia).

Family Hirundinidae VIGORS, 1825
Genus *Hirundo* LINNAEUS, 1758
Hirundo † gracilis nova sp.
(Plate III. Figure 8 A-B)

Type locality and age: Polgárdi 4, 5 Late Miocene (MN 13).

Holotype: Ulna sin. with damaged proximal epiphysis (Polgárdi 5, MÁFI V.11.97.1; V.29172).

Paratype: Ulna dext. with damaged proximal epiphysis (Polgárdi 4 (MÁFI V.11.82.1; V.29157).

Measurements: Ulna A= 24-25 mm; E=1.78 mm; F=2.57-2.72 mm; G=2.03-2.06 mm.

Comparative material: Hirundo rustica (MTM n=1: A=23.92 mm; C=3.54 mm; E=1.61 mm; F=3.01

mm; G=1.94 mm); *Delichon urbica* (MTM n=1: A=20.80 mm; C=3.32 mm; E=1.47 mm; F=2.68 mm; G=1.94 mm); *Riparia riparia* (MTM n=1: A=20.05 mm; C=3.06 mm; E=1.55 mm; F=2.72 mm; G=1.82 mm);

Diagnosis: Medium sized swallow species. On proximal epiphysis of ulna in cranial view (Fig. 8A), the *cotyla dorsalis* is asymmetrical rounded and *cotyla ventralis* (a) has circular shape. *Tuberculum lig. colateralis ventralis* (b) is strongly protuding. On distal epiphysis in medial view (Fig. 8B), lateral edge of *condylus dorsalis* (c) bends in arch. *Sulcus intercondylaris* (d) is straight, while it draws mildly concave arch in recent genus. *Condylus ventralis* (e) is obliquely conical, more than in recent genus. *Tuberculum carpale* (f) is protruding and semicircular.

Name: Its name refers to the slenderness of bones.

Description: More slender than the recent species.

Hirundo † major nova sp.
(Plate III. Figure 9 A-B)

Type locality: Csarnóta 2, Pliocene (MN 15-16).

Holotype: Ulna dext. (distal fragment) (MÁFI V.11.14.1; V.29089/1).

Paratype: Tibiotarsus dext. (distal fragment) (MÁFI V.11.14.2; V.29089/2).

Dimensions: 1. Ulna E=1.86 mm; F=3.18 mm; G=1.97mm; 2. tibiotarsus E=0.89 mm; F=1.97 mm; G=1.81 mm.

Comparative material: Hirundo rustica (MTM n=1; 1. ulna: E=1.61 mm; F=3.01 mm; G=1.94 mm; 2. tibiotarsus: E=0.89 mm; F=2.04 mm; G=1.99 mm).

Diagnosis: On distal epiphysis of ulna in medial view (Fig. 9A), the *condylus dorsalis* (c) has hook-like shape, but it is less pointed than in recent species. *Sulcus intercondylaris* (d) is less concave than in recent genus. *Condylus ventralis* (e) is obliquely conical. *Tuberculum carpale* (f) has wide hook-like shape and it is less protruding than in recent species.

On tibiotarsus the distal epiphysis in cranial view (Fig. 9B), the *tuberositas retinaculi m. fibularis* (a) is flattened. The distal end of the s*ulcus extensorius* (b) is rounded. *Pons tendineus* (c) is wide and oblique. *Condylus lateralis* (d) has distaly rounded conical shape. *Incisura intercondylaris* (e) has strongly concave shape. C*ondylus medialis* (f) is distaly pointed oval shaped.

Etymology: after its large size.

Description: It corresponds in characteristics with recent genus, but its dimensions are larger. This material was reported as *Hirundo* sp. from Csarnóta 2 by JÁNOSSY (1979a). The fossil species *Hirundo* †*gracilis* KESSLER, 2012 from Polgárdi (Late Miocene, MN 13) is smaller than the Csarnótian specimen. The its *condylus dorsalis* is more rounded and the *incisura intercondylaris* is less concave.

Distribution: The genus is known from the Early Pliocene (MN 15) from Ivanovce I. - Slovakia (Švec, P. 1985: In: FEJFAR & HEINRICH 1985; MLÍKOVSKÝ 2002). It was described in the Early Pleistocene (MQ1) as recent species *H. rustica* (LINNAEUS, 1758) from Betfia 2 (ČAPEK 1917; LAMBRECHT 1933; JÁNOSSY 1979a; KESSLER 1975; Gál 2002); Betfia 9 (Romania), (GÁL 2002); Deutsch-Altenburg 4B, 2C - Austria, (JÁNOSSY 1981; DÖPPES, D & RABEDER, 1997; MLÍKOVSKÝ 1998); Osztramos 8 (Hungary), (JÁNOSSY & KORDOS 1976; JÁNOSSY 1986).

The genus was reported outside the Carpathian Basin with the recent species *Hirundo rustica* LINNAEUS, 1758 from Early Pleistocene (MQ1) in Koneprusy and Stranská skála – Czech Republic (JÁNOSSY 1972; MLÍKOVSKÝ 1996) and from younger sites.

Genus *Delichon* MOORE, 1854
Delichon † polgardiensis nova sp.
(Plate III. Figure 10 A-B)

Type locality and age: Polgárdi 5, Late Miocene (MN 13).

Holotype: Coracoideum dext. (MÁFI V.11.94.1; V.29169).

Paratypes: Ulna sin., with damaged proximal epiphysis; 4 distal fragments of ulnae - 3 dext. and one sin. (MÁFI V.11.118.5; V.29193/1-5).

Measurements: 1. coracoid A=16.27 mm, B=15.67 mm; C=3.39 mm, D=2.24 mm, E=1.03 mm; G=3.26 mm; 2. ulna: E=1.69-1.93 mm; F=2.92-3.07 mm; G=2.07-2.27 mm.

Comparative material: Delichon urbica (MTM n=1: 1. coracoid A=16,86 mm, B=16,15 mm; C=3,66 mm, D=3,54 mm, E=1,36 mm; G=3,56 mm; 2. ulna E=1,47 mm; F=2,68 mm; G=1,94 mm.

Diagnosis: Medium sized swallow species. On coracoid in dorsal view (Fig. 10A), the *acrocoracoid* (a) is strongly protruding, the end is rounded, the medial end bulges mildly. *Processus accesorius* (b) is short, hook-like and blunted. Edge of s*ulcus m. supracoracoidei* (c) forms asymmetrical concave line. *Facies artic. humeralis* (d) is bulged and rounded. Point of *processus procoracoidei* (e) does not exceed medial edge of corpus.

On distal epiphysis of ulna in medial view (Fig. 10B), *condylus dorsalis* (a) is more rounded and claw shaped. *Sulcus intercondylaris* (b) is mildly concave. *Condylus ventralis* (c) is oblique conical. *Tuberculum carpale* (d) is more protruding asymmetrical rectangle shape.

Name: refers to the type locality.

Description: It corresponds in its characters to recent species, but differs in its sizes.

Delichon † pusillus nova sp.
(Plate III. Figure 11)

Type locality and age: Csarnóta 2, Pliocene (MN 15-16).

Holotype: Proximal fragment of carpometacarpus sin. (MÁFI V.11.21.1; V.29096).

Measurements: Carpometacarpus C=2.78 mm.

Comparative material: Delichon urbica (MTM n=1; carpometacarpus: C=3.75 mm).

Diagnosis: On proximal epiphysis of carpometacarpus in ventral view (Figure 4), the *trochlea carpalis* (a) has asymmetrically conical and it more bulging than in recent species. *Proc. extensorius* (b) has slightly oblique, rounded beak-like shape. *Processus alularis* (c) has obliquely rectangular shape and the *fovea subalularis* (d) is weakly developed.

Name: The name reffer to it smaller size.

Description: It is smaller as the recent species, but in the characteristics mostly corresponds to it.

Delichon † *major* nova sp.
(Plate III. Figure 12)

Type locality and age: Beremend 26, Pliocene (MN 15-16).

Holotype: Carpometacarpus dext. (BKA)

Measurements: Carpometacarpus A=15.59 mm; B=13.42 mm; C=4.21 mm; D=3.27 mm; E=3.74 mm; F=3.56 mm.

Comparative material: Delichon urbica (MTM n=1: carpometacarpus A=14.99 mm; B=11.80 mm; C=3.90 mm; D=1.70 mm; E=2.90 mm; F=2.80 mm); the extinct species *Delichon pusillus* (carpometacarpus C=2.78 mm).

Diagnosis: On the proximal epiphysis of carpometacarpus in ventral view (Fig. 11), the *trochlea carpalis* (a) has symmetrically conical shape. *Proc. extensorius* (b) has slightly oblique, asymmetrically beak-like shape. *Processus alularis* (c) has rectangular shape and the *fovea subalularis* (d) is well developed angle shaped. *Protuberantia metacarpalis* (e) has triangular shape. The basis of the *metacarpus majus* (f) is wide and rounded.

Name: Was named after its big dimensions.

Description: It corresponds in characters with rececent species, but has larger sizes.

Distribution: The genus is known with recent species only from the Early Pleistocene (MQ1) from the Czech Republic (Stránská skála, MLÍKOVSKÝ 1995); Romania (Betfia 2 , ČAPEK 1917; LAMBRECHT 1933; JÁNOSSY 1979a; KESSLER 1975; GÁL 2002 and Betfia 9, GÁL 2002) and Spain (Quibas, MONTOYA et al. 1999).

Genus *Riparia* FORSTER, 1817
Riparia †*minor* nova sp.
(Plate IV. Figure 13 A-C)

Type locality and age: Polgárdi 4, Late Miocene (MN 13).

Holotype: Coracoideum sin. (MÁFI V.11.66.1; V.29141).

Paratypes: Ulna sin., with damaged proximal epiphysis (MÁFI); 3 ulnae dext., distal fragments (MÁFI V.1.83.4; V.29158/1-4).

Measurements: 1. coracoid C=2.28 mm; D=2.69 mm; E=1.56 mm; 2. ulna A=23-24 mm; E=1.60-1.78 mm; F=2.51-2.72 mm; G=1.89-2.08 mm.

Comparative material: Riparia riparia (MTM n=1: 1. coracoid: C=2.48 mm; D=3.32 mm; E=1.79 mm; 2. ulna: A=20.05 mm; C=3.06 mm; E=1.55 mm; F=2.72 mm; G=1.82 mm);

Diagnosis: Small sized swallow species. On coracoid in dorsal view (Fig. 12A), the *acrocoracoid* (a) has asymmetrical blunt conical shape, its medial edge bulges strongly. *Processus accesorius* (b) is short, hook-like and blunted. *Sulcus m. supracoracoidei* (c) is asymmetrical concave line. Point of *processus procoracoidei* (d) does not exceed medial edge of corpus. *Facies articularis humeralis* (e) is rounded.

On proximal epiphysis of ulna in cranial view (Fig. 12B), *cotyla ventralis* (a) has circular shape. C*otyla dorsalis* (b) is angular and asymmetric (but is damaged). *Tuberculum ligamenti colateralis ventralis* (c) is weakly protruding. *Tuberculum biccipitale* (d) and *incisura radialis* (e) are well expresssed. *Depressio m. brachialis* (f) is deep. On distal epiphysis of ulna in medial view (Fig. 12C), *condylus dorsalis* (g) has blunted and rounded claw shape. *Sulcus intercondylaris* (h) is slightly concave. *Condylus ventralis* (i) has oblique conical shape. *Tuberculum carpale* (j) is obliquely protuding and rounded.

Name: after its small dimensions.

Description: The coracoid differs from recent species in some morphological characters and in its smaller sizes.

Distribution: The genus is known only from the Early Pleistocene (MQ1) from Czech Republic (Stránská skála, MLÍKOVSKÝ 1995) and Romania (Betfia 9, GÁL 2002) with recents species.

Family Aegithalidae, REICHENBACH 1850
Genus *Aegithalos* HERMANN, 1804
Aegithalos † *gaspariki* nova sp.
(Plate IV. Figure 14 A-B)

Type locality and age: Polgárdi 4, 5, Late Miocene (MN 13).

Holotype: Carpometacarpus dext. (*os metacarpale minus* missing), (Polgárdi 5, MÁFI V.11.90.1; V.29165).

Paratype: Humerus sin. (proximal fragment), (Polgárdi 4, MÁFI V.11.76.1; V.29151).

Measurements: 1. humerus C=4.18 mm; 2. carpometacarpus A=7.93 mm; C=2.43 mm; F=2.15 mm.

Comparative material: Aegithalos caudatus (MTM n=1: humerus C=3.78 mm; 2. carpometacarpus A=8.42 mm; C=2.37 mm; F=1.86 mm).

Diagnosis: Larger sized species than recent one. On proximal epiphysis of humerus in caudal view (Fig. 7A), damaged *crista pectoralis* constitutes a mildly bulging line. *Tuberculum dorsale* (a) constitutes weakly developed rounded rectangle. *Caput humeri* (b) has flattened concave shape. *Tuberculum ventrale* (c) is weakly developed. *Crista bicipitalis* (d) constitutes pointed, asymmetric protruding beak shape. *Crus fossae* (e) mildly divides *fossa pneumotricipitalis* (e) into two.

On proximal epiphysis of carpometacarpus in ventral view (Fig. 7B), *trochlea carpalis* (a) has semicircular shape. *Proc. extensorius* (b) has short and truncated conical shape. *Processus alularis* (c) has rounded rectangular shape and *fovea subalularis* (d) has weakly developed acute angle shape. *Protuberantia metacarpalis* (e) is in the external edge of *os metacarpale majus* and forms small and triangular bulgle.

Name: After the name of Mihály GASPARIK, Hungarian paleontologist.

Description: It corresponds more in characters and sizes to recent species of the genus.

Aegithalos † *congruis* nova sp.
(Plate IV. Figure 15 A-B)

Type locality and age: Csarnóta 2, Pliocene (MN 15-16).

Holotype: Tibiotarsus dext. (distal fragment), (MÁFI V.11.15.1; V.29090).

Paratype Coracoid dext. (proximal fragment), (MÁFI V.11.46.1; V.29121).

Measurements: 1. Coracoid C=1,88 mm; D=1.65 mm; 2. tibiotarsus F=1.76 mm; G=1.51 mm.

Comparative material: Aegithalos caudatus (MTM n=1; 1. coracoid: C=1.93 mm; D=1.48 mm; 2. tibiotarsus: F=1.92 mm; G=1.72 mm).

Diagnosis: On cranial part of coracoid (Figure 5A), the *processus acrocoracoidalis* (a) is rounded and strongly protruding. *Processus accesorius* (b) has short and pointed hook-shape. The lateral edge of *facies articularis humeralis* (c) is oblique and strongly bulged. The edge of *sulcus musculi supracoracoidei* (d) is arched. *Processus procoracoidalis* (e) is blunt pointed and it weakly exceeds the medial edge of bones.

On tibiotarsus the distal epiphysis in cranial view (Figure 5B), the *tuberositas retinaculi m. fibularis* (a) is weakly developed and blunted. *Sulcus extensorius* (b) is oblique and has asymmetrical distal end. *Pons supratendinous* (c) is wide and oblique. *Condylus lateralis* (d) has slightly pointed oval shape. *Incisura intercondylaris* (e) has straight and wavy line. *Condylus medialis* (f) has slightly pointed oval-like shape. The its lateral edge is bulged.

Name: The name refer to lat. *congruis*=agreement, corresponding.

Description: It mostly corresponds with recent species in the characters and sizes.

Distribution: The family annd genus is known in fossil material with recent species *Aegithalos caudatus* (LINNAEUS, 1758) from the Early Pleistocene (MQ1) from Betfia 2– Romania (ČAPEK 1917) and S'Onix-Mallorca – Spain (SONDAAR et al. 1995).

Fam. Paridae BOIE, 1826
Genus *Parus* LINNAEUS, 1758
Parus † *robustus* nova sp.
(Plate IV. Figure 16 A-D)

Type locality and age: Csarnóta 2, Pliocene (MN 15-16).

Other locality: Beremened 26, Pliocene (MN 15-16).

Holotype: Ulna sin. (distal fragment), (Csarnóta 2, MÁFI V.11.16.1; V.29091).

Paratypes: Carpometacarpus dext. and sin. (proximal fragments), (Csarnóta 2, MÁFI V.11.47.2; V.29122); Humerus dext., distal fragment of humerus dext. (Beremend 26, BKA).

Measurements: 1. humerus A=18,16 mm; B=6,27 mm; C=6,01 mm; D=5,03 mm; E=1,75mm; F= 5,00-5,06 mm; G=2,45-2,53 mm; 2. ulna E=1.23 mm; F=2.45 mm; G=1.75 mm; 3. carpometacarpus C=2.43-2.77 mm.

Comparative material: Parus major (MTM n=1; 1. ulna: E=1.13 mm; F=1.94 mm; G=1.49 mm, 2. carpometacarpus: C=2.24 mm), *P. palustris* (MTM n=1; 1. humerus A=13,95 mm; B= 4,87 mm; C=4,49 mm; D=4,04 mm; E=1,26 mm; F=3,74 mm; G=1,72 mm; 2. carpometacarpus: C=2.31 mm).

Diagnosis: On proximal epiphysis of humerus in caudal view (Fig. 16A), *crista pectoralis* form rounded contour and the *tuberculum dorsale* (a) has rounded rechtangle shape. C*aput humeri* (b) has wide and slightly convex shape. *Tuberculum ventrale* (c) forms protruding circular spur. *Crista bicipitalis* (d) has protruding and rounded shape. *Crus fossae* (e) is less developed, the *fossae pneumotricipitalis* (f) is not divided into two part. On distal epiphysis in cranial view (Fig. 16B), the *tuberculum supracondylare ventrale* (g) is less developed. *Epicondylus ventralis* (h) is flatten. *Processus flexorius* (i) is strongly protruding and rounded. *Condylus ventralis* (j) has lying oval shape. *Incisura intercondylaris* (k) is wide and has angle shape. *Condylus dorsalis* (l) is crooked oval shaped. *Epicondylus dorsalis* (m) is rounded. *Processus supracondylaris dorsalis* (n) is long, bent and has two unequal branches.

On distal epiphysis of ulna in medial view (Fig. 16C), the *condylus dorsalis* (c) has wide and blunted claw-like shape. *Sulcus intercondylaris* (d) is less concave than in recent genus. *Condylus ventralis* (e) has strongly rounded and obliquely blunted conical shape. *Tuberculum carpale* (f) has asymmetrical

blunted conical shape, but it is narrower than in recent species. .

On proximal epiphysis of carpometacarpus in ventral view (Fig. 16D), the *trochlea carpalis* (a) has bulging blunted conical shape. *Proc. extensorius* (b) has short, rounded and straight beak-like shape. *Processus alularis* (c) forms slightly obliquely and rounded rectangular shape and the *fovea subalularis* (d) has wide acute angle shape.

Name: Was named after its large dimensions.

Description: It is fossil species with larger dimensions than recent *Parus major*.

Parus † *parvulus* nova sp.
(Plate V. Figure 17)

Type locality and age: Csarnóta 2, Pliocene (MN 15-16).

Holotype: Cranial fragment of coracoideum sin. (MÁFI V.11.17.1; V.29092).

Measurements: Coracoid C=2.17 mm; D=1.68 mm.

Comparative material: Parus ater (MTM n=1; coracoid: C=2.23 mm D=2.49 mm), *P. coeruleus* (MTM n=1; coracoid: C= 2.19 mm; D=2.50 mm).

Diagnosis: On coracoid in medial view (Figure 7), the *acrocoracoid* (a) has conical shape. *Processus accesorius* (b) is hook-like. *Sulcus m. supracoracoidei* (c) has semicircular shape. The point of *processus procoracoidei* (d) is blunted and just exceed the medial edge of the corpus.

Name: The name refers to its sizes.

Description: It is small Tit species. The end of the *processus acessorius* is damaged, but this does no hinder the identification.

Parus † *medius* nova sp.
(Plate V. Figure 18 A-B)

Type locality and age: Beremend 26, Pliocene (MN 15-16).

Holotype: Humerus dext. (BKA).

Paratype: Distal fragment of humerus dext. (BKA).

Measurements: Humerus A=14,92 mm; B=5,93 mm; C=4,71 mm; D=3,61 mm; E=1,31-1,44 mm; F=3,57-3,79 mm; G=1,98-2,04 mm.

Comparative material: Parus coeruleus (MTM n=1 humerus A=14,33 mm; B=5,80 mm; C=4,91 mm; D=3,95 mm; E=1,33 mm; F=4,17 mm; G=1,87 mm); *Parus palustris* (MTM n=1: humerus A=13,95 mm; B=4,87 mm; C=4,49 mm; D=4,04 mm; E=1,26 mm; F=3,74 mm; G=1,72 mm).

Diagnosis: On proximal epiphysis of humerus in caudal view (Fig. 18A), *crista pectoralis* forms rounded contour and the *tuberculum dorsale* (a) has rounded rechtangle shape. The c*aput humeri* (b) is wide and slightly convex. *Tuberculum ventrale* (c) forms protruding circular spur. *Crista bicipitalis* (d) has protruding and pointed shape. *Crus fossae* is less developed, the *fossae pneumotricipitalis* (e) is not divided into two part. On distal epiphysis in cranial view (Fig. 6B), the *tuberculum supracondylare ventrale* (f) is less developed; the *epicondylus ventralis* (g) is less rounded. *Processus flexorius* (h) is strongly protruding and rounded. *Condylus ventralis* (i) has lying oval shape. *Incisura intercondylaris* (j) is wide and has angle shape. *Condylus dorsalis* (k) is crooked oval shaped. *Epicondylus dorsalis* (l) is rounded. *Processus supracondylaris dorsalis* (m) has two unequal branches.

Name: Was named after its medium size dimensions.

Description: It is among the medium-sized tits.

Distribution: The genus is known only from Lower Pliocene in the Carpathian Basin as *Parus* sp. foss.indet. from Beremend 26 - Hungary (MN 15) (KESSLER 2010) The recent species was reported in Early Pleistocene (MQ1-2) as *Parus coeruleus* LINNAEUS, 1758 from Betfia 9 –Romania (GÁL 2002); as *Parus major* LINNAEUS, 1758 from Betfia 2, 9-Romania (ČAPEK 1917; LAMBRECHT 1933; JÁNOSSY 1979a; KESSLER 1975; GÁL 2002); Chi□cău 2. - România (KESSLER 1982; JURCSÁK & KESSLER 1988; GÁL 2002); as *Parus lugubris* TEMMINCK, 1820 from Betfia 2 –Romania (GÁL 1917).

The family is known outside the Carpathian Basin only from the Late Pliocene from Varsets (MN 17, Bulgaria) as *Parus* sp. (BOEV 1987b, 2000a); Stránská skalá (MQ1, Czechia) as *Parus major* LINNAEUS, 1758 (JÁNOSSY 1972); *Parus cristatus* C. L. BREHM, 1839; *P. ater* LINNAEUS, 1758 and *P. major* LINNAEUS, 1758 (SOONDAR et al. 1995) (MONTOYA et al. 1999, 2001) and Tarchankut (MQ1, Ukraine) as *Parus major* LINNAEUS, 1758 (VOJINSTVENS'KYJ 1967).

Family Sittidae (BONAPARTE, 1831)
Genus *Sitta* LINNAEUS, 1758
Sitta †*gracilis* nova sp.
(Plate V. Figure 19)

Type locality and age: Polgárdi 4, Late Miocene (MN 13).

Holotype: Carpometacarpus sin. (proximal fragment), (MÁFI V.11.60.1; V.29135).

Measurements: Carpometacarpus C=2.82 mm, D=1.42 mm.

Comparative material: Sitta europaea (MTM n=1: C=3.21 mm; D=1.57 mm).

Diagnosis: Small-sized slider species. On proximal epiphysis of carpometacarpus in ventral view (Fig.19), *trochlea carpalis* (a) has strongly protruding semicircular shape. *Proc. extensorius* (b) is short and asymmetrically rounded. *Processus alularis* (c) is undeveloped and has asymmetric and pointed cone shape. *Fovea subalularis* (d) has acute angled pit.

Name: The name was given after its slenderness.

Description: Its size is smaller than in recent species.

Sitta † *pusilla* nova sp.
(Plate V. Figure 20 A-B)

Type locality and age: Csarnóta 2, Pliocene (MN 15-16), (KESSLER, 2010a).

Holotype: Carpometacarpus dext. (proximal fragment), (MÁFI V.11.34.1; V.29109).

Paratypes: Carpometacarpus dext. (proximal fragment), 2 tarsometatarsi sin. (distal fragments) (MÁFI V.11.53.3; V.29128).

Measurements: 1. carpometacarpus C= 2.22-2.39 mm; 2. tarsometatarsus E=0.99-1.26 mm; F=1.92-2.11 mm; G=1.22-1.57 mm.

Comparative material: Sitta europaea (MTM n=1; 1. carpometacarpus: C=2.99 mm; 2. tarsometatarsus: E=1.11 mm; F=2.15 mm; G=1.46 mm).

Diagnosis: The characteristics corresponds with recent species, but the sizes differ more in carpometacarpus and less in tarsometatarsus.

On proximal epiphysis of carpometacarpus in ventral view (Figure 20A), the *trochlea carpalis* (a) has strongly protruding semicircular shape. *Proc. extensorius* (b) is straight and with rounded end. *Processus alularis* (c) has rounded conical shape. *Fovea subalularis* (d) has acute-angled pit shape.

On distal epiphysis in dorsal view of tarsometatarsus (Figure 20B), the *trochlea metatarsi* II. (a) has laterally protruding, pointed and claw-like shape. *Incisura intertrochlearis medialis* (b) is wider and deep. *Trochlea metatarsi tertii* (c) is wide and in middle it significantly immersed. *Incisura intertrochlearis lateralis* (d) is deep and wide. *Trochlea metatarsi* IV. (e) has blunt conical shape.

Name: The name refers to very small sizes of the species.

Description: The dimensions of fossil species is smaller than of recent species. The *Sitta gracilis* from Polgárdi was described also on the basis of carpometacarpus. It is larger than the Csarnótian specimen (carpometacarpus C=2.82 mm, D=1.42 mm) and differ to it in shape of the *processus extensorius*. The Polgárdi specimen is shorter than in the Csarnótian remains. The *processus alularis* is more pointed. The characteristics corresponds in generaly to recent species. JÁNOSSY (1995) reported this bones as *Sitta* sp.

Sitta † *villanyensis* KESSLER, 2012
(Plate V. Figure 21)

Type locality and age: Beremend 26, Pliocene (MN 15-16).

Holotype: Carpometacarpus dext. (BKA).

Measurements: Carpometacarpus A=12,41 mm; B=11,13 mm; C=3,71 mm; E=3,32 mm; F=2,89 mm.

Comparative material: Sitta europaea (MTM n=1: A=12,61 mm; B=10,90 mm; C=3,64 mm; E=3,43 mm; F= 2,69 mm).

Diagnosis: A small sized slider species. On proximal epiphysis of carpometacarpus in ventral view (Fig. 21), the *trochlea carpalis* (a) has blunt conical shape. *Proc. extensorius* (b) has asymmetrically conical shape. *Processus alularis* (c) is rounded rechtangle shaped. *Fovea subalularis* (d) has acute angled pit. *Protuberantia metacarpalis* (e) is undeveloped, wide and flattened. The basis of the *facies articularis digiti major* (f) is asymmetrically angle shaped. The end of *os metacarpi minus* (g) is beveled.

Name: Was named after the Villány Hill.

Description: It corresponds in characters and size with recent species and differ in these to extinct species from Polgárdi and Csarnóta, which are much smaller.

Distribution: The family and genus were reported from the Carpathian Basin as Sittidae gen et sp. foss. indet. from Subpiatra 2 – Romania (Middle Miocene, MN 6) (KESSLER & VENCZEL 2009). The recent species is known from the Early Pleistocene (MQ1-2) as *Sitta europea* LINNAEUS, 1758 from Betfia 9 - Romania (GÁL 2002); Deutsch-Altenburg 4B – Austria (JÁNOSSY 1981) and from Somssich-Hill 2 – Hungary (JÁNOSSY 1979a, 1980).

The genus is known outside the Carpathian Basin only from the Early Pliocene (MN 16) from Rebielice Królowskie I. (Poland) as *Sitta* sp. (also with smaller sizes) (JÁNOSSY 1974) and from the Late Pliocene from Varsets (MN 17, Bulgaria) (BOEV 1996, 2000). The fossil species *Sitta senogalliensis* PORTIS, 1887 from Senigallia (Upper Miocene, MN 13, Italy) was put by MLÍKOVSKÝ (2002) into „*Family incertae sedis"*.

Family Certhiidae (VIGORS, 1825).
Genus *Certhia* LINNAEUS, 1758
Certhia † *immensa* nova sp.
(Plate V. Figure 22 A-C)

Type locality and age: Csarnóta 2, Pliocene (MN 15-16).

Holotype: Coracoideum dext. (cranial fragment), (MÁFI V.11.22.1; V.29097).

Paratypes: One right and one left side carpometacarpus (proximal fragments); tarsometatarsus sin. (distal fragment), (MÁFI V.11.42.3; V.29117).

Measurements: 1. coracoid: C=2.62 mm; D=2.16 mm; 2. carpometacarpus C=2.47-2.52 mm; 3. tarsometatarsus E=1.03 mm, F=1.84 mm.

Comparative material: Certhia brachydactyla (MTM n=1; 1. coracoid: C=2.14 mm; D=1.36 mm; 2.

carpometacarpus: C=2.15 mm; 3. tarsometatarsus: E=0.76 mm, F=1.56 mm).

Diagnosis: On medial side of coracoid (Figure 22A) in cranial end, the *acrocoracoideum* (a) has asymmetrical rounded cone shape. Its medial edge bulges mildly. The end of *processus accesorius* (b) is damaged, but it is elongated hook-like. The edge of *sulcus m. supracoracoideumei* (c) is mildly flattened concave shape. *Facies articularis humeralis* (d) has cranial edge strongly bulges. The point of *processus procoracoideumei* (e) exceeds the medial edge of corpus.

On proximal epiphysis of carpometacarpus in ventral view (Figure 22B), the *trochlea carpalis* (a) is asymmetrically bulging. *Proc. extensorius* (b) is obliquely blunted conical shaped with rounded end. *Processus alularis* (c) is small, protruding and has asymmetrical conical shape. *Fovea subalularis* (d) has asymmetrical truncated conical shape.

On distal epiphysis of tarsometatarsus in dorsal view (Figure 9C), the edge (a) between *fossa metatarsi* I. and *trochlea metatarsi* II. is weakly waved. *Trochlea metatarsi II.* (b) has truncated conical shape. *Incisura intertrochlearis medialis* (b) is mildly wide and deep. *Trochlea metatarsi III.* (c) is wide, and its end is strongly and wide concave. *Incisura intertrochlearis lateralis* (d) is wide and deep. *Trochlea* metatarsi IV. (e) has rounded blunt conical shape.

Name: The name reffer to larger dimensions of species.

Description: The sizes are larger than in recent species.

Distribution: The family and genus was reported with fossil species only from the Carpathian Basin. Certhiidae gen. et sp. foss.indet. was reported from Subpiatra 2. – Romania (Middle Miocene, MN6), (KESSLER & VENCZEL 2009) and *Certhia janossyi* KESSLER et HÍR, 2012 from Rudabánya (Upper Miocene, MN 9) (KESSLER & HÍR 2012b). The recent species was reported from Betfia 2-Romania (Lower Pleistocene MQ1) (ČAPEK 1917; LAMBRECHT 1933; JÁNOSSY 1979a; KESSLER 1975; GÁL 2002).

Family Tichodromidae SWAINSON, 1827
Genus *Tichodroma* ILLIGER, 1811
Tichodroma †capeki nova sp.
(Plate VI. Figure 23 A-B)

Type locality and age: Polgárdi 4, Late Miocene (MN 13).

Holotype: Humerus dext. (proximal fragment), (MÁFI V.11.68.1; V29143).

Measurements: Humerus B=5.04 mm; C=5.13 mm; D=4.91 mm; E=1.89 mm.

Comparative material: Tichodroma muraria (MTM n=1: B=5.66 mm; C=5.67 mm; D=5.26 mm; E=1.93 mm).

Diagnosis: Fossil species, smaller than recent one. On proximal epiphysis of humerus in cranial view (Fig. 23A), c*aput humeri* (a) is convex, but not too protruding. *Tuberculum dorsale* (b) is less rounded up than in recent genus. *Sulcus lig. transversus* (c) is more wide and deep than in recent species. *Crista bicipitalis* (d) is protruding in a point similarly to, but more blunted than in recent species, distal edge is similarly concave. In caudal view (Fig. 23B), *tuberculum ventrale* (e) is well developed and rounded. C*rus fossae* (f) is weakly developed and the two parts of *fossa pneumotricipitalis* (g) can be separated with dificulty.

Name: After the name of Waclav ČAPEK, Czech paleornithologist.

Description: Its characters correspond to recent species.

Distribution: The family and genus are not known in other fossil materials.

Family Muscicapidae VIGORS, 1825
Genus *Muscicapa* LINNAEUS, 1766
Muscicapa † miklosi nova sp.
(Plate VI. Figure 24).

Type locality and age: Polgárdi 4, Late Miocene (MN 13).

Holotype: Femur sin. (distal fragment), (MÁFI V.11.67.1; V.29142).

Measurements: Femur E=1.28 mm; F=2.51 mm; G=1.98 mm.

Comparative material: Muscicapa albicollis (MTM n=1: E=0.95 mm; F=2.05 mm; G=1.59 mm); *M. hypoleuca* (MTM n=1: F=2.46 mm); *M. parva* (MTM n=1: E=0.94 mm; F=2.01 mm; G=1.79 mm); *M. striata* (MTM n=1: E=1.24 mm; F=2.37 mm; G=2.09 mm).

Diagnosis: Small flycatcher species. On distal epiphysis of femur in caudal view (Fig. 24), *trochlea fibularis* (a) is slightly pointed in contrast with recent species. Distal end of *condylus lateralis* (b) constitutes an arc. *Incisura intercondylaris* (c) is concave-like, but less than in recent genus. *Condylus medialis* (d) is oblique, but more pointed than in recent genus. *Epicondylus medialis* (e) and *epicondylus lateralis* are rounded, but weakly developed.

Name: After the name of Miklós KRETZOI, Hungarian paleornithologist.

Description: It corresponds in characteristics and sizes to recent species of the genus. The fossil species *Muscicapa leganyii* KESSLER et HÍR, 2012 from the Middle Miocene (MN 7/8) of Felsőtárkány-Felnémet 2/3 (KESSLER & HÍR 2012) was identified based on the coracoid. This bone also corresponds in characteristics and sizes to recent species, but its age is older than Polgárdi specimen.

Muscicapa † petényii nova sp.
(Plate VI. Figure 25)

Type locality and age: Beremend 26, Pliocene (MN 15-16).

Holotype: Carpometacarpus dext. (BKA).

Measurements: Carpometacarpus A=11,29 mm; F=2,79 mm.

Comparative material: Muscicapa striata (MTM n=1: carpometacarpus A=11,84 mm; F=2,06 mm); *Muscicapa parva* ((MTM n=1: carpometacarpus A=10,09 mm; F=1,96 mm); *Ficedula albicollis* (MTM n=1: carpometacarpus A=11,49 mm; F=2,33 mm).

Diagnosis: On proximal epiphysis of carpometacarpus in ventral view (Fig. 9), the *trochlea carpalis* (a) is symmetrical bulging, with rounded and conical shape. *Processus alularis* (b) has rounded rechtangle shape. *Fovea subalularis* (c) has acute angled pit. *Protuberantia metacarpalis* (d) is well developed, wide and pointed. The basis of *facies articularis digiti major* (e) is symmetrically angle shaped. The end of *os metacarpi minus* (g) is beveled.

Name: Was named after Hungarian paleontologist Salamon János PETÉNYI.

Description: It corresponds in characters and in dimensions to recent species of *Muscicapa (Ficedula)* genus. The missing *processus extensorius* does not prevent the identification. The extinct species known from the Carpathian Basin differ in age to Beremendian specimen, and were described from other type of bones.

Distribution: The genus was reported as *Muscicapa leganyii* KESSLER et HÍR, 2012 from the Middle Miocene (MN 7/8) of Felsőtárkány-Felnémet 2/3 (KESSLER & HÍR 2012) and the Late Pliocene – Early Pleistocene boundary (MN 17-18) from S'Onix - Mallorca (Spain) as *Muscicapa striata* (PALLAS, 1764), (SONDAAR et al. 1995); from Varshets (Bulgaria) as *Muscicapa* sp. (BOEV 1996, 2000); from Mas Ramboult (France) as *Ficedula hypoleuca* (PALLAS, 1764), (MOURER-CHAUVIRÉ 1975) and as *Ficedula* sp. from Montoussé (France) (CLOT et al. 1976).

Genus *Luscinia* FORSTER, 1817
Luscinia †denesi nova sp.
(Plate VI. Figure 26)

Type locality and age: Polgárdi 4, Late Miocene (MN 13)

Holotype: Humerus dext. (distal fragment), (MÁFI V.11.72.1; V.29147).

Measurements: Humerus E=1.52 mm; F=3.92 mm; G=2.23 mm.

Comparative material: Luscinia luscinia (MTM n=1: E=1.68 mm; F=4.26 mm; G=2.29 mm); *L. megarhynchos* (MTM n=1: E=1.59 mm; F=4.05 mm; G=2.39 mm); *L. svecica* (MTM n=1: E=1.55 mm; F=4.04 mm; G=2.16 mm).

Diagnosis: Smaller species than recent species of the genus. In cranial view (Fig.11) of distal epiphysis of humerus, the *tuberculum ventrale* is undeveloped; *epicondylus ventralis* (a) is well developed but is protruding more strongly than in recent genus. *Processus flexorius* (b) is wide, rounded and less protruding than in recent genus. *Condylus ventralis* (c) has stretched oval shape. *Incisura intercondylaris* (d) has deep and pointed pit. *Condylus dorsalis* (e) has mildly bent oval shape. *Epicondylus dorsalis* (f) is rounded. *Proc. supracondylaris dorsalis* (g) is averagely long, widening between it and diaphysis is deeper and wider than in recent genus.

Name: After the name of Dénes JÁNOSSY, Hungarian paleornithologist.

Description: It corresponds in characters to the recent genus. The fossil species *Luscinia praeluscinia* KESSLER ET HÍR, 2012 from the Early Miocene (MN5) from Litke 2 (North Hungary) was identified based on the coracoid, so there is no basis of comparasion. The fossil species *Luscinia jurcsáki* KESSLER et VENCZEL, 2011 from Subpiatra (Middle Miocene, MN 6, Romania) was identified also on the basis of its humerus, and differs from the Polgárdi specimen in characters of *epicondylus lateralis* (the *tuberculum supracondylare ventrale* is not protruding, the *processus flexorius* is much wider and protruding), therefore it is somewhat larger. The Polgárdi specimen has intermediate size between recents species *Luscinia luscinia* (LINNAEUS, 1758) and *L. megarhynchos* C. L. BREHM, 1831. This material was described as *Luscinia* sp. by JÁNOSSY (1992, 1995) and KESSLER (2010).

Luscinia † pliocaenica nova sp.
(Plate VI. Figure 27 A-B)

Type locality and age: Beremend 26, Pliocene (MN 15-16).

Holotype: Distal fragment of humerus dext. (BKA).

Paratype: Carpometacarpus sin. (damaged) (BKA).

Measurements: 1, humerus E=1,75 mm; F=4,32 mm; G=2,29 mm; 2**.** carpometacarpus A=14,92 mm; E=2,75 mm; F=3,14 mm.

Comparative material: Luscinia megarhynchos (MTM n=1: humerus E=1,61 mm; F=4,31 mm; G= 2,25 mm; carpometacarpus A=12,51 mm; E=3,00 mm; F=3,18 mm); *Luscinia luscinia* (MTM n=1: humerus E=1,59 mm; F=4,26 mm; G=mm; carpometacarpus A= 24,02 mm; E=3,89 mm; F=4,85 mm) .

Diagnosis: On distal epiphysis in cranial view of humerus (Fig. 27A), the *tuberculum ventrale* (a) is well developed; the *epicondylus ventralis* (b) is rounded. *Processus flexorius* (c) is rounded and less protruding. *Condylus ventralis* (d) is strongly bulged. *Incisura intercondylaris* (e) has deep and wide pit shape. *Condylus dorsalis* (f) has mildly bent oval

shape. *Epicondylus dorsalis* (g) is rounded. *Proc. supracondylaris dorsalis* (h) is short but probable it is damaged.

On proximal epiphysis of carpometacarpus in ventral view (Fig. 27B), the *trochlea carpalis* (a) is symmetrical bulging. *Fovea subalularis* (b) is wide and less concave shaped. *Protuberantia metacarpalis* (c) is well developed and pointed. The end of *os metacarpalis minus* (d) is asymmetrically rounded.

Name: Was named after the age of the sites.

Description: The characters of carpometacarpus corresponds to recent genus despite its damages, however, it has largest dimensions than in recent species.

Distribution: The genus is known for extinct species from Litke 2 - Hungary (Lower Miocene, MN5) as *Luscinia* † *praeluscinia* KESSLER et HÍR, 2012 (KESSLER & HÍR 2012); from Subpiatra - Romania (MIidle Miocene, MN6) as *Luscinia* † *jurcsaki* KESSLER et VENCZEL, 2011 (KESSLER & VENCZEL 2011). The recent species are known from the Pleistocene as *Luscinia luscinia* (LINNAEUS, 1758) from Betfia 9 (Q1, GÁL 2002); as *Luscinia megarhynchos* C. L. BREHM, 1831 from Betfia 9 (Q1, GÁL 2002); as *Luscinia svecica* (LINNAEUS, 1758) from Hundsheim (Q3, MLÍKOVSKỳ 2009), etc.

The genus was reported outside the Carpathian Basin as *Luscinia svecica* (LINNAEUS, 1758) by JÁNOSSY from Rebielice I. (Upper Pliocene, Poland), (JÁNOSSY 1974) and from Stránská skála (MQ1, Czechia), (JÁNOSSY 1972).

Genus *Erithacus* CUVIER, 1801
Erithacus † *minor* nova sp.
(Plate VI. Figure 28 A-B)

Type locality and age: Beremend 26, Pliocene (MN 15-16).

Holotype: Carpometacarpus dext. (BKA).

Paratypes: Two fragment distal of humeri (dext. and sin.) (BKA).

Measurements: 1. humerus E=1,43-1,55 mm; F=3,55-3,77 mm; G=1,84-1,85 mm; 2. carpometacarpus A=8,98 mm; C=2,54 mm; E=2,17 mm; F=2,36 mm.

Comparative material: Erithacus rubecola (MTM n= 1: humerus E=1,53 mm; F=3,88 mm; G=1,97 mm; 2. carpometacarpus A=10,27 mm; C=2,71 mm, E=2,35 mm; F=2,45 mm).

Diagnosis: On distal epiphysis in cranial view of humerus (Fig. 28A), the *tuberculum ventrale* (a) is well developed; the *epicondylus ventralis* (b) is well developed and rounded. *Processus flexorius* (c) is wide, rounded and less protruding than in recent genus. *Condylus ventralis* (d) is strongly bulged. *Incisura intercondylaris* (e) has deep and wide pit shape. *Condylus dorsalis* (f) has mildly bent oval shape. *Epicondylus dorsalis* (g) is rounded. *Proc. supracondylaris dorsalis* (h) is long and has two small branches.

On proximal epiphysis of carpometacarpus in ventral view (Fig. 28B), the *trochlea carpalis* (a) is symmetrical bulging, with rounded and conical shape. *Processus extensorius* (b) is asymmetrically oblique conical shaped. *Processus alularis* (c) is less developed. *Fovea subalularis* (d) has depp and triangular shape. *Protuberantia metacarpalis* (e) is small but well developed and pointed. The basis of *facies articularis digiti major* (f) is straight. The end of *os metacarpalis minus* (g) is asymmetrically rounded.

Name: The name refers to its sizes.

Description: It corresponds in characters to recent species, but it is smaller.

Distribution: The extinc species *Erithacus* † *horusitskyi* KESSLER et HÍR, 2012 is known from Mátraszölős 1., (Middle Miocene, MN 7/8) (KESSLER & HÍR 2012). As *Erithacus* sp. was reported from Beremend 17 (Q1- Lower Pleistocene) (JÁNOSSY 1992, 1995). Recent species *Erithacus rubecola* was reported from Betfia 2, 9 - Q1 (KORMOS 1913, ČAPEK 1917; LAMBRECHT 1933; JÁNOSSY 1979; KESSSLER 1975; GÁL 2002); Q3/I: Hundsheim (MLÍKOVSKY 2009); Q4/I: Velika Pecina (M. MALEZ 1975; V. MALEZ 1984, 1988); and from the Early Pleistocene of Spain and from the Middle Pleistocene of England, France, Israel and Italy (TYRBERG 1998).

Genus *Phoenicurus* FORSTER, 1817
Phoenicurus † *erikai* nova sp.
(Plate VII. Figure 29).

Type locality and age: Csarnóta 2, Pliocene (MN 15-16).

Holotype: Ulna dext. (distal fragment) (MÁFI V.11.25.1; V.29100).

Measurements: Ulna F=2.43 mm; G=1.55 mm.

Comparative material: Phoenicurus ochrurus (MTM n=1; ulna: F=2.53 mm; G=1.61 mm); *Phoenicurus phoenicurus* (MTM n=1; ulna: F=2.77 mm; G=1.85 mm).

Diagnosis: On distal epiphysis in medial view (Fig. 29), *condylus dorsalis* (a) has wide and blunt claw shape. *Sulcus intercondylaris* (b) is slightly concave. *Condylus ventralis* (c) has semicircular shape. *Tuberculum carpale* (d) has asymmetrical, blunt conical shape.

Name: named after Hungarian paleornithologist Erika GÁL.

Description: It corresponds in characteristics to recent genus, but it resemble in sizes with smaller recent species.

Phoenicurus † *baranensis* nova sp.
(Plate VII. Figure 30)

Type locality and age: Beremend 26, Pliocene (MN 15-16).

Holotype: Humerus dext. with damaged proximal epiphysis (BKA).

Paratypes: Distal fragments of the right and left side humerus (BKA).

Measurements: Humerus A=18,08 mm; B=6,86 mm; E=1,71-1,78 mm; F=4,73-5,05 mm; G=2,50-2,59 mm.

Comparative material: Phoenicurus ochrurus (MTM n=1: humerus A=15,29 mm; B=5,17 mm; E=1,47 mm; F=4,23 mm; G=2,09 mm); *Phoenicurus phoenicurus* (MTM n=1: humerus A=17,40 mm; B=5,86 mm; E=1,60 mm; F=4,54 mm; G=2,17 mm);

Diagnosis: On distal epiphysis of humerus in cranial view (Fig. 30), the *tuberculum supracondylare ventrale* (a) is well developed. *Epicondylus ventralis* (b) is asymmetrically rounded. *Processus flexorius* (c) is protruding and has rounded end. *Condylus ventralis* (d) has oval shape. *Incisura intercondylaris* (e) has wide acute angle shape. *Condylus dorsalis* (f) has bented oval shape. *Epicondylus dorsalis* (g) is rounded. *Proc. supracondylaris dorsalis* (h) is wide and has two unequal branches.

Name: refers to name of Baranya County.

Description: It characteristics corresponds to recent genus, but has alargest dimensions.

Distribution: The genus was reported only from Quibas – Spain (Lower Pleistocene, Q1) (MONTOYA et al. 1999) and the recent species from some localities from the Middle and the Late Pleistocene in Europa (TYRBERG 1998).

Genus *Monticola* Boie, 1822
Monticola † *pongraczi* nova sp.
(Plate VII. Figure 31)

Type locality and age: Beremend 26, Pliocene (MN 15-16).

Holotype: Distal fragment of humerus sin. (BKA)

Measurements: Humerus F=6,35 mm; G=3,08 mm.

Comparative material: Monticola saxatilis (MTM n=1: humerus F=6,36 mm; G=3,36 mm).

Diagnosis: On distal epiphysis of humerus in cranial view (Fig. 31), the *tuberculum supracondylare ventrale* (a) is well developed. *Epicondylus ventralis* (b) is strongly rounded. *Processus flexorius* (c) is protruding and has rounded end. *Condylus ventralis* (d) has oval shape. *Incisura intercondylaris* (e) has wide acute angle shape. *Condylus dorsalis* (f) has bented oval shape. *Epicondylus dorsalis* (g) is rounded. *Proc. supracondylaris dorsalis* (h) is long and has two small branches.

Name: Was named after the name of László PONGRÁCZ who created the „Beszélő Kövek" Foundation.

Description: It corresponds mostly in characteristics and size to recent species.

Distribution: The genus is known only the Middle and the Late Pleistocene to recent species from Cyprus, France, Italy and Romania (TYRBERG 1998).

Genus Saxicola BECHSTEIN, 1892
Saxicola †*lambrechti* nova sp.
(Plate VII. Figure 32 A-D)

Type locality and age: Polgárdi 4, 5; Late Miocene (MN 13).

Holotype: Humerus sin. (Polgárdi 5, MÁFI V.11.106.1; V.29181).

Paratypes: Three humeri sin. (2 proximal fragments) (Polgárdi 4,5); ulna sin. (proximal fragment), (Polgárdi 4) (MÁFI V.11.110.3, V.11.128.2); tibiotarsus sin. (distal fragment), (Polgárdi 5) (MÁFI V.29185).

Measurements: 1. humerus A=16.41-17.07 mm; B=3.93 mm; C=4.99-5.51 mm; E=1.65 mm; F=4.21 mm; G=2.37 mm; 2. ulna B=2.67 mm; C=2.88 mm; F=2.41 mm; G=1.56mm; 3. tibiotarsus F=2.49 mm; G=2.43 mm.

Comparative material: Saxicola rubetra (MTM N=1: humerus A=16.42 mm; C=4.36 mm; E=1.44 mm; F=4.04 mm; ulna B=2.45 mm; C=2.64 mm; tibiotarsus F=2.37 mm; G=2.09 mm); *S. torquata* (MTM N=1: humerus A=15.45 mm; B=3.93 mm; C=4.99-5.51 mm; E=1.54-1.66 mm; F=3.73-3.88 mm; G=2.17-2.58 mm; ulna B=2.38 mm; C=2.60 mm; E=1.25 mm; F=2.30 mm; G=1.70 mm; tibiotarsus F=2.24 mm).

Diagnosis: Fossil species, that corresponds in size to recent species of genus. On proximal epiphysis of humerus in caudal view (Fig. 32A), *tuberculum dorsale* (a) is rounded. *Caput humeri* (b) is wide, flat and hardly bulging. *Tuberculum ventrale* (c) is well developed and has circular shape. *Crista bicipitalis* (d) is asymmetrical rounded and protruding. C*rus fossae* (e) is well developed and *fossae pneumotricipitalis* (f) is divided into two parts. On distal epiphysis in cranial view (Fig. 32B), *tuberculum supracondylare ventrale* (g) is developed. *Epicondylus ventralis* (h) forms straight line. *Processus flexorius* (i) is protruding and has rounded end. *Condylus ventralis* (j) has stretched oval shape. *Incisura intercondylaris* (k) is deeper than in recents speceies. *Condylus dorsalis* (l) has bented oval shape. *Epicondylus dorsalis* (m) forms straight line, while in recent genus is rounded. (*Proc. supracondylaris dorsalis* (n) is damaged).

On proximal epiphysis of ulna in cranial view (Fig. 32C), the *oleocranon* (a) is long, with blunted end. *Cotyla dorsalis* (b) has protruding semicircular shape. C*otyla ventralis* (c) has circular shape.

Tuberculum lig. colat. ventralis (d) and *depressio m. brachialis* (e) are well developed.

On tibiotarsus the distal epiphysis in cranial view (Fig. 32D), the *tuberositas retinaculi m. fibularis* (a) is small and asymmetrically triangular. *Sulcus extensorius* (a) is less wide and has narrowing end. *Pons supratendinous* (c) is wide and straight. *Condylus lateralis* (d) has reverse oval shape, and is laterally flattened and distally pointed. *Incisura intercondylaris* (e) has concave and wavy line. *Condylus medialis* (f) has oval shape.

Name: After the name of Kálmán LAMBRECHT, Hungarian paleornithologist.

Description: It corresponds in characters and sizes to recent species of the genus.

Saxicola † *baranensis* nova sp.
Plate VII. Figure 33 A-C)

Type locality and age: Pliocene (MN 15-16).

Other locality: Beremend 26, Pliocene (MN 15-16).

Holotype: Ulna dext. (proximal fragment), (Csarnóta 2, MÁFI V.11.18.1; V.29093).

Paratypes: Distal fragment of humerus dext., distal fragment of ulna dext. (Beremend 26, BKA).

Measurements: 1. humerus E=1,59 mm; F=4,42 mm, G=2,28 mm; 2. ulna B=2.65 mm; C=2.92 mm; F=2,76 mm; G=1,73 mm.

Comparative material: Saxicola rubetra (MTM n=1; humerus E=1,51 mm; F=4,38 mm, G=2,15 mm; ulna: B=2.45 mm; C=2,64 mm; F=2,47 mm); *Saxicola torquata* (MTM n=1; humerus E=1,44 mm; F=4,04 mm, G=1,95 mm; ulna: B=2.38 mm; C=2.57 mm; F=2,30 mm).

Diagnosis: On distal epiphysis of humerus in cranial view (Fig. 33A), the *tuberculum supracondylare ventrale* (a) is well developed. *Epicondylus ventralis* (b) is strongly rounded. *Processus flexorius* (c) is protruding and has rounded end. *Condylus ventralis* (d) has extended oval shape. *Incisura intercondylaris* (e) has acute angle shape. *Condylus dorsalis* (f) has bented oval shape. *Epicondylus dorsalis* (g) is rounded. *Proc. supracondylaris dorsalis* (h) is long and has two unequal branches.

On proximal epiphysis of ulna in cranial view (Fig. 33B), the *oleocranon* (a) is not very long, straight with rounded end. *Cotyla dorsalis* (b) is projecting and has semicircular end. *Cotyla ventralis* (c) has circular shape. The *tuberculum lig. colat. ventralis* (d) and the *depressio m. brachialis* (e) are well developed.

On distal epiphysis of ulna in medial view (Fig. 33C), the *condylus dorsalis* (a) has wide and claw-like shape. *Sulcus intercondylaris* (b) has less concave shape. *Condylus ventralis* (c) has semicircular shape.

Name: refers to Baranya County .

Description: Its characteristics corresponds to recent genus and has larger sizes than recent species.

Saxicola †*parva* nova sp.
(Plate VIII. Figure 34)

Type locality and age: Csarnóta 2, Pliocene (MN 15-16).

Holotype: Ulna dext. (proximal fragment), (MÁFI V.11.24.1; V.29099).

Paratype: Ulna sin. (proximal fragment), (MÁFI V.11.43.1; V.29118).

Measurements: Ulna B=2.21 mm; C=2.49-2.51 mm.

Comparative material: Saxicola rubetra (MTM n=1; ulna: B=2.45 mm; C=2.64 mm); *Saxicola torquata* (MTM n=1; ulna: B=2.38 mm; C=2.57 mm).

Diagnosis: On proximal epiphysis of ulna in cranial view (Figure 11), the *oleocranon* (a) is long and has conical shape with rounded end. *Cotyla dorsalis* (b) is less projecting than in *Saxicola baranensis* and has asymmetrical conical shape with rounded end. C*otyla ventralis* (c) has circular shape. The *tuberculum lig. colat. ventralis* (d) and the *depressio m. brachialis* (e) are well developed.

Name: The name refers to smaller sizes of species.

Description: It is smaller than *S. baranensis*. The characteristics and dimensions corresponds to smaller species of recent genus.

Saxicola † *magna* nova sp.
(Plate VIII. Figure 35)

Type locality and age: Beremend 26, Pliocene (MN 15-16).

Holotype: Distal fragment of humerus sin. (BKA).

Paratype: Distal fragment of humerus sin. (BKA).

Measurements: Humerus F=4,73-4,84 mm; G=2,53-2,59 mm.

Comparative material: Saxicola rubetra (MTM n=1: humerus F=4,38 mm, G=2,15 mm); *Saxicola torquata* (MTM n=1: humerus F=4,04 mm, G=1,95 mm).

Diagnosis: On distal epiphysis of humerus in cranial view (Fig. 13A), the *tuberculum supracondylare ventrale* (a) is well developed. *Epicondylus ventralis* (b) is strongly rounded. *Processus flexorius* (c) is protruding and has rounded end. *Condylus ventralis* (d) has oval shape. *Incisura intercondylaris* (e) has wide acute angle shape. *Condylus dorsalis* (f) has bent oval shape. *Epicondylus dorsalis* (g) is rounded. *Proc. supracondylaris dorsalis* (h) is long and wide and has two unequal branches.

Name: Was named after its larger dimensions.

Description: Its characteristics corresponds to recent genus and has larger sizes than recent species.

Distribution: The recent species was reported from Betfia 2 and 9 –Romania (Lower Pleistocene, Q1) as *Saxicola rubetra* (Betfia 9, GÁL 2002) and *Saxicola torquata* (Betfia 2; ČAPEK 1917; LAMBRECHT 1933; JÁNOSSY 1979a; KESSLER 1975; GÁL 2002).

The genus is known outside the Carpathian Basin only from Early Pleistocene (MQ1) from Voigstedt (Germany) (JÁNOSSY 1965) and from Quibas (Spain) (MONTOYA et al.1999).

Genus *Oenanthe* VIELLOT, 1816
Oenanthe †*kormosi* nova sp.
(Plate VIII. Figure 36 A-D)

Type locality and age: Polgárdi 5, Late Miocene (MN 13).

Holotype: Femur dext. (MÁFI V.11.103.1; V.29178).

Paratypes: Carpometacarpus dext. (proximal fragment); tibiotarsus dext. (distal fragment); tarsometatarsus sin. (distal fragment), (MÁFI V.11.125.3; V.29200).

Measurements: 1. carpometacarpus C=3.91 mm; 2. femur A=18.71 mm; B=17.55 mm; C=3.32 mm; D=2.11 mm; E=1.59 mm; F= 3.45 mm; G=2.46 mm; 3. tibiotarsus E=1.45 mm; F=3.04 mm; G=2.78 mm.; tarsometatarsus E=1.29 mm; F=2.56 mm; G=1.53 mm.

Comparative material: Oenanthe oenanthe (MTM n= 1: 1. carpometacarpus C=3.55 mm; 2. femur A=17.49 mm; B=16.21 mm; C=3.18 mm; D=2.01 mm; E=1.51 mm; F=3.21 mm; G=2.52 mm; 3. tibiotarsus E=1.46 mm; F=2.76 mm; G=2.72 mm; 4. tarsometatarsus E=1.27 mm; F=2.33 mm; G= 1.43 mm). *O. hispanica* (MTM n=1: 1. carpometacarpus C=2.55 mm; 2. tibiotarsus E=1.34 mm; F= 2.86 mm; 3. tarsometatarsus E=1.24 mm; F=1.75 mm; G=1.23 mm).

Diagnosis: Fossil species, larger than species of recent genus. On proximal epiphysis of carpometacarpus in ventral view (Fig. 36A), *trochlea carpalis* (a) is slightly asymmetrically bulging, with rounded and conical shape, as in recent genus. *Processus extensorius* (b) has long and stretched beak-like shape, with rounded end. *Processus alularis* (c) has small conical shape. *Fovea subalularis* (d) has asymmetrical mangled conical shape.

On proximal epiphysis of femur in caudal view (Fig. 36B), the *trochanter femoris* (a) is rounded. *Fossa trochanteris* (b) is weakly concave. *Facies articularis acetabularis* (c) has round pit. *Impressiones obturatoriae* (d) has stretched oval shape. On distal epiphysis, *trochlea fibularis* (e) is rounded. *Crista tibiofibularis* (f) is well developed. *Condylus lateralis* (g) is rounded distally. *Incisura intercondylaris* (h) has deeply concave line. *Condylus medialis* (i) has oblique conical shape and is more pointed than in recent genus. *Epicondylus medialis* (j) is undeveloped.

On distal epiphysis of tibiotarsus in cranial view (Fig. 36C), the *tuberositas retinaculi m. fibularis* (a) is wide with rounded point. *Sulcus extensorius* (b) is wide and pointed distally. *Pons supratendinous* (c) is wide and straight. *Condylus lateralis* (d) has oval shape. *Incisura intercondylaris* (e) has slightly oblique and wavy line. *Condylus medialis* (f) has oval shape.

On distal epiphysis of tarsometatarsus in dorsal view (Fig. 36D), the *trochlea metatarsi* II. (a) has thin and claw-like shape. *Incisura intertrochlearis medialis* (b) is wide and deep. *Trochlea metatarsi* III. (c) is weakly wide with slightly concave ende. *Incisura intertrochlearis lateralis* (d) is slightly wide and deep. *Trochlea* metatarsi IV. (e) has thin and flattened blunt conical shape.

Name: After the name of Tivadar KORMOS, Hungarian paleontologist.

Description: In its characteristics and sizes close to the recent species *Oenanthe oenanthe* (LINNAEUS, 1758), but is somewhat larger, also than the species from rest of the family, but it is smaller than *Monticola.*

Oenanthe † *pongraczi* nova sp.
(Plate VIII. Figure 37 A-D)

Type locality and age: Csarnóta 2, Pliocene (MN 15-16).

Other locality: Beremend 26, Pliocene (MN 15-16).

Holotype: Ulna dext. (distal fragment), (Csarnóta 2, MÁFI V.11.23.1; V.29098).

Paratypes: Distal fragment of humerus sin., carpometacarpus sin. and phalanga alae 1. dig.II. (Beremend 26, BKA).

Measurements: 1, humerus F=4,78 mm; G=2,38 mm; F=4,73-4,84 mm; G=2,53-2,59 mm; 2. ulna F=3.09 mm; G=2.11 mm; 3. carpometacarpus A=15,78 mm; B=13,04 mm; C=3,68 mm; E= 3,55 mm; F=3,45 mm; 4. ph.alae A=7,88 mm; C=2,23 mm, E=2,65 mm; F=2,39 mm.

Comparative material: Oenanthe oenanthe (MTM n=1; humerus F=4,79 mm; G=2,58 mm; ulna: F=3.05 mm; G=2.17 mm; carpometacarpus A=14,40 mm; B= 12,04mm; C=3,30 mm; E=3,02mm; F= 3,19 mm; ph.alae A=7,51 mm); *Oenanthe hispanica* (MTM n=1; humerus F=4,51 mm; G=2,21 mm; ulna: F=2.41 mm; G=1.74 mm; carpometacarpus A=13,35 mm; B=11,56 mm; C=2,55 mm; E=3,15 mm; F= 3,12 mm).

Diagnosis: On distal epiphysis of humerus in cranial view (Fig. 37A), the *tuberculum supracondylare ventrale* (a) is well developed. *Epicondylus ventralis* (b) is rounded. *Processus flexorius* (c) is less protruding and has rounded end. *Condylus ventralis* (d) has oval shape. *Incisura intercondylaris* (e) has wide acute angle shape.

Condylus dorsalis (f) has bent oval shape. *Epicondylus dorsalis* (g) is rounded. *Proc. supracondylaris dorsalis* (h) has conical shape.

On distal epiphysis of ulna in cranial view (Fig. 37B), the *condylus dorsalis* (a) has pointed claw shape. *Sulcus intercondylaris* (b) is wide and slightly concave, less than in the recent species. *Condylus ventralis* (c) has wide and blunted conical shape. *Tuberculum carpale* (d) is semicircular protruding. Between it and the condylus ventralis one deep pit can be found.

On carpometacarpus in ventral view (Fig. 37C), the *trochlea carpalis* (a) is symmetrical bulging, with rounded and conical shape, as in the recent genus. *Processus extensorius* (b) has long and oblique beak-like, with rounded end. *Processus alularis* (c) has rounded rectangular shape. *Fovea subalularis* (d) has asymmetrical mangled conical shape. *Protuberantia metacarpalis* (e) has blunted triangular shape. The basis of the *facies articularis digiti major* (f) is asymmetrical triangular shaped. The distal end of the *os metacarpalis minus* (g) is cut off in straight line.

In phalanga alae (Fig. 37D) the proximal edge (c) is projecting in asymetrically rounded form, The ventral point (a) has conical shape. The dorsal point (b) is laterally projecting in conical form. The dorsal edge (d) is bended, while the distal edge (e) is rounded.

Name: after László PONGRÁCZ, who created the „Beszélő Kövek" Foundation.

Description: It mostly corresponds in charachteristics to recent species *Oenanthe oenanthe,* but differ in sizes (it is larger).

Distribution: The earliest report of the genus outside the Carpathian Basin is only the Early Pleistocene (MQ1) from Stránská skála (Czech Republic) (JÁNOSSY 1972); Montoussé 5. (France) (CLOT et al. 1976) Quibas (Spain) (MONTOYA et al. 1999).

Family Turdidae RAFINESQUE, 1815
Genus † *Turdicus* KRETZOI, 1962
†*Turdicus pannonicus* nova sp.
(Plate IX. Figure 38 A-B)

Type locality and age: Polgárdi 4, 5; Late Miocene (MN 13).

Holotype: Ulna sin. (distal fragment) (Polgárdi 5, MÁFI V.11.105.1; V.29180).

Paratypes: Tibiotarsus dext. (distal fragment, damaged lateral) (Polgárdi 4, MÁFI V.11.85.1; V.29160).

Measurements: 1. ulna E=2.03 mm; F=3.56 mm; G=2.39mm; 2. tibiotarsus E=.91 mm; F=3.29 mm; G=3.65 mm.

Comparative material: T. illiacus (MTM n=1: 1. ulna E=2.31mm; F=3.80 mm; 2. tibiotarsus E=1.71mm; F=3.36mm); *T. philomelos* (MTM n=1: 1. ulna E=2.16 mm; F=3.91 mm; G=2.65 mm; 2. tibiotarsus E=1.88 mm; F=3.62 mm; G=3.83 mm).

Diagnosis: This species is similar in its sizes to recent smaller species (*Turdus illiacus/philomelos*). On distal epiphysis of ulna in medial view (Fig. 38A), the *condylus dorsalis* (a) has blunted claw shape; *sulcus intercondylaris* (b) has concave line (but it is damaged). *Condylus ventralis* (c) is protruding and rounded. *Tuberculum carpale* (d) has semicircular shape.

On distal epiphysis of tibiotarsus in cranial view (Fig. 38B), the *tuberositas retinaculi m. fibularis* (a) is undevoleped. *Sulcus extensorius* (b) is wide, its distal end is pointed. *Pons supratendineus* (c) is wide and slant. *Condylus lateralis* (d) has asimmetrically oval shape and distally is rounded. Line of *incisura intercondylaris* (e) is walvy and obliquely. *Condylus medialis* (f) has reverse and pointed oval shape.

Name: Was named after Pannonia region.

Description: Sulcus intercondylaris and *condylus lateralis* got partly damaged. The ulnae of the fossil species *Turdicus minor* KESSLER ET HÍR, 2012 from Litke 2 - Hungary (Lower Miocene, MN5) are smaller (E=1,73-1,84 mm; F=3,32-3,33 mm; G=2,12-2,22 mm) than the Polgárdi specimen and the *condylus ventralis* is more rounded (KESSLER & HÍR 2012). The type species *Turdicus tenuis* KRETZOI 1962 was described from Betfia 5 (MQ1, Romania) as new genus and species, but without sizes and photos (KRETZOI 1962). The holotype cannot be found, therefore this species was considered as „*nomen nudum*" (MLÍKOVSKÝ 2002).

Distribution: The fossil genus has not been reported yet from external zone of the Carpathian Basin. In the Carpathian Basin there it is present continuously in the Neogene.

Genus *Turdus* LINNAEUS, 1758
Turdus † *miocaenicus* nova sp.
(Plate IX. Figure 39 A-B)

Type locality and age: Polgárdi 5, Late Miocene (MN 13).

Holotype: Ulna sin. (distal fragment) (MÁFI V.11.102.1; V.29177).

Paratypes: Coracoid sin. (with damaged cranial part) (MÁFI V.11.124.1; V.29199).

Measurements: 1. coracoid E=1.81 mm; 2. ulna E=2.78 mm; F=4.75 mm; G=3.58 mm.

Comparative material: Turdus pilaris (1. coracoid E=1.85 mm; 2. ulna E=2.76 mm; F=4.94 mm); *T.viscivorus* (1. coracoid E=1.78 mm; 2. ulna E=2.74 mm; F=4.89 mm; G=3.55); *T. torquatus* (MTM n=1: 1. coracoid E=1,90 mm; 2. ulna E=2.51mm; F= 4.82 mm).

Diagnosis: Similar in its characteristics and sizes to larger recent species (*Turdus pilaris/ viscivorus/torquatus* size), On the medial side of coracoid (Fig. 15A), the *acrocoracoid* (a) and its

medial edge are lopsided and steep. *Facies articularis humeralis* (b) has lateral edge that strongly bulges. Edge of the s*ulcus m.supracoracoidei* (c) forms straight line. *Processus procoracoidei* (d) is triangular and well developed.

On distal epiphysis of the ulna in medial view (Fig.15B), the *condylus dorsalis* (a) is claw shaped, but more blunt than in recents species of genus. S*ulcus intercondylaris* (b) is less concave. *Condylus ventralis* (c) is lopsided and narrow conical. *Tuberculum carpale* (d) has asymmetrically and obliquely conical shape.

Name: named after its type strata.

Description: Its size and characters are very similar to recent larger trushes (*Turdus pilaris/viscivorus/torquatus* size), but the shape of *tuberculum carpale* differ to (it is not a semicircular shape). The fossil species *Turdicus minor* KESSLER ET HÍR, 2012 from the Hungarian Lower and Middle Miocene (Litke 2, MN 5; rather Mátraszölős 2. and 3. MN 7/8) has smaller sizes (1. coracoid: E=1.52 mm;.2. ulna: E=1.73-1.84 mm; F=3.32-3.33 mm; G=2.12-2.22 mm) and the shape of *condylus ventralis* and *tuberculum carpale* differ (KESSLER & HÍR 2012).

Turdus † *polgardiensis* nova sp.
(Plate IX. Figure 40 A-B)

Type locality and age: Polgárdi 5, Late Miocene (MN 13).

Holotype: Ulna dext. (with damaged proximal epiphysis), (MÁFI V.11.100.1; V.29175).

Measurements: Ulna A=approx. 33-35 mm; C=4.31 mm; E=2.11 mm; F=4.15 mm; G=2.81 mm.

Comparative material: T. merula (MTM n=1: A=34.29 mm; C=4.72 mm; E=2.37 mm; F=4.25 mm; G=3.06 mm); *T. philomelos* (MTM n=1: A= 30.67 mm; C=4.32 mm; E=2.16mm; F=3.91 mm; G=2.65 mm).

Diagnosis: In dimensions it is similar to middle sized recent species (*Turdus merula* size), but in characteristics resembles larger size recent species. On proximal epiphysis of the ulna in cranial view (Fig. 40A), *cotyla dorsalis* (a) is conical shaped. *Cotyla ventralis* (b) has circular shape. *Tuberculum lig. colateralis ventralis* (c) is well developed. *Depressio m. brachialis* (e) has circular shape and it is well developed. On the distal epiphysis in medial view (Fig. 40B), the *condylus dorsalis* (f) is rounded. *Sulcus intercondylaris* (g) is less concave than in recents species. *Condylus ventralis* (e) has weakly lopsided conical shape. *Tuberculum carpale* (f) has pointed conical shape, while in the recents species has rather claw-like shape.

Name: Was named after the name of type locality.

Description: The partly damaged oleocranon makes the identification difficult, but in its sizes itis similar to medium size thrushes (*Turdus merula* size). In the morphological characters it is more similar to larger species of genus, but the shape of the *tuberculum carpale* also differs.

Turdus † *major* nova sp.
(Plate IX. Figure 41 A-E)

Type locality and age: Csarnóta 2, Pliocene (MN 15-16).

Other locality: Beremend 26, Pliocene (MN 15-16).

Holotype: Humerus sin. (distal fragment), (Csarnóta 2, MÁFI V.11.19.1; V.29094)

Paratypes: Proximal fragment of humerus dext.; carpometacarpus sin. and proximal fragment of the right side bone; two phalanga alae 1. dig.II. and 4 fragments distal of tarsometatarsus (Beremend 26, BKA).

Measurements: 1. humerus C= 9,89 mm, D= 8,49 mm F=7.58 mm; G=3.52 mm; 2. carpometacarpus A=22,13 mm, B=19,20 mm; C=5,23-5,47 mm; E'=1,75 mm; F=4,35 mm; 3. ph-alae A= 10,19-10,72 mm; C=3,30-3,61mm; E=3,37-3,52 mm; F=3,35- 3,40 mm; 4. tarsometatarsus E=2,12-2,34 mm; F=4,01-4,49 mm; G=2,49-2,78 mm.

Comparative material: Turdus torquatus (MTM n=1; humerus: C= 9,82 mm, D= 8,41 mm, F=7.88 mm; carpometacarpus A=22,14 mm, B=19,20 mm; C=5,27 mm; E'=1,94 mm; F=4,62mm; ph-alae A=10,12 mm; C=3,09 mm; E=3,49 mm; tarsometatarsus E=1,71 mm; F=3,86 mm; G=mm); *Turdus pilaris* (MTM n=1: humerus C= 10,25 mm, D= 9,09 mm, F=8,21 mm; carpometacarpus A=23,63 mm, B=20,38 mm; C=5,93 mm; E'=2,17 mm; F=5,09 mm; ph-alae A=11,36 mm; C=3,31 mm; E=3,52 mm; tarsometatarsus E=1,63 mm; F=4,13 mm; G=2,32 mm; *Turdus viscivorus* (MTM n=1: humerus C=10,81 mm, D= 9,32 mm, F=7.28 mm; carpometacarpus A=25,10 mm, B=20,86 mm; C=5,17 mm; E'=2,56 mm; F=5,25mm; ph-alae A=12,16 mm; C=4,24 mm; E=4,84 mm; tarsometatarsus E=1,78 mm; F=4,16 mm; G=2,44mm).

Diagnosis: On proximal epiphysis of humerus in caudal view (Fig. 41A), the *crista pectoralis* forms rounded contour and the *tuberculum dorsale* (a) has rounded shape. *Caput humeri* (b) is wide and slightly convex. *Tuberculum ventrale* (c) forms well developed circular spur. *Crista bicipitalis* (d) has protruding and cut-off shape. *Crus fossae* (e) is developed, the *fossae pneumotricipitalis* (f) is divided into two part.

On distal epiphysis in cranial view of humerus (Fig. 41B), the *tuberculum ventrale* (a) is well developed. *Epicondylus ventralis* (b) is weakly arches. *Processus flexorius* (c) is obliquely protruding and rounded. *Condylus ventralis* (d) has extended oval shape. *Incisura intercondylaris* (e) is deep and blunted as in the recent species. *Condylus dorsalis* (f) has curved ovalic shape. *Epicondylus dorsalis* (l) is mildly

protruding and rounded. *Processus supracondylaris dorsalis* (h) is short and bent with blunted end.

On carpometacarpus in ventral view (Fig. 41C), the *trochlea carpalis* (a) has conical shape, as in the recent genus. *Processus extensorius* (b) has long and oblique beak-like shape, with rounded end. *Processus alularis* (c) has rounded rectangular shape. *Fovea subalularis* (d) has acut angle pit shape. *Protuberantia metacarpalis* (e) is undeveloped. The basis of the *facies articularis digiti major* (f) is rounded triangular shaped. The distal end of the *os metacarpalis minus* (g) has asymmetrical straight line.

On phalanga alae (Fig. 41D), the ventral point of the proximal edge (a) is projecting lateral in conical shape. The dorsal point (b) is laterally projecting in rounded form. The proximal edge (c) is less rounded. The dorsal edge (d) is bended, while the distal edge (e) is rounded.

On distal epiphysis of tarsometatarsus in dorsal view (Fig. 41E), the *trochlea metatarsi tertii* (a) is wide and has oblique cut-off end. *Incisura intertrochlearis medialis* (b) is narrow and deep. *Trochlea metatarsi tertii* (c) is wide and has concave end. *Incisura intertrochlearis lateralis* (d) is wide and deep. *Trochlea* metatarsi IV. (e) has rectangle shape with rounded end.

Name: Was named after the its larger dimensions.

Description: In its characteristics seem to recent species and has the sizes of *T. torquatus*.

Turdus † *medius* nova sp.
(Plate X. Figure 42 A-F)

Type locality and age: Csarnóta 2, Pliocene (MN 15-16).

Other locality: Beremend 26, Pliocene (MN 15-16).

Holotype: Humerus dext. (distal fragment), (Csarnóta 2, MÁFI V.11.26.1; V.29101).

Paratypes: Ulna dext. (distal fragment), (MÁFI); tibiotarsus dext. (distal fragment), (Csarnóta 2, MÁFI V.11.44.2; V.29119); proximal and distal fragments of the left side humerus; two carpometacacarpus dext. (missing *os metacarpus minus*); distal fragments of the right and left side tarsometatarsus (Beremend 26, BKA).

Measurements: 1. humerus B=11,02 mm; C=9,03 mm; D=8,28 mm; E=2,69 mm; F=6,30-6,35 mm; G=3,19-3,57 mm; 2. ulna: F=4.03 mm; G=2.88 mm; 3. carpometacarpus A=19,79-20,13 mm, B=16,69 mm; C=5,13 mm; E'=1,72-1,74 mm; F=4,35-4,48 mm; 4. tibiotarsus F=3.68 mm; G=3.55 mm; 5. tarsometatarsus F=3,88 mm; G=2,26-2,38 mm.

Comparative material: Turdus merula (MTM n=1; humerus: B=11,39 mm; C=9,46 mm; D=8,67 mm; E=2,75 mm; F=6.46 mm; G=3.38 mm; ulna: F=4.23 mm; G=3.09 mm; carpometacarpus A=20,36 mm, B=16,63 mm; C=5,10 mm; E'=2,27 mm; F=4,16 mm; tibiotarsus: F=3.89 mm; G=3.85 mm; tarsometatarsus F=3,82 mm; G=2,14 mm).

Diagnosis: On proximal epiphysis of humerus in caudal view (Fig. 42A), the *tuberculum dorsale* (a) is rounded. *Caput humeri* (b) is wide and weakly bulging. *Tuberculum ventrale* (c) is well developed and has circular shape. *Crista bicipitalis* (d) hass protruding cut-off shape. C*rus fossae* (e) is weakly developed and the *fossae pneumotricipitalis* (f) is divided into two part.

On distal epiphysis in cranial view of humerus (Fig. 42B) the *tuberculum ventrale* (a) is well developed and weakly protruding. The *epicondylus ventralis* (b) is arched. *Processus flexorius* (c) is obliquely protruding and rounded. *Condylus ventralis* (d) has laying oval shape. *Incisura intercondylaris* (e) is deep acute angle pit. The *condylus dorsalis* (f) has curved ovalic shape. *Epicondylus dorsalis* (l) is mildly protruding and rounded. *Processus supracondylaris dorsalis* (h) is bent and curved and has branched end.

On distal epiphysis of ulna in medial view (Fig. 42C), the exterior edge of *condylus dorsalis* (a) is laying arched and has asymmetricaly blunted conical shape. *Sulcus intercondylaris* (b) is wide and slightly concave. It is straighter than in the recent species. *Condylus ventralis* (c) is oblique and wide blunted conical. *Tuberculum carpale* (d) is semicircular-like protruding.

On proximal epiphysis of carpometacarpus in ventral view (Fig. 42D), the *trochlea carpalis* (a) has rounded and conical shape, as in recent genus. *Processus extensorius* (b) has wide and oblique beak-like, with rounded end. *Processus alularis* (c) has rectangular shape. *Fovea subalularis* (d) has acute angle shape. *Proeminentia metacarpalis* (e) is undevelepod and flatten. The basis of the *facies articularis digiti major* (f) has tiangle shape. The end of the *metacarpus minus* (g) is less concave.

On distal epiphysis of tibiotarsusus in cranial view (Fig. 42E), the *pons supratendineus* (a) is wide and oblique. *Condylus lateralis* (b) has flat and pointed oval shape. The line of i*ncisura intercondylaris* (c) has concave and slightly wavy. C*ondylus medialis* (d) is distaly pointed and reversed oval shaped.

On distal epiphysis of tarsometatarsusus in dorsal view (Fig. 42F), the *trochlea metatarsi tertii* (a) has rectangle shape with less rounded end. *Incisura intertrochlearis medialis* (b) is wide and deep. *Trochlea metatarsi tertii* (c) is wide and has concave end. *Incisura intertrochlearis lateralis* (d) is narrow and deep. *Trochlea* metatarsi IV. (e) is conical shaped.

Name: Was named after its middle seize dimensions.

Description: It corresponds in characteristies to recent genus, and its dimensions seem to *Turdus merula.*

Turdus † minor nova sp.
(Plate X. Figure 43 A-D)

Type locality and age: Csarnóta 2, Pliocene (MN 15-16).

Other locality: Beremend 26, Pliocene (MN 15-16).

Holotype: Humerus sin. (distal fragment), (Csarnóta 2, MÁFI V.11.27.1; V.29102).

Paratypes: Two carpometacarpus dext. (proximal fragments); tarsometatarsus dext. (distal fragment), (Csarnóta 2, MÁFI V.11.45.2; V.29120); Proximal and distal fragment of humerus sin. (Beremend 26, BKA).

Measurements: 1. humerus C=7,67 mm; E=2,42 mm; F=mm; G=mm; F=5,82-6.09 mm; G=2,95-3.01 mm; 2. carpometacarpus C=4.17-4.25 mm; 3. tarsometatarsus E=1.35 mm; G=1.81 mm.

Comparative material: Turdus philomelos (MTM n=1; 1. humerus: C=8,45 mm; F=5.65 mm; G=3.40 mm; 2. carpometacarpus: C=4.56 mm; 3. tarsometatarsus: E=1.25 mm; G= 1.82 mm).

Diagnosis: On proximal epiphysis of humerus in caudal view (Fig. 43A), the c*aput humeri* (a) is wide and rounded. *Tuberculum ventrale* (b) is well developed and has pointed circular shape. *Crista bicipitalis* (c) is less protruding and rounded. C*rus fossae* (d) is well developed and the *fossae pneumotricipitalis* (e) is divided into two part. On distal epiphysis of humerus in cranial view (Fig. 43B) the *tuberculum ventrale* (a) is well developed. The *epicondylus ventralis* (b) is rounded. *Processus flexorius* (c) is obliquely protruding and rounded. *Condylus ventralis* (d) has rounded oval shape. *Incisura intercondylaris* (e) has deep acute angle pit shape. *Condylus dorsalis* (f) has curved ovalic shape. *Epicondylus dorsalis* (l) is rounded. *Processus supracondylaris dorsalis* (h) is bent and has asymmetrically conical shape.

On proximal epiphysis of carpometacarpusus in ventral view (Fig. 43C), the *trochlea carpalis* (a) is asymmetrically bulging. It has conical shape with rounded end. *Proc. extensorius* (b) has long, mildly oblique rectangular shape with rounded end. *Processus alularis* (c) is small and conical. *Fovea subalularis* (d) is wide and conical pit.

On distal epiphysis of tarsometatarsus in dorsal view (Fig. 43D), the edge between *fossa metatarsalis* I. and *trochlea metatarsi* II. (a) is wide and wavy. *Trochlea metatarsi tertii* (b) is wide and asymmetrical with mildly concave end. *Incisura intertrochlearis lateralis* (c) is medium wide and deep.

Trochlea metatarsi IV. (e) has flattened blunt conical shape.

Name: The name refers to smaller sizes of species.

Description: It corresponds in characteristies to recent genus, and has dimensions seem to *Turdus philomelos,* but it is smaller. The distal epiphyisis of tibiotarsus is damaged. Lateral edge of tarsometatarsus is incomplete and *trochlea metatarsi II.* missed.

Distribution: The thrushes are represented better in fossil matarials becausse of their relatively larger stature (between the songbirds). In the Carpathian Basin they were described from Middle Miocene (MN7/8) of Mátraszölős 2 – Hungary (GÁL et al. 2000) as Turdidae gen et sp. foss. indet., from Middle Miocene (MN7/8) of Felsőtárkány-Hungary (HÍR et al. 2001) as *Turdus* sp. foss. indet. from the Early Pliocene (MN 15-16) of Ivanovce I – Slovakia (ŠVEC in FEJFAR & HEINRICH 1985; MLÍKOVSKÝ 2002); also from Csarnóta 2 – Hungary (Lower Pliocene, MN 15), (JÁNOSSY 1979a; KESSLER 2010); from the Early Pliocene (MN 15) of Beremend 26 – Hungary (KESSLER 2010a) and from Early Pleistocene (MQ1-MQ2) in some other localities of the Carpathian Basin: Betfia 9 – Romania (GÁL 2002); Deutsch Altenburg 4B –Austria (JÁNOSSY 1981; DÖPPES & RABEDER 1997; MLÍKOVSKÝ 1998a.); Beremend 17 (KESSLER 2010); Nagyharsányhegy 1-4 - Hungary (LAMBRECHT 1916, 1933; JÁNOSSY 1979). On the recent species was reported: *Turdus torquatus* (LINNAEUS), 1758 in Betfia 9 – Romania (Lower Pleistocene, MQ1) (GÁL 2002); *Turdus merula* LINNAEUS, 1758 in Betfia 13-Romania (Upper Pliocene, MN 16-17) (KESSLER 1975, GÁL 2002); Betfia 2 – Romania (Lower Pleistocene, MQ1) (ČAPEK 1917; LAMBRECHT 1933; JÁNOSSY 1979; KESSLER 1975; GÁL 2002); Betfia 9-Romania (Lower Pleistocene, MQ1) (KESSLER 1975; GÁL 2002); *Turdus philomelos* Brehm, 1831 Beremend 16 - Hungary (Upper Pliocene, MN 16-17) (Jánossy 1991, 1992); Betfia 2- Romania (Lower Pleistocene, MQ1) (ČAPEK 1917; LAMBRECHT 1933; JÁNOSSY 1979; KESSLER 1975; Gál 2002); Betfia 9 -Romania (Lower Pleistocene, MQ1) (KESSLER 1975; Gál 2002); Deutsch Altenburg -Ausztria (Lower Pleistocene, MQ1) (JÁNOSSY 1981); *Turdus iliacus* LINNAEUS, 1766 from Polgárdi 4 - Hungary (Upper Miocene, MN 13) (JÁNOSSY 1991, 1995); Betfia 2-Romania (Lower Pleistocene, MQ1) (ČAPEK 1917; LAMBRECHT 1933; JÁNOSSY 1979; KESSLER 1975; GÁL 2002); Betfia 9 - Romania (Lower Pleistocene, MQ1) (KESSLER 1975; GÁL 2002); Q2: Nagyharsányhegy 1-4 (Lower Pleistocene Q2) (KESSLER 2010a); *Turdus viscivorus* LINNAEUS, 1758 from Csarnóta 2- Hungary (Lower Pliocene, MN15) (JÁNOSSY 1979); from Betfia 2 - Romania (Lower Pleistocene, MQ1) (ČAPEK 1917; LAMBRECHT 1933; JÁNOSSY 1979; KESSLER 1975; GÁL 2002); from Betfia 9 - Romania (Lower Pleistocene, MQ1) (KESSLER 1975; GÁL 2002); Deutsch- Altenburg - Austria (Lower Pleistocene, MQ1) (JÁNOSSY 1981); *Turdus pilaris* LINNAEUS, 1758 from Betfia 2 - Romania (Lower Pleistocene, MQ1) (ČAPEK 1917; LAMBRECHT 1933; JÁNOSSY 1979; KESSLER 1975; GÁL 2002); Betfia 9 - Romania (Lower Pleistocene, MQ1) (KESSLER 1975; GÁL 2002).

The genus it is known outside of the Carpathian Basin from Credinta –Romania (Middle Miocene, MN 8) as *Turdus* sp. (GÁL & KESSLER 2006), while from the Late Pliocene from Rebielice Królowskie I. – Poland (JÁNOSSY 1974), Varshets – Bulgaria (BOEV 1996, 2000), Sandalja I. - Croatia (V. MALEZ-BACIC 1979) and from the Early Pleistocene from some localities and countries in Europe (Austria, Bulgaria, Czech Republic. France, Germany, Romania, Spain, etc.) (TYRBERG 1998).

Fam. Oriolidae BOIE, 1826
Genus *Oriolus* LINNAEUS, 1758
Oriolus † beremendensis nova sp.
(Plate XI. Figure 44 A-E)

Type locality and age: Beremend 26, Pliocene (MN 15-16).

Holotype: Carpometacarpus dext. (BKA)

Paratypes: Distal fragment of humerus sin.; ulna sin.; proximal fragment of ulna sin.; distal fragment of tibiotarsus sin. (BKA).

Measurements: 1. humerus E=2,76 mm; F=6,26 mm; G=3,14 mm; 2. ulna A=37,59 mm; B=4,58-4,87 mm; C=5,00-5,15 mm; E=2,68 mm; F=4,45 mm;G=3,17 mm; 3. carpometa-carpus A=22,00 mm; B=19,36 mm; C=5,69 mm; E=4,01 mm; F=4,64 mm; 4. tibiotarsus .E=1,81 mm; F=3,63 mm; G=3,60 mm.

Comparative material: Oriolus oriolus (MTM n=1: humerus E=3,10 mm; F=6,98 mm; G=4,11 mm; ulna A=40,26 mm; B=4,73 mm;C=5,17 mm; E=2,33 mm;F=4,83 mm;G=3,42 mm; carpometacarpus A=24,02 mm; B=21,01 mm; C=5,37 mm; E=3,89mm; F=4,85 mm; tibiotarsus .E=1,79 mm;F=3,78 mm; G=3,51 mm).

Diagnosis: On distal epiphysis of humerus in cranial view (Fig. 44A), the *tuberculum supracondylare ventrale* (a) is developed. *Epicondylus ventralis* (b) is rounded. *Processus flexorius* (c) is less protruding and has rounded end. *Condylus ventralis* (d) has oval shape. *Incisura intercondylaris* (e) is deep and wide. *Condylus dorsalis* (f) has bented oval shape. *Epicondylus dorsalis* (g) is rounded. *Proc. supracondylaris dorsalis* (h) is long and bented.

On proximal epiphysis of ulna in cranial view (Fig. 44B), the *oleocranon* (a) is long, with blunted end. *Cotyla dorsalis* (b) has asymmetrical conical shape. C*otyla ventralis* (c) has circular shape. The *tuberculum lig. colat. ventralis* (d) and the *depressio m. brachialis* (e) are well developed.

On distal epiphysis in medial view of ulna (Fig. 44C), the *condylus dorsalis* (f) has wide and blunted claw-like shape. *Sulcus intercondylaris* (g) is wide and slightly concave. It is straighter than in recent species. *Condylus ventralis* (h) has wide and blunted conical shape. *Tuberculum carpale* (i) is semicircular-like protruding.

On proximal epiphysis of carpometacarpus in ventral view (Fig. 44D), the *trochlea carpalis* (a) is asymmetrical bulging. *Processus extensorius* (b) has blunted conical shape. *Processus alularis* (c) has distally rounded rectangular shape. *Fovea subalularis* (d) has acute angle shape. *Proeminentia metacarpalis* (e) is undeveloped and flatten. The basis of the *facies articularis digiti major* (f) has tiangle shape. The end of the *metacarpus minus* (g) is asymmetrical rounded

On tibiotarsus the distal epiphysis in cranial view (Fig. 44E), the *sulcus extensorius* (a) is narrow with rounded end. *Pons supratendinous* (b) is wide and oblique. *Condylus lateralis* (c) has oval shape. *Incisura intercondylaris* (d) has concave and wavy line. *Condylus medialis* (f) has reverse oval-like shape.

Name: Was named after the name of the localities.

Description: It corresponds partially with charateristics and size the recent species.

Distribution: The genus has no extinct species. The recent species *Oriolus oriolus* (LINNAEUS, 1758) is known from Betfia 9- Romania (Q1) (GÁL 2002); Vindija - Croatia (Q3) (M. MALEZ 1975; V. MALEZ 1984, 1988) and some localities from the Late Pleistocene in Europa (TYRBERG 1998)

Family Sylviidae VIGORS, 1825
Genus *Acrocephalus* NAUMANN, 1811
Acrocephalus † major nova sp.
(Plate XI. Figure 45 A-E)

Type locality and age: Polgárdi 4, Late Miocene (MN 13).

Holotype: Ulna dext. (MÁFI V.11.107.1; V.29182).

Paratypes: Five humeri (one proximal fragment of sin. and 4 distal fragment – 2 sin. and 2 dext.), 19 ulnae (3 complete, 9 proximal and 5 distal fragments), 2 tibiotarsi sin. (distal fragments) (MÁFI V.11.87.26; V.29162).

Measurements: 1. humerus C=5.27 mm; E=1.62-1.92 mm; F=4.12-4.45 mm; G=2.32-2.44 mm; 2. ulna A=21.61-22.30 mm; B=2.64-3.23 mm; C=2.58-3.25 mm; E=1.42-1.69 mm; F=2.42-3.03 mm; G=1.71-2.06 mm; 3. tibiotarsus F=2.89-2.94 mm; G=1.74-2.06 mm.

Comparative material: Acrocephalus arrundinaceus (MTM n=1: 1. humerus C=5.71 mm; E=1.59 mm; F=4.12 mm; G=2.68 mm; 2. ulna A=24.25 mm; B=3.21 mm; C=3.42 mm; E=1.61 mm; F=2.71 mm; G=2.18 mm; 3. tibiotarsus F=3.14 mm; G=3.06 mm); *A. scirpaceus* (MTM n=1: 1. humerus A=19.05 mm; C=5.77 mm; E=1.77 mm; F=4.03 mm; 2. ulna A=23.54 mm; C=3.08 mm; E=1.58 mm; F=2.77 mm; 3. tibiotarsus F=3.17 mm).

Diagnosis: Corresponds in its characteristics and sizes to recent larger species of genus. On proximal epiphysis of humerus in caudal view (Fig. 45A), the *tuberculum dorsale* (a) is rounded. *Caput humeri* (b) is wide and convex, but not outstanding. *Tuberculum ventrale* (c) is wide and stretched. *Crista bicipitalis*

(d) is mildly pointed and asymmetrically protruding. *Crus fossae* (e) is well developed, therefore *fossae pneumotricipitalis* (f) is divided in two. On distal epiphysis in cranial view (Fig. 45B), the *epicondylus ventralis* (g) is mildly convex. *Processus flexorius* (h) is strongly protruding and rounded. *Condylus ventralis* (i) has stretched oval shape. *Incisura intercondylaris* (j) is deeper and narrow. *Condylus dorsalis* (k) has bent and strongly oval shape. *Epicondylus dorsalis* (l) is rounded. *Processus supracondylaris dorsalis* (m) is short, blunt and mildly branches off. The widening between it and diaphysis is deep and narow.

On proximal epiphysis in cranial view of ulna (Fig. 45C), the *oleocranon* (a) is long, thin and even. *Cotyla dorsalis* (b) has asymmetrical and rounded conical shape. *Cotyla ventralis* (c) has circular shape. *Tuberculum lig. colat. ventralis* (d) is well developed. On distal epiphysis in medial view (Fig, 45D), *condylus dorsalis* (e) is semicircular shaped. *Sulcus intercondylaris* (f) is slightly concave. *Condylus ventralis* (g) has wide conical shape. *Tuberculum carpale* (h) has semicircular shape.

On tibiotarsus the distal epiphysis in cranial view (Fig. 45E), the *tuberositas retinaculi m. fibularis* (a) is wide and flattened. *Sulcus extensorius* (b) is wide and even. *Pons supratendinous* (c) also is wide and even. C*ondylus lateralis* (d) has oval shape. The line of *incisura intercondylaris* (e) is concave and wavy. *Condylus medialis* (f) has flattened oval shape.

Name: Was named after its larger dimensions.

Description: It corresponds in characteristics to recent greater species of genus. On proximal epiphysis of humerus the *crista pectoralis* is damaged.

Acrocephalus †*minor* n. sp.
(Plate XII. Figure 46 A-E)

Type locality and age: Polgárdi 4, Late Miocene (MN 13).

Holotype: Humerus sin. (proximal epiphysis) (MÁFI V.11.71.1; V.29146).

Paratypes: One sin. and two humeri dext. (distal fragments); 2 ulnae sin. (proximal and distal fragments); tibiotarsus sin.(distal fragment) (MÁFI V.11.88.10; V.29163).

Measurements: 1. humerus C=4.67-4.81 mm; E=1.59-1.68 mm; F=3.88-3.99 mm; G=2.26-2.36 mm; 2. ulna E=1.43 mm-1.45; F=2.49-2.52 mm, G=1.67-1.71 mm; 3. tibiotarsus E=1.09 mm; F=2.03-2.25 mm; G=1.83-2.20 mm.

Comparative material: Acrocephalus schoenobenus (MTM n=1: humerus A=14.35 mm; C=4.26 mm; E=1.26 mm; F=3.21 mm; G=1.88; ulna A=15.42 mm; C=2.12 mm; E= 0.97 mm; F=2.03 mm; tibiotarsus F=2.29 mm; G=2.12 mm); *A. palustris* (MTM n=1: ulna F=2.07 mm; tibiotarsus F=2.29 mm);

Diagnosis: Corresponds in characteristics to smaller species of genus. On proximal epiphysis of humerus in caudal view (Fig. 46A), the *tuberculum dorsale* (a) has angular shape. *Caput humeri* (b) is convex. *Tuberculum ventrale* (c) has oustanding cone-shape. *Crista bicipitalis* (d) is pointed and has asymmetrical protruding shape. *Crus fossae* (e) is well developed but it is short. *Fossae pneumotricipitalis* (f) is partly divided in two parts. On distal epiphysis in cranial view (Fig. 46B), the *epicondylus ventralis* (g) has convex shape. *Processus flexorius* (h) is protruding and rounded. *Condylus ventralis* (i) has stretched oval shape. *Incisura intercondylaris* (j) has acute angled pit shape. *Condylus dorsalis* (k) has bent oval shape. **(***Processus supracondylaris dorsalis* (m) is damaged. The widening between it and diaphysis is deep and narrow).

On proximal epiphysis in cranial view of ulna (Fig. 46C), the *oleocranon* (a) is long, thin and slightly oblique. *Cotyla dorsalis* (b) has asymmetrical and rounded conical shape. *Cotyla ventralis* (c) has circular shape. *Tuberculum lig. colat. ventralis* (d) and the *depressio m. brachialis* (e) are well developed. On distal epiphysis in medial view, *condylus dorsalis* (e) has rounded claw-like shape. *Sulcus intercondylaris* (f) is slightly concave. *Condylus ventralis* (g) has wide conical shape. *Tuberculum carpale* (h) has semicircular shape. On distal epiphysis of ulna in medial view (Fig. 46D), the *condylus dorsalis* (a) is bented and rounded claw shaped. *Sulcus intercondylaris* (b) is slightly concave. *Condylus ventralis* (c) has blunted cone-shape. *Tuberculum carpale* (d) has wide and rounded conical shape.

On tibiotarsus the distal epiphysis in cranial view (Fig. 46E), the *tuberositas retinaculi m. fibularis* (a) is undeveloped and flat. *Sulcus extensorius* (b) is wide. *Pons supratendinous* (c) is wide and straight. C*ondylus lateralis* (d) has pointed and flattened oval shape. Line of *incisura intercondylaris* (e) is concave, oblique and wavy. *Condylus medialis* (f) has rounded oval shape.

Name: Was named after its smaller dimensions.

Description: It corresponds in characteristics to smaller species of the recent genus. On humerus the *crista pectoralis* is damaged. *Processus supracondylaris dorsalis* is also damaged.

Acrocephalus † *kretzoii* nova sp.
(Plate XII. Figure 47 A-B)

Type locality and age: Csarnóta 2, Pliocene (MN 15-16).

Other locality: Beremend 26, Pliocene (MN 15-16).

Holotype: Carpometacarpus sin. (proximal fragment), (Csarnóta 2, MÁFI V.11.1.1; V.29076).

Paratypes: Two carpometacarpus sin (proximal fragments); tarsometatarsus dext. (distal fragment), (Csarnóta 2, MÁFI V.11.39.3; V.29144); distal fragments of the right and left side tarsometatarsus (Beremend 26, BKA).

Measurements: 1. carpometacarpus C=3.25-3.73 mm; 2. tarsometatarsus F=1,88 -2,07 mm; G=1,13-1,19 mm.

Comparative material: Acrocephalus arrundinaceus (MTM n=1; carpometacarpus: C=3.44 mm; tarsometatarsus: F=1.74 mm; G=1.07 mm).

Diagnosis: On proximal epiphysis of carpometacarpusus in ventral view (Fig. 47A), the *trochlea carpalis* (a) is symmetrically bulging. It has strongly bulging conical shape with rounded end, than in recent species. *Proc. extensorius* (b) has obliquely blunted conical shape. *Processus alularis* (c) has rounded rechtangle shape. *Fovea subalularis* (d) has blunted conical shape.

On distal epiphysis of tarsometatarsus in dorsal view (Fig. 47B), the edge between *fossa metatarsalis* I. and *trochlea metatarsi* II. (a) is strongly wavy. *Trochlea metatarsi* II. (b) has oglique and blunted conical shape. *Incisura intertrochlearis medialis* (b) has acute angle shape. *Trochlea metatarsi tertii* (d) is wide and with a bellow mildly concave end. *Incisura intertrochlearis lateralis* (e) is strongly wide. (T*rochlea metatarsi* IV. (f) is strongly damaged).

Name: Was named after Hungarian paleoornithologist Miklós KRETZOI.

Description: Its characteristics correspond to recent genus, but in dimensions refer to a larger species.

Acrocephalus † kordosi nova sp.
(Plate XII. Figure 48)

Type locality and age: Csarnóta 2, Pliocene (MN 15-16).

Holotype: Carpometacarpus dext. (proximal fragment), (MÁFI V.11.2.1; V.29077).

Measurements: Carpometacarpus C=2.88 mm.

Comparative material: Acrocephalus schoenobenus (MTM n=1; carpometacarpus: C=2.88 mm); *Acrocephalus palustris* (MTM n=1; carpometacarpus: C=2.82 mm);

Diagnosis: On proximal epiphysis of carpometacarpus in ventral view (Fig. 48), the *trochlea carpalis* (a) is symmetrically bulging. It has strongly bulging conical shape with rounded end, than in the recent species. *Proc. extensorius* (b) is obliquely blunted conical shaped with rounded lateral edge. *Processus alularis* (c) has rounded rechtangle shape. *Fovea subalularis* (d) has blunted conical shape.

Name: Was named after Hungarian paleontologist László KORDOS.

Description: Its characteristics corresponds to recent genus, but in dimensions ist among from smaller species.

Distribution: The genus was reported from the Carpathian Basin as *Acrocephalus* sp. foss. indet. from the Late Miocene of Rudabánya - Hungary (MN 9) and the Early Pleistocene of Betfia 9 - Romania (MQ1) (GÁL 2002). The recent species *Acrocephalus palustris* was reported from the Early Pleistocene of Betfia 2 –Romania (MQ1) (ČAPEK 1917; LAMBRECHT 1933; JÁNOSSY 1979; KESSLER 1975, GÁL 2002**).**

Genus *Cettia* BONAPARTE, 1838
Cettia † janossyi nova sp.
(Plate XII. Figure 49).

Type locality and age: Polgárdi 4, Late Miocene (MN 13).

Holotype: Humerus dext. (with damaged proximal epiphysis), (MÁFI V.11.100.2; V.29176).

Measurements: Humerus A=16,87 mm; C=aprox. 4,60 mm; E=1,66 mm; F=3,48; G=1,78 mm.

Comparative material: Cettia ceti (MTM n=1: humerus A=15,42 mm; C=5,04 mm; E=1,63 mm; F=3,54 mm; G=1,81 mm).

Diagnosis: Corresponds in its characteristics and sizes to recent species. On proximal epiphysis of humerus in cranial view (Fig. 49), the *tuberculum dorsale* (a) is rounded. *Caput humeri* (b) is wide and convex. On distal epiphysis in cranial view, the *epicondylus ventralis* (c) is arches strongly. *Processus flexorius* (d) is protruding and rounded. *Condylus ventralis* (e) has lying oval shape. *Incisura intercondylaris* (f) is wide and concave. *Condylus dorsalis* (g) is oval shaped. *Epicondylus dorsalis* (h) is strongly arching in semicircular shape. *Processus supracondylaris dorsalis* (i) is long and its end branches off.

Name: Was named after the Hungarian paleontologist, Dénes JÁNOSSY.

Description: In generaly it corresponds in its characters and sizes to recent species, but it is more slender.

Cettia †kalmani nova sp.
(Plate XII. Figure 50)

Type locality and age: Csarnóta 2, Pliocene (MN 15-16).

Holotype: Distal fragment of the humerus dext. (MÁFI V.11.28.1; V.29103).

Measurements: Humerus F=4.45 mm; G=2.31 mm.

Comparative material: Cettia ceti (MTM n=1; humerus: F= 3.54 mm; G=1.81 mm) ,*Sylvia communis* (MTM n=1; humerus: F=3.48 mm; G=1.83 mm).

Diagnosis: On the distal epiphysis in cranial view of humerus (Fig. 50), the *tuberculum ventrale* (a) is well developed. The *epicondylus ventralis* (b) is strongly arches. *Processus flexorius* (h) is straighter protruding and asymmetrically rounded. *Condylus ventralis* (d) is extended oval shaped. *Incisura intercondylaris* (e) is deeper and pointed pit than in the recent genus.

Condylus dorsalis (f) is oval shaped and less oblique than in the recent species. *Epicondylus dorsalis* (g) is rounded. *Proc. supracondylaris*

dorsalis (h) is wide and olique and has two short braches.

Name: Was named after Hungarian paleornithologist Kálmán LAMBRECHT.

Description: Its characteristics corresponds to recent species, but the fossil species is bigger in sizes than extinct species from Polgardi *Cettia janossyi* or than the recent species.

Distribution: The genus was reported only from Polgárdi as *Cettia* sp. by D. JÁNOSSY (1991). This material was identified in this paper.

Genus *Hippolais* C. VON BALDENSTEIN , 1827
Hippolais †*veterior* nova sp.
(Plate XIII. Figure 51 A-C)

Type locality and age: Polgárdi 4, Late Miocene (MN 13).

Holotype: Carpometacarpus sin. (MÁFI V.11.70.1; V.29145).

Paratypes: Three humeri dext. (distal fragments); carpometacarpus sin. (proximal fragment); one sin. and one dext. distal fragment of tibiotarsus (MÁFI V.11.84.5; V.29159).

Measurements: 1. carpometacarpus C=2.96-3.01 mm; 2. humerus F=3.86-4.01 mm; G=2.09-2.39 mm; 3. tibiotarsus E=1.14 mm; F=2.25-2.36 mm; G=2.06-2.26 mm.

Comparative material: Hippolais icterina (MTM n=1: carpometacarpus C=2.91 mm; humerus F=4.17 mm; G=2.13 mm; tibiotarsus E=1.11 mm; F=2.31 mm; G=2.11 mm); *H. pallida* (MTM n=1: carpometacarpus C=2.53 mm; humerus F=3.94 mm; tibiotarsus E=1.10 mm; F=2.22 mm).

Diagnosis: Its characteristics mostly correspond to those of recent genus**.** On distal epiphysis in cranial view of humerus (Fig. 51A), the *tuberculum supracondylare ventrale* (a) is well developed. *Epicondylus ventralis* (b) is more rounded than in the recent species. *Processus flexorius* (c) has semicircular shape. *Condylus ventralis* (d) has stretched oval shape *Incisura intercondylaris* (e) is profound and in acute angle hollow. *Condylus dorsalis* (f) is oval shaped. *Epicondylus dorsalis* (l) is rounded. *Processus supracondylaris dorsalis* (m) is short, blunt and mildly bented.

On proximal epiphysis of carpometacarpus in ventral view (Fig. 51B), the *trochlea carpalis* (a) is rounded, symmetrically and strongly convex. *Proc. extensorius* (b) is massive and asymmetrically conical. *Processus alularis* (c) is well developed and has rectangular shape. *Fovea subalularis* (d) is profound and conical. *Protuberantia metacarpalis* (e) is located in the external edge of the *os metacarpale majus* and forms undeveloped triangular bulge.

On tibiotarsus the distal epiphysis in cranial view (Fig. 51C), the *tuberositas retinaculi m. fibularis* (a) has blunt triangular shape. *Sulcus extensorius* (b) is wide. *Pons supratendineus* (c) is wide and straight. *Condylus lateralis* (d) has oval shape. *Incisura intercondylaris* (e) has deeper concave line. C*ondylus medialis* (f) is distaly pointed and reverse oval shaped.

Name: Was named after its age (lat. *veterior*=old).

Description: Its characteristics and sizes mostly corresponds to recent species.

Distribution: The genus was reported only from France (Upper Pleistocene) (TYRBERG 1998).

Genus *Sylvia* SCOPOLI, 1769
Sylvia †*intermedia* nova sp.
(Plate XIII. Figure 52 A-E)

Type locality and age: Polgárdi 4, Late Miocene (MN 13).

Holotype: Carpometacarpus dext. (missing *os metacarpale minus*), (MÁFI V.11.69.1; V.29144).

Paratypes: Thre humeri dext. (on missed proximal epiphysys, on proximal and on distal fragment); 2 tibiotarsi dext. (distal fragments); 4 tarsometatarsi (3 sin. and 1 dext. distal fragments) (MÁFI V.11.86.9; V.29161).

Measurements: 1. humerus A=aprox.16-18 mm; C=5.24 mm; E=1.69mm; F=3.83-4.73 mm; G=2.09-2.47 mm; 2. carpometacarpus A=12.22 mm; C=2.97 mm; F=2.51 mm; 3. tibiotarsus E=1.07-1.08 mm; F=1.97-2.12 mm; G=1.83-2.07 mm; 4. tarsometatarsus E=1.01 mm; F=1.86-2.04 mm; G=1.06-1.13 mm.

Comparative material: Sylvia atricapilla (MTM n=1: humerus A=16.06 mm; C=5.03 mm; E=1.53 mm; F=3.71 mm; carpometacarpus A=1036 mm; C=2.38 mm; tibiotarsus E=0.96 mm; F=2.11 mm; tarsometatarsus E=0.84 mm; F=1.47 mm); *S. borin* (MTM n=1: humerus A=16.79; C=5.51mm; E=1.69mm; F=4.45 mm; G=2.28 mm; carpometacarpus A=12.71 mm; C=3.11 mm; F=2.83 mm; tibiotarsus E=1.27 mm; F=2.65 mm; tarsometatarsus E=1.11 mm; F=1.92 mm; G=1.18 mm); *S. communis* (MTM n=1: humerus A=16.41; C=4.90 mm; E=1.52 mm; F=3.70 mm; carpometacarpus A=11.62 mm; C=2.46 mm; tibiotarsus E=1.12 mm; F=2.28 mm; tarsometatarsus E=0.87 mm; F= 1.78 mm); *S. curruca* (MTM n=1: humerus A=13.46 mm; C=4.47 mm; E=1.34 mm; F=3.09 mm; carpometacarpus A=10.05 mm; C=2.52 mm; tibiotarsus E=1.05 mm; F=2.13 mm; G=1.99 mm; tarsometatarsus E=1.07 mm; F=1.52 mm).

Diagnosis: The bones belong to on middle size species. On proximal epiphysis of the humerus in caudal view (Fig. 52A), the *caput humeri* (a) is wide and convex. *Tuberculum ventrale* (b) has lying S-shape. *Crista bicipitalis* (c) is protruding with rounded end. *Crus fossae* (d) is developed, therefore *fossae pneumotricipitalis* (e) is divided in two. *Tuberculum dorsale* (f) is rounded. On distal epiphysis in cranial view (Fig. 52B), the *tuberculum supracondylare ventrale* (g) is developed. Lateral edge of *epicondylus ventralis* (h) is very mildly bulging. *Processus*

flexorius (i) is more protruding, slightly lopsided and more rounded than in the recent species. *Condylus ventralis* (j) has stretched oval shape. *Incisura intercondylaris* (k) has a profound pit. *Condylus dorsalis* (l) has a bent strongly oval shape, with pointed distal end. *Epicondylus dorsalis* (m) is rounded. (*Processus supracondylaris dorsalis* (n) is damaged. The widening between it and the diaphysis is deeper and more narrowed than in the recent species)

On proximal epiphysis of carpometacarpus in ventral view (Fig. 52C), the *trochlea carpalis* (a) is asymmetrically bulging, wide and flattened. It has rounded end, as the recent species. *Proc. extensorius* (b) has oblique beak-like shape with rounded end. *Processus alularis* (c) is weakly developed and has rechtangle shape. Bellow it the *fovea subalularis* (d) is acute angled. *Protuberantia metacarpalis* (e) is wide and flat.

On tibiotarsus the distal epiphysis in cranial view (Fig. 52D), the *tuberositas retinaculi m. fibularis* (a) is weakly developed, bellow it the diaphysis narrowing. *Sulcus extensorius* (a) is wide, with rounded end. *Pons supratendinous* (c) is wide and straight. *Condylus lateralis* (d) is oval and flattened, with pointed end. Line of *incisura intercondylaris* (e) is concave. C*ondylus medialis* (f) has reversed oval shape.

On distal epiphysis of tarsometatarsus in dorsal view (Fig. 52E), the edge (b) between *fossa metatarsi* I. (a) and *trochlea metatarsi* II. is wavy. *Trochlea metatarsi* II. (c) has lopsided conical shape. *Incisura intertrochlearis medialis* (d) is wide and weakly deep. *Trochlea metatarsi III.* (e) is wide and its end is slightly concave. *Incisura intertrochlearis lateralis* (f) is wide and deep. *Trochlea* metatarsi IV. (g) has short conical shape with blunted end.

Description: It is a medium-sized species. The *crista pectoralis* is damaged. The tibiotarsi are relatively smaller than the other bones.

Sylvia † pussila nova sp.
(Plate XIII. Figure 53 A-C)

Type locality and age: Csarnóta 2, Pliocene (MN 15-16).

Other locality: Beremend 26, Pliocene (MN 15-16).

Holotype: Carpometacarpus sin. (proximal fragment), (Csarnóta 2, MÁFI V.11.7.1; V.29082).

Paratypes: Carpometacarpus dext. (proximal fragment); one right and one left side tarsometatarsus (distal fragments), (Csarnóta 2, MÁFI V.11.108.3; V.29183); proximal fragment of humerus dext. (Beremend 26, BKA).

Measurements: 1. humerus B=5,03 mm; C=4,71 mm; D=3,37 mm; E=1,47 mm 2. carpometacarpus C=2.,43-2.53 mm; 3. tarsometatarsus F=1.64-1.68 mm; G=1.09-1.27 mm.

Comparative material: Sylvia atricapilla (MTM n=1; humerus B=4,88 mm; C=5,07 mm; D=3,73 mm; E=1,48 mm; carpometacarpus: C=2.38 mm; tarsometatarsus: F=1.47 mm); *S. borin* (MTM n=1; humerus C=5,48 mm; E=1,69 mm; carpometacarpus: C=3.11 mm; tarsometatarsus: F=1.92 mm; G=1.18 mm); *S. communis* (MTM n=1; humerus C=4,90 mm; E=1,52 mm; carpometacarpus: C=2.46 mm; tarsometatarsus: F=1.78 mm); *S. curruca* (MTM n=1; humerus C=4,47 mm; E=1,34 mm; carpometacarpus: C=2.52 mm; tarsometatarsus: F=1.52 mm).

Diagnosis: On proximal epiphysis of humerus in cranial view (Fig. 53A), the c*aput humeri* (a) is wide and less convex. *Tuberculum ventrale* (b) forms oval-like spur. *Crista bicipitalis* (c) is rounded and strongly protruding. *Crus fossae* (d) is well developed, therefore *fossae pneumotricipitalis* (e) is divided in two.

On proximal epiphysis of the carpometacarpusus in ventral view (Fig. 53B), the *trochlea carpalis* (a) is symmetrically bulged conical shape. *Proc. extensorius* (b) is obliquely and strongly blunted conical shaped. *Processus alularis* (c) has rectangle shape. *Fovea subalularis* (d) has pointed conical shape.

On distal epiphysis of tarsometatarsusus in dorsal view (Fig. 53C), the edge between *fossa metatarsalis* I. and *trochlea metatarsi* II. (a) is wavy. *Trochlea metatarsi* II. (b) is damaged. *Incisura intertrochlearis medialis* (c) has wide acute angle shape. *Trochlea metatarsi tertii* (d) is wide and with bellow concave end. *Incisura intertrochlearis lateralis* (e) is strongly wide. T*rochlea metatarsi* IV. (f) has asymmetrically rounded shape.

Name: Its name refers to smaller size of species.

Description: The bones become to one smaller size species. The *trochlea metatarsi* II. is damaged.

Distribution: The genus was described also from the Carpathian Basin as *Sylvia* sp. foss.indet. in the Late Miocene of Polgárdi (MN13) (JÁNOSSY 1991); from Csarnóta 2 and Beremend 26 - Hungary (Lower Pliocene, MN 15) (KESSLER 2010); and in the Early Pleistocene of Betfia 9-Romania (MQ1) (GÁL 2002). The recent species was reported also from the Early Pleistocene (MQ1) as *Sylvia atricapilla* (LINNAEUS, 1758) from Betfia 9-Romania (GÁL 2002) and Deutsch-Altenburg -Austria (JÁNOSSY 1981); *Sylvia communis* LATHAM, 1787 from Betfia 2-Romania (ČAPEK, 1917; LAMBRECHT 1933; JÁNOSSY 1979; KESSLER 1975; GÁL 2002); and from Betfia 9 – Romania (KESSLER 1975; GÁL 2002).

The genus it is known outside the Carpathian Basin from the Early Pleistocene of S'Onix – Mallorca, Spain (MN 18) (SONDAAR et al. 1995) with recent species.

Genus *Locustella* KAUP, 1829
Locustella † kordosi nova sp.
(Plate XIV. Figure 54 A-D)

Type locality and age: Polgárdi 4, 5; Late Miocene (MN 13).

Holotype: Humerus dext. (proximal fragment), (MÁFI V.11.104.1; V.29179).

Paratypes: Humerus sin. (proximal fragment); ulna sin. (distal fragment); 8 tibiotarsi (4 sin. and 4 dext. distal fragments), (MÁFI V.11.111.1, V.11.126.9; V.29186, V.29201).

Measurements: 1. humerus C=3.83-4.14 mm; 2. ulna F=2.36 mm, G=1.71 mm; 3. tibiotarsus E=1.09 mm; F=2.03-2.25 mm; G=1.83-2.20 mm.

Comparative material: Locustella fluviatilis (MTM n=1: ulna F=2,69 mm, G=1.89 mm; tibiotarsus E=1.14 mm; F=2.55 mm); *L. luscinia* (MTM n=1: humerus C=4.61 mm; ulna F=2.29 mm, G=1.67 mm; tibiotarsus E=1.13 mm; F=2.22 mm; G=2.17 mm); *L. naevia* (MTM n=1: humerus C=4.18 mm; ulna F=2.43 mm; tibiotarsus E=1.07 mm; F=2.16 mm).

Diagnosis: Corresponds in characteristics to species of recent genus. On proximal epiphysis of humerus in caudal view (Fig. 54A), the *tuberculum dorsale* (a) is angular. *Caput humeri* (b) is wide and convex. *Tuberculum ventrale* (c) is well developed and has one semicircular shape. *Crus fossae* (e) is well developed, therefore *fossae pneumotricipitalis* (f) is divided in two. In cranial view (Fig. 54B), the *crista bicipitalis* (d) is asymmetrically protruding and rounded.

On distal epiphysis of ulna in medial view (Fig. 54C), the *condylus dorsalis* (a) has claw-like shape. *Sulcus intercondylaris* (b) is less concave. *Condylus ventralis* (c) is wide and blunt, oblique, conical shaped. *Tuberculum carpale* (d) is protruding and has simmetrically rounded shape.

On tibiotarsus the distal epiphysis in cranial view (Fig. 54D), the *tuberositas retinaculi m. fibularis* (a) is weakly developed and flattened, bellow it the diaphysis is narrowing. *Sulcus extensorius* (b) is wide. *Pons supratendinous* (c) is narrow and slightly lopsided. *Condylus lateralis* (d) is oval. Line of i*ncisura intercondylaris* (e) is concave and slightly wavy. C*ondylus medialis* (f) has flattened oval shape.

Name: Was named after László KORDOS, Hungarian paleontologist.

Description: It is corresponds in characteristics and sizes to the recent species of the genus. On proximal epiphysis of humerus the *crista pectoralis* is damaged. On ulna the *condylus dorsalis* is more pointed than in the recent species.

Locustella † janossyi nova sp.
(Plate XIV. Figure 55 A-B)

Type locality and age: Csarnóta 2, Pliocene (MN 15-16).

Other locality: Beremend 26, Pliocene (MN 15-16).

Holotype: Tibiotarsus dext. (distal fragment), (Csarnóta 2, MÁFI V.11.35.1; V.29110).

Paratype: Distal fragment of humerus sin. (Beremend 26, BKA).

Measurements: humerus F=3,73 mm; G=2,08 mm; tibiotarsus E=1.14 mm; F=1.77 mm; G=2.02 mm.

Comparative material: Locustella luscinia (MTM n=1; tibiotarsus: E=1.16 mm; F=2.15 mm; G=2.28 mm); *Locustella naevia* (MTM n=1: humerus F=3,59 mm; G=1,90 mm; tibiotarsus: E=1.28 mm; F=3,31); *Locustella luscinoides* (MTM n=1: humerus F=2,91 mm; G=1,75 mm; tibiotarsus: E=1.23 mm; F=2,91).

Diagnosis: On distal epiphysis in cranial view of humerus (Fig. 55A), the *tuberculum ventrale* (a) is well developed. The *epicondylus ventralis* (b) is strongly arches. *Processus flexorius* (c) is less protruding and rounded. *Condylus ventralis* (d) has extended oval shape. *Incisura intercondylaris* (e) is deep and wide. *Condylus dorsalis* (f) has bented oval shape. *Epicondylus dorsalis* (g) is rounded. *Proc. supracondylaris dorsalis* (h) has pointed shape (but it is damaged).

On distal epiphysis of tibiotarsusus in cranial view (Fig. 55B), the *tuberositas retinaculi m. fibularis* (a) is wide and flattened. *Sulcus extensorius* (b) is wide and distally rounded. *Pons supratendineus* (c) is wide and weakly obliquely. *Condylus lateralis* (d) is damaged, but has laterally flatted and distaly pointed shape. Line of i*ncisura intercondylaris* (e) is concave and slightly wavy. C*ondylus medialis* (f) is distaly pointed and lateraly flattened shaped.

Name: Was named after the Hungarian paleornithologist Dénes JÁNOSSY.

Description: Corresponds in its characteristics to recent genus and in dimensions with smaller sizes recent species. The extinct species identified from Polgárdi – Hungary (Upper Miocene, MN 13) as *L. kordosi* KESSLER, 2012 differ it in bigger size and in the shape of *pons tendineus* and *condylus medialis* (the previosly is narrow and the latter is more stodgy than the Polgárdi specimen).

Locustella † magna nova sp.
(Plate XIV. Figure 56 A-B)

Type locality and age: Beremend 26, Pliocene (MN 15-16).

Holotype: Humerus sin. (BKA)

Measurements: Humerus A=16,91 mm; B=7,11 mm; C=5,73 mm; D=4,68 mm: E=1,61 mm; F=4,48 mm; G=2,36 mm.

Comparative material: Locustella luscinioides (MTM n=1: humerus A=15,21 mm; B=5,43 mm; C=4,66 mm; D=3,81 mm: E=1,48 mm; F=3,69 mm; G=1,89 mm); *L. naevia* (MTM n=1: humerus

A=13,14 mm; B=mm; C=4,18 mm; D=mm: E=1,28 mm; F=3,34 mm).

Diagnosis: On proximal epiphysis of humerus in cranial view (Fig. 56A), the *tuberculum dorsale* (a) is rounded. C*aput humeri* (b) is wide and convex. *Tuberculum ventrale* (c) forms semicircular spur. *Crista bicipitalis* (d) is asymmetrical rounded and strongly protruding. *Crus fossae* (e) is well developed, therefore *fossae pneumotricipitalis* (f) is divided in two.

On distal epiphysis in cranial view of humerus (Fig. 56), the *tuberculum ventrale* (g) is developed. The *epicondylus ventralis* (h) is rounded. *Processus flexorius* (i) is protruding and rounded. *Condylus ventralis* (j) has extended oval shape. *Incisura intercondylaris* (k) is deep and wide. *Condylus dorsalis* (l) has bent oval shape. *Epicondylus dorsalis* (m) is rounded. *Proc. supracondylaris dorsalis* (n) is wide with rounded end.

Name: Was named after its large size.

Description: Corresponds in its characteristics to recent species, but it is more larger in its sizes.

Distribution: The genus was reported as *Locustella* sp. foss.indet. from the Late Miocene of Rudabánya – Hungary (MN 9), (JÁNOSSY 1994) and as *Locustella fluviatilis* (WOLF, 1810) from the Early Pleistocene (MQ1) of Betfia 9 - Romania (GÁL 2002).

Outside of the Carpathian Basin the genus is known only from the Late Pleistocene of Czech Republic (TYRBERG 1998).

Genus *Regulus* VIEILLOT, 1807
Regulus † *pliocaenicus* nova sp.
(Plate XIV. Figure 57)

Type locality and age: Beremend 26, Pliocene (MN 15-16).

Holotype: Humerus sin. with damaged distal epiphysis (BKA).

Measurements: Humerus A=apr.11,50 mm; B=3,40 mm; C=3,36 mm; D=3,17 mm: E=1,20 mm; F= apr.2,60 mm; G=apr.1,50 mm.

Comparative material: Regulus regulus (MTM n=1: humerus A=10,27 mm; B=3,50 mm; C=2,90 mm; D=1,32 mm: E=0,98 mm; F=2,79 mm; G=1,24 mm).

Diagnosis: On proximal epiphysis of humerus in cranial view (Fig. 57), the *tuberculum dorsale* (a) is rounded. C*aput humeri* (b) is wide and convex. *Tuberculum ventrale* (c) forms semicircular spur. *Crista bicipitalis* (d) is asymmetrical rounded. *Crus fossae* (e) is less developed, but *fossae pneumotricipitalis* (f) is divided into two. On distal epiphysis in cranial view of humerus, the *proc. supracondylaris dorsalis* (g) is located low and away from the corpus of epiphysis.

Name: Was named after the age of site.

Description: Corresponds in its characteristics to recent species, but it is larger in its sizes.

Distribution: The genus is known with the extinct species *Regulus bulgaricus* BOEV, 1999 from Varshets - Bulgaria (Late Pliocene, MN 17) (BOEV 1999). The recent species was reported from S'Onix - Mallorca, Spain (Early Pleistocene, Q1) (SONDAAR et el.1995) and from Hundsheim - Austria (Middle Pleistocene, Q3) (LAMBRECHT 1933; JÁNOSSY 1974, 1979) and from some sites of the the Late Pleistocene from Europa (TYRBERG 1998).

Genus *Phylloscopus* BOIE, 1826
Phylloscopus † *venczeli* nova sp.
(Plate XV. Figure 58 A-C)

Type locality and age: Polgárdi 4, Late Miocene (MN 13).

Holotype: Carpometacarpus dext. (MÁFI V.11.74.1; V.29149).

Paratypes: Two ulnae sin. (one complete and one proximal fragment); carpometacarpus dext. (proximal fragment), (MÁFI V.11.89.4; V.29164).

Measurements: 1. carpometacarpus A=9.19 mm; C=2.21-2.42 mm; E=1.77 mm; F= 2.18 mm; 2. ulna A=14.73 mm; B=2.49-2.76 mm; C=2.09-2.46 mm; E= 1.09 mm; F=2.14 mm; G=1.66 mm;

Comparative material: Phylloscopus collybita (MTM n=1: 1. carpometacarpus A=9.51 mm; C=2.22 mm; 2. ulna A=16.73 mm; B=2.62 mm; C=2.23 mm; E=1.02 mm; F=2.09 mm; G=1.61 mm); *P.sibilatrix* (MTM n=1: 1. carpometacarpus A=9.17 mm; C=2.39 mm; E=1.78 mm; F=2.19 mm; 2. ulna A=16.66 mm; B=2.58 mm; C=2.44 mm; E= 1.18 mm; F=2.01 mm; G=1.53 mm); *P. trochilus* (MTM n=1: 1. carpometacarpus A=10.35 mm; C=1.95 mm; 2. ulna A=15.76 mm; C=2.14 mm; E=1.03 mm; F=1.97mm).

Diagnosis: Corresponds in its characteristics to recent species of the genus. On proximal epiphysis of ulna in cranial view (Fig. 58A), the *oleocranon* (a) is long, even and blunt. *Cotyla dorsalis* (b) has protruding symmetrically semicircular shape. C*otyla ventralis* (c) has symmetrically circular shape. *Tuberculum lig. colat. ventralis* (d) and *depressio m. brachialis* (e) are developed. On distal epiphysis in medial view (Fig. 58B), *condylus dorsalis* (f) has rounded blunt claw shape. *Sulcus intercondylaris* (b) is slightly concave. *Condylus ventralis* (c) is oblique and blunt conical. *Tuberculum carpale* (f) has truncated conical shape.

On proximal epiphysis of carpometacarpus in ventral view (Fig. 58C), the *trochlea carpalis* (a) is semicircular (but partially damaged). *Proc. extensorius* (b) is short, stout and oblique conical. *Processus alularis* (c) is small and rectangular shaped, below it, the *fovea subalularis* (d) is acute angle shaped. *Protuberantia metacarpalis* (e) is small and has triangular shape.

Name: Was named after the Hungarian paleontologist from Romania, Márton VENCZEL.

Description: It corresponds in characteristics and sizes to recent species of the genus. The genus was reported from Felsőtárkány–Hungary (Middle Miocene, MN 7/8) as *Phylloscopus miocaenicus* KESSLER et HÍR 2012 in basis of phalanga alae 1. dig. II. did, but this bone it is not in Polgardi's material. (KESSLER & HÍR 2012).

Phylloscopus †*pliocaenicus* nova sp.
(Plate XV. Figure 59)

Type locality and age: Csarnóta 2, Pliocene (MN 15-16).

Holotype: Humerus dext. (with damaged proximal epiphysis), (MÁFI V.11.3.1; V.29078).

Measurements: Humerus A=aprox.13-14 mm; E=1.29 mm; F=3.55 mm; G=1.84 mm.

Comparative material: Phylloscopus trochillus (MTM n=1; humerus: A=13.25 mm; E=1.43 mm; F=3.25 mm; G=1.74 mm), *Phylloscopus collybita* (MTM n=1; humerus: A=12.30 mm; E=11.80 mm; F=3.01 mm; G=1.66 mm).

Diagnosis: On distal epiphysis in cranial view of humerus (Fig. 59), the *tuberculum ventrale* (a) is well developed. The *epicondylus ventralis* (b) is strongly arches. *Processus flexorius* (h) has semicircular shape. *Condylus ventralis* (d) has extended oval shape. *Incisura intercondylaris* (e) is deep and narrow. *Condylus dorsalis* (f) has oval shape and less oblique than in the recent species. *Epicondylus dorsalis* (g) is strongly rounded.

Name: Its name refers to age of sediment.

Description: Its characteristics corresponds to recent genus. The *proc. supracondylaris dorsalis* missed. On recent species it is long with blunted end. The hollow. between it and the diaphysis is wide.

Distribution: Outside of Carpathian Basin the genus is known the the Late Pliocene from Varsets (MN 17, Bulgaria) as *Phylloscopus* sp. (BOEV 1996, 2000); from Cerdzenica – Bulgaria (Lower Pleistocene, MQ1), (BOEV 2000) and from Israel (Middle Pleistocene) (TYRBERG 1998).

The family was identified in Neogene only from the Carpathian Basin.

Family Motacillidae (VIGORS, 1825)
Genus *Anthus* BECHSTEIN, 1807
Anthus † *híri* nova sp.
Plate XV. Figure 60 A-C)

Type locality and age: Polgárdi 5, Late Miocene (MN 13).

Holotype: Carpometacarpus dext. (MÁFI V.11.98.1; V.29173).

Paratypes: Two carpometacarpi (proximal fragments dext. and sin.), tarsometatarsus sin. (distal fragment) (MÁFI V.11.122.3; V.29197).

Measurements: 1. carpometacarpus A=11.83 mm; C=2.61-3.09 mm; F=2.58 mm; 2. tarsometatarsus F=2.19 mm; G=1.38 mm.

Comparative material: Anthus campetris (MTM n=1: carpometacarpus A=15.13 mm; C=3.41 mm; F=3.22 mm; tarsometatarsus F=2.34 mm; G=1.39 mm); *A. pratensis* (MTM n=1: carpometacarpus A=14.28 mm; C=3.76 mm; F=2.93 mm; tarsometatarsus F=2.33 mm; G=1.35 mm); *A. spinoletta* (MTM n=1: carpometacarpus A=14.09 mm; C=3.48 mm; F=2.68 mm; tarsometatarsus F=2.37 mm; G=1.18 mm); *A. trivialis* (MTM n=1: carpometacarpus A=12.83 mm; C=3.15 mm; F=2.79 mm; tarsometatarsus F=2.14 mm; G=1.11mm).

Diagnosis: Its characteristics corresponds to recent *Anthus* genus, in sizes to smaller species as *A. spinoletta* and *A. trivialis.* On proximal epiphysis of carpometacarpus in ventral view (Fig. 60A), the *trochlea carpalis* (a) is symmetrically bulging semicircular. *Proc. extensorius* (b) is short, obliquely asymmetric and has rounded end. *Processus alularis* (c) is rectangular shaped, below it, *fovea subalularis* (d) has mangled conical shape (in dorsal view, Fig. 60B). The large p*rotuberantia metacarpalis* (e) is triangular.

On distal epiphysis of tarsometatarsus in dorsal view (Fig. 60C), *trochlea metatarsi II.* (a) has asymmetrical conical shape. *Incisura intertrochlearis medialis* (b) is acute angle shaped. *Trochlea metatarsi III.* (c) is wide, and its end is concave. *Incisura intertrochlearis lateralis* (d) is acute angle shaped. *Trochlea* metatarsi IV. (e) is wider claw-like.

Name: Was named after Hungarian paleontologist János HÍR.

Description: It correspond in its characters to recent genus *Anthus* its sizes is between recent *A. spinoletta* and *A. trivialis,* id est belongs to the pipits with a smaller stature. The fosssil species *Anthus antecedens* KESSLER et HÍR, 2012 from Mddle Miocene of Felsőtárkány (MN 7/8) was identified based on one phalanga alae (KESSLER & HÍR 2012), otherwise it is assigned to pipits with larger stature.

Anthus † *baranensis* nova sp.
(Plate XV. Figure 61 A-B)

Type locality and age: Csarnóta 2, Pliocene (MN 15-16).

Holotype: Coracoid dext. (cranial fragment) (MÁFI V.11.8.1; V.29083).

Paratypes: Ulna sin. (distal fragment) (MÁFI V.11.36.1; V.29111).

Measurements: 1. coracoid C=2.93 mm; D=2.49 mm; 2. ulna F=3.03 mm.

Comparative material: Anthus trivialis (MTM n=1; coracoid: C=3.15 mm; D=2.42 mm; ulna: F=2.86 mm).

Diagnosis: On medial side of coracoideum (Fig. 61A) in cranial end, the *acrocoracoideum* (a) has

symmetrical blunted cone shape. Its medial edge bulges mildly. End of *processus accesorius* (b) has elongated beak-like shape. Edge of *sulcus m. supracoracoideumei* (c) is mildly flattened concave shape. *Facies articularis humeralis* (d) has cranial edge, strongly bulges and rounded. Point of *processus procoracoideumei* (e) more exceeds the medial edge of corpus.

On distal epiphysis in medial view of ulna (Fig. 61B), the *condylus dorsalis* (a) is strongly rounded and has conical shape. *Sulcus intercondylaris* (b) is wide and slightly concave. *Condylus ventralis* (c) has asymmetrical semicircular shape. *Tuberculum carpale* (d) has asymmetrical blunted conical shape.

Etymology: Was named after the name of the Baranya County.

Description: It corresponds in its characteristics to smaller size recent species.

Distribution: The genus was reported also as *Anthus* sp. foss.indet. from Beremend 15 – Hungary (Late Pliocene, MN 16) by JÁNOSSY (1992); from Betfia 2 – Romania (Early Pleistocene, MQ1), (ČAPEK 1917; LAMBRECHT 1933; JÁNOSSY 1979; KESSLER 1975; GÁL 2002); and from Betfia 9-Romania (Early Pleistocene, MQ1), (KESSLER 1975; GÁL 2002).

On outside the Carpathian Basin the genus is known from Rebielice Królowskie 1 – Poland (Upper Pliocene, MN 16) (JÁNOSSY, 1974); Varseths - Bulgaria (Upper Pliocene, MN 16, MN 17) (BOEV 1996, 2000) and with recent species from the Early Pleistocene of Bulgaria, Czech Republic, France and Spain (Tyrberg 1998). The fossil species *Anthus bosniaskii* PYCRAFT, 1909 from Gabbro – Italy (Upper Miocene, MN 13) was put by MLÍKOVSKÝ into „*Family incertae sedis"* (MLÍKOVSKÝ 2002).

Genus *Motacilla* LINNAEUS, 1758
Motacilla †*intermedia* nova sp.
(Plate XVI. Figure 62 A-G)

Type locality and age: Polgárdi 4,5; Late Miocene (MN 13).

Holotype: Humerus sin. (proximal fragment (MÁFI V.11.95.1; V.29170).

Paratypes: Humerus dext. (with damaged proximal epiphysis); 4 sin. and dext. humeri (distal fragments); 2 ulnae sin.(distal fragments); 3 dext. and one sin. complete carpometacarpi; one dext. and one sin. carpometacarpi (missing *os metacarpale minus*), 4 femura (distal fragments, 2 dext. and 2 sin.); tibiotarsi dext. (distal fragment); 4 tarsometatarsi sin. (distal fragments) (MÁFI V.11.114.7, V.11.119.9; V.29189, V.29154).

Measurements: 1.humerus A=14.75 mm; B=5.69 mm; C=5.79 mm; E=1.48-1.86 mm; F= 3.66-4.41 mm; G=1.98-2.38 mm; 2. ulna E=1.61 -1,91 mm; F=2.65-3.30 mm; G=1.69-2.22 mm; 3. carpometacarpus A=11.85-12.39 mm; C=2.84-2.97 mm; F=2.47mm; 4. femur E=1.18-1.33 mm; F=2.61-2.93 mm; G=2.01-2.29 mm; 5. tibiotarsus F=2.36 mm; G=2.18 mm; 6. tarsometatarsus E=0.93-1.12 mm; F=2.05-2.19 mm; G=1.13-1.15 mm.

Comparative material: Motacilla alba (MTM n= 1: humerus A=18.50 mm; B=5.86 mm; C=5.99 mm; E=2.07 mm; F=4.54 mm; G=2.49 mm; ulna E=1.53 mm; F=2.99 mm; G=2.12 mm; carpometacarpus A=14.28 mm; C=3.53 mm; F= 2.81mm; femur E=1.34 mm; F=2.92 mm; G=2.33 mm; tibiotarsus F= 2.43 mm; G=2.38 mm; tarsometatarsus E=1.08 mm; F=2.21 mm; G=1,23 mm); *M cinerea* (MTM n= 1: humerus A=17.40 mm; B=5.48 mm; E=1.48-1.86 mm; F=3.69 mm; G=2.44 mm; ulna E=1.38 mm; F=2.54 mm; G=1.83 mm; carpometacarpus A=12.63 mm; C=3.01 mm; F=2.62mm; femur E=1.01 mm; F=1.93 mm; G=1.85 mm; tibiotarsus F= 2.36 mm; G=2.18 mm; tarsometatarsus E=1.01mm; F=2.05-2.19 mm; G=113mm); *M. flava* (MTM n= 1: humerus A=17.04 mm; B=5.30 mm; C=6.04 mm; E=1.60 mm; F=4.83 mm; G=2.28 mm; ulna E=1.47 mm; F=2.64 mm; G=1.78 mm; carpometacarpus A=12.63 mm; C=3.82 mm; F=2.78 mm; femur E=1.18 mm; F=2.52 mm; G=2.00 mm; tibiotarsus F=2.36 mm; G=2.32 mm; tarsometatarsus E=1.48 mm; F=2.07 mm; G=1.16 mm).

Diagnosis: On proximal epiphysis of humerus in caudal view (Fig. 62A), the *tuberculum dorsale* (a) is rounded. *Caput humeri* (b) is wide and convex, but not too outstanding. *Tuberculum ventrale* (c) is semicircular and smaller than in recent species. *Crista bicipitalis* (d) is slightly pointed and has protruding beak shape. *Crus dorsale fossae* is weakly developed, therefore the two parts of *fossa pneumotricipitalis* (e) are shown together. On distal epiphysis in cranial view (Fig. 62B), the *tuberculum supracondylare ventrale* (f) is developed. *Epicondylus ventralis* (g) is rounded. *Processus flexorius* (h) is slightly lopsided and rounded. *Condylus ventralis* (i) is extended oval shaped. *Incisura intercondylaris* (j) is in acute angle. *Condylus dorsalis* (k) has strongly curved ovale shaped. *Epicondylus dorsalis* (l) is rounded. *Proc. supracondylaris dorsalis* (m) is slightly pointed.

On distal epiphysis of ulna in medial view (Fig. 62C), the *condylus dorsalis* (a) is laterally rounded and has a distally pointed claw-like shape. *Sulcus intercondylaris* (b) is concave. *Condylus ventralis* (c) has oblique conical shape. *Tuberculum carpale* (d) is asymmetrically rounded and protruding.

On proximal epiphysis of the carpometacarpus in ventral view (Fig. 62D), the *trochlea carpalis* (a) is symmetrically bulging. It is semicircular, as in the recent species. *Proc. extensorius* (b) has short, oblique conical-like shape with rounded end. *Processus alularis* (c) is conical, below it, the *fovea subalularis* (d) has acute angle shape. *Protuberantia metacarpalis* (e) is large and has triangular shape.

On distal epiphysis of femur in caudal view (Fig. 62E), the exterior side of *trochlea fibularis* (a) is rounded. Distal end of *condylus lateralis* (b) forms

one arc. *Incisura intercondylaris* (c) is concave. *Condylus medialis* (d) has oblique, strongly blunted conical shaped. *Epicondylus medialis* (e) is well developed.

On distal epiphysis of tibiotarsus in cranial view (Fig. 62F), the *tuberositas retinaculi m. fibularis* (a) is flat and underdeveloped. *Sulcus extensorius* (b) is narrow with rounded distal end. *Pons supratendinous* (c) is wide and straight. *Condylus lateralis* (d) has oval shape, with distaly rounded end. Line of i*ncisura intercondylaris* (e) is concave and wavy. C*ondylus medialis* (f) is distally rounded oval shaped.

On distal epiphysis of tarsometatarsus in dorsal view (Fig. 62G), the *trochlea metatarsi II.* (a) is distal widening conical, with cut-off end. *Incisura intertrochlearis medialis* (b) is narow and deep. *Trochlea metatarsi* III. (c) is wide with mildly concave end. *Incisura intertrochlearis lateralis* (d) is deep and widening. *Trochlea metatarsi* IV. (e) is asymmetric conical with rounded end.

Name: Was named after its intermediate charateristics.

Description: The sizes is intermediate between to *M. alba* and *M. cinerea* , but in morphological characteristics it resembles *M. alba*. In several characters it exhibits the mixture of the characters of *Anthus* and *Motacilla* types.

Motacilla † *minor* nova sp.
(Plate XVI. Figure 63)

Type locality and age: Beremend 26, Pliocene (MN 15-16).

Holotype: Carpometacarpus dext. (BKA).

Measurements: Carpometacarpus A=12,37 mm; B=10,28 mm; C=3,22 mm; F=2,30 mm.

Comparative material: Motacilla alba (MTM n=1: A=14,28 mm; C=3,53 mm; F= 2,81mm); *M cinerea* (MTM n= 1: A=12,63 mm; C=3,01 mm; F= 2,62mm); *M. flava* (MTM n= 1: A=12,94 mm; C=3,82 mm; F=2,78 mm).

Diagnosis: On proximal epiphysis of carpometacarpus in ventral view (Fig. 26), the *trochlea carpalis* (a) has asymmetrically bulging conical shape. *Proc. extensorius* (b) is obliquely asymmetrical shaped with rounded end. *Processus alularis* (c) is rounded rechtangle shaped, below it, *fovea subalularis* (d) has mangled conical shape. *Protuberantia metacarpalis* (e) is undeveloped.

Name: Was named after its small size.

Description: It corresponds in its characteristics with recent *Motacilla flava*, but has intermediate dimensions between *M. flava* and *M. cinerea*.

Motacilla † *robusta* nova sp.
(Plate XVI. Figure 64)

Type locality and age: Beremend 26, Pliocene (MN 15-16).

Holotype: Proximal fragment of humerus sin. (BKA).

Measurements: Humerus B=7,31 mm; C=6,91 mm; E=2,18 mm.

Comparative material: Motacilla alba (MTM n=1: humerus B=6,91 mm; C=5,80 mm; E= 1,72 mm); *M cinerea* (MTM n=1: humerus B=5,93 mm; C=5,23 mm; E=1,84 mm); *M. flava* (MTM n=1: humerus B=6,24 mm; C=5,21 mm; E=1,89 mm).

Diagnosis: On proximal epiphysis of humerus in caudal view (Fig. 64), the *tuberculum dorsale* (a) is rounded. *Caput humeri* (b) is wide and less convex, not too outstanding. *Tuberculum ventrale* (c) is semicircular and smaller than in the recents species. *Crista bicipitalis* (d) is protruding with pointed cut-off end. *Crus dorsale fossae* is weakly developed, therefore the two parts of *fossa pneumotricipitalis* (e) are shown together.

Name: Was named after its bigger dimensions.

Description: It is more robust than the recent species.

Distribution: In the Carpathian Basin the genus was reported also from Mátraszölős 1 - Hungary (Middle Miocene, MN 7/8) as *Motacilla* sp. indet. based on a claw (KESSLER & HÍR 2012), from Csarnóta 2 – Hungary (Lower Pliocene, MN 15), (KESSLER 2010); from Beremend 26 – Hungary (Lower Pliocene, MN 15) (KESSLER 2010) and from Polgárdi (Upper Miocene, MN 13) by JÁNOSSY (1991). The recent species is known from the Early Pleistocene (MQ1) as *Motacilla alba* LINNAEUS, 1758 Q1 from Betfia 2 - Romania (ČAPEK 1917; LAMBRECHT 1933; JÁNOSSY 1979a; KESSLER 1975; GÁL 2002); from Betfia 9 - Romania (KESSLER 1975; GÁL 2002); as *Motacilla flava* LINNAEUS, 1758; Q1 from Betfia 9 - Romania (GÁL 2002) and as *Motacilla cinerea* TUNSTALL, 1771; Q1 from Betfia 9 - Romania (GÁL 2002).

The genus was described outside of the Carpathian Basin from Varshets – Bulgaria (Upper Pliocene, MN 17) by BOEV (1996, 2000), and from Stránská skálá – Czech Republic (Lower Pleistocene, MQ1) by MLÍKOVSKÝ (1995). The fossil species *Motacilla humata* MILNE-EDWARDS 1871 and *Motacilla major* MILNE-EDWARDS 1871 (MILNE-EDWARDS 1871) from Saint-Gerand-le-Puy – France (Lower Miocene, MN 2) has a disputed situation (MLÍKOVSKÝ 2002).

Family Bombycillidae (SWAINSON), 1832
Genus *Bombycilla* (SWAINSON), 1832
Bombycilla †*brevia* nova sp.
(Plate XVII. Figure 65 A-C)

Type locality and age: Polgárdi 5, Late Miocene (MN 13).

Holotype: Coracoideum dext. (MÁFI V.11.96.1; V.29171).

Paratypes: Humerus dext. (with damaged proximal epiphysis); tibiotarsus sin. (distal fragment) (MÁFI V.11.120.2; V.29195).

Measurements: 1. coracoid A=17.95 mm; B=17.11 mm; C=2.48 mm; D=3.19 mm; E=1.56 mm; G=4.28 mm; 2. humerus A= approx. 22-23 mm; E=2.41 mm; F=5.91 mm; G=3.22 mm; 3. tibiotarsus F=2.94 mm; G=2.62 mmm.

Comparative material: Bombycilla garrulus (MTM n=1: coracoid A=24.44 mm; B=23.96 mm; C=3.78 mm; D=4.55 mm; E=2.35 mm; G=6.39 mm; humerus A=26.12 mm; E=2.65 mm; F=6.53 mm; G=3.71 mm; tibiotarsus E=1.45 mm; F=3.28 mm; G=3.22 mmm).

Diagnosis: Coracoid and tibiotarsus are smaller than in recent species. On the dorsal side of coracoid (Fig. 65A), the *acrocoracoid* (a) is short and has truncated conical shape. *Processus accesorius* (b) has short and blunted conical shape. Edge of *sulcus m. supracoracoidei* (c) forms strongly concave line. *Processus procoracoidei* (d) is triangular and its point strongly exceeds the medial edge of the corpus. *Facies aricularis humeralis* (e) has straight medial edge with a rounded cranial end.

On the distal epiphysis in cranial view of the humerus (Fig. 65B), the *tuberculum supracondylare ventrale* (a) is rounded and less bulged than in the recent species. *Processus flexorius* (b) is protruding and distally rounded. *Condylus ventralis* (c) is oval shaped with pointed end. *Incisura intercondylaris* (d) is concave and deep. *Condylus dorsalis* (e) has strongly curved oval shape, more than in the recent species. *Epicondylus dorsalis* (f) is less rounded than in recent genus. *Proc. supracondylaris dorsalis* (g) is short, blunt, forked, but the distal larger branch is shorter than in the recent species.

On tibiotarsus the distal epiphysis in cranial view (Fig. 65C), the *tuberositas retinaculi m. fibularis* (a) is wide and rounded, situated distantly the distal epiphysis. *Sulcus extensorius* (b) is wide. *Pons supratendinous* (c) is wide and straight. *Condylus lateralis* (d) is distally rounded oval. The line of i*ncisura intercondylaris* (e) is wavy. C*ondylus medialis* (f) is distally rounded and laterally flattened oval.

Name: Its name is after the brevity of the bones last.

Description: The dimensions of the coracoid and tibiotarsus are much smaller than in the recent species. The humerus is already less. The tibiotarsus of the fossil species *Bombycilla hamori* KESSLER et HÍR, 2012 identified from Litke 2- Hungary (Lower Miocene, MN 5) is much larger than the Polgardi specimen. (F=3,32 mm; G=3,03 mm). In the morphological characters the two species are similar in that the *tuberositas retinaculi musculus fibularis* is rounded; the distal end of *sulcus extensorius* is wide; the *incisura intercondylaris* forms a wavy line; but the *condylus lateralis* and *condylus medialis* distally are not rounded but narrowing (KESSLER & HÍR 2012).

Bombycilla † *kubinyii* nova sp.
(Plate XVII. Figure 66 A-B)

Type locality and age: Beremend 26, Pliocene (MN 15-16).

Holotype: Humerus sin. with missed proximal epiphysis (BKA);

Paratypes: Distal fragment of the left side tibiotarsus (BKA).

Measurements: Humerus E=2,88 mm; F=7,95 mm; G=3,64 mm; tibiotarsus E=1,80 mm; F=3,44mm; G=2,99 mmm.

Comparative material: Bombycilla garrulus (MTM n=1: humerus E=2,65 mm; F=6,53 mm; G= 3,71 mm; tibiotarsus E=1,45 mm; F=3,51 mm; G=3,31 mmm).

Diagnosis: On distal epiphysis in cranial view of humerus (Fig. 66A), the *tuberculum supracondylare ventrale* (a) is rounded and less bulged than in the recent species. *Epicondylus ventralis* (b) is rounded. *Processus flexorius* (c) is protruding and distally rounded. *Condylus ventralis* (d) has oval shape. *Incisura intercondylaris* (e) is concave, wide and deep. *Condylus dorsalis* (f) is less rounded. *Epicondylus dorsalis* (g) is less rounded. *Proc. supracondylaris dorsalis* (h) is short, wide and blunt.

On tibiotarsus the distal epiphysis in cranial view (Fig. 66B), the *tuberositas retinaculi m. fibularis* (a) is small and flatted. *Sulcus extensorius* (b) is narrow and distally pointed. *Pons supratendinous* (c) is wide and straight. *Condylus lateralis* (d) is distally pointed ovalic. Line of i*ncisura intercondylaris* (e) is wavy. C*ondylus medialis* (f) is distally rounded and lateray flattened oval shaped.

Name: Was named after the name of Hungarian paleontologist Ferenc KUBINYI.

Description: It corresponds in its characteristics and size to recent species.

Distribution: The family and genus are known in fossil material in the Neogene and Quaternary only from the Carpathian Basin as *Bombycilla* sp. foss. indet. from Csarnóta 2 –Hungary (Lower Pliocene, MN 15) (KESSLER 2010), Beremend 26 - Hungary (Lower Pliocene, MN 15) (KESSLER 2010); Beremend 17 (Lower Plaistocene, MQ1) (JÁNOSSY 1992) and Betfia 9 –Romania (Lower Pleistocene, MQ1) (GÁL 2002).

Family Troglodytidae VIEILLOT, 1807
Genus *Troglodytes* VIEILLOT, 1807
Troglodytes †*robustus* nova sp.
(Plate XVII. Figure 67 A-E)

Type locality and age: Polgárdi 4, 5; Late Miocene (MN 13).

Holotype: Humerus sin. (Polgárdi 4, MÁFI V.11.64.1; V.29139).

Paratypes: Ulna dext. (proximal fragment); carpometacarpus dext.; tibiotarsus sin. (distal fragment) (Polgárdi 5, MÁFI V.11.121.3; V.29196).

Measurements: 1. humerus A=12.91 mm; B=3.39 mm; C=3.74 mm; D=3.35 mm; E=1.22 mm; F=3.07 mm; G=1.54 mm; 2. ulna B=2.51 mm; C=2.13 mm; E=1.42 mm; 3. carpometacarpus A=8.49 mm; C=2.69 mm; E=2.14 mm; F=2.19 mm; 4. tibiotarsus F=2.22 mm; G=2.08 mm.

Comparative material: Troglodytes troglodytes (MTM n=1; humerus A=11.96 mm; B=2.67 mm; C=3.22 mm; D=2.39 mm; E=1.11 mm; F=3.12 mm; G=1.55 mm; ulna B=2.38 mm; C=1.81 mm; E=1.26 mm; carpometacarpus A=7.97 mm; C=2.03 mm; E=2.06 mm; F=1.97 mm; tibiotarsus F=1.97 mm; G=1.83 mm).

Diagnosis: The fossil species differs of the recent in larger sizes and robustness of the bones. On the proximal epiphysis of humerus in caudal view (Fig. 67A), the *tuberculum dorsale* (a) is cut-off lateraly. *Caput humeri* (b) is wide, convex and flat. *Tuberculum ventrale* (c) is well developed and forms ovale-like spur. *Crista bicipitalis* (d) is rounded and protrouding. *Crus dorsale fossae* (e) is weakly developed and short, therefore the two parts of *fossa pneumotricipitalis* (f) are visible together. On distal epiphysis in cranial view of humerus (Fig. 67B), the *tuberculum supracondylare ventrale* (g) is well developed. *Epicondylus ventralis* (h) is mildly arched. *Processus flexorius* (i) is claw-like bent, its end is protrouding and rounded. *Condylus ventralis* (j) is well developed and has symmetrical oval shape. *Incisura intercondylaris* (k) is a wide pit. *Condylus dorsalis* (l) is distaly rounded. *Epicondylus dorsalis* (m) is rounded and well developed. *Processus supracondylaris dorsalis* (n) is wide, short and bented.

On proximal epiphysis of ulna in cranial view (Fig. 67C), the *oleocranon* (a) has long and blunted conical shape. *Cotyla dorsalis* (b) is asymmetrically rounded. C*otyla ventralis* (c) has mildly stretched circular shape. The *tuberculum lig. colat. ventralis* (d) is undeveloped. *Depressio m. brachialis* (e) is developed.

On proximal epiphysis of carpometacarpus in ventral view (Fig. 67D), the *trochlea carpalis* (a) is asymmetrically bulging. It has conical shape, but less blunted than in the recent species. *Proc. extensorius* (b) is short, with rounded end. *Processus alularis* (c) has rounded rectangular shape, below it the *fovea subalularis* (d) is acute angle shaped. *Protuberantia metacarpalis* (e) is a wide, blunt odontoid spur.

On tibiotarsus the distal epiphysis in cranial view (Fig. 67E), the *tuberositas retinaculi m. fibularis* (a) is conical, but pointed than in the recent species. *Sulcus extensorius* (b) is arched and its distally end is wide. *Pons supratendinous* (c) is wide and straight. *Condylus lateralis* (d) is wide ovalic, the distally end weakly narrowed. Line of *incisura intercondylaris* (e) is strongly concave and wider than in the recent specis. C*ondylus medialis* (f) is asymmetrically reverse oval shaped. *Arrow transverses* (g) is developed.

Name: Its name is after the robustness of the bones.

Description: The fossil species differs to the recent in its larger size.

Distribution: The family and genus are known only to recent species from S'Onix- Mallorca – Spain (Early Pleistocene, MN 18) (SONDAAR et al. 1995).

Family Cinclidae (CABANIS, 1847)
Genus *Cinclus* BORKHAUSEN, 1897
Cinclus † *gaspariki* nova sp.
(Plate XVIII. Figure 68)

Type locality and age: Polgárdi 5, Late Miocene (MN 13).

Holotype: Carpometacarpus sin. (proximal epiphysis) (MÁFI V.11.99.1; V.29174).

Measurements: Carpometacarpus C=3,79 mm.

Comparative material: Cinclus cinclus (MTM n=1: C=3,72 mm).

Diagnosis: The fossil bone differs from the recent species in a small difference in size. On proximal epiphysis of carpometacarpus in ventral view (Fig. 68), the *trochlea carpalis* (a) is symmetrical but lopsided blunt conical. *Proc. extensorius* (b) has obliquely, rounded beak-like shape. Larger than in recent species. *Processus alularis* (c) has rectangular shape. More developed than in the recent species. *Fovea subalularis* (d) is acute-angled and deep.

Name: Was named after Hungarian paleontologist Mihály GASPARIK.

Description: The remanins in generally correspond in characters to the recent species. The fossil species *Cinclus major* KESSLER et HÍR, 2012 was identified in the Early Miocene (MN 5) from Litke 2 (Hungary) based from on one fragment of a carpometacarpus. It is larger than the Polgardi specimen (C=4,54 mm), (KESSLER & HÍR 2012b).

Cinclus † *minor* nova sp.
(Plate XVIII. Figure 69)

Type locality and age: Csarnóta 2, Pliocene (MN 15-16).

Holotype: Ulna dext. (distal fragment) (MÁFI V.11.9.1, V.29084).

Measurements: Ulna F=2.78 mm; G=1.78 mm.

Comparative material: Cinclus cinclus (MTM n=1; ulna: F= 3.41 mm; G=2.52 mm).

Diagnosis: On distal epiphysis of ulna in medial view (Fig. 69), the *condylus dorsalis* (a) has blunted claw-like shape. *Sulcus intercondylaris* (b) is wide and concave. *Condylus ventralis* (c) has symmetrical but

oblique conical shape. *Tuberculum carpale* (d) has flattened semicircular shape.

Name: Its name refers to smaller dimensions of species.

Description: It is smaller than the recent species. The extinct species *Cinclus* †*gaspariki* from Polgárdi – Hungary (Upper Miocene, MN 13) has also small sizes, but it was described from one carpometacarpus and its age is older than the Csarnotánian specimen.

Distribution: The fossil species *Cinclus major* KESSLER et HÍR, 2012 was identified in the Early Miocene (MN 5) Litke 2 (Hungary) (KESSLER & HÍR 2012b). It is larger than the Polgardi and the Csarnotánian specimen.

The recent species *Cinclus cinclus* (LINNAEUS, 1758) was described from Betfia 9 - Romania (Lower Pleistocene, MQ1) (GÁL 2002). It is also known in the Middle Pleistocene from localities in France and Germany (TYRBERG 1998).

Family Prunellidae RICHMOND, 19o8
Genus *Prunella* VIEILLOT, 1818
Prunella † *freudenthali* nova sp.
(Plate XVIII. Figure 70 A-C)

Type locality and age: Polgárdi 5, Late Miocene (MN 13)

Holotype: Humerus sin., proximal fragment (MÁFI V.11.101.1, V.29176).

Paratypes: Two humeri sin. (proximal fragments); 2 ulnae sin.(with damaged proximal epiphysis); femur dext. (distal fragment) (MÁFI V.11.123.5; V.29198).

Measurements: 1. humerus B=4.65-4.95 mm; C=5.25-5.54 mm; D=4.57-5.52 mm; 2. ulna A aprox. 18-aprox. 22; E=1.14-1.34 mm; F=2.07-2.28 mm; G=1.63-1.77 mm; 3. femur F= 2.67 mm; G=1.92 mm.

Comparative material: Prunella modularis (MTM n=1: humerus B=4.85 mm; C=5.52 mm; D=5.41 mm;. ulna E=1.35 mm; F=2.56 mm; G=1.65 mm; femur F=3.22 mm; G=2.56 mm); *P. collaris* (MTM n=1: humerus B=4.85 mm; C=5.52 mm; D=5.41 mm; ulna E=2.19 mm; F=3.42 mm; femur F=4.13 mm).

Diagnosis: Dimensions of humerus correspond to recent *P. modularis*. On proximal epiphysis of humerus in caudal view (Fig. 70A), the *tuberculum dorsale* (a) is rounded. *Caput humeri* (b) is wide and slightly bulging. *Tuberculum ventrale* (c) forms asymmetrical circular spur. *Crista bicipitalis* (d) is protruding with rounded end. *Crus dorsale fossae* (e) is underdeveloped, therefore the two parts of *fossa pneumotricipitalis* (f) are visible together

On distal epiphysis of ulna in medial view (Fig. 70B), the *condylus dorsalis* (a) is claw shaped. *Sulcus intercondylaris* (b) is slightly concave. *Condylus ventralis* (c) is lopsided blunt conic shaped. *Tuberculum carpale* (d) is semicircular.

On distal epiphysis of femur in caudal view (Fig. 70C), the *trochlea fibularis* (a) is rounded. Distal end of *condylus lateralis* (b) forms one arc. *Incisura intercondylaris* (c) is strongly concave. *Condylus medialis* (d) is oblique and blunt conical. *Epicondylus medialis* (e) is protruding and rounded.

Name: Was named after the Dutch paleontologist, Mathias FREUDENTHAL.

Description: The sizes of the humerus corresponds to the recent species *P. modularis*. The sizes of ulna and femur is slightly smaller than in the recent species.

Prunella †*kormosi* nova sp.
(Plate XVIII. Figure 71 A-D)

Type locality and age: Csarnóta 2, Pliocene (MN 15-16).

Other locality: Beremend 26, Pliocene (MN 15-16).

Holotype: Coracoideum sin. (cranial fragment), (Csarnóta 2, MÁFI V.11.4.1; V.29079).

Paratypes: Humerus dext. (proximal epiphysis); 2 right and 2 left side ulnae (distal fragments) (Csarnóta 2, MÁFI V.11.40.5; V.29155); distal fragment of the tarsometatarsus dext. (Beremend 26, BKA).

Measurements: 1. coracoid C=2.97 mm; D=2.74 mm; E=1.77 mm; 2. humerus B=4.37 mm; C=5.67 mm; D=5.14 mm; 3. ulna E=1.31 mm; F=2.54-2.84 mm; G=1.67-1.97 mm; 4. tarsometatarsus E=1,31mm; F=2,95 mm; G=1,73 mm.

Comparative material: Prunella collaris (MTM n=1; humerus: B=4.85 mm; C=5.52 mm; D=5.41 mm; tarsometatarsus E=1,03 mm; F= 2,66 mm; G=1,77 mm); *Prunella modularis* (MTM n=1; coracoid: C=2.87 mm; D=2.51 mm; E=1,01 mm; humerus: B=4.85 mm; C=5.52 mm; D=5.41 mm; ulna: E=1.35 mm; F=2.57 mm; G= 1.81 mm; tarsometatarsus E=0,94 mm; F= 2,23 mm).

Diagnosis: On medial side of coracoideum in cranial end (Figure 71A), the *acrocoracoideum* (a) has symmetrical blunted cone shape. Its medial edge bulges mildly. *Processus accesorius* (b) has elongated claw-like shape with cut-off end. Edge of *sulcus m. supracoracoideumei* (c) is asymmetrically concave shape. *Facies articularis humeralis* (d) has cranial edge strongly bulges and rounded. Point of *processus procoracoideumei* (e) more exceeds the medial edge of corpus.

On proximal epiphysis of humerus in caudal view (Figure 71B), the *tuberculum dorsale* (a) is asymmetrical rounded. *Caput humeri* (b) is wide and convex, but not too outstanding. *Tuberculum ventrale* (c) is protruding, but it is damaged. *Crista bicipitalis* (d) is protruding and rounded. *Fossa pneumotricipitalis* (e) is not divided in two parts.

On distal epiphysis of ulna in medial view (Figure 71C), the *condylus dorsalis* (a) has rounded and blunted claw-like shape. *Sulcus intercondylaris* (b) is

wide and concave. *Condylus ventralis* (c) has obliquely blunt conical shape. *Tuberculum carpale* (d) has protruding semicircular shape.

On distal epiphysis of tarsometatarsusus in dorsal view (Fig. 71D), the edge between metatarsus I. and the *trochlea metatarsi* II. (a) is wavy. *Trochlea metatarsi* II. (b) has rectangular shape. *Incisura intertrochlearis medialis* (c) is narrow and deep. *Trochlea metatarsi* III. (d) is wide and with bellow mildly concave end. *Incisura intertrochlearis lateralis* (e) is wide and deep. T*rochlea metatarsi* IV. (f) has curved and rounded conical shape.

Name: Was named after Hungarian paleontologist Tivadar KORMOS.

Description: It is larger than recent *P.modularis*, but smaller than *P.collaris.*

Distribution: The genus is known outside of the Carpathian Basin only with recent species from the Early Pleistocene (MQ1) as *Prunella modularis* (LINNAEUS, 1758) from S'Onix Mallorca - Spain (SONDAAR et al.1995) and Boxgrove-Quarry 2 - England (HARRISON & STEWART 1999); and as *P. collaris* (SCOPOLI, 1769) from Stránská skála – Czech Republic (Lower Pleistocene, MQ1) (JÁNOSSY 1972).

Family Laniidae SWAINSON, 1834
Genus *Lanius* LINNAEUS, 1758
Lanius †*capeki* nova sp.
(Plate XIX. Figure 72)

Type locality and age: Polgárdi 4, Late Miocene (MN 13).

Holotype: Coracoideum dext. (cranial fragment) (MÁFI V.11.54.1; V.29129).

Measurements: Coracoid C=2.93 mm; D=3.48 mm; E=1.45 mm.

Comparative material: Lanius collurio (MTM n=1: C=2.99 mm; D=3.32 mm; E=1.35 mm); *L.excubitor* (MTM n=1: C=4.52 mm; D=4.37 mm; E=1.50 mm); *L.minor* (MTM n=1: C=3.33 mm; D=3.80 mm; E=1.49 mm).

Diagnosis: Corresponds in characteristics and sizes to recent smaller species of genus. On dorsal side of coracoid (Fig. 72), the *acrocoracoid* (a) is blunt conical shape, and its medial edge weakly bulges. *Processus accesorius* (b) is elongated and narrowed claw-like, with more pointed ende than in the recent species. Edge of *sulcus m. supracoracoidei* (c) has flattened concave shape. The edge of the *facies articularis humeralis* (d) is straight and its cranial end is strongly rounded. Point of *processus procoracoidei* (e) exceeds the medial edge of the corpus, as is recent *L. excubitor* LINNAEUS, 1758, but it is missingng in others species of genus.

Name: Was named after Czech paleornitologist Waclav ČAPEK.

Description: In general it corresponds in characters and sizes to the recent *L. colurio* LINNAEUS, 1758. The fossil species *Lanius schreteri* KESSLER ET HÍR 2012 from Felsőtárkány- Felnémet 2/3 – Hungary (Middle Miocene, MN 7/8) was described based of the other types of bones (scapula) and ist much larger than the Polgárdi species. *Lanius minor* GMELLIN, 1788 was reported also from Polgárdi 2 by JÁNOSSY (1991), but presumably those are the remains described in this paper.

Lanius † *hungaricus* nova sp.
(Plate XIX. Figure 73 A-E)

Type locality and age: Csarnóta 2, Pliocene (MN 15-16).

Holotype: Coracoid sin. (cranial fragment), (MÁFI V.11.5.1; V.29080).

Paratypes: Coracoid sin. (cranial fragment); scapula sin. (cranial fragment); carpometacarpus sin. (proximal fragment), (MÁFI V.1.41.2; V.29116).

Measurements: 1. coracoid C= 3.02-3.09 mm; D=2.64-2.66 mm; 2. scapula B=3.65 mm; D=1.86 mm; E=1.95 mm; 3. carpometacarpus C=3.16 mm.

Comparative material: Lanius collurio (MTM n=1; coracoid: C=2.97 mm; D=3.32 mm; scapula: B=3.65 mm; D=2.01 mm; E= 1.92 mm; carpometacarpus: C=3.19 mm).

Diagnosis: On medial side of coracoideum in cranial end (Fig. 73A), the *acrocoracoideum* (a) has asymmetrical and pointed cone shape. Its medial edge is bulges. *Processus accesorius* (b) has elongated and pointed claw-like shape with curved end. Edge of *sulcus m. supracoracoideumei* (c) is asymmetrically concave shape. *Facies articularis humeralis* (d) has rounded cranial edge. On lateral side (Fig. 73B), the point of *processus procoracoideumei* (e) is not exceeds the medial edge of corpus.

On cranial end of scapula (Fig. 73C), the lateral branch (a) has wide and rounded end. Edge between the two branches (b) forms wide but oblique concave line. Medial branch (c) is short and wide blunted conical shape. F*acies atricularis humeralis* (d) has an asymmetrical circular shape, with conical proeminence in medial part.

On proximal epiphysis of carpometacarpus in ventral view (Fig. 73D), the *trochlea carpalis* (a) has symmetrically bulged conical shape. *Proc. extensorius* (b) is obliquely and strongly blunted conical. *Processus alularis* (c) is rectangular shape. On dorsal view (Fig. 73E), the *fovea subalularis* (d) has rectangular shape.

Etymology: Was named after the name of the country.

Description: It corresponds in size to recent *Lanius collurio*.

Lanius † *major* nova sp.
(Plate XIX. Figure 74 A-D)

Type locality and age: Beremend 26, Pliocene (MN 15-16).

Holotype: Humerus dext. (BKA).

Paratypes: Distal fragments of humerus sin. and dext.; carpometacarpus sin.; distal fragment of tarsometatarsus sin. (BKA).

Measurements: 1. humerus A=25,62 mm; B=8,64 mm; C=7,30 mm; D=7,48 mm; E=2,12-2,28 mm; F=6,18-6,23 mm; G=2,95-3,05 mm; 2. carpometacarpus B=17,15 mm; C=5,63 mm; D=3,05 mm; E'=2,22 mm; tarsometatarsus E=1,93 mm; F=3,64 mm; G=2,10 mm.

Comparative material: Lanius excubitor (MTM n=1: humerus A= 27,00 mm; B=10,00 mm; C=8,34 mm; E=2,53 mm; F=6,91 mm; G=3,36 mm; carpometacarpus B=16,43 mm; C=4,34 mm; D=2,20mm; E'=1,67 mm; tarsometatarsus E=1,41 mm; F=2,72 mm; G=1,73 mm); *L.minor* (MTM n=1: humerus A=23,35 mm; B=10,22 mm; C=7,18 mm; D=6,21 mm; E=1,98 mm; F=5,64 mm; G=3,13 mm; carpometacarpus B=14,08 mm; C=3,80 mm; D=2,02 mm; E'=1,57 mm).

Diagnosis: On proximal epiphysis of humerus in caudal view (Fig. 74A), the *tuberculum dorsale* (a) is rounded. *Caput humeri* (b) is wide and convex. *Tuberculum ventrale* (c) is large and has semicircular sape. *Crista bicipitalis* (d) is less protruding and rounded. *Crus dorsale fossae* is developed, therefore the *fossa pneumotricipitalis* (e) is divided into two parts.

On distal epiphysis of humerus in cranial view (Fig. 74B), the *tuberculum supracondylare ventrale* (a) is rounded and less bulged than in the recent *L. excubitor*. *Epicondylus ventralis* (b) is rounded. *Processus flexorius* (c) is protruding and distally rounded. *Condylus ventralis* (d) has oval shape. *Incisura intercondylaris* (e) is concave, wide and deep. *Condylus dorsalis* (f) is rounded distally. *Epicondylus dorsalis* (g) is rounded. *Proc. supracondylaris dorsalis* (h) is short, wide and pointed.

On proximal epiphysis of carpometacarpusus in ventral view (Fig. 74C), the *trochlea carpalis* (a) has asymmetrically bulged conical shape. *Proc. extensorius* (b) is obliquely and strongly blunted conical. *Processus alularis* (c) is asymmetrical rectangular shape. *Fovea subalularis* (d) has acute-angle shape. *Protuberantia metacarpalis* (e) is wide and flatted,

On distal epiphysis of tarsometatarsusus in dorsal view (Fig. 74D), the edge (a) between trochlea metatarsi I. and *trochlea metatarsi* II. is wavy. *Trochlea metatarsi* II. (b) has bent asymmetrical conical shape. *Incisura intertrochlearis medialis* (c) is wide and deep. *Trochlea metatarsi* III. (d) is wide and with bellow mildly concave end. *Incisura intertrochlearis lateralis* (e) is narow and deep. T*rochlea metatarsi* IV. (e) has rounded conical shape.

Etymology: Was named after its larger dimensions.

Description: The remains derived from two different sizes specimen. The humerus is mostly smaller than the recent *L. excubitor,* the carpometacarpus and tarsometatarsus derived from the large specimens.

Lanius † *intermedius* nova sp.
(Plate XX. Figure 75 A-B)

Type locality and age: Beremend 26, Pliocene (MN 15-16).

Holotype: Carpometacarpus dext. (BKA).

Paratypes: Proximal fragment of humerus dext. (BKA).

Measurements: 1. humerus C=5,53 mm; D=4,34 mm; 2.carpometacarpus A=14,61 mm; B=12,07 mm; C=3,67 mm; D=2,20 mm; E=2,88 mm; F=3,39 mm.

Comparative material: L.collurio (MTM n=1: humerus C=5,94 mm; D=4,98 mm; carpometacarpus A=14,10 mm; B=11,80 mm; C=3,30 mm; D=1,45 mm; E=2,18 mm; F=3,07 mm); *L.minor* (MTM n=1: humerus C=7.18mm; D=6,21 mm; carpometacarpus A=17,09 mm; B=14,23 mm; C=3,99 mm; D=2,99 mm; E=3,01 mm; F=3,57 mm).

Diagnosis: On proximal epiphysis of humerus in caudal view (Fig. 75A), the *tuberculum dorsale* (a) is rounded. *Caput humeri* (b) is wide and convex. *Tuberculum ventrale* (c) is big and has semicircular sape. *Crista bicipitalis* (d) is protruding and rounded. *Crus dorsale fossae* (e) is developed, therefore the *fossa pneumotricipitalis* (f) is divided into two parts.

On proximal epiphysis of carpometacarpusus in ventral view (Fig. 75B), the *trochlea carpalis* (a) has asymmetrically bulged conical shape. *Proc. extensorius* (b) is obliquely and has asymmetrically blunted conical shape. *Processus alularis* (c) has rectangular shape. *Fovea subalularis* (d) has concave shape. *Protuberantia metacarpalis* (e) is wide and flatted,

Description: It has intermediate dimensions between recent species *L. minor* and *L. collurio* and differs in characters to much smaller *L. hungaricus* KESSLER, 2012 from Csarnóta.

Distribution: In the Carpathian Basin the genus was described as *Lanius* sp. foss. indet. from Subpiatra 2-Romania (Middle Miocene, MN 6) (KESSLER & VENCZEL 2009); from Csarnóta 2 – Hungary (Lower Pliocene, MN 15) (KESSLER 2010) and from Beremend 26 – Hungary (Lower Pliocene, MN 15) (KESSLER 2010a). The recent species are known as *Lanius excubitor* LINNAEUS, 1758 from Betfia 9-Romania (Lower Pleistocene, MQ1) (GÁL 2002); as *Lanius collurio* LINNAEUS, 1758 from Betfia 13-Romania (Upper Pliocene, MN 16) (KESSLER 1975, GÁL 2002); from Betfia 7-_Romania (Lower Pleistocene, MQ1-2) (KESSLER 1975, GÁL 2002); as *Lanius minor* GMELIN, 1788 from Betfia 2-Romania (Lower Pleistocene, MQ1) (ČAPEK 1917; LAMBRECHT 1933; JÁNOSSY 1979a; KESSLER 1975; GÁL 2002);

Betfia 9 - Romania (Lower Pleistocene, MQ1) (KESSLER 1975; GÁL 2002).

The family and genus are known outside the Carpathian Basin from the Late Pliocene from of Varshets (MN 17, Bulgaria) as *Lanius* sp. (BOEV 1996, 2000); from Petralona 24 – Greece (Lower Pleistocene) as *Lanius* cf. *minor* GMELLIN, 1788 by Miklós KRETZOI (1977). The fossil species *Lanius miocaenus* MILNE-EDWARDS, 1871 (MILNE-EDWARDS 1969-71) from Saint-Gérand-le-Puy – France (Lower Miocene, MN 2) was put into „*Family incertae sedis"* by MLÍKOVSKÝ (2002).

Family Sturnidae VIGORS, 1825
Genus *Sturnus* LINNAEUS, 1758
Sturnus † *brevis* nova sp.
(Plate XX. Figure 76 A-C)

Type locality and age: Polgárdi 4, 5; Late Miocene (MN 13).

Holotype: Coracoideum dext.(Polgárdi 4, MÁFI V.11.55.1, V.29130).

Paratype: Humerus dext. (damaged proximal epiphysis), (Polgárdi 5); tibiotarsus dext. (distal fragment) (Polgárdi 5), (MÁFI V.11.115.2; V.29190).

Measurements: 1. coracoid C=3.37 mm; D=4.11 mm; E=1,33 mm; 2. humerus A=aprox. 23-24 mm; E=2.47 mm; F=5.27 mm; G=3.38 mm; 3 . tibiotarsus F=2.94 mm; G=2.62 mm.

Comparative material: Sturnus vulgaris (MTM n=1: coracoid C=4.11 mm; D=5.32 mm; E=1.69 mm; humerus A= 26.86 mm; E=2.76 mm; F=6.61 mm; G=3.81 mm; tibiotarsus F=3.61 mm; G=3.33 mm); *S. roseus* (MTM n=1: coracoid D=5.52 mm; humerus A=27.95 mm; E=2.78 mm; F=6.47 mm; tibiotarsus F=4.55 mm).

Diagnosis: The new species differs to recent species in its sizes. On dorsal side of coracoid (Fig. 76A), the *acrocoracoid* (a) has slightly asymmetrical blunt conical shape. *Processus accesorius* (b) is hook-like with cut-off end. Edge of s*ulcus m. supracoracoidei* (c) forms strongly concave line. Edge of *facies articularis humeralis* (d) is straight. *Processus procoracoidei* (e) is well developed.

On distal epiphysis of humerus in cranial view (Fig. 76B), the *tuberculum supracondylare ventrale* (a) is bulging. *Epicondylus ventralis* (b) is flat. *Processus flexorius* (c) has oblique conical shape. *Condylus ventralis* (d) has oval shape. *Incisura intercondylaris* (e) is well developed, the its acute angle hollow. is in point than in the recent species. The *condylus dorsalis* (f) has curved ovalic shape. *Epicondylus dorsalis* (g) is rounded. *Processus supracondylaris dorsalis* (h) is short and blunt and has two unequal branches.

On tibiotarsus the distal epiphysis in cranial view (Fig. 31C), the *tuberositas retinaculi m. fibularis* (a) is weakly developed and flat. *Sulcus extensorius* (b) is wide. *Pons supratendinous* (c) is wide and straight. *Condylus lateralis* (d) is oval (but damaged). *Incisura intercondylaris* (e) has flattened concave shape. C*ondylus medialis* (f) is lateraly flattened and asymmetrically conical.

Name: Was name after its shape (Lat. *brevis*=short).

Description: It differs in its smaller sizes from the recent species. The fossil species *Sturnus kretzoii* KESSLER et HÍR, 2012 (KESSLER & HÍR 2012) from Rudabánya – Hungary (Upper Miocene, MN 9) was described based on a carpometacarpus is also smaller than the recent species.

Sturnus † *pliocaenicus* nova sp.
(Plate XX. Figure 77 A-C)

Type locality and age: Beremend 26, Pliocene (MN 15-16).

Holotype: Humerus dext., with damaged proximal epiphysis (BKA).

Paratypes: Proximal and distal fragments of humerus dext.; distal fragments of tarsometatarsus dext. (BKA).

Measurements: Humerus A=approx. 28,50-29,00 mm; B=9,96 mm, C=9,33 mm; D=8,25 mm; E=2,6-2,92 mm; F=6,55-7,68 mm; G=3,60-4,15 mm; tarsometa-tarsus E=1,63 mm; F=3,39-3,46 mm; G=2,02-2,04 mm.

Comparative material: Sturnus vulgaris (MTM n=1: humerus A=26,86 mm; B=9,59 mm, C=8,64 mm; D=7,59 mm;E=2,76 mm; F= 6,61 mm; G=3,81 mm; tarsometatarsus E=1,65 mm; F=3,28 mm; G=2,13 mm); *S. roseus* (MTM n=1: humerus A=27,95 mm; B=9,83 mm, C=8.85 mm; D=7.53 mm; E=2,78 mm; F=6,47 mm).

Diagnosis: On proximal epiphysis of humerus in caudal view (Fig. 77A), the *tuberculum dorsale* (a) is rounded. *Caput humeri* (b) is wide and convex. *Tuberculum ventrale* (c) is large and has semicircular sape, while in the recent genus. *Crista bicipitalis* (d) is less protruding. *Crus dorsale fossae* (e) is weakly developed, therefore the *fossa pneumotricipitalis* (f) is divided into two parts.

On distal epiphysis of humerus in cranial view (Fig. 77B), the *tuberculum supracondylare ventrale* (g) is bulging. *Epicondylus ventralis* (h) is rounded. *Processus flexorius* (i) is protrunding and rounded. *Condylus ventralis* (j) has oval shape. *Incisura intercondylaris* (k) is wide in acute-angle. The *condylus dorsalis* (l) has curved oval shape. *Epicondylus dorsalis* (m) is weakly rounded. *Processus supracondylaris dorsalis* (n) is long, wide with two unequal branches.

On distal epiphysis of tarsometatarsusus in dorsal view (Figure 77C), the edge (a) between trochlea metatarsi I. and *trochlea metatarsi* II. is wavy. *Trochlea metatarsi* II. (b) has bented rectangalar shape. *Incisura intertrochlearis medialis* (c) is narrow. *Trochlea metatarsi* III. (d) is wide and with bellow

mildly concave end. *Incisura intertrochlearis lateralis* (e) is wide and deep. T*rochlea metatarsi* IV. (e) has pointed conical shape.

Name: Was named after the age of the site. .

Description: It differs to known extinct and recent species with much larger dimensions.

Sturnus † *baranensis* nova sp.
(Plate XX. Figure 78 A-B)

Type locality and age: Beremend 26, Pliocene (MN 15-16).

Holotype: Proximal fragment of humerus dext. (BKA)

Paratype: Distal fragment of humerus dext. (BKA)

Measurements: Humerus B=8,91 mm; C=8,47 mm; D=7,48 mm; E= 2,78 mm, F=5,65 mm; G=2,95 mm.

Comparative material: Sturnus vulgaris (MTM n=1: humerus B=9,59 mm, C=8,64 mm; D=7,59 mm; E=2,76 mm; F= 6,61 mm; G=3,81 mm); *S. roseus* (MTM n=1: humerus B=7.85 mm, C=8,36 mm; D=6,70 mm; E=2,78 mm; F=6,47 mm).

Diagnosis: On proximal epiphysis of humerus in caudal view (Fig. 78A), the *tuberculum ventrale* (a) is big and has semicircular sape, while in the recent genus. *Crista bicipitalis* (b) is less protruding. *Crus dorsale fossae* (c) is weakly developed, therefore the *fossa pneumotricipitalis* (d) is divided into two parts.

On distal epiphysis of humerus in cranial view (Fig. 78B), the *tuberculum supracondylare ventrale* (e) is bulging. *Condylus ventralis* (f) has oval shape. *Incisura intercondylaris* (g) is wide in acute-angle shaped. The *condylus dorsalis* (h) has curved oval shape. *Epicondylus dorsalis* (i) is weakly rounded. *Processus supracondylaris dorsalis* (j) is long, wide with two unequal branches.

Name: Was named after the name of Baranya county.

Description: It differs from recent and extinct species in its dimensions.

Distribution: In the Carpathian Basin the genus was reported as *Sturnus* sp. foss. indet. from Beremend 16, 17 - Hungary (Lower Pleistocene, MQ1) by JÁNOSSY (1991, 1992), and the recent *Sturnus vulgaris* LINNAEUS, 1758 is known from Betfia 2 - Romania (Lower Pleistocene, MQ1-2) (ČAPEK 1917; LAMBRECHT 1933; JÁNOSSY 1979; KESSLER 1975; GÁL 2002); Betfia 9 - Romania (KESSLER 1975; Gál 2002); Betfia 5 – Romania (KESSLER 1975; JÁNOSSY 1979; GÁL 2002).

The family and genus were described outside the Carpathian Basin as *Sturnus* sp. in the Late – Pliocene and the Early Pleistocene localities from Varseths – Bulgaria (MN 17 – MQ1) by BOEV (1996, 2000), West Runton and Boxgrove – England (HARRISON 1979, HARRISON & STEWART 1999) and Prezletice – Czech Republic (ČAPEK 1917, JÁNOSSY 1983, 1992).

Family Passeridae (ILLIGER, 1811)
Genus *Passer* KOCH, 1816
Passer † *híri* nova sp.
(Plate XXI. Figure 79 A-C)

Type locality and age: Polgárdi 4, Late Miocene (MN 13).

Holotype: Ulna sin. (proximal fragment) (MÁFI V.11.61.1, V.29136).

Paratypes: Three carpometacarpi sin. (missing os metacarpale minus); tibiotarsus sin. (distal fragment) (MÁFI V.11.78.4; V.29153).

Measurements: 1. ulna B=3.28 mm; C=2.85 mm; E=1.61 mm; 2. carpometacarpus A=11.74-12.56 mm; C=3.04-3.14 mm; F=2.71-2.81 mm; 3. tibiotarsus F=2.32 mm; G=2.05 mm.

Comparative material: Passer domesticus (MTM n=1: ulna B=3.49 mm; C=3.06 mm; E=1.61 mm; carpometacarpus A= 11.12 mm; C=3.03 mm; F=2.74 mm; tibiotarsus F=2.89 mm; G=2.65 mm); *P. montanus* (MTM n=1: ulna B=2.96 mm; C=2.96 mm; E=1.49 mm; carpometacarpus A= 11.29 mm; C= 2.46 mm; tibiotarsus F=2.45mm; G=2.32 mm).

Diagnosis: It is smaller than the recent species, but corresponds with its in morphological characteristics. On the proximal epiphysis of ulna in cranial view (Fig. 79A), the *oleocranon* (a) is long, straight and blunt ended. *Cotyla dorsalis* (b) is asymmetrically conical shaped, with rounded lateral edge. *Cotyla ventralis* (c) has slightly flattened circular shape. *Tuberculum lig. colat. ventralis* (d) is mostly developed. *Depressio m.brachialis* (e) has circular shape.

On the proximal epiphysis of carpometacarpus in ventral view (Fig. 79B), the *trochlea carpalis* (a) is symmetrically bulging. *Proc. extensorius* (b) has obliquely and asymmetrically conical-like shape. *Processus alularis* (c) has rectangular shape. *Fovea subalularis* (d) has acute angle pit shape. *Protuberantia metacarpalis* (e) is small and pointed.

On tibiotarsus the distal epiphysis in cranial view (Fig. 79C), the *tuberositas retinaculi m. fibularis* (a) is underdeveloped. *Sulcus extensorius* (a) is wide. *Pons supratendinous* (c) is moderately wide and straight. *Condylus lateralis* (d) is laterally flattened and distally pointed oval. *Incisura intercondylaris* (e) is slightly concave-like line. *Condylus medialis* (f) has wider egg shape.

Name: Was named after Hungarian paleontologist János HÍR.

Description: Its size is smaller than the recent species, but corresponds to it in its characters.

Passer † *minusculus* nova sp.
(Plate XXI. Figure 80)

Type locality and age: Csarnóta 2, Pliocene (MN 15-16).

Holotype: Coracoid dext. (cranial fragment), (MÁFI V.11.6.1; V.29081).

Measurements: C=2.54 mm; D=2.14 mm.

Comparative material: Paser montanus (MTM n=1; coracoid: C=3.28 mm; D=2.62 mm); *Passer domesticus* MTM n=1; coracoid: C=3.05 mm; D=2.79 mm).

Diagnosis: On medial side of coracoideum in cranial end (Fig. 80), the *acrocoracoideum* (a) has bulged symmetrical and blunted cone shape. *Processus accesorius* (b) is damaged. Edge of *sulcus m. supracoracoideumei* (c) has flattened concave shape. *Facies articularis humeralis* (d) has rounded cranial edge. Point of *processus procoracoideumei* (e) is more exceeds the medial edge of corpus.

Name: The name refers to very smaller dimensions of species.

Description: Ist very little in comparison to recent sepcies of genus, but corresponds it in its characteristics. The *processus acessorius* is partially damaged.

Passer † *pannonicus* nova sp.
(Plate XXI. Figure 81)

Type locality and age: Beremend 26, Pliocene (MN 15-16).

Holotype: Carpometacarpus sin. (BKA)

Measurements: Carpometacarpus: A=12,23 mm; B=9,63 mm; C=2,78 mm; E=2,32 mm; F=3,06 mm.

Comparative material: Passer domesticus (MTM n=1: carpometacarpus A=11,12 mm; C=3,03 mm; F=2,74 mm); *P. montanus* (MTM n=1: carpometacarpus A=11,29 mm; C=2,46 mm; F=2,43 mm).

Diagnosis: On proximal epiphysis of carpometacarpus in ventral view (Fig. 81), the *trochlea carpalis* (a) is symmetrically bulging. *Processus alularis* (b) is large and has rectangular shape. *Fovea subalularis* (c) has asimetrical acute angle pit shape. *Protuberantia metacarpalis* (d) is developed and pointed. Basis of the *facies articularis digiti major* (e) is asymmetrical rounded. End of the *metacarpus minus* (f) is less concave.

Name: Was named after the Pannonia region.

Description: It corresponds mostly in dimensions and characteristics to recent species. The extinct species from Polgardi and Csarnóta are smaller. The missing of *proc. extensorius* not prevent the determination.

Distribution: The earliest report of family and genus is from Saint-Gérand-le-Puy - France (Lower Miocene, MN 2) as *Passer* sp. (MOURER-CHAUVIRÉ 1995), but it is not known in other localities from Neogene. The recent species outside the Carpathian Basin is known from the Middle Pleistocene in Europe.

The recent species *Passer montanus* (LINNAEUS, 1758) was described from the sites of Betfia – Romania (Lower Pleistocene, MQ1): Betfia 2 (MQ1) (ČAPEK 1917; LAMBRECHT 1933; JÁNOSSY 1979; KESSLER 1975; GÁL 2002); Q2: Betfia 5 (MQ1) (KESSLER 1975; JÁNOSSY 1979; GÁL 2002).

Family Fringillidae LEACH, 1820
Genus *Fringilla* LINNAEUS, 1758
Fringilla †*kormosi* nova sp.
(Plate XXI. Figure 82 A-C)

Type locality and age: Polgárdi 4, 5; Late Miocene (MN 13).

Holotype: Humerus dext. (Polgárdi 4, MÁFI V.11.56.1; V.29131).

Paratype: Coracoideum sin. (cranial fragment) (Polgárdi 5, MÁFI V.11.75.1; V.29150).

Measurements: 1. coracoid D=3.04 mm. 2. humerus A=20.95 mm; B=5.87 mm; C=6.21 mm; D=5.92 mm; E=1.97 mm; F=5.46 mm; G=2.98 mm. *Comparative material: Fringilla coelebs* (MTM n=1: coracoid D=2.62 mm; humerus A=18,12 mm; B=6.35 mm; C=6.09 mm; D=5.22 mm; E=1.70 mm; F=4.62 mm; G=2.57 mm); *F. montifringilla* (MTM n=1: coracoid D=2.89 mm; humerus A=19.28 mm; B=5.43 mm; C=6.22 mm; D=5.34 mm; E=1.83 mm; F=5.04 mm; G=1.69 mm.).

Diagnosis: Although basically its sizes it is similar to that of *Pyrrhula* and *Loxia* genera, but in its characteristics corresponds to the genus *Fringilla*.

On coracoid in dorsal view (Fig. 82A), the *acrocoracoid* (a) is asymmetrical blunted conical shaped and has bulging medial edge. *Processus accesorius* (b) is hook-like and has blunted end. Edge of *sulcus m. supracoracoidei* (c) forms strongly concave shape. *Facies aricularis humeralis* (d) has rounded cranial end. Point of *processus procoracoidei* (e) does not exceed the medial edge of corpus.

On proximal epiphysis of humerus in cranial view (Fig. 82B), the cranial end on *crista pectoralis, tuberculum dorsale* (a) is rounded. *Caput humeri* (b) is wide and slightly convex. *Tuberculum ventrale* (c) is well developed. *Crista bicipitalis* (d) forms rounded beak-like shape. C*rus dorsale fossae* is underdeveloped and the two parts of *fossa pneumotricipitalis* (e) can not be separated (Fig. 82C., in caudal view). On distal epiphysis in cranial view (Fig. 82B), the *tuberculum supracondylare ventrale* (f) is developed. *Epicondylus ventralis* (g) is rounded. *Processus flexorius* (h) is protruding and weakly rounded. *Condylus ventralis* (i) has lying oval shape. *Incisura intercondylaris* (j) has acute angle hollow.. *Condylus dorsalis* (k) is strongly bent oval. *Epicondylus dorsalis* (l) is rounded. *Processus supracondylaris dorsalis* (m) is developed and has two small proeminences. The widening between it and the diaphysis is deep.

Name: Was named after Hungarian paleontologist, Tivadar KORMOS.

Description: It is large size *Fringilla* species. The genus was described as *Fringilla* sp. indet. from Litke 2 –Hungary (Lower Miocene, MN 5) and Mátraszölős 2 (Middle Miocene, MN 7/8) on the basis of a one distal fragment of a humerus respectively one a proximal fragment of a radius, with larger sizes (humerus F=5.26 mm; G=2.59 mm; radius: C=1.72 mm; E=1.04 mm). (KESSLER & HÍR 2012). While the *processus accessorius* of the humerus is damaged and the radius is missing in the Polgardi material, they can not regarded as referred materials.

Fringilla † *petenyii* nova sp.
(Plate XXI. Figure 83 A-B)

Type locality and age: Csarnóta 2, Pliocene (MN 15-16).

Holotype: Tibiotarsus dext. (distal fragment),(MÁFI 11.49.1; V.29124).

Paratype: Tarsometatarsus dext. (distal fragment), (MÁFI V.11.29.1; V.29104).

Measurements: 1. tibiotarsus E=1.12 mm; F=2.35 mm; G=2.16 mm; 2. tarsometatarsus F=2.04 mm; G=1.29 mm.

Comparative material: Fringilla fringilla (MTM n=1; tibiotarsus: E=1.09 mm; F=2.38 mm; G=2.30 mm; tarsometatarsus: F=2.04 mm; G=1.21 mm); *Fringilla montifringilla* (MTM n=1; tibiotarsus: E=1.13 mm; F=2.42 mm; G=2.39 mm; tarsometatarsus: F=2.06 mm; G=1.21 mm).

Diagnosis: On distal epiphysis of tibiotarsusus in cranial view (Figure 83A), the *tuberositas retinaculi m. fibularis* (a) is wide and flattened. *Sulcus extensorius* (b) is more wide and distally pointed. *Pons supratendineus* (c) is narrow and weakly obliquely. *Condylus lateralis* (d) has lateraly rounded shape. The line of i*ncisura intercondylaris* (e) is concave. C*ondylus medialis* (f) is distally and laterally rounded shaped.

On distal epiphysis of tarsometatarsusus in dorsal view (Figure 83B), the. *trochlea metatarsi* II. (a) has oblique conical shape. *Incisura intertrochlearis lateralis* (b) has wide acute angle shape. *Trochlea metatarsi* III. (c) is wide and with slightly concave end. *Incisura intertrochlearis medialis* (d) is wide. T*rochlea metatarsi* IV. (f) has rounded conical shape.

Name: Was named after hungarian paleontologist Salamon János PETÉNYI.

Description: Its characteristics and dimensions corresponds to recent genus.

Distribution: In the Carpathian Basin it was described as *Fringilla* † sp. foss. indet. from Litke 2 – Hungary (Lower Miocene, MN 5) and from Mátraszölős 2 - Hungary (Middle Miocene, MN 7/8) (KESSLER & HÍR 2012) and as Fringillidae gen et sp. foss. indet. from Csarnóta 2 - Hungary (Lower Pliocene, MN 15), (KESSLER 2010). The recents species of the genus it is known from the Early Pleistocene (MQ1-2) as *Fringilla montifringilla* LINNAEUS, 1758 from Betfia 2-Romania (ČAPEK 1917; LAMBRECHT 1933; JÁNOSSY 1979; KESSLER 1975; GÁL 2002) and Betfia 9-Romania (KESSLER 1975; GÁL 2002) and as *Fringilla coelebs* Linnaeus, 1758 from Betfia 2-Romania (ČAPEK 1917; LAMBRECHT 1933; JÁNOSSY 1979; KESSLER 1975; GÁL 2002); Betfia 9-Romania (KESSLER 1975; GÁL 2002) and Chi□că u-Bear Cave 2-Romania (KESSLER 1982; JURCSÁK & KESSLER 1988; GÁL 2002).

The genus is known outside of the Carpathian Basin from the Lower Pliocene (MN 16) from Hostalets de Pierola- Spain as *Fringilla* sp. (VILLALTA 1963), from the Late Pliocene – Early Pleistocene (MN 17-MQ1) from Varshets – Bulgaria (BOEV 1996, 1997); S'Onix (Mallorca) – Spain (SONDAAR et al. 1995) and Tarchankut-Ukraine (VOJINTSVENS'KY 1967) as *F.* cf. *coelebs* LINNAEUS, 1758. The other genera are known as *Serinus* sp. from Beremend 15-Hungary (Late-Pliocene, MN 16), (JÁNOSSY 1992); from Saint-Gerand-le Puy – France (Lower Miocene, MN 2), (MOURER-CHAUVIRÉ 1995). Fringilidae gen. et sp. indet. was reported from Csarnóta 2 – Hungary (Lower Pliocene, MN 15) (KESSLER 2010).

Genus *Carduelis* BRISSON, 1760
Carduelis †*kretzoii* nova sp.
(Plate XXII. Figure 84 A-F)

Type locality and age: Polgárdi 4, 5; Late Miocene (MN 13).

Holotype: Humerus dext. (Polgárdi 5, MÁFI V.V.11.91.1; V.29166).

Paratypes: Two coracoidea sin. (cranial fragments), (Polgárdi 5); 12 humeri (2 completes sin., 9 proximal fragments dext.and sin., one distal fragment sin.), (Polgárdi 4, 5); carpometacarpus dext. (Polgárdi 4); femur dext. (distal fragment) (Polgárdi 5); 2 tibiotarsi sin.(distal fragments) (Polgárdi 5), (MÁFI V.11.112.9; V.11.116.7; V.29187, V.29191).

Measurements: 1. coracoid C=2.41-2.56 mm; D=2.61-2.84 mm; 2. humerus A=15.54-17.52 mm; B= 4.17-5.01 mm; C= 4.22-5.46 mm; E=1.51-1.87 mm; F=3.43-3.98 mm; G=2.07-2.13 mm;. 3. carpometacarpus A=9.93 mm; C=3.04 mm; E=2.16 mm; F= 2.31 mm; 4. femur E=1.32 mm; F=2.48 mm; G=1.93 mm; 5. tibiotarsus F=2.26-2.34 mm; G=2.04-2.16 mm;

Comparative material: Carduelis carduelis (MTM n=1: coracoid C=3.00 mm; D=2.52 mm; E=0.92 mm; humerus A=16.55 mm; C= 5.57 mm; E= 1.65 mm; F=4.46 mm; G=2.32 mm; ulna F=2.60 mm; carpometacarpus A=10.37 mm; C=2.86 mm; E=1.99 mm; F=2.66 mm; femur E=1.24 mm; F=2.54 mm; tibiotarsus F=2.29 mm; G=2.12 mm); *C. flammea* (MTM n=1: coracoid C= 2.93 mm; D=2.44 mm; humerus A= 12.82 mm; C=4.76 mm; E=1.45 mm; F=3.75 mm; G=2.28 mm; ulna F=2.29 mm; G=1.90 mm; carpometacarpus A=12.17 mm; C=3.19 mm; E=2.84 mm; F=2.28 mm; femur E=1.14 mm, F=2.30

mm; G=1.57 mm; tibiotarsus F=2.15 mm); *C. canabina* (MTM n=1: coracoid C=2.90 mm; D=3.19 mm; humerus A=16.83 mm; C=5.84 mm; E=1.78 mm; F=4.09 mm; G=2.22 mm; ulna F=2.77 mm; carpometacarpus A=12.11 mm; C=3.55 mm; E=2.35 mm; F=2.46 mm; femur E=1.03 mm; F=2.41 mm; G=1.91 mm; tibiotarsus F=2.22 mm; G=1.96 mm); *C. flavirostris* (MTM n=1: coracoid C=2.38 mm; D=2.99 mm; humerus A=15.67 mm; C=5.37 mm; E=1.59 mm; F=4.14 mm; G=2.21 mm; ulna F=2.50 mm; carpometacarpus A=11.65 mm; C=2.84 mm; E=2.44 mm; F=2.49 mm; femur E=1.09 mm; F=2.41 mm; tibiotarsus F=1.99 mm; G=1.78 mm); *C. spinus* (MTM n=1: coracoid C=2.59 mm; D= 2.91 mm; humerus A=13.49 mm; C=5.02 mm; E=1.73 mm; F=3.85 mm; G=1.90 mm; ulna F=2.59 mm; G=1.79 mm; carpometacarpus A=10.38 mm; C=2.68 mm; E=2.44 mm; F=2.34 mm; femur E=1.16 mm; F= 2.44 mm; G=2.09 mm; tibiotarsus F=1.99 mm; G=1.78 mm).

Diagnosis: Basically its sizes it is between smaller species such as *C. carduelis* , *C. flammea* and *C. spinus*. On coracoid in dorsal view (Fig. 84A), the *acrocoracoid* (a) is blunted conical shaped. *Processus accesorius* (b) is short and hook-like (but with damaged end). Edge of *sulcus m. supracoracoidei* (c) has flattened arched shape. Edge of *facies articularis humeralis* (d) is straight. Point of *processus procoracoidei* (e) exceed the medial edge of the corpus.

On proximal epiphysis of humerus in caudal view (Fig. 84B), the *tuberculum dorsale* (a) is rounded. *Caput humeri* (b) is wide and convex. *Tuberculum ventrale* (c) forms asymmetrical semicircular spur. *Crista bicipitalis* (d) is protruding with rounded end. C*rus dorsale fossae* is underdeveloped and the two parts of *fossa pneumotricipitalis* (e) can not be separated. On distal epiphysis of humerus in cranial view (Fig. 84C) the *tuberculum supracondylare ventrale* (f) is flattened but well developed. *Epicondylus ventralis* (g) is rounded. *Processus flexorius* (h) has cut-off end and it is much shorter than in the recent genus. *Condylus ventralis* (i) has stretched oval shape. *Incisura intercondylaris* (j) has wide and acute angled pit. *Condylus dorsalis* (k) has strongly bent oval shape. *Epicondylus dorsalis* (l) is rounded. *Processus supracondylaris dorsalis* (m) is short and has spherical shape. The widening between it and the diaphysis is deep.

On proximal epiphysis of carpometacarpus in ventral view (Fig. 84D), the *trochlea carpalis* (a) is rounded and it is slightly asymmetrically bulging. *Proc. extensorius* (b) has asymmetrical, oblique conical–like shape. *Processus alularis* (c) has asymmetrical protruding cone shape. *Fovea subalularis* (d) has acute angled pit. *Protuberantia metacarpalis* (e) is small and triangular.

On distal epiphysis of femur in caudal view (Fig. 84E), the *trochlea fibularis* (a) is rounded. Distal end of *condylus lateralis* (b) constitutes one arc. *Incisura intercondylaris* (c) has deeply and widely concave shape. *Condylus medialis* (d) has oblique and blunt conical shape. *Epicondylus medialis* (e) is flat.

On tibiotarsus the distal epiphysis in cranial view (Fig.84F), the *tuberositas retinaculi m. fibularis* (a) is less developed and flattened. *Sulcus extensorius* (b) is wide, but its distal end is narrowing. *Pons supratendineous* (c) is wide and straight. *Condylus lateralis* (d) has narrow oval shape with pointed end. *Incisura intercondylaris* (e) is slightly concave and has wavy line. *Condylus medialis* (f) has distal rounded and regular ovalic shape.

Name: Was named after Miklós KRETZOI, Hungarian paleornithologist

Description: It corresponds in its sizes to recent smaller and medium size species of genus, such as *C. carduelis* (LINNAEUS, 1758), *C. flammea* (LINNAEUS, 1758) and *C. spinus* (LINNAEUS, 1758).

Carduelis † *lambrechti* nova sp.
(Plate XXII. Figure 85 A-C)

Type locality and age: Polgárdi 4, Late Miocene (MN 13).

Holotype: Humerus sin. (MÁFI V.11.58.1; V.29133).

Paratypes: Coracoideum dext. and sin. (cranial fragments); humerus dext. and sin. (in the left side specimen the proximal epiphysis is damaged). (MÁFI V.11.77.4; V.29152).

Measurements: 1. humerus A=17.28-17.51 mm; C=5.32-5.39 mm; E=1.56-1.78 mm; F=3.92-4.32 mm; G=2.21-2.38 mm; 2. coracoid C=2.75-2.92 mm; D=3.48-3.55 mm; E=1.23 mm.

Comparative material: Carduelis carduelis (MTM n=1: 1. coracoid C=3.03 mm; D=2.52 mm; E=0.92 mm; 2. humerus A=16.55 mm; C=5.57 mm; E= 1.65 mm; F=4.46 mm; G=2.32 mm); *C. chloris* (MTM n=1: coracoid C=2.85 mm; D=3.53 mm; E=1.19 mm; humerus A=18.19 mm; C=6.14 mm; E=1.89 mm; F=4.13 mm).

Diagnosis: Its sizes corresponds to recent *Carduelis chloris* . On coracoid in dorsal view (Fig. 85A), the *acrocoracoid* (a) is blunted conical shaped, its medial edge slightly bulging. *Processus accesorius* (b) is hook-like with bent and pointed end. Edge of s*ulcus m. supracoracoidei* (c) forms flattened concave line. Exterior edge of the *facies articularis humeralis* (d) is straight line. Point of *processus procoracoidei* (e) exceed the medial edge of corpus.

On proximal epiphysis of humerus in caudal view (Fig. 85B), the *tuberculum dorsale* (a) is rounded. *Caput humeri* (b) is wide and slightly convex. *Tuberculum ventrale* (c) forms oval spur. *Crista bicipitalis* (d) is protruding and rounded. C*rus dorsale fossae* is underdeveloped and the two parts of *fossa pneumotricipitalis* (e) can not be separated. On distal epiphysis of humerus in cranial view (Fig.85C), the

tuberculum supracondylare ventrale (a) is weakly developed. *Epicondylus ventralis* (g) is rounded. *Processus flexorius* (h) is obliquely protruding and has rounded end. *Condylus ventralis* (i) has laying oval shape. *Incisura intercondylaris* (j) has acute angle hollow. *Condylus dorsalis* (e) has strongly bent oval shape. *Epicondylus dorsalis* (l) is rounded. *Processus supracondylaris dorsalis* (m) is long with semispherical end. The widening between it and the diaphysis is deep.

Name: Was named after Kálmán LAMBRECHT, Hungarian paleornithologist.

Description: Its size corresponds to recent *Carduelis chloris* (LINNAEUS, 1758)

Carduelis † *parvulus* nova sp.
(Plate XXIII. Figure 86 A-B)

Type locality and age: Csarnóta 2, Pliocene (MN 15-16).

Holotype: Coracoideum dext. (cranial fragment), (MÁFI V.11.10.1; V.29085).

Paratype: Coracoideum dext. (cranial fragment); ulna sin. (distal fragment), (MÁFI V.11.37.1; V.29112).

Measurements: 1. coracoid C=2.34-2.46 mm; D=2.07- 2.16 mm; 2. ulna E=1.29 mm; F=2.33 mm; G=1.62 mm.

Comparative material: Carduelis spinus (MTM n=1; coracoid: C=2.70 mm; D=1.96 mm; ulna: E=1.38 mm; F=2.42 mm; G=1.79 mm); *Carduelis cannabina* (MTM n=1; coracoid: C=2.75 mm; D=2.41 mm; ulna: E=1.32 mm; F=2.56 mm; G=2.39 mm); *Carduelis flammea* (MTM n=1; coracoid: C=2.93 mm; D=2.29 mm; ulna: E=1.36 mm; F=2.66 mm; G=1.90 mm).

Diagnosis: On medial side of coracoideum in cranial end (Fig. 86A), the *acrocoracoideum* (a) has asymmetrical cone shape with cut-off end. *Processus accesorius* (b) has regular claw-like shape. Edge of *sulcus m. supracoracoideumei* (c) has flattened concave shape. *Facies articularis humeralis* (d) has bulged and rounded cranial edge. Point of *processus procoracoideumei* (e) exceeds the medial edge of corpus and has extended and flattened shape.

On distal epiphysis of ulna in medial view (Fig. 28 B), the *condylus dorsalis* (a) has rounded and proximal blunted claw-like shape. *Sulcus intercondylaris* (b) is wide and concave. *Condylus ventralis* (c) has obliquely blunt conical shape. *Tuberculum carpale* (d) has protruding semicircular shape.

Name: Was named after its dimensions.

Description: It corresponds in characteristics to genus and in dimensions to little sized species.

Carduelis † *medius* nova sp.
(Plate XXIII. Figure 87)

Type locality and age: Csarnóta 2, Pliocene (MN 15-16).

Holotype: Coracoideum sin. (cranial fragment) (MÁFI V.11.11.1, V.29086).

Paratype: Coracoideum sin. (cranial fragment) (MÁFI V.11.38.1; V.29113).

Measurements: Coracoid C=2.67-3.37 mm; D=2.37-2.65 mm.

Comparative material: Carduelis cannabina (MTM n=1; coracoid: C=2.75 mm; D=2.41 mm); *Carduelis flammea* (MTM n=1; coracoid: C=2.93 mm; D=2.29 mm); *Carduelis carduelis* (MTM n=1; coracoid:C=3.00 mm; D=2.20 mm);

Diagnosis: On medial side of coracoideum in cranial end (Figure 87), the *acrocoracoideum* (a) has asymmetrical cone shape with slightly rounded end. *Processus accesorius* (b) has regular claw-like shape with rounded end. Edge of *sulcus m. supracoracoideumei* (c) has flattened concave shape. *Facies articularis humeralis* (d) has bulged and rounded cranial edge. Point of *processus procoracoideumei* (e) more exceeds the medial edge of corpus.

Name: Was named after its medium sizes.

Description: Corresponds in its characteristics and sizes with one medium sized recent species of genus.

Distribution: In the Carpathian Basin the genus was reported as *Carduelis* sp. from Beremend 17 – Hungary (Lower Pleistocene, MQ1) by JÁNOSSY (1992). Recent species are known from Betfia 9-Romania (Lower Pleistocene, MQ1) as: *Carduelis chloris* (LINNAEUS, 1758), *Carduelis carduelis* (LINNAEUS, 1758), *Carduelis spinus* (LINNAEUS, 1758) és *Carduelis cannabina* (LINNAEUS, 1758), (GÁL 2002).

The genus was described outside of the Carpathian Basin from the Late Pliocene – Early Pleistocene, (MN 17 – MQ1) in Varshets and Cerzenica – et al. Bulgaria by BOEV (1996, 2000), Quibas and S'Onix-Spain by MONTOYA et al. (1999) and SONDAAR et al. (1995); Mas Ramboult -France by MOURER-CHAUVIRÉ (1995) and Stránská skála- Czech Republic by JÁNOSSY (1972).

Genus *Pyrrhula* (LINNAEUS, 1758)
Pyrrhula †*gali* nova sp.
(Plate XXIII. Figure 88 A-C)

Type locality and age: Polgárdi 5, Late Miocene (MN 13).

Holotype: Humerus sin. (MÁFI V.11.129.1; V.29204).

Paratypes: Humerus sin.; ulna sin. (proximal fragment) (MÁFI V.11.129.1; V.29204/3).

Measurements: 1. humerus A=16.61-17.16 mm; B=4.43-4.69 mm; C=5.37-5.91 mm; D=4.33 mm; E=1.58 -1.68 mm; F=3.99- 4.05 mm; G=2.11-2.21 mm; 2. ulna B=3.39 mm; C=2.76 mm; E=1.36-1.38 mm;

Comparative material: Pyrrhula pyrrhula (MTM n=1: humerus A=19.68 mm; B=5.71 mm; C=6.61 mm; D=5.28 mm; E=1.96 mm; F=5.54 mm; G=2.71 mm; ulna C=2.76 mm; E=1.36 mm); *Pinicola enucleator* (MTM n=1: ulna C=2.76 mm; E=1.36 mm); *Loxia curvirostra* (MTM n=1: humerus A=18.58 mm; B=7.46 mm; C=7.15 mm; D=5.81 mm; E=2.05 mm; F=5.73 mm; G=3.02 mm; ulna B= 3.68 mm; C=2.76 mm; E=1.36 mm).

Diagnosis: On proximal epiphysis of humerus in caudal view (Fig. 88A), the *tuberculum dorsale* (a) is rounded. *Caput humeri* (b) is wide and slightly convex. *Tuberculum ventrale* (c) forms circular spur. *Crista bicipitalis* (d) is laterally protruding and has cut-off end. C*rus dorsale fossae* is underdeveloped and the two parts of *fossa pneumotricipitalis* (e) can not be separated. On the distal epiphysis of humerus in cranial view (Fig. 88B), the *tuberculum supracondylare ventrale* (f) is weakly developed. *Epicondylus ventralis* (g) is protruding. *Processus flexorius* (h) is obliquely protruding and has cut-off end. *Condylus ventralis* (i) has lying oval shape. *Incisura intercondylaris* (j) is wide acute angle hollow. *Condylus dorsalis* (e) has strongly bent oval shape. *Epicondylus dorsalis* (l) is rounded. *Processus supracondylaris dorsalis* (m) is short and has two unequal branches. The larger branches have semispherical end.

On proximal epiphysis of ulna in cranial view (Fig. 88C), the *oleocranon* (a) is long, thin and slightly bent. *Cotyla dorsalis* (b) has conical shape with a rounded end. *Cotyla ventralis* (c) has circular shape. *Tuberculum lig. colateralis ventralis* (d) is well developed. *Depressio m. brachialis* (e) is weakly hollow.

Name: Was named after Hungarian paleornithologist, Erika GÁL.

Description: Corresponds in its characters to recent species of the genus.

Pyrrhula † *minor* nova sp.
(Plate XXIII. Figure 89 A-C)

Type locality and age: Csarnóta 2, Pliocene (MN 15-16).

Holotype: Humerus sin.(distal fragment), (MÁFI V.11.12.1, V.29087).

Paratípus: Coracoideum sin. (cranial fragment); ulna dext. (distal fragment), (MÁFI V.11.48.2; V.29123).

Measurements: 1. coracoid C=2.84 mm; D=2.36 mm; 2. humerus F=3.54 mm; G=2.31 mm; 3. ulna F=1.58 mm; G=2.85 mm; E=1.41 mm.

Comparative material: Pyrrhula pyrrhula (MTM n=1; coracoid: C=2.95 mm; D=2.54 mm; humerus: F=4.76 mm; G=2.55 mm; ulna: E=1.54 mm; F=3.03 mm; G=2.51 mm).

Diagnosis: On medial side of coracoideum in cranial end (Figure 89A), the *acrocoracoideum* (a) has symmetrical cone shape with rounded end. *Processus accesorius* (b) has regular claw-like shape with strongly rounded end. Edge of *sulcus m. supracoracoideumei* (c) is deep concave shape. *Facies articularis humeralis* (d) has rounded cranial edge.

On distal epiphysis of humerus in cranial view (Figure 89B), the *tuberculum ventrale* (a) is well developed. *Epicondylus ventralis* (b) is strongly arched. *Processus flexorius* (h) has rounded claw-like shape. *Condylus ventralis* (d) has strongly bulged oval shape. *Incisura intercondylaris* (e) has deep and pointed pit. *Condylus dorsalis* (f) has curved oval shape. *Epicondylus dorsalis* (g) is rounded. *Proc. supracondylaris dorsalis* (h) is wide and oblique and has two short braches.

On distal epiphysis of ulna in medial view (Figure 89C), the *condylus dorsalis* (a) has strongly arched and wide edge. *Sulcus intercondylaris* (b) is concave in acute angle. *Condylus ventralis* (c) has regular semicircular shape. *Tuberculum carpale* (d) has asymmetrical conical shape with bulged lateral edge.

Name: Its name refers to smaller dimensions of species.

Description: Corresponds in its characteristics to recent genus, but differs in dimensions.

Distribution: The genus was reported as *Pyrrhula* sp. foss. indet. from Beremend 16, 17, - Hungary (Lower Pliocene – Lower Pleistocene, MN 15-MQ1) (KESSLER 2010) and as recent *Pyrrhula pyrrhula* LINNAEUS, 1758 from Betfia 9 –Romania (Lower Pleistocene, MQ1) (GÁL 2002).

The genus was reported outside the Carpathian Basin from the Late Pliocene – Early Pleistocene, (MN 17 – MQ1) in Varshets– Bulgaria by BOEV (1996, 1997) and Stránská skála- Czech Republic by JÁNOSSY (1972).

Loxia † c*sarnotanus* nova sp.
(Plate XXIV. Figure 90 A-C)

Type locality and age: Csarnóta 2, Pliocene (MN 15-16).

Other locality: Beremend 26, Pliocene (MN 15-16).

Holotype: Humerus dext. (distal fragment), (Csarnóta 2, MÁFI V.11.30.1; V.29105).

Paratype: Ulna sin. (distal fragment), (Csarnóta 2, MÁFI V.11.50.1, V.29125); two humeri sin, with damaged proximal epiphysises; distal fragment of tibiotarsus dext. (Beremend 26, BKA).

Measurements: 1. humerus F=4.48 mm; G=2.41 mm; 2. ulna F=3.27 mm; G=2.23 mm; E=2,10-2,14

mm; F=4,48--6,05 mm; G=2,41-2,92 mm. 2. tibiotarsus E=1,56 mm; F=3,03 mm; G=3,15 mm.

Comparative material: Loxia curvirostra (MTM n=1; humerus: F=5.59 mm; G=3.08 mm; ulna: F=3.45mm; G=2.45 mm; tibiotarsus E=1,53 mm; F=3,17 mm); *Loxia leucoptera* (MTM n=1; humerus: F=4.70 mm; G=2.60 mm; ulna: F=3.05mm; G=2.23 mm; tibiotarsus E=1,49 mm; F=2,79 mm).

Diagnosis: On distal epiphysis in cranial view of humerus (Fig. 90A), the *tuberculum ventrale* (a) is developed. *Epicondylus ventralis* (b) is rounded. *Processus flexorius* (h) has obliquely rounded conical shape. *Condylus ventralis* (d) has oval shape. *Incisura intercondylaris* (e) has wide and pointed pit. *Condylus dorsalis* (f) has oval shape (but damaged). *Epicondylus dorsalis* (g) is rounded. *Proc. supracondylaris dorsalis* (h) has asymmetrically blunted conical shape.

On distal epiphysis in medial view of ulna (Fig. 90B), the *condylus dorsalis* (a) has asymmetrically bulged conical shape. *Sulcus intercondylaris* (b) is slightly concave. *Condylus ventralis* (c) has blunt conical shape. *Tuberculum carpale* (d) has flattened semicircular shape.

On distal epiphysis of tibiotarsus in cranial view (Fig. 90C), the *tuberositas retinaculi m. fibularis* (a) is weakly developed. *Sulcus extensorius* (b) is narrow and distally rounded. *Pons supratendineus* (c) is narrow and oblique. *Condylus lateralis* (d) has lateraly rounded shape. The line of i*ncisura intercondylaris* (e) is wavy. C*ondylus medialis* (f) has distally pointed shape.

Name: Was named after the name of type locality.

Description: Its characteristics corresponds with recent genus, but has smaller dimensions.

Distribution: In the Carpathian Basin it is known only as *Loxia curvirostra* Linnaeus, 1758 from Betfia 9 –Romania (Early Pleistocene, Q1), (GÁL 2002); In outside of the Carpathian Basin was reported as *Loxia* sp. from Saint-Gerand-le Puy-France (Lower Miocene, MN 2) , (MOURER-CHAUVIRÉ 1995) and as *Loxia patevi* BOEV, 1999 from Varshets -Bulgary (Upper Pliocene, MN 17), (BOEV 1999).

Genus *Pinicola* VIEILLOT, 1807
Pinicola † *kubinyii* nova sp.
(Plate XXIV. Figure 91)

Type locality and age: Csarnóta 2, Pliocene (MN 15-16).

Holotype: Scapula sin. (with damaged corpus), (MÁFI V.11.31.1; V.29106).

Measurements: Scapula B=4.19 mm; C=1.82 mm; D=2.74 mm; E=1.84 mm.

Comparative material: Pinicola enucleator (MTM n=1; scapula: B=5.23 mm; C=1.92 mm; D=2.83 mm; E=1.97 mm).

Diagnosis: On cranial end of scapula (Figure 91), the lateral branch (a) has wide and rectangular shape with cut-off end. Edge between the two branches (b) forms wide concave line. Medial branch (c) is long and pointed. F*acies atricularis humeralis* (d) has reversed conical shape.

Name: Was named after the Hungarian geologist Ferenc KUBINYI.

Description: It is smaller in dimensions than the recents species.

Spreading: The genus *Pinicola* with recent species it is known only from the Pleistocene localities of Europa (TYRBERG 1998). In the Carpathian Basin was reported as *Pinicola enucleator* (Linnaeus, 1758) from Deutsch-Altenburg – Austria (Lower Pleistocene, Q1), (JÁNOSSY 1981).

Genus *Coccothraustes* BRISSON, 1760
Coccothraustes † *major* KESSLER, 2012
(Plate XXIV. Figure 92 A-F)

Type locality and age: Beremend 26, Pliocene (MN 15-16).

Holotype: Proximal fragment of humerus sin. (BKA).

Paratypes: 8 fragments of mandibulae and maxillae; distal fragment of the right and left side humerus; distal fragment of the right and left side tarsometatarsus; (BKA).

Measurements: Humerus B=10,94 mm; C=8,97 mm; D=7,02 mm; E=2,46-2,69 mm; F=6,24-6,28 mm; G=3,42-3,46 mm; tarsometatarsus E=1,57-,67 mm; F=2,81-3,01 mm; G=1,64-1,70 mm.

Comparative material: Coccothraustes coccothraustes (MTM n=1: humerus B=8,36 mm; C= 7,19 mm; D=6,70 mm; E= 2,46 mm F=5,87 mm; G=3,33 mm; tarsomeatarsus E=1,26 mm; F=2,80 mm; G=1,75 mm).

Diagnosis: The fragments of mandibulae (Fig. 92A,B) and maxillae (Fig. 92C) are tipically for genus, but weakly bigger than in the recent species. On proximal epiphysis of humerus in caudal view (Fig. 92D), the *tuberculum dorsale* (b) is rounded. *Caput humeri* (a) is wide and asymmetrical convex. *Tuberculum ventrale* (c) forms semicircular spur. *Crista bicipitalis* (d) is protruding with cut-off end. C*rus dorsale fossae* is undeveloped and the two parts of *fossa pneumotricipitalis* (e) can be weakly separated. On distal epiphysis in cranial view (Fig. 92E) of humerus the *tuberculum supracondylare ventrale* (f) is developed. *Epicondylus ventralis* (g) is rounded. *Processus flexorius* (h) is protruding and rounded. *Condylus ventralis* (i) has oval shape. *Incisura intercondylaris* (j) has wide and acute angled pit. *Condylus dorsalis* (k) has strongly bent oval shape. *Epicondylus dorsalis* (l) is pointed. *Processus supracondylaris dorsalis* (m) is long, curved and pointed.

On distal epiphysis of tarsometatarsus in dorsal view (Figure 92F), the. *trochlea metatarsi* II. (a) has rounded conical shape. *Incisura intertrochlearis*

lateralis (b) has wide acute angle shape. *Trochlea metatarsi* III. (c) is wide and with slightly concave end. *Incisura intertrochlearis medialis* (d) is narrow and deep. T*rochlea metatarsi* IV. (e) has asymmetrical cut-off end shape.

Name: Was named after its dimensions.

Description: It differs to recent species in its dimensions, more larger than in recent species, and corresponds much in its characters. It should be noted that do not meet with this genus in other songbirds-rich materials (Polgárdi, Csarnóta).

Distribution: The genus was reported with extinct species only from Bulgaria (Varshets and Slivnita, Upper Pliocene - Early Pleistocene, MN 17-Q1) as *Coccothraustes simeonovi* BOEV, 1998 and *C. balcanicus* BOEV, 1998 (BOEV 1998). The recent species is known of the Early Pleistocene from some localities in Europe (TYRBERG 1998).

Family Emberizidae VIGORS, 1831
Genus *Emberiza* VIGORS, 1831
Emberiza † pannonica nova sp.
(Plate XXV. Figure 93 A-D)

Type locality and age: Polgárdi 4, 5; Late Miocene (MN 13).

Holotype: Humerus dext. (proximal fragment) (Polgárdi 5, MÁFI V.11.92.1; V.29167).

Paratypes: Ulna sin. (proximal fragment) (Polgárdi 5); carpometacarpus dext. (missing *os metacarpale minus*), (Polgárdi 4); one right and 2 left side tibiotarsi (distal fragments), (Polgárdi 4), (MÁFI V.V.11.113.3, V.11.117.1; V.29188, V.29192).

Measurements: 1. humerus B=6.41 mm, C=7.23 mm; D=5.19 mm; 2. ulna B=3.61 mm; C=3.33 mm; E=1.55 mm; 3. carpometacarpus A=13.83 mm; C=3.33 mm; F=3.01 mm; 4. tibiotarsus F=2.57-3.08 mm; G=2.44-2.83 mm.

Comparative material: Emberiza cyrlus (MTM n=1: humerus C=5.98 mm; ulna C=3.18 mm; E=1,50 mm; carpometacarpus A=12.55 mm; C= 4.17 mm; tibiotarsus F=2.95 mm); *E. cia* (MTM n=1: humerus B=5.32 mm, C=6.53 mm; D=4.35 mm; ulna B=3.61 mm; C=3.43 mm; E=1.58 mm; carpometacarpus A=12.52 mm; C=3.39 mm; F=2.92 mm; tibiotarsus F=2.75 mm; G=2.41 mm); *E. citrinella* (MTM n=1: humerus B=6.30 mm; C=6.65 mm; D=5.55 mm; ulna C=3.44 mm; E=1.65 mm; carpometacarpus A=12.35 mm; C= 3.25 mm; F=2.88 mm; tibiotarsus F=2.72 mm; G=1.21 mm).

Diagnosis: On proximal epiphysis of humerus in caudal view (Fig. 93A), the *tuberculum dorsale* (a) is rounded. *Caput humeri* (b) is wide and convex, but not too protruding. *Tuberculum ventrale* (c) has well developed circular shape. *Crista bicipitalis* (d) forms blunt beak-like shape. C*rus dorsale fossae* (e) is undeveloped and the two parts of *fossa pneumotricipitalis* (f) can not be separated.

On proximal epiphysis of ulna in cranial view (Fig. 93B), the *oleocranon* (a) is long, thin, straight and has blunt end. *Cotyla dorsalis* (b) has asymmetrically and rounded conical shape. *Cotyla ventralis* (c) has oblique oval shape. *Tuberculum lig. colat. ventralis* (d) is well developed. *Depressio m.brachialis* (e) is weakly developed.

On the proximal epiphysis of carpometacarpus in ventral view (Fig. 93C), the *trochlea carpalis* (a) is asymmetrically bulging and protruding**.** *Proc. extensorius* (b) has obliquely conical-like shape. *Processus alularis* (c) is rectangular shape and the *fovea subalularis* (d) has slightly acute angle pit. *Protuberantia metacarpalis* (e) is triangular bulgle.

On tibiotarsus the distal epiphysis in cranial view (Fig. 93D), the *tuberositas retinaculi m. fibularis* (a) is rounded. *Sulcus extensorius* (a) has pointed distal end. *Pons supratendinous* (c) is wide and weakly oblique. *Condylus lateralis* (d) has pointed oval shape. *Incisura intercondylaris* (e) is concave and wavy line. *Condylus medialis* (f) has flattened oval shape.

Name: The name refers to Pannonia region.

Description: It corresponds to middle size recent species (*E. citrinella, E.cia, E.cyrlus*). The fossil species *Emberiza bartkoi* KESSLER et HÍR, 2012 from Litke 2 – Hungary (Lower Miocene, MN 5) seems similar in it sizes to Polgardi specimen, but was described from a distal fragment of a humerus. **(**KESSLER & HÍR 2012).

Emberiza † polgardiensis nova sp.
(Plate XXV. Figure 94 A-F)

Type locality and age: Polgárdi 4, 5; Late Miocene (MN 13).

Holotype: Tibiotarsus sin. (distal fragment) (Polgárdi 4, MÁFI V.11.61.1; 29137).

Paratypes: Four sin. and dext. humeri (1 proximal and 3 distal fragment), (Polgárdi 4,5); 4 ulnae (one right side with damaged proximal epiphysis, one right side and 2 left side distal fragments), (Polgárdi 5); 4 tibiotarsi sin. (distal fragments), (Polgárdi 4); 7 dext. and sin. tarsometatarsi (distal fragments), (Polgárdi 4),(MÁFI V.11.79.19; V.29154).

Measurements: 1. humerus A=16.61 mm; B=4.21-4.43 mm; C=5.26-5.37 mm; E=1.58 mm; F=3.66-3.99 mm; G=2.11-2.35 mm; 2. ulna F=2.41-2.59 mm; G=1.51-1.59 mm; 3. tibiotarsus E=1.25 mm; F=2.15-2.41 mm; G=2.01-2.18 mm; 4. tarsometatarsus E=1.16 mm; F=1.93-2.18 mm; G=0.93-1.19 mm.

Comparative material: Emberiza schoeniclus (MTM n=1: humerus A= 18.02 mm; B=4.65 mm; C=5.61 mm; E=1.71 mm; F=4.45 mm; G=2.42 mm; ulna B=3.34 mm; C=3.05 mm; E=1.52 mm; F=2.69 mm; G=1.93 mm; tibiotarsus E=1,09 mm; F=2,44 mm; G=2,36 mm; tarsometatarsus E=1.26; F=2.16 mm; G=1.22 mm).

Diagnosis: On proximal epiphysis of humerus in caudal view (Fig. 94A), the *tuberculum dorsale* (a) is

obliquely rounded shape. *Caput humeri* (b) is wide and convex, but not too protruding. *Tuberculum ventrale* (c) is well developed and it forms oval-like spur. *Crista bicipitalis* (d) has blunt beak-like shape. C*rus dorsale fossae* (e) is underdeveloped and the two parts of *fossa pneumotricipitalis* (f) can not be separated. On distal epiphysis in cranial view (Fig. 38B), the *tuberculum supracondylare ventrale* (g) is weakly developed. *Epicondylus ventralis* (h) is rounded. *Processus flexorius* (i) is slightly protruding and pointing sideways. *Condylus ventralis* (j) has wide and blunted conical-shape. *Incisura intercondylaris* (k) is deep hollow. *Condylus dorsalis* (l) has bent oval shape. *Epicondylus dorsalis* (m) is rounded. *Processus supracondylaris dorsalis* (n) is short, wide and has two small branches. The widening between it and the diaphysis is wide.

On proximal epiphysis of ulna in cranial view (Fig. 94C), the *oleocranon* (a) is long, thin and even. *Cotyla dorsalis* (b) has asymmetrically and rounded conical shape. *Cotyla ventralis* (c) has circular shape. *Tuberculum lig. colat. ventralis* (d) is weakly developed. *Depressio m.brachialis* (e) is developed. On distal epiphysis of ulna in medial view (Fig. 94D), the *condylus dorsalis* (a) has claw-like shape. *Sulcus intercondylaris* (b) has concave shape. *Condylus ventralis* (c) is wide conical. *Tuberculum carpale* (d) has semicircular shape.

On tibiotarsus the distal epiphysis in cranial view (Fig. 94E), the *tuberositas retinaculi m. fibularis* (a) is flattened and less develloped. *Sulcus extensorius* (a) is wide and has triangular distal end. *Pons supratendinous* (c) is wide and weakly oblique. *Condylus lateralis* (d) has flattene oval shape. *Incisura intercondylaris* (e) has slightly concave and obliquely wavy line. *Condylus medialis* (f) has oval shape.

On distal epiphysis of tarsometatarsus in dorsal view (Fig. 94F), the *trochlea metatarsi* II. (a) has wide and obliquely truncated rectangular shape. *Incisura intertrochlearis medialis* (b) has wide acute angle pit. *Trochlea metatarsi* III. (c) has concave end. *Incisura intertrochlearis lateralis* (d) has narrow acute angle pit. *Trochlea* metatarsi IV. (e) has flattened blunt conical shape.

Name: The name refers to the fossil locality.

Description: In its sizes it is similar to the smaller recent species (*E. schoeniclus*).

Emberiza † media nova sp.
(Plate XXVI. Figure 95 A-C)

Type locality and age: Csarnóta 2, Pliocene (MN 15-16).

Holotype: Humerus sin. (MÁFI V.11.33.1; V.29108)

Paratype : Ulna dext. (distal fragment), (MÁFI V.11.51.1; V.29126).

Measurements: 1. humerus: A=18.72 mm; B=7.91 mm; C=5.50 mm; D=5.07 mm; E=1.84 mm; F=4.67 mm; G=2.31 mm; 2. ulna F=3.18 mm; G=2.39 mm.

Comparative material: Emberiza cia (MTM n=1; humerus: A=18.65 mm; C=5.96 mm; E=1.96 mm; F=3.96 mm; ulna: F=2.97 mm; G=2.11 mm); *Emberiza citrinella* (MTM n=1; humerus: E=2.29; F=4.81 mm; ulna: F=2.88 mm; G=2.59 mm); *Emberiza schoeniclus* (MTM n=1: humerus: A=17.62 mm; C=5.63 mm; E=1.79 mm; F=4.38 mm; G=2.33 mm; ulna: F=2.69 mm; G=1.93 mm).

Diagnosis: On proximal epiphysis of humerus in caudal view (Fig. 95A), the *tuberculum dorsale* (a) is bulged in conical shape. *Caput humeri* (b) is convex. *Tuberculum ventrale* (c) has oval shape. *Crista bicipitalis* (d) is protruding with cut-off end. *Fossa pneumotricipitalis* (e) is not divided in two parts. On distal epiphysis of humerus in cranial view (Fig. 95B), the *tuberculum ventrale* (f) is weakly developed. *Epicondylus ventralis* (g) is slightly rounded. *Processus flexorius* (h) has rounded rectangular shape. *Condylus ventralis* (i) has oval shape. *Incisura intercondylaris* (j) has wide concave pit. *Condylus dorsalis* (k) has oval shape. *Epicondylus dorsalis* (l) is less rounded. *Proc. supracondylaris dorsalis* (m) is short, wide and pointed.

On distal epiphysis of ulna in medial view (Fig. 95C), the *condylus dorsalis* (a) has asymmetrically bulged conical shape. *Sulcus intercondylaris* (b) is concave. *Condylus ventralis* (c) has semicircular shape. *Tuberculum carpale* (d) has asymmetrical conical shape.

Name: Its name refers to middle sized dimensions of species.

Description: It corresponds to characteristics of recent genus.

Emberiza † parva nova sp.
(Plate XXVI. Figure 96 A-C)

Type locality and age: Csarnóta 2, Pliocene (MN 15-16).

Holotype: Coracoideum dext. (cranial fragment), (MÁFI V.11.32.1; V.29107).

Paratypes: One right and 2 left side humeri (distal epiphysis); 2 right and 2 left side ulnae (distal fragments), (MÁFI V.11.52.6, V.29127).

Measurements: 1. coracoid C=2.87 mm; D=2.44 mm; 2. humerus F=3.54-3.55 mm; G=1.84-2.02 mm; 3. ulna F=2.59-2.95 mm; G=1.55-1.92 mm.

Comparative material: Emberiza schoeniclus (MTM n=1: coracoid C=2,99 mm; humerus: F=4.38 mm; G=2.33 mm; ulna: F=2.69 mm; G=1.93 mm).

Diagnosis: On medial side of coracoideum in cranial end (Fig. 96A), the *acrocoracoideum* (a) has symmetrical and bulged semicircular shape. *Processus accesorius* (b) has elonged and curved claw-like shape. Edge of *sulcus m. supracoracoideumei* (c) has flattened concave shape. *Facies articularis humeralis* (d) has rounded and bulged edge. Point of the

processus prococarcoidalis (e) more exceeds the medial edge of corpus

On distal epiphysis of humerus in cranial view (Fig. 96B), the *tuberculum ventrale* (a) is well developed. *Epicondylus ventralis* (b) is slightly rounded. *Processus flexorius* (c) has short and wide rectangular shape. *Condylus ventralis* (d) has oval shape. *Incisura intercondylaris* (e) has wide concave pit. *Condylus dorsalis* (f) has oval shape. *Epicondylus dorsalis* (g) is bulged. *Proc. supracondylaris dorsalis* (h) is long, wide and with rounded end.

On distal epiphysis of ulna in medial view (Fig. 35 C), the *condylus dorsalis* (a) has bulged claw-like shape with rounded end. *Sulcus intercondylaris* (b) is concave. *Condylus ventralis* (c) has conical shape. *Tuberculum carpale* (d) has asymmetrical semicircular shape.

Name: Its name refers to smaller sized of species.

Description: Corresponds in its characteristics to recent genus.

Emberiza † *gaspariki* nova sp.
(Plate XXVI. Figure 97 A-C)

Type locality and age: Beremend 26, Pliocene (MN 15-16).

Holotype: Humerus sin. (BKA).

Paratypes : Distal fragment of humerus sin.; Three carpometacarpi dext. (BKA).

Measurements: 1. humerus: A=22,26 mm; B=6,99 mm; C=7,56 mm; D=6,18 mm; E=2,24 mm; F= 5,66-5,80 mm; G=2,68-3,17 mm; 2. carpometacarpus: A=16,84-17,49 mm; B=13,84-15,33 mm; C=4,27-4,63 mm; E=2,98-3,40 mm; F=3,76-4,11 mm;

Comparative material: Emberiza calandra (MTM n=1 humerus: A=24,99 mm; B=8,71 mm; C=8,05 mm; D=6,68 mm; E=2,32 mm; F=6,18 mm; G=3,48 mm; carpometacarpus: A=16,94 mm; B=13,67 mm; C=4,00 mm; E=3,15 mm; F=3,79 mm); *Emberiza cia* (MTM n=1 humerus: A=18,65 mm; C= 5,96 mm; E=1,96 mm; F=3,96 mm; carpometacarpus A=12,52 mm; C= 3,39 mm; F=2,92 mm); *Em-beriza citrinella* (MTM n=1: humerus: E=2,29; F=4,81 mm; carpometacarpus A=12,35 mm; C= 3,25 mm; F=2,88 mm); *Emberiza schoeniclus* (MTM n=1: humerus: A=17,62 mm; C=5,63 mm; E=1,79 mm; F=4,38 mm; G=2,33 mm; carpometacarpus A=12,25 mm; C= 3,35 mm; F=2,92 mm).

Diagnosis: On proximal epiphysis of humerus in caudal view (Fig. 97A), the *tuberculum dorsale* (a) is rounded. *Caput humeri* (b) is convex. *Tuberculum ventrale* (c) is damaged. *Crista bicipitalis* (d) is protruding with rounded end. *Fossa pneumotricipitalis* (e) is not divided into two parts. On distal epiphysis of humerus in cranial view (Figure 97B), the *tuberculum ventrale* (f) is well developed. *Epicondylus ventralis* (g) is slightly rounded. *Processus flexorius* (h) has oblique and rounded rectangular shape. *Condylus ventralis* (i) has oval shape. *Incisura intercondylaris* (j) has wide concave pit. *Condylus dorsalis* (k) has oval shape. *Epicondylus dorsalis* (l) is rounded. *Proc. supracondylaris dorsalis* (m) is short, wide and blunt.

On carpometacarpus in ventral view (Fig. 97C), the *trochlea carpalis* (a) is asymmetrically bulging and protruding**.** *Proc. extensorius* (b) has obliquely conical shape wit cut-off end. *Processus alularis* (c) has rectangular shape and the *fovea subalularis* (d) has slightly acute angle pit. *Protuberantia metacarpalis* (e) has wide and flat triangular shape.

Name: Was named after the Hungarian paleontologist Mihály GASPARIK.

Description: It corresponds in its characteristics to recent species, but has larger dimensions.

Distribution: In the Carpathian Basin was described the fossil species *Emberiza bartkoi* KESSLER et HÍR, 2012 from Litke 2 – Hungary (Lower Miocene, MN 5) (KESSLER & HÍR 2012). The remains of *Emberiza* sp.foss. indet. it is known from Nagyharsányhegy 1-4 – Hungary (Lower Pleistocene, MQ2) (JÁNOSSY 1979). The recent species *Emberiza calandra* LINNAEUS, 1758 was identified from Betfia 2 - Romania (Lower Pleistocene, MQ1) (ČAPEK 1917; LAMBRECHT 1933; JÁNOSSY 1979a; KESSLER 1975; GÁL 2002) and Betfia 9 - Romania (KESSLER 1975; GÁL 2002) and *Emberiza citrinella* LINNAEUS, 1758 also from Betfia 9 - Romania (GÁL 2002).

The genus it is known outside the Carpathian Basin from the Late Pliocene - Early Pleistocene (MN 17- MQ1) sediments from Varshets and Slivnita - Bulgaria (BOEV 1996, 1997, 2000) and Stránská skála - Czech Republic (JÁNOSSY 1972).

Genus *Plectrophenax* STEJNEGER, 1882
Plectrophenax †*veterior* nova sp.
(Plate XXVI. Figure 98)

Type locality and age: Polgárdi 4, Late Miocene (MN 13).

Holotype: Tibiotarsus sin. (distal fragment) (MÁFI V.11.59.1; V.29134).

Measurements: Tibiotarsus E=1.64 mm; F=2.59 mm; G=2.31 mm.

Comparative material: Plectrophenax nivalis (MTM n=1: E=1.65 mm; F=2.65 mm; G=2.52 mm); *E.calandra* (MTM n=1: E=1.70 mm; F=3.40 mm); *E. citrinella* (MTM n=1: E=1.43 mm; F=1.88 mm; G=2.46 mm).

Diagnosis: Its characteristics corresponds those tof the recent genus and species.

On tibiotarsus the distal epiphysis in cranial view (Fig. 98), the *tuberositas retinaculi m. fibularis* (/a) is less develloped and has lying shape. *Sulcus extensorius* (b) has deep and narrow distal end. *Pons supratendinous* (c) is straight and much wider than in the recent species. *Canalis extensorius* (d) has oval shape*. Condylus lateralis* (e) has flattened oval shape. *Incisura intercondylaris* (f) is wide and forms slightly

obliquely and wavy line. *Condylus medialis* (g) has less ovalic shape than in the recent species.

Name: The name refers to the age of the bone (Lat. *veterior*=old).

Description: It corresponds in its characters to the recent species.

Distribution: The genus is known only with recent species from Middle Pleistocene sediments from France and Ukraine (TYRBERG 1998).

Discussion

The fossil deposits on the W and SW of Hungary yielded extraordinarily rich passerine bone material in the 20th century. Identifying and classifying the material, however, has occurred to family and genus level at most, with the exception of the large Corvidae. Firstly, no such studies have been made globally for passerines and in consequence at the turn of the century only a couple of dozen extinct species had been identified, most of which were from large Corvidae and Menuridae families. Secondly, the skeletal parts of the fossil representatives of the order known only from the Upper Oligocene across Europe show morphologically unusually large homogeneity with recent material. The differences for both family and genus are very dinstinctive, which facilitates identification at this level. For this reason material of this kind has been reported from many sites across Europe, including Hungary through the good offices of Kálmán LAMBRECHT, Miklós KRETZOI and Dénes JÁNOSSY among others. However, very few attempts have been made at identification at species level and even these were received critically.

Mostly attempts were made to synonymise these with recent species (see MLIKOVSKY 2002).

This tendency does not take account of the laws of the process of evolution. Every living creature originates from its parents and modern specimens are separated from their ancestors by countless generations going backwards in time over millions of years. Since passerines, with the exception of larger birds such as Corvidae, reach sexual maturity at the age of one year old, we must count on at least a million generations over a million years. Due to the genetic characteristics inherited over so many generations, minimal differences between parent and offspring must surely arise in the area of morphology as well. Over many hundred thousand or a million generations these differences could be fairly large from both a morphological and biometrical viewpoint, and an individual from a generation a million years ago and one from today cannot be regarded as identical. All the less so because we are only able to study the skeletal traits without knowing anything about the other anatomical traits, such as the intestines, or the former characteristics of the plumage, behaviour and lifestyle.

In this paper this approach, as well as the morphological and size differences demonstrable in diagnoses are used to identify the parts of skeleton suitable for classification at species level bearing in mind that the material from Polgárdi, Csarnóta and Beremend are separated from today's related recent species by about 3-6 million years. But even the extinct species of the small mammals determining Pleistocene stratigraphy, which could produce several generations a year, existed only for a time band lasting between a few tens of thousands of generations and a few hundred thousand generations. On this basis, we believe it is entirely justified to hold that the species longevity of passerines should be fixed at one million generations at least, while we do not accept criticism of this approach and hold that it is unsound to synonymise fossil taxa that are described from 10- to 15-million-year-old remains with recent species citing none too obvious differences.

The same principles were used to identify and describe the new taxa of passerine birds from the Neogene material. These principles were that passerines usually reach sexual maturity at the age of one year, thus there have been approximately 3-6 million generations between the recent and fossil material. In view of this, more than enough time has elapsed for there to be morphological and ethological differences between them which make the identification and description of new taxa possible.

The passerines which have already been classified at species level appeared as a new element in the fauna of the Upper Oligocene and Lower Miocene. This is a global novelty in avian palaeontology as, although most of the 9,000 extant species of bird are passerines (about 5,500 species), the fossil remains of only a couple of dozen have been described at species level. According to the current status of science, they spread after their traits had evolved from Australia and its environs to the whole world during the Oligocene. The earliest known Palaearctic remains come from the Upper Oligocene (MP 30) from sites at Coderet and Gannat (Allier) in France (MOURER-CHAUVIRÉ ET AL. 1989). Typically these finds already bear the osteomorphological signs indicating passerines. Thereafter, fossils from Europe, Asia, and also from North and South America are only known from the Lower Miocene. In the last of these continents passerine remains have been described from the Lower Miocene in Patagonia (NORIEGA & CHIAPPE 1993). This means that the spread of the passerines ended at this time.

Results and conclusions

From the territory of Hungary, new 113 extinct taxa represent Neogene Passeriformes including the material from Polgárdi (39 taxa), from Csarnóta (35 taxa) and from Beremend (24 taxa), as well as those described from North Hungary (KESSLER & HÍR 2012) (15 taxa).

The Late Miocene avian fauna at Polgárdi has been identified from extraordinarily rich material. From the several hundred bone finds (JÁNOSSY mentions 308), the three researchers who have studied the material to date have identified 955 bones from the three Polgárdi sites (2, 4, 5), (ČAPEK [in papers by KORMOS 1911, and LAMBRECHT 1912 and 1933], Jánossy, 1992, 1995; KESSLER 2010 and 2012). Of these one taxon only has been identified at class level (Aves indet.), 2 taxa at order level (Galliformes és Passeriformes indet.), 3 taxa at family level (Anatidae, Fringillidarum, Emberizidae), and 18 at genus level (see Table of Species).

It should be noted that on the last occasions classifications were made (2010, 2012) most of this material was identified at genus level at most. The passerines noted by Dénes JÁNOSSY in 1992 and 1995 and by the author in 2010, which were identified only at genus level, are in most cases classified at species level in this work. JÁNOSSY (1992) only listed 21 bones for passerines, but from this and the unidentified material 39 passerine taxa were identified at species level and a few at genus level. This is not to mention the unidentified material.

Of the total of 71 identified species, there were 63 extinct species and 2 extinct subspecies (*Falco tinnunculus atavus* and *Athene noctua veta*), and 48 of these species and 2 subspecies were from Polgárdi.

If the extinct species of passerines described from Polgárdi (39 species) are taken into account, together with the other 10 new extinct taxa (9 species: *Egretta polgardiensis* KESSLER, 2010; *Anas albae* JÁNOSSY, 1991; *Palaeocryptonix hungaricus* JÁNOSSY, 1991; *Porzana kretzoii* KESSLER, 2010*,, Rallicrex polgardiensis* JÁNOSSY*,*1991; *Calidris janossyi* KESSLER, 2010*,, Charadrius lambrechti* KESSLER, 2010*, Tyto campiterrae* JÁNOSSY*,* 1991; *Cuculus pannonicus* KESSLER, 2010 and one subspecies: *Porzana estramosi veterior* JÁNOSSY, 1991) described from there (a total of 49), the site's palaeontological significance and the extraordinary wealth and diversity of the former avian fauna of the area, as well as its endemic nature are proven.

Comparing the species list of the three sites, we may establish that in the case of Polgárdi 2, it is not possible to deduct more considerable inferences from the skimpy list of species.

The species list of the Polgardi 4 and Polgárdi 5 not differ fundamentally, 29 species it is common, 24 species are not on the Polgárdi 5, but reversely it is only 9. The species from aquatic/wetland environment differ and the list of Polgárdi 4 is richer from this viewpoint. Also differ the composition of the list in open grass and shrub land environment, while the species from forest and rocky habitats mostly correspond.

Most of the bone remains from Polgárdi sites originate from small birds; medium-sized birds account for an insignificant amount, and large birds are almost entirely absent from the fauna. The largest sized birds were two species of peacock (*Pavo*), as well as hawk (*Buteo*), bustard (*Otis*) and duck (*Anas*), and those in the small to medium-sized category were partridge (*Palaeortyx*), snipe (*Gallinago*), cuckoo (*Cuculus*) and crows (*Corvus*). All the rest were far smaller in size. Naturally, the two nocturnal predators, the medium-sized barn owl (*Tyto*) and the small-sized little owl (*Athene*) must not be forgotten. It is more than likely that the majority of the bones accumulated in the rock cavities and fissures of Szárhegy were due to their activity. In part their size determines the size of their prey animals as well.

The barn owl was well represented in the fossil material, with 17 bones from Site 4 and 93 from Site 5.

The composition of the list of species suggests very varied ecological conditions on the western shore of the Pannonian Lake, which was regressed and drying out, with habitats ranging from shoreline marshland, areas covered with reed beds and gallery forests to more open grassland and cliffs with woody vegetation.

Sixteen species (23%) indicate an aquatic/wetland environment, 19 species (27%) an open grass and shrub land environment, 27 species (37%) deciduous forests and 9 species (13%) rocky habitats if taxa identified at genus and species level are considered.

The Csarnóta sites (or more precisely Site 2 as only one species was classified from Site 4) yielded 63 taxa. Of these, 59 were identified at species level, 2 at genus level, and 2 at order or class level. 57 (53 species and 4 subspecies) of the 59 species are fossil or extinct taxa. Of these, 40 species were first recorded at Csarnóta. 61 recent taxa belong to 10 orders, 28 families and 52 genera.

As regards the ecotypes of the classified taxa, an aquatic/wetland environment was typical of 7 taxa (11%), an open grass and shrub land environment of 12 taxa (20%), a rocky environment of 6 taxa (10%), and forest and wooded areas of 36 taxa (59%). The percentages of open environment and rocky habitat species were approximately the same as those of the Late Miocene material (MN13) from Polgárdi, where the former was 23% and the latter 13%, but there was a significant difference for those of the wetland and forest species of avian fauna (23% and 27%

respectively). This clearly reflects the differences in environmental conditions before and after the Pannonian Lake silted up. There was a marked reduction of aquatic and wetland habitats (only one open water species is on the list of fauna), but the forest avian fauna doubled. Common related taxa are as follows: *Anas alba, Falco tinnunculus atavus, Palaeortyx brevipes, Rallicrex polgardiensis, Porzana kretzoii, Otis kalmani, Galinago veterior, Athene noctua veta, Apus baranensis, Miocorvus larteti*, whereas other extinct species of songbirds genera from Polgárdi (*Galerida, Lullula, Hirundo, Delichon, Anthus, Sitta, Certhia, Saxicola, Oenanthe, Turdus, Cettia, Acrocephalus, Locustella, Phylloscopus, Cinclus, Prunella, Lanius, Passer, Fringilla, Carduelis, Pyrrhula* és *Emberiza*) may be direct predecesors of the Csarnótan's species, considering the 2.5 to 3 million year difference in the age of the sites.

After NAGYMAROSSY and HÁMOR (2012) in the Pannonian Basin the Pliocene continental beds indicate an arid or semiarid climate, similar to the present desert. In contrast KRETZOI (1969) signaled that increased humidity and heat-intensive forest faunas existed in Csarnótanum.

The bird fauna from Csarnóta 2 confirmed this idea with 70% aquatic/wetland and forest areas ecotype species composition.

The Beremend 26 site yielded 66 taxa. Of these, 56 were identified at species level, 10 at genus level. 56 (52 species and 4 subspecies) of the 66 taxa are extinct taxa. The 66 taxa belong to 10 orders, 30 families and 53 genera.

Of these, 37 species were first recorded at Beremend 26 (24 species) and Csarnóta 2 (13 species, which are known from the holotype and which are paratypes in Beremend 26) . All 37 species belong to the order Passeriformes. The five Corvidae taxa was signaled in 2010 (KESSLER 2010).

As regards the ecotypes of the classified taxa, an aquatic/wetland environment was typical of 11 taxa (17%), an open grass and shrub land environment of 12 taxa (18%, but this a rocky environment of 3 taxa, 4,5%), and forest and wooded areas of 43 taxa (65%). It proves that the KRETZOI's (1969) assumption regarding the climate of Csarnótanum was adequate.

Compared to the similar age bird fauna from Csarnóta – near only a few kilometers distant to the Beremend – we can be concluded that 25 taxa of the same (apr. 37-38%); the ecotypes are almost similar; in Beremend more the aquatic/wetland ecotype taxa, in Csarnóta more the rocky ecotypes.

However it should be noted, that while in the Csarnóta 2 the fully fossil material was examined, from Beremend 26 only a part of the fossil remains has been saved.

This my explain also that, while in the Csarnóta 2 faunas can be found of great stature *Bubo bubo* (that pray a larger-bodied birds), in Beremend this is missing, while in the fossil material can occur bustards, herons, black grouse and capercaillie.

The bones of some prey species compared to others are better represented in fossil material (*Delichon polgardiensis, Saxicola lambrechti, Acrocephalus major, A. minor, Hippolais veterior, Sylvia intermedia, Locustella kordosi, Motacilla intermedia, Carduelis kretzoii* and *Emberiza polgardiensis* in Polgárdi; *Prunella kormosi* and *Emberiza parva* in Csarnóta; *Turdus major, T.medius, T.minor, Oriolus beremendensis, Lanius major, Sturnus pliocaenicus* and *Coccothraustes major* in Beremend), what on the one hand proved the density of individuals or preference of the predators.

Table 1. Songbirds bones from Hungarian Neogene. (Abrevations: PC - Polgárdi complete bones; PF - Polgárdi fragmentary bones; PT - Polgárdi total bones; CsC - Csarnóta complete bones; CsF - Csarnóta fragmentary bones; CsT - Csarnóta total bones; BC - Beremend complete bones; BF - Beremend fragmentary bones; BT - Beremend total bones; TC - total complete bones; TG - total fragmentary bones; TG - total number bones).

Bones	PC	PF	PT	CsC	CsF	CsT	BC	BF	BT	TC	TF	TG
max+mand.								8	8		8	8
coracoid	6	9	15		14	14				6	23	29
scapula					2	2					2	2
humerus	16	47	63	2	11	13	10	34	44	28	92	120
ulna	10	46	56	1	22	23	1	2	3	12	70	82
carpomtcp.	16	5	21		13	13	13	3	16	29	21	50
ph.alae							2		2	2		2
femur	1	7	8							1	7	8
tibiotarsus		36	36		7	7		3	3		46	46
tarsometts.		18	18	1	9	10	3	7	10	4	34	38
Total	49	168	217	4	78	82	29	49	78	82	303	385

The above data suggest the following taphonomical conclusions:

1. The longest bones (tibiotarsi, tarsometatarsi) in most cases were fragmented. It refers to small- or medium-sized predators.

2. The number of complete bones from Polgárdi suggest medium-sized predators (*Tyto, Strix, Surnia, Asio*).

3. A small number of complete bones from Csarnóta suggest that they were prey to a small owl (probable *Athene noctua*).

4. Six types of bones (coracoid, humerus, ulna, carpometacarpus, tibiotarsus and tarsometatarsus) represented a overwhelming majority from fossil remains (96% in Polgárdi, 90% in Csarnóta and 84% in Beremend).

5. Three wing bones (humeri, ulnae and carpometacarpi) represent 66% from total remains.

6. The rate of bones/species is 5,56 in Polgárdi, 2,34 in Csarnóta and 2,11 in Beremend.

The identification of 114 songbird taxa from Carpathian Basin (113 from Hungary and one from Romania: *Luscinia jurcsaki* KESSLER et VENCZEL 2011 from the Middle Miocene, MN 6 of Subpiatră, Bihor County[KESSLER & VENCZEL 2011]) means to start a new chapter in palaeornithology.

The author hopes that the research of the Neogene passeriformes will produce new and interesting results both in Europe and in other part of the world.

Acknowledgements

The author wishes to express his deep gratitude to Dr. László KORDOS (GGIH) and László PONGRÁCZ (collector of fossil materials and creator of the Foundation "Beszélő Kövek") for access to fossil remains. Dr. Mihály GASPARIK is thanked for providing access to fossil and recent bird bone collections in the Natural History Museum of Hungary and to Dr. Erika GÁL, Dr. László KORDOS, László MAKÁDI and Dr. Piroska PAZONYI for the help in revision of the text.

References

BAUMEL, J. J., KING, A. S., LUCAS, A. M., BREAZILE, J. E., EVANS, H. E. 1979: *Nomina anatomica avium.* Academic Press, London, 637 p.

BOEV, Z. N. 1996: Tertiary avian localities of Bulgaria. In: MLIKOVSKY (ed): Tertiary avian localities of Europa. – *Acta Universitatis Carolinae, Geologica* 39, 541–545.

BOEV, Z. N. 1997: *Chauvireria balcanica* gen. n., sp. n. (Phasianidae – Galliformes) from the Middle Villafranchian of Western Bulgaria. *Geologica Balcanica* 27, 69–78.

BOEV, Z. N. 1998: Late Pliocene hawfinches (*Coccothraustes* Brisson, 1760) (Aves: Fringillidae) from Bulgaria. – *Historia Naturalis Bulgarica* 9, 87–99.

BOEV, Z. N. 1999: Earliest finds of crossbills (genus *Loxia*) (Aves: Fringillidae) fromVarshets (NW Bulgaria). – *Geologica Balcanica* 29(3–4), 51–57.

BOEV, Z. N. 2000: Neogene avifaunas of Bulgaria. – *Vertebrata Palasiatica* 38, (Supplement): 2– 10.

BOEV, Z. N. 2012: Neogene Larks (Aves: Alaudidae (Vigors, 1825) from Bulgaria. – *Acta zoologica bulgarica*, 64 (3), 295–318.

BRODKORB, P. 1960: How many species of birds have existed? – *Bulletin of the Florida State Museum, Biological Sciences* 5, 41–53.

ČAPEK, V. 1917: A püspökfürdői preglaciális madárfauna. – *Barlangkutatás* 5, 66–74.

CLOT, A., CHALINE, J., HEINTZ, E., JAMMOT, D., MOURER-CHAUVIRÉ, C. & RAGE. J.C. 1976: Montoussé 5 (Hautes-Pyrénées), un nouveau remplissage de fissure à faune de vertébrés du Pléstocène inférieur. – *Géobios* 9, 511–514.

DÖPPES, D & RABEDER, G (eds) 1997. *Pliozäne und Pleistozäne Faunen Österreichs*. – Mitteilungen der Kommission für Quartärforschung der Österreichischen Akademie der Wissenschaften, Vol 10, Wien, pp. 411.

DRIESCH, A. VON DEN. 1976: A guide to the measurements of animal bones from archaeological sites. – *Peabody Museum Bulletin* 1.

FREUDENTHAL, M. & KORDOS, L. 1989: *Cricetus polgardiensis* sp.nov. and *Cricetus kormosi* SCHAUB , 1930 from the Late Micene Polgárdi localities (Hungary). – *Scripta Geologica* 89, 71–95.

GÁL, E. 2002: Avifauna pleistocena a Romaniei. [Not published doctoral thesis: Pleistocene birds faunas from Romania]. Bucuresti. 263 pp.

GÁL E., HÍR J., KESSLER E., KÓKAY J. & VENCEL M. (2000): Középső-miocén ősmaradványok a Mátraszőlős, Rákóczi-kápolna alatti útbevágásból. II. A Mátraszőlős 2. lelőhely. – *Folia Historico Naturalia Musei Matraensis* 24: 39–75.

GÁL, E. & KESSLER, E. 2006. Songbird remains from the Miocene (Middle Sarmatian) site Credinta (Dobrogea, South-East Romania). In: Z. CSIKI (ed.) *Volume dedicated to Dan Grigorescu on his 65th birthday*. University of Bucharest Printing House.

GILBERT, M. B., MARTIN, L.D. & SAVAGE, H.G 1981: *Avian Osteology* . Laramie, Wyoming. 240 pp.

HARRISON, C.J.O. & STEWART, J.R. 1999: Avifauna. In: ROBERTS M.B. & PARFITT S.A. (eds): Boxgrove. *A middle Pleistocene hominid site at Eartham Quarry, Boxgrove, West Sussex.* – English Heritage Archaeological Report (London) 17: 187–196.

HARRISON C.J.O. (1979): Small non-passerine birds of the Lower Tertiary as exploiters of ecological niches now occupied by passerines. – Nature 281: 562–563.

HIR, J. KÓKAY, J., VENCZEL, M., GÁL, E. & KESSLER, E. 2001. Előzetes beszámoló a felsőtárkányi „Gödör-kert" n. őslénytani lelőhelykomplex újravizsgálatáról. – *Folia Historico-Naturalia Musei Matraensis* 25: 41–65.

HORÁČEK, I. 1985: Survey of the fossil vertebrate localities Včeláre 1–7. – *Časopis pro Mineralogii a Geologii* 30, 353–366.

JÁNOSSY, D. 1965: Vogelreste aus den altpleistozänen Ablagerungen von Voigtstedt in Thüringen. – *Paläontologische Abhandlungen (A)* 2, 336–361.

JÁNOSSY, D. 1972: Die mittelpleistozäne Vogelfauna der Stránská Skála. – *Anthropos* 21 (12), 35–64.

JÁNOSSY, D. 1974: Die mittelpleistozäne Vogelfauna von Hundsheim (Niederösterreich). – *Sitzber. Österr. Akad. Wiss. Mathem.-Naturw*. Kl., Abt. 1, 182, 211–257.

JÁNOSSY, D. 1978: Új finomrétegtani szint Magyarország pleisztocén őslénytani sorozatában. – *Földrajzi Közlemények* 26(1–3), 161–174.

JÁNOSSY, 1979: Plio-pleistocene Bird Remains from the The Carpathian Basin. IV. Anseriformes, Gruiformes, Charadriiformes, Passeriformes. – *Aquila* 85, 11–39.

JÁNOSSY, D. 1980: Plio-pleistocene Bird Remains from the The Carpathian Basin. VI. Systematical and Geographical Catalogue. – *Aquila* 87, 9–22.

JÁNOSSY, D. 1981: Die altpleistozänen Vogelfaunen von Deutsch-Altenburg 2 und 4 (Niederösterreich). – *Beiträge zur Palaontologie von Österreich* 8, 375–391.

JÁNOSSY, D. 1983: Die mittelpleistozäne Vogelfauna von Přezletice bei Prag (ČSSR). In: Heinrich W.-D. (ed.): Wirbeltier-Evolution und Faunenwandel im Känozoikum. – *Schriftenreihe für Geologische Wissenschaften* 19–20, 247–269.

JÁNOSSY, D. 1986: *Pleistocene vertebrate faunas of Hungary*. Budapest: Akadémiai Kiadó & Amsterdam: Elsevier, pp. 208.

JÁNOSSY, D. 1991: Late Miocene bird remains from Polgárdi (W-Hungary). – *Aquila* 98, 13–35.

JÁNOSSY, D. 1992: Lower Pleistocene Bird Remains from Beremend (S-Hungary, Loc. 15. and 16.). – *Aquila* 99, 9–25.

JÁNOSSY, D. 1993: Bird remains from the Upper Miocene (MN9) of Rudabánya (N-Hungary). – *Aquila* 100, 53–70.

JÁNOSSY, D. 1995: A late Miocene avifauna from Polgárdi, western Hungary. *In:* Peters D.S. (ed.): *Acta palaeornithologica. – Courier Forschunsinstitut Senckenberg* 181, 203–206.

JÁNOSSY, D. & KORDOS, L. 1976: Az Osztramos gerinces lelőhelyeinek faunisztikai és karszt-morfológiai áttekintése (1974-ig). – *Fragmenta Mineralogica et Paleontologica* 8, 39–92.

JURCSÁK, T. & KESSLER, E. 1988. Evoluţia avifaunei pe teritoriul României (III). – *Crisia* 18: 647–688.

KESSLER, E. 1975: Contribuţii noi la studiul avifaunei fosile de la Betfia, jud. Bihor. – *Nymphaea.* 3, 53–59.

KESSLER J. 2009a: Új eredmények a Kárpát-medence neogén és negyedidőszaki madárvilágához, I. rész. [New results with regard to the Neogene and Quaternary Avifauna of the Carpathian basin. Part I.] – *Földtani Közlöny* 139/1, 67–82.

KESSLER J. 2009b: Új eredmények a Kárpát-medence neogén és negyedidőszaki madárvilágához II.rész. [New results with regard to the Neogene and Quaternary Avifauna of the Carpathian basin. Part II.] – *Földtani Közlöny* . 139/3, 251–271.

KESSLER, J. 2010: Új eredmények a Kárpát-medence neogén és negyedidőszaki madárvilágához, III.rész [New results with regard to the Neogene and Quaternary Avifauna of the Carpathian basin. Part III.] – *Földtani Közlöny*. 140/1, 53–72.

KESSLER, J. 2012–2013: A Kárpát-medence madárvilágának őslénytani kézikönyve. [Palaeornithological Handbook of birds fauna from Carpathian Basin]. Könyvmühely Kiadó Miskolc, 458 p.+ 48 Táblakép.

KESSLER J. & Hír, E. 2012: Észak-Magyarország madárvilága a miocénben II. rész. [The avifauna in North Hungary during the Miocene. Part II.] – *Földtani közlöny.* – 142/2, 149–168.

KESSLER, E. & Venczel, M 2009: Bird remains from the Middle Miocene of Subpiatră (W-Romania). – *Nymphaea, Folia naturae Bihariae* 36, 27–36 Oradea.

KESSLER, E. & Venczel, M 2011: A new passeriform bird from the Middle Miocene of Subpiatră (W-Romania). – *Nymphaea, Folia naturae Bihariae* , Oradea 38, 17–22.

KORDOS, L. 1991a: Mezőföld, Polgárdi, késő-miocén ősgerinces lelőhelyek [Late Miocene paleovertebrate

localities, Polgárdi, Mezőföld]. *Magyarország Geológiai Alapszelvényei*, MÁFI Kiadvány. pp. 1–6.

KORDOS, L, 1991b: Villányi-hegység, Villány, alsó-pleisztocén ősgerinces lelőhelyek. *Magyarország geológiai alapszelvényei,* MÁFI Kiadvány, pp. 1–6.

KORDOS, L. 2001: Beremendi alapszelvény. Gerinces őslénytani vizsgálatok, [Kézirat], MÁFI, Budapest.

KORDOS, L. 2004: *Beremend. Pliocén gerinces lelőhelyek.* Kirándulásvezető .7. Magyar Őslénytani Vándorgyülés. P. 54–57.

KORMOS, T. 1911: Die pliozäne Knochenfund bei Polgárdi (vorläufiger Bericht). – *Földtani Közlöny* 41, 171–189.

KORMOS, T. 1913: Kleinere Mitteilungen aus dem ungarischen Pleistocan. – *Centralblatt für Mineralogie, Geologie und Palaontologie* 1913: 13–17.

KRETZOI, M. 1952: Die Raubtiere der Hipparion-fauna von Polgárdi. – *Jahrbuch Ungarische Geological Anstalt*, 40, 1–12.

KRETZOI, M., 1956: A Villányi hegység alsó pleisztocén gerinces faunái. – *Geologica Hungarica. Series. Paleontologica*, 27: 1–264.

KRETZOI, M., 1962: A csarnótai fauna és faunaszint. – *A Magyar Állami Földtani Intézet Évi Jelentése az 1959. évről* pp. 297–395.

KRETZOI, M., 1969: A magyarországi quarter és pliocén szárazföldi biosztratigráfiájának vázlata. – Földrajzi Közlemények, 18 (3): 179–204.

KRETZOI, M. 1977: The fauna of small vertebrates of the Middle Pleistocene at Petralona. – *Anthropos* (Athena) 4, 131–143.

LAMBRECHT, K. 1912: Magyarország fossilis madarai. Die fossilen Vögel Ungarns. – *Aquila* 19, 288–320.

LAMBRECHT, K. 1916: Az első magyar preglaciális madárfauna. Die erste ungarische praglaziale Vogelfauna. – *Aquila* 22**,** 165–172.

LAMBRECHT, K. 1933: *Handbuch der Palaornithologie*. Bornträger Edit. Berlin. pp. 1024.

MALEZ, M. 1975: Ornitofauna iz kvartarnih naslaga velike pecine na ravnoj gori u sjeve-rozapadnoj Hrvatskoj. *Larus* 26/28: 45–54.

MALEZ, V. 1984: Paleornitološki ostaci iz kvartarnih naslaga nekih spilja Hrvatske i Slovenije. *In*: *Deveti jugoslavenski speleoloski kongres*, Zbornik predavanja: 711–719.

MALEZ, V. 1988: Pleistocenska ornitofauna iz spilje Vindije u sjevernozapadnoj Hrvatskoj. – *Rad Jugoslavenske Akademije Znanosti i Umjetnosti, Varazdin* 2: 31–203.

MALEZ-BAČIĆ V. 1979. Pleistocenska ornitofauna iz Šandalje u Istri te njezino stratigrafsko i paleoekološko značenje, – *Palaeontologia Jugoslavica* 21, 1–46.

MILNE-EDWARDS, A. 1869–1871. *Recherches anatomiques et paléontologiques pour servir àl'histoire des oiseaux fossiles de la France.* Vol. 2. Paris: G. Masson, 627 pp. + pls. 97.

MLÍKOVSKÝ J. 1989: Ptáci staršího a středního pleistocénu Československa: současný stav aperspektivy výzkumu In: SEITL, L. (ed.): *Současný stav a perspektivy331výzkumu kvartéru v ČSSR* . 63–67. Brno: Moravské muzeum & Universita J.E. Purkyně.

MLÍKOVSKÝ, J. 1995: Early Pleistocene birds of Stránská skála: 1. Musil's talus cone. In: MUSIL, R. (ed.): Stránská skála Hill: Excavations of open-air sediments 1964–1972. – *Anthropos (Brno)* 26, 111–126.

MLÍKOVSKÝ, J. (ed.) 1996. Tertiary avian localities of Europe. – *Acta Universitatis Carolinae, Geologica.* 39, 517–848.

MLÍKOVSKÝ, J. 1998. Early Pleistocene birds of Deutsch-Altenburg, Austria. – *Acta Societatis Zoologicae Bohemicae* 62:135–141.

MLÍKOVSKÝ, J. 2002: *Cenozoic Birds of the World. Part 1*: *Europe.* Ninox Press, Praha, 407 pp.

MLÍKOVSKÝ, J. 2009: Middle Pleistocene birds of Hundsheim, Austria. – *Journal of the National Museum (Prague), Natural History Series* 177 (7): 69–82.

MONTOYA, P. ET AL. 1999: La fauna del Pleistoceno inferior de la Sierra de Quibas (Abanilla,Murcia). – *Estudios Geológicos* 55, 127–161.

MONTOYA, P. ET AL. 2001: Une faune très diversifiée du Pléistocène inférieur de la Sierra de Quibas (province de Murcia, Espagne). – *Comptes Rendus de l'Académie des Sciences(Paris), Sciences de la Terre et des Planètes* 332, 387–393.

MOURER-CHAUVIRÉ, C. 1975: Les oiseaux du Pléistocène moyen et supérieur de France. – *Documents des Laboratoires de Géologie de la Faculté des Sciences de Lyon* 64, 1–624.

MOURER-CHAUVIRÉ, C. 1995: Dynamics of the avifauna during the Paleogene and the Early Neogene of France. Settling of the recent fauna. – *Acta Zoologica Cracoviensia* 38(3): 325–342.

MOURER-CHAUVIRÉ C., HUGUENEY M. & JONET P. 1989: Découverte de Passeriformes dans l'Oligocène supérieur de France. – *Comptes Rendus Hebdomadaires de l'Académie des Sciences (Paris), Sciences de la Terre et des Planètes* 309, 843–849.

NORIEGA, J. I. & CHIAPPE, L. 1993: An Early Miocene Passeriform from Argentina. – *The Auk* 110(4), 936–938.

PONGRÁCZ, L. 1999: A beremendi Szőlő-hegy természettudományi kutatásának 150 éve. *PeténYi emlékkönyv*. Beremend.

PORTIS, A. 1887: Contribuzioni alla ornitolitologia italiana. Parte II. – *Memorie Regia Accademia Scienze (Torino)* (2) 38, 181–203.

SONDAAR, P.Y., MCMINN M., SEGUÍ, B. & ALCOVER J.A. 1995: Interès paleontològic del jaciments càrstic de les Gimnésies i les Pitiüses. – *Endins* **20**, 155–170

ŠVEC, P. 1985: In: FEJFAR O. & HEINRICH W.-D. (Eds,) 1985: Zur Bedeutung der Wirbeltier fundstätten von Ivanovce und Hajnáčka für die Säugetierpaläontologie im Pliozän und frühen Pleistozän in Europa:Kentnisstand und Probleme. – *Věstník Ústředního Ústavu Geologického* 60, 213–224.

TCHERNOV, E. 1980: The Pleistocene Birds of Ubeidiya, JordanValley. In: *The Pleistocene of the Central Jordan Valley.The excavation at Ubeidiya.* The Israel Acad. of Sci.,Humanities, Jerusalem, 1–83.

TYRBERG T. 1998: *Pleistocene birds of the Palearctic: a catalogue*. Cambridge, Mass.: Nuttall Ornithological Club, ix + pp. 720.

VILLALTA, J. F. de 1963. Las aves fósiles del Mioceno español. – *Boletín de la Real Sociedad Española de Historia Natural Geología* 61: 263–285

ZELENKOV, N. 2011: *Neogene Birds of Central Asia.* Ph. D. Thesis, Paleontological Institute, RAN, Moscow, 1–304.

ZELENKOV, V.N. & KUROCHKIN, E.N. 2012: The first representative Pliocene assemblages of passerine birds

in Asia (Northern Mongolia and Russian Transbaikalia). – *Geobios* 45 (2012) 323–334

VOJINSTVENS'KYJ M. A. 1967: Iskopaemaja ornitofauna Ukrainy. – *Prirodnaja Obstanovka i Fauny Prošlogo* 3**,** 3–76.

Table 2. Species from Polgárdi localities (sp.foss= extinct species; sp.end. = endemic extinct species)

Taxa	Sp. foss.	Sp. end.	Capek (KORMOS, 1911)	JÁNOSSY 1991, 1995	KESSLER 2009a,b 2010	KESSLER in this paper	Polgárdi 2/4/5
Egretta polgardiensis	x	x			x		4
Anas albae	x	x	x	x			2
A. clypeata					x		4
Anatidae indet.					x		4,5
Buteo sp.					x		4
Falco cherrug					x		4
F. tinnunculus atavus	x				x		5
Palaeocryptonix hungaricus	x	x	x	x			2,4,5
Pavo arhiaci	x		x	x	x		2,4,5
Palaeortyx gallica	x				x		4,5
P. brevipes	x				x		4,5
Galliformes indet.	x				x		4,5
Porzana estramosi veterior	x	x		x			4,5
P. estramosi	x				x		4,5
P. kretzoii	x	x			x		4,5
Rallicrex polgardiensis	x	x		x	x		4,5
Otis khosiatzki	x			x			5
O. kalmani	x				x		4
Gallinago sp.				x			4
G. veterior	x				x		4
Limosa sp.					x		5
Tringa sp.				x	x		4
Cursorius sp.				x			4
Calidris janossyi	x	x			x		5
Charadrius lambrechti	x	x			x		4
Tyto campiterrae	x	x		x	x		4,5
Athene noctua veta	x		x		x		4
Surnia robusta	x				x		4,5
Cuculus pannonicus	x	x			x		4
Apus baranensis	x				x		4
Chaetura baconica	x			x	x		4,5
Alauda tivadari	x	x				x	4
Calandrella gali	x	x				x	4,5
Lullula minor	x	x				x	4,5
Hirundo gracilis		x					4,5
Delichon polgardiensis		x					5
Riparia minor		x					4
Corvus sp.				x	x		4
C. pliocaenus	x				x		5
Miocorvus larteti	x				x		4
Motacilla sp.				x	x		5
M. intermedia	x	x				x	4,5
Anthus sp.					x		4
A. hiri	x	x				x	5
Bombycilla sp.						x	4,5
B. brevia	x	x				x	5

Taxa	Sp. foss.	Sp. end.	Capek (KORMOS, 1911)	JÁNOSSY 1991, 1995	KESSLER 2009a,b 2010	KESSLER in this paper	Polgárdi 2/4/5
Cinclus gaspariki	x	x				x	5
Troglodytes sp.	x	x				x	4
T. robustus	x	x				x	4,5
Turdus sp.				x	x		4,5
T. polgardiensis	x	x				x	5
T.miocaenicus	x	x				x	5
Turdicus pannonicus	x	x				x	4,5
Prunella sp.					x		4
P. freudenthali	x	x				x	5
Luscinia sp.				x	x		4
L. denesi	x	x				x	4
Muscicapa miklosi	x	x				x	4
Saxicola lambrechti	x	x				x	4,5
Oenanthe kormosi	x	x				x	5
Muscicapiidae sp. indet.					x		5
Tichodroma capeki	x	x				x	4
Certhia sp.					x		4
Sitta sp.					x		5
S. gracilis	x	x				x	4
Aegithalos gaspariki	x	x				x	4,5
Acrocephalus sp.1.				x			5
A. sp.2				x			4
A. sp.					x		4
A. major	x	x				x	4
A. minor	x	x				x	4
Hippolais veterior	x	x				x	4
Cettia sp.				x			4
C. janossyi	x	x				x	4
Sylvia sp.				x			4
S. intermedia	x	x				x	4
Locustella kordosi	x	x				x	4,5
Phylloscopus venczeli	x	x				x	4
Lanius sp.			x	x	x		2,5
L.capeki	x	x				x	4
Sturnus sp.					x		4
S. brevis	x	x				x	4,5
Passer hiri	x	x				x	4
Fringiilidarum indet.				x	x		5
Fringilla kormosi	x	x				x	4,5
Carduelis kretzoii	x	x				x	4,5
C. lambrechti	x	x				x	4
Pyrrhula gali	x	x				x	5
Emberizidae indet.					x		5
Emberiza polgardiensis	x	x				x	4,5
E. pannonica	x	x				x	4,5
Plectrophenax veterior	x	x				x	4
Passeriformes indet.					x	x	4
Aves indet.			x		x	x	2,4,5

Table 3.Species from Csarnóta localities (subsp.= subspecies; sp.foss= extinct species; sp.end. = endemic extinct species)

Taxa	subsp.	sp.foss.	sp.end.	JÁNOSSY 1969, 79	KESSLER 2009, 10	KESSLER in this paper	Csarnóta 2,4.
Podiceps csarnoanus		x	x		x		2
Anas albae		x					2.15
Falco tinnunculus atavus	x	x			x		2
Palaeortyx brevipes		x			x		2,18; 2.21;
Gallus beremendensis		x			x		2
Francolinus capeki		x		x			2
Tetrao paeurogallus		x		x			2
T. partium		x			x		4
Rallicrex polgardiensis		x		x	x		2.15
Porzana kretzoii		x	x		x		2
Otis kalmani		x			x		2
Galinago veterior		x		x			2
Cuculus csarnotanus		x	x	x			2
Bubo bubo				x			2
Aegolius sp.				x			2
Glaucidium baranensis		x	x		x		2.13; 2.24;
Athene noctua veta	x	x			x		2.2
Apus baranensis		x			x		2
Garrulus glandarius				x			2
Pyrrhocorax graculus vetus	x	x		x			2
Corvus harkanyensis		x	x		x		2
Miocorvus larteti		x			x		2
Pica pica major	x	x			x		2
Galerida pannonica		x	x			x	2.22
Lullula parva		x	x			x	2.10
Hirundo major		x	x	x	x	x	2.22
Delichon pusillus		x	x			x	2.21
Aegithalos congruis		x	x			x	2.21
Parus robustus		x	x			x	2.16
P. parvulus		x	x			x	2
Sitta pussila		x	x	x	x	x	2.21
Certhia immensa		x	x		x	x	2.21
Saxicola baranensis		x	x		x	x	2
S. parva		x	x		x	x	2
Phoenicuros erikai		x	x		x	x	2
Oenanthe pongraczi		x	x		x	x	2
Turdus major		x	x	x	x	x	2
T. medius		x	x		x	x	2.17
T. minor		x	x		x	x	2.17
Turdoides borealis		x		x			2
Cettia kalmani		x	x			x	2
Acrocephalus kretzoii		x	x			x	2.17
A. kordosi		x	x			x	2
Sylvia pussila		x	x		x	x	2.18
Locustella janossyi		x	x			x	2.21
Phylloscopus pliocaenicus		x	x			x	2
Bombycilla sp.		?			x		2
Anthus baranensis		x	x			x	2

Taxa	subsp.	sp.foss.	sp.end.	JÁNOSSY 1969, 79	KESSLER 2009, 10	KESSLER in this paper	Csarnóta 2,4.
Cinclus minor		x	x		x	x	2
Prunella kormosi		x	x		x	x	2
Lanius hungaricus		x	x		x	x	2.10
Passer minusculus		x	x			x	2
Carduelis parvulus		x	x		x	x	2
C. medius		x	x		x	x	2
Pyrrhula minor		x	x		x	x	2
Fringilla petényii		x	x		x	x	2
Loxia csarnotanus		x	x		x	x	2
Pinicola kubinyii		x	x		x	x	2.06
Emberiza media		x	x		x	x	2
E. parva		x	x		x	x	2
Passeriformes indet.		?			x	x	2
Aves indet.		?			x	x	2

Table 4. Species from Beremend localities (subsp.= extinct subspecies; sp.foss= extinct species; sp.end. = endemic extinct species; Obs. Csarnóta= Species indentificate also from Csarnóta)

Taxa	ssp. foss.	sp. foss.	sp. end.	KESSLER 2009a,b	KESSLER 2010	KESSLER 2012 and in this paper	Obs. Csarnóta
Podiceps sp.				x			
Egretta sp.				x			
Accipiter sp.				x			
Falco tinnunculus atavus	x			x			
Falco sp.				x			
Tetrao praeurogallus		x		x			
Tetrao partium		x		x			
Gallus beremendensis		x		x			
Francolinus capeki		x		x			
Palaeocryptonix hungaricus		x		x			
Perdix perdix jurcsaki	x			x			
Rallicrex polgardiensis		x		x			
Miorallus major		x		x			
Porzana sp.				x			
Otis lambrechti		x		x			
Otis kalmani		x		x			
Tringa sp.				x			
Chlidonias sp.				x			
Columba sp.				x			
Glaucidium baranensis		x		x			
Athene noctua veta	x			x			
Strix intermedia		x		x			
Picus pliocaenicus		x	x			X (2012)	
Dendrocopus praemedius		x				X (2012)	
Melanocorypha minor		x	x			x	
Galerida pannonica		x				x	x
Lullula parva		x				x	x
Lullula minuscula		x	x			x	
Delichon major		x	x			x	
Corvus pliocaenus		x			X		
Corvus sp.					X		

Taxa	ssp. foss.	sp. foss.	sp. end.	KESSLER 2009a,b	KESSLER 2010	KESSLER 2012 and in this paper	Obs. Csarnóta
Miocorvus larteti		x			X		
Pica pica major	x				X		
Nucifraga sp.					X		
Parus robustus		x				x	x
Parus medius		x	x			x	
Sitta villanyensis		x	x			x	
Muscicapa petényii		x	x			x	
Luscinia pliocaenica		x	x			x	
Phoenicurus baranensis		x	x			x	
Oenanthe pongraczi		x				x	x
Saxicola baranensis		x				x	x
Saxicola magna		x	x			x	
Erithacus minor		x	x			x	
Monticola pongraczi		x	x			x	
Turdus major		x				x	x
Turdus medius		x				x	x
Turdus minor		x				x	x
Oriolus beremendensis			x			x	
Acrocephalus kretzoii						x	x
Sylvia pusilla						x	x
Locustella magna			x			x	
Locustella janossyi			x			x	x
Regulus pliocaenicus			x			x	
Motacilla minor			x			x	
Motacilla robusta			x			x	
Bombycilla kubinyii			x			x	
Prunella kormosi						x	x
Lanius major			x			x	
Lanius intermedius			x			x	
Sturnus pliocaenicus			x			x	
Sturnus baranensis			x			x	
Passer pannonicus			x			x	
Coccothraustes major			x			x	
Loxia csarnotanus						x	x
Emberiza gaspariki			x			x	

Plate I

Figure 1 A. *Alauda* † *tivadari* nova sp. – coracoid dext. (Polgárdi, MÁFI V.11.63.1; V.29138), caudal view, a. *acrocoracoid*; b. *processus accesorius*; c. *sulcus m. supracoracoidei*; d. *facies aricularis humeralis*; e. *processus procoracoidei*.

Figure 1 B. *Alauda* † *tivadari* nova sp. – tibiotarsus sin. (Polgárdi, MÁFI V.11.801; V.29155), cranial view, a. *tuberositas retinaculi m. fibularis*; b. *sulcus extensorius*; c. *pons supratendineus*; d. *condylus lateralis*; e. *incisura intercondylaris*; f. *condylus medialis.*

Figure 2A. *Galerida* † *pannonica* nova sp. – humerus sin. (Beremend, BKA), cranial view: a. *tuberculum supracondylare ventrale*; b. *epicondylus ventralis*; c. *processus flexorius*; d. *condylus ventralis*; e. *incisura intercondylaris*; f. *condylus dorsalis*; g. *epicondylus dorsalis*; h. *processus supracondylaris dorsalis.*

Figure 2 B. *Galerida* † *pannonica* nova sp. – carpometacarpus sin. (Beremend, BKA), ventral view: a. *trochlea carpalis*; b. *proc. extensorius*; c. *processus alularis*; d. *fovea subalularis*; e. *protuberantia metacarpalis;* f. *facies arrticularis digiti major.*

Figure 2 C. *Galerida* † *pannonica* nova sp. – tibiotarsus sin. (Csarnóta, MÁFI V.11.13.1; V.29088). cranial view, a. *tuberositas retinaculi m. fibularis*; b. *sulcus extensorius*; c. *pons supratendineus*; d. *condylus lateralis*; e. *incisura intercondylaris*; f. *condylus medialis.*

Figure 2 D *Galerida* † *pannonica* nova sp. – tarsometatarsus sin. (Beremend, BKA), dorsal view: a. *trochlea metatarsi* II.; b. *incisura intertrochlearis medialis*; c. *trochlea metatarsi* III.; d. *incisura intertrochlearis lateralis*; e. *trochlea* metatarsi IV.

Figure 3 A. *Lullula* † *minor* nova sp. – humerus sin. (Polgárdi, MÁFI V.11.81.2; V.29156/1), cranial view, a. *tuberculum ventrale*; b. *epicondylus ventralis*; c. *processus flexorius*; d. *condylus ventralis*; e. *incisura intercondylaris*; f. *condylus dorsalis*; g. *epicondylus dorsalis*; h. *processus supracondylaris ventralis.*

Figure 3 B. *Lullula* † *minor* nova sp. – ulna sin. (Polgárdi, MÁFI V.11.93.1; V.29168), cranial view, a. *oleocranon*; b. *cotyla dorsalis*; c. *cotyla ventralis*; d. *tuberculum lig. colat. ventralis*; e. *depressio m. brachialis*.

Figure 3 C. *Lullula* † *minor* nova sp. – ulna sin. (Polgárdi, MÁFI V.11.93.1; V.29168), medial view, f. *condylus dorsalis*; g. *sulcus intercondylaris*; h. *condylus ventralis*; i. *tuberculum carpale.*

Figure 3 D. *Lullula* † *minor* nova sp. – tarsometatarsus sin. (Polgárdi, MÁFI V.11.81.2; V.29156/2), dorsal view, a. *trochlea metatarsi* II.; b. *incisura intertrochlearis lateralis*; c. *trochlea metatarsi tertii*; d. *incisura intertrochlearis medialis*; e. *trochlea metatarsi* IV.

Plate I

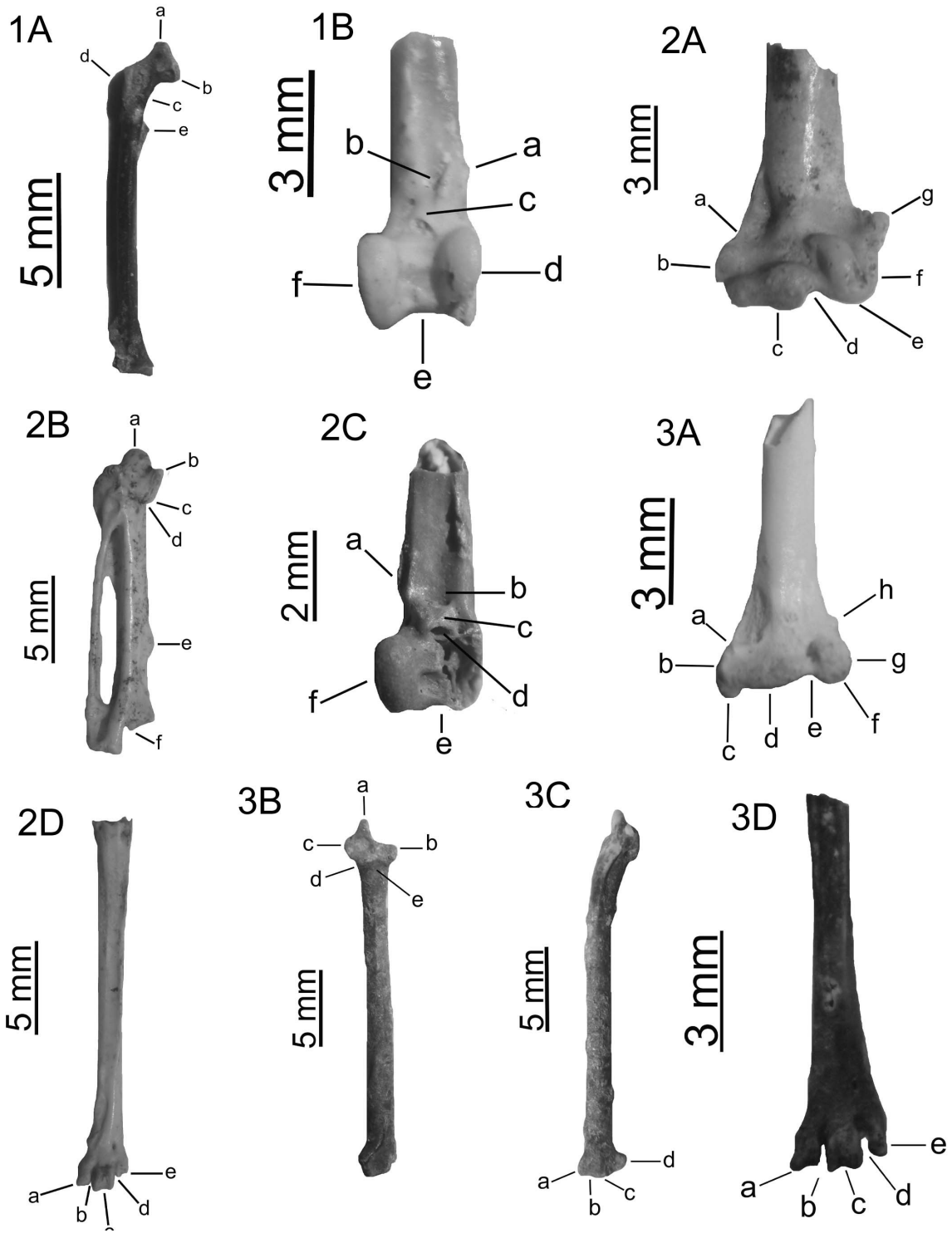
1A
5 mm
1B
3 mm
2A
3 mm
2B
5 mm
2C
2 mm
3A
3 mm
2D
5 mm
3B
5 mm
3C
5 mm
3D
3 mm

Plate II

Figure 4A. *Lullula* † *parva* nova sp. – humerus dext. (Beremend, BKA), caudal view: a. *tuberculum dorsale*; b. *caput humeri*; c. *tuberculum ventrale*; d. *crista bicipitalis*; e. *crus fossae*; f. *fossae pneumotricipitalis*.

Figure 4 B. Lullula † parva nova sp. – humerus dext. (Beremend, BKA), cranial view: g. tuberculum supracondylare ventrale; h. epicondylus ventralis; i. processus flexorius; j. condylus ventralis; k. incisura intercondylaris; l. condylus dorsalis; m. epicondylus dorsalis; n. processus supracondylaris dorsalis.

Figure 4 C. *Lullula* † *parva* nova sp. – tibiotarsus sin. (Csarnóta, MÁFI V.11.20.1; V.29095), cranial view, a. *tuberositas retinaculi m. fibularis*; b. *sulcus extensorius*; c. *pons supratendineus*; d. *condylus lateralis*; e. *incisura intercondylaris*; f. *condylus medialis.*

Figure 5 A. *Lullula* † *minuscula* nova sp. – humerus dext. (Beremend, BKA), caudal view: a. *tuberculum dorsale*; b. *caput humeri*; c. *tuberculum ventrale*; d. *crista bicipitalis*; e. *crus fossae*; f. *fossae pneumotricipitalis*.

Figure 5 B. *Lullula* † *minuscula* nova sp. – humerus dext. (Beremend, BKA), cranial view: f. *tuberculum supracondylare ventrale*; g. *epicondylus ventralis*; h. *processus flexorius*; i. *condylus ventralis*; j. *incisura intercondylaris*; k. *condylus dorsalis*; l. *epicondylus dorsalis*; m. *processus supracondylaris dorsalis.*

Figure 6 A. *Calandrella* † *gali* nova sp. – coracoid dext. (Polgárdi, MÁFI V.11.109.1; V.29184), dorsal view, a. *acrocoracoid*; b. *processus accesorius*; c. *sulcus m. supracoracoidei*; d. *facies aricularis humerális*; e. *processus procoracoidei*.

Figure 6 B. *Calandrella* † *gali* nova sp. – humerus sin. (Polgárdi, MÁFI V.11.65.1; V.29140), caudal view, a. *tuberculum dorsale*; b. *caput humeri*; c. *tuberculum ventrale*; d. *crista bicipitalis*; e. *crus fossae*; f. *fossae pneumotricipitalis*.

Figure 6 C. *Calandrella* † *gali* nova sp. – humerus sin. (Polgárdi, MÁFI V.11.65.1; V.29140), cranial view, g. *epicondylus ventralis*; h. *processus flexorius*; i. *condylus ventralis*; j. *incisura intercondylaris*; k. *condylus dorsalis*; l. *epicondylus dorsalis*; m. *processus supracondylaris dorsalis.*

Figure 4 D. *Calandrella* † *gali* nova sp. – tibiotarsus dext. (Polgárdi, MÁFI V.11.127.1; V.29202), cranial view, a. *tuberositas retinaculi m. fibularis*; b. *sulcus extensorius*; c. *pons supratendineus*; d. *condylus lateralis*; e. *incisura intercondylaris*; f. *condylus medialis.*

Plate II

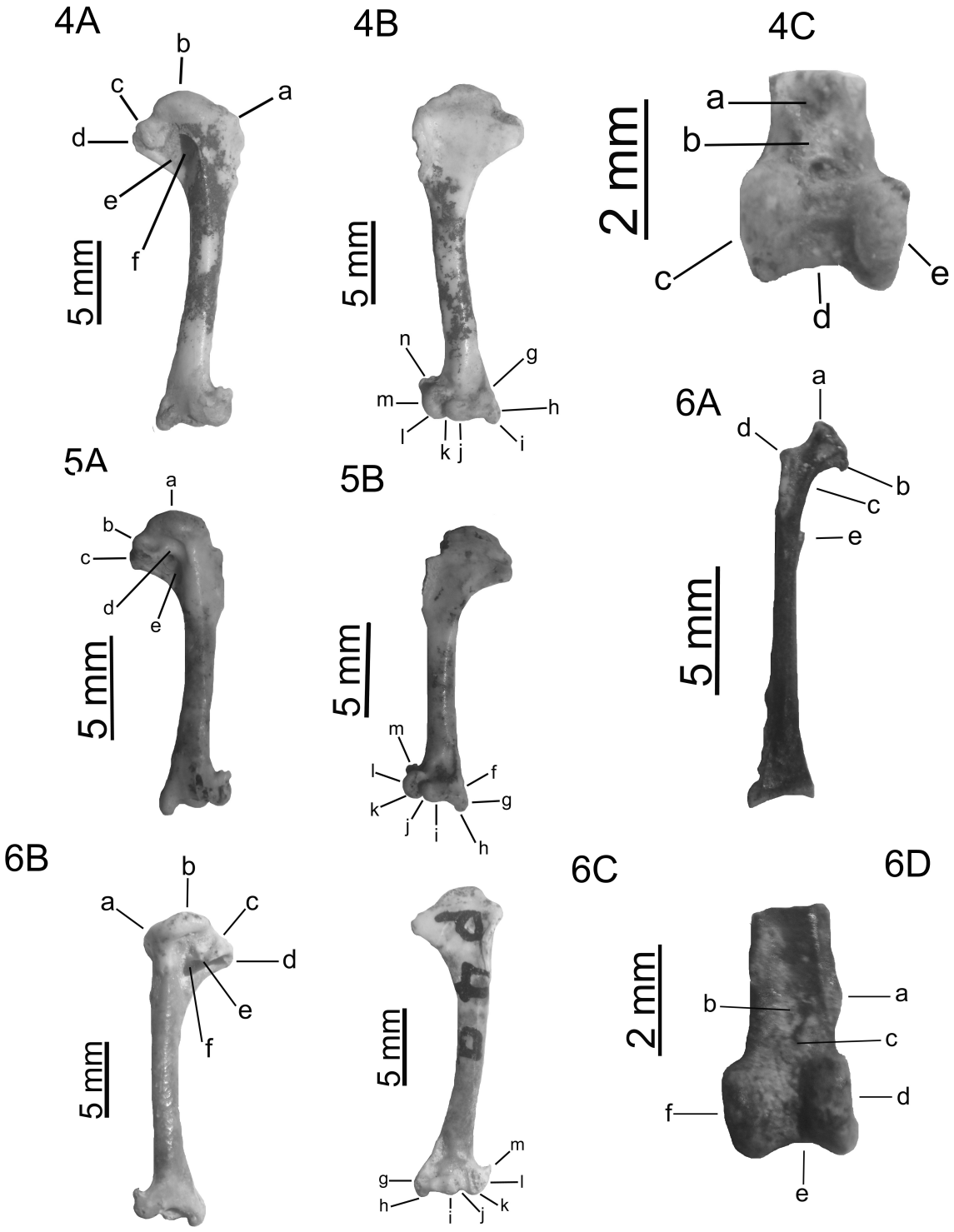
4A
b
c
a
d
e
f
5 mm
4B
5 mm
n
g
m
h
l
k j
i
4C
2 mm
a
b
c
e
d
5A
a
b
c
d
e
5 mm
5B
5 mm
m
l
f
k
g
j
i
h
6A
a
d
b
c
e
5 mm
6B
b
a
c
d
e
f
5 mm
6C
5 mm
m
g
l
h
i
j
k
6D
2 mm
b
a
c
f
d
e

Plate III

Figure 7 A. *Melanocorypha † minor* nova sp. – humerus sin. (Beremend, BKA), caudal view: a. *tuberculum dorsale*; b. *caput humeri*; c. *tuberculum ventrale*; d. *crista bicipitalis*; e. *crus fossae*; f. *fossae pneumotricipitalis*.

Figure 7 B. *Melanocorypha † minor* nova sp. – humerus sin. (Beremend, BKA), cranial view: g. *tuberculum supracondylare ventrale*; h. *epicondylus ventralis*; i. *processus flexorius*; j. *condylus ventralis*; k. *incisura intercondylaris*; l. *condylus dorsalis*; m. *epicondylus dorsalis*; n. *processus supracondylaris dorsalis.*

Figure 8 A. *Hirundo † gracilis* nova sp. – left side ulna (Polgárdi, MÁFI V.11.97.1; V.29172), cranial view, a. *cotyla ventralis*; b. *tuberculum lig. colat. ventralis*.

Figure 8 B. *Hirundo † gracilis* nova sp. – right side ulna (Polgárdi, MÁFI V.11.82.1; V.29157), medial view, c. *condylus dorsalis*; d. *sulcus intercondylaris*; e. *condylus ventralis*; f. *tuberculum carpale.*

Figure 9 A. *Hirundo † major* nova sp. – ulna dext. (Csarnóta, MÁFI V.11.14.1; V.29089/1), medial view, a. *condylus dorsalis*; b. *sulcus intercondylaris*; c. *condylus ventralis*; d. *tuberculum carpale.*

Figure 9 B. *Hirundo † major* nova sp. – tibiotarsus dext. (distal fragment) (Csarnóta, MÁFI V.11.14.2; V.29089/2), cranial view, a. *tuberositas retinaculi m. fibularis*; b. *sulcus extensorius*; c. *pons supratendineus*; d. *condylus lateralis*; e. *incisura intercondylaris*; f. *condylus medialis.*

Figure 10 A. *Delichon † polgardiensis* nova sp. – coracoid dext. (Polgárdi, MÁFI V.11.94.1; V.29169),), dorsal view, a. *acrocoracoid*; b. *processus accesorius*; c. *sulcus m. supracoracoidei*; d. *processus procoracoidei*.

Figure 10 B. *Delichon † polgardiensis* nova sp. – ulna sin. (Polgárdi, MÁFI V.11.118.5; V.29193/1–5), medial view, a. *condylus dorsalis*; b. *sulcus intercondylaris*; c. *condylus ventralis*; d. *tuberculum carpale.*

Figure 11. *Delichon † pusillus* nova sp. – carpometacarpus sin. (Csarnóta, MÁFI V.11.21.1; V.29096), ventral view, a. *trochlea carpalis*; b. *proc. extensorius*; c. *processus alularis*; d. *fovea subalularis*; e. *protuberantia metacarpalis.*

Figure 12. *Delichon † major* nova sp. – carpometacarpus dext. (Beremend, BKA), ventral view: a. *trochlea carpalis*; b. *proc. extensorius*; c. *processus alularis*; d. *fovea subalularis*; e. *protuberantia metacarpalis;* f. basis of the *metacarpus majus.*

Plate III

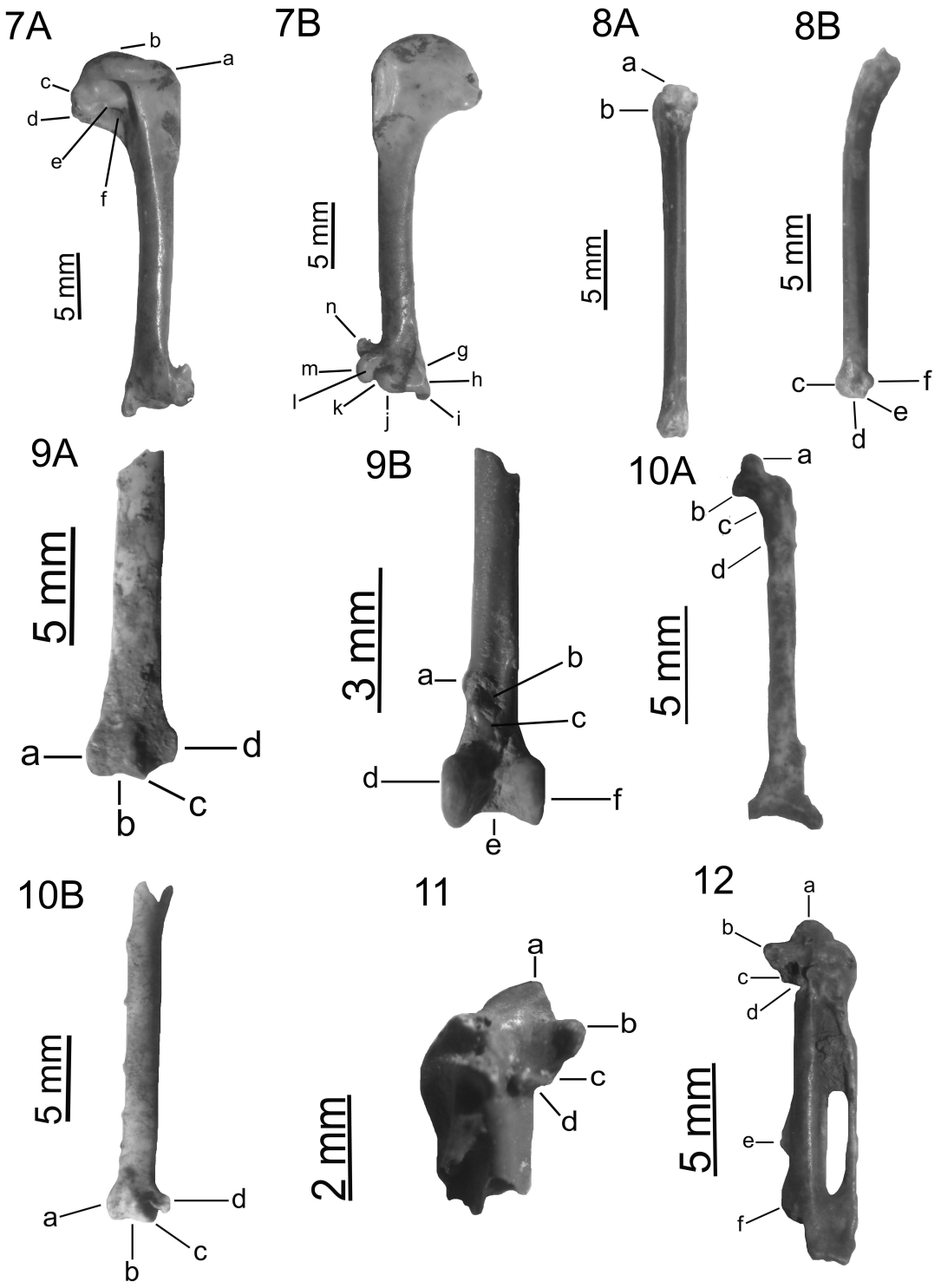
7A
b
a
c
d
e
f
5 mm
7B
5 mm
n
g
m
h
l
k
j
i
8A
a
b
5 mm
8B
5 mm
c
f
e
d
9A
5 mm
a
d
b
c
9B
3 mm
a
b
c
d
f
e
10A
a
b
c
d
5 mm
10B
5 mm
a
d
b
c
11
a
b
c
d
2 mm
12
a
b
c
d
e
f
5 mm

Plate IV

Figure 13 A. *Riparia †minor* nova sp. – coracoid sin. (Polgárdi, MÁFI V.11.66.1; V.29141), dorsal view, a. *acrocoracoid*; b. *processus accesorius*; c. *sulcus m. supracoracoidei*; d. *processus procoracoidei;* e. *facies articularis humeralis.*

Figure 13 B. *Riparia †minor* nova sp. – ulna sin. (Polgárdi, MÁFI V.1.83.4; V.29158/1–4), cranial view, a. *cotyla ventralis*; b. *cotyla dorsalis*; c. *tuberculum lig. colat. ventralis*; d. *tuberculum biccipitale*; e. *incisura radialis*; f. *depressio m. brachialis*.

Figure 13 C. *Riparia †minor* nova sp. – ulna dext. (Polgárdi, MÁFI V.1.83.4; V.29158/1–4), medial view, g. *condylus dorsalis*; h. *sulcus intercondylaris*; i. *condylus ventralis*; j. *tuberculum carpale.*

Figure 14 A. *Aegithalos †gaspariki* nova sp. – humerus sin. (Polgárdi, MÁFI V.11.76.1; V.29151), caudal view, a. *tuberculum dorsale*; b. *caput humeri*; c. *tuberculum ventrale*; d. *crista bicipitalis*; e. *crus fossae*; f. *fossae pneumotricipitalis*.

Figure 14 B. *Aegithalos †gaspariki* nova sp. – carpometacarpus dext. (Polgárdi, MÁFI V.11.90.1; V.29165), ventral view, a. *trochlea carpalis*; b. *proc. extensorius*; c. *processus alularis*; d. *fovea subalularis*; e. *protuberantia metacarpalis.*

Figure 15 A. *Aegithalos † congruis* nova sp. – coracoideum dext. (Csarnóta, MÁFI V.11.46.1; V.29121), dorsal view, a. *acrocoracoideum*; b. *processus accesorius*; c. *sulcus m. supracoracoidei*; d. *processus procoracoidei*.

Figure 15 B. *Aegithalos † congruis* nova sp. – tibiotarsus dextr (MÁFI V.11.15.1; V.29090), cranial view, a. *tuberositas retinaculi m. fibularis*; b. *sulcus extensorius*; c. *pons supratendineus*; d. *condylus lateralis*; e. *incisura intercondylaris*; f. *condylus medialis.*

Figure 16 A. *Parus † robustus* nova sp. – humerus dext. (Beremend, BKA), caudal view: a. *tuberculum dorsale*; b. *caput humeri*; c. *tuberculum ventrale*; d. *crista bicipitalis*; e. *crus fossae;* f. *fossae pneumotricipitalis*.

Figure 16 B. *Parus † robustus* nova sp. – humerus dext. (Beremend, BKA), cranial view: g. *tuberculum supracondylare ventrale*; h. *epicondylus* vedntralis; i. *processus flexorius*; j. *condylus ventralis*; k. *incisura intercondylaris*; l. *condylus dorsalis*; m. *epicondylus dorsalis*; n. *processus supracondylaris dorsalis.*

Figure 16 C. *Parus † robustus* nova sp. – ulna sin. (Csarnóta, MÁFI V.11.16.1; V.29091) caudal view, a. *condylus dorsalis*; b. *sulcus intercondylaris*; c. *condylus ventralis*; d. *tuberculum carpale.*

Figure 16 D. *Parus † robustus* nova sp. – carpometacarpus dext. (Csarnóta, MÁFI V.11.47.2; V.29122), ventral view, a. *trochlea carpalis*; b. *proc. extensorius*; c. *processus alularis*; d. *fovea subalularis*; e. *protuberantia metacarpalis.*

Plate IV

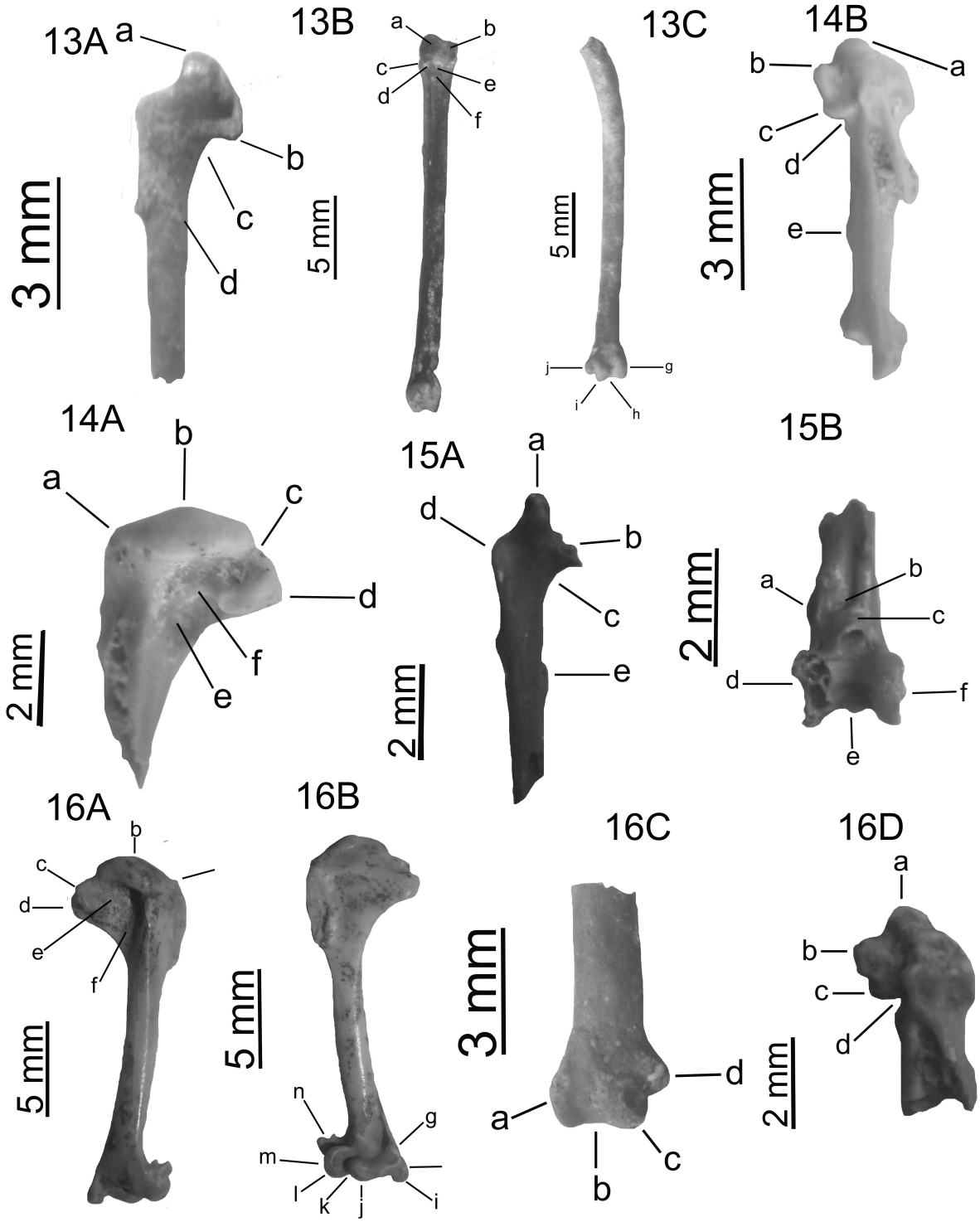
13A
a
b
c
d
3 mm
13B
a
b
c
d
e
f
5 mm
13C
5 mm
j
g
i
h
14B
b
a
c
d
e
3 mm
14A
b
a
c
d
f
e
2 mm
15A
a
d
b
c
e
2 mm
15B
a
b
c
d
f
e
2 mm
16A
b
c
d
e
f
5 mm
16B
5 mm
n
g
m
l
k
j
i
16C
3 mm
d
a
c
b
16D
a
b
c
d
2 mm

Plate V

Figure 17. *Parus* † *parvulus* nova sp. – coracoideum sin. (Csarnóta, MÁFI V.11.17.1; V.29092), dorsal view, a. *acrocoracoideum*; b. *processus accesorius*; c. *sulcus m. supracoracoidei*; d. *processus procoracoidei*.

Figure 18 A. *Parus* † *medius* nova sp. – humerus dext. (Beremend, BKA), caudal view: a. *tuberculum dorsale*; b. *caput humeri*; c. *tuberculum ventrale*; d. *crista bicipitalis*; e. *fossae pneumotricipitalis*.

Figure 18 B. *Parus* † *medius* nova sp. – humerus dext. (Beremend, BKA), cranial view: f. *tuberculum supracondylare ventrale*; g. *epicondylus ventralis*; h. *processus flexorius*; i. *condylus ventralis*; j. *incisura intercondylaris*; k. *condylus dorsalis*; l. *epicondylus dorsalis*; m. *processus supracondylaris dorsalis.*

Figure 19. *Sitta* †*gracilis* nova sp. – carpometacarpus sin. (Polgárdi, V.11.60.1; V.29135), ventral view, a. *trochlea carpalis*; b. *proc. extensorius*; c. *processus alularis*; d. *fovea subalularis.*

Figure 20 A. *Sitta* † *pusilla* nova sp. – carpometacarpus dext. (Csarnóta, MÁFI V.11.34.1; V.29109). ventral view, a. *trochlea carpalis*; b. *proc. extensorius*; c. *processus alularis*; d. *fovea subalularis*; e. *protuberantia metacarpalis.*

Figure 20 B. *Sitta* † *pusilla* nova sp. – tarsometatarsus sin. (Csarnóta, MÁFI V.11.53.3; V.29128), dorsal view, a. *trochlea metatarsi* II.; b. *incisura intertrochlearis medialis*; c. *trochlea metatarsi* III.; d. *incisura intertrochlearis lateralis*; e. *trochlea* metatarsi IV.

Figure 21. *Sitta* † *villanyensis* nova sp. – carpometacarpus dext. (Beremend, BKA), ventral view: a. *trochlea carpalis*; b. *proc. extensorius*; c. *processus alularis*; d. *fovea subalularis*; e. *protuberantia metacarpalis;* f. basis of the *metacarpus majus;* g. end of the *os metacarpi minus.*

Figure 22 A. *Certhia* † *immensa* nova sp. – coracoideum dext. (Csarnóta, MÁFI V.11.22.1; V.29097), dorsal view, a. *acrocoracoideum*; b. *processus accesorius*; c. *sulcus m. supracoracoidei*; d. *processus procoracoidei*.

Figure 22 B. *Certhia* † *immensa* nova sp. – carpometacarpus dext. (Csarnóta, MÁFI V.11.42.3; V.29117), ventral view, a. *trochlea carpalis*; b. *proc. extensorius*; c. *processus alularis*; d. *fovea subalularis*; e. *protuberantia metacarpalis.*

Figure 22 C. *Certhia* † *immensa* nova sp. – tarsometatarsus sin. (Csarnóta, MÁFI V.11.42.4; V.29117). dorsal view, a. *trochlea metatarsi* II.; b. *incisura intertrochlearis medialis*; c. *trochlea metatarsi* III.; d. *incisura intertrochlearis lateralis*; e. *trochlea* metatarsi IV.

Plate V

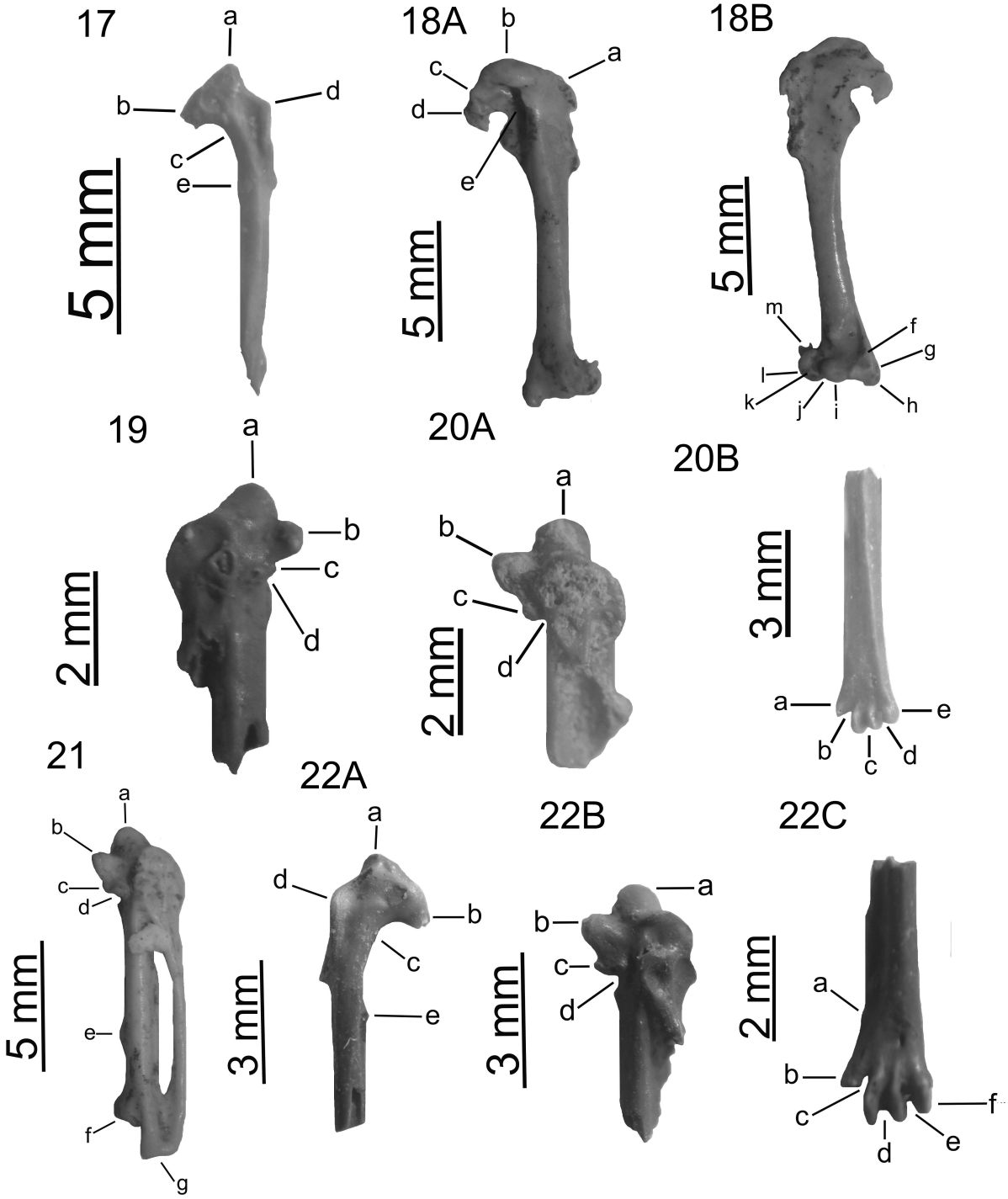
17
a
b
c
d
e
5 mm
18A
b
a
c
d
e
5 mm
18B
5 mm
m
f
g
l
k
j
i
h
19
a
b
c
d
2 mm
20A
a
b
c
d
2 mm
20B
3 mm
a
e
b
c
d
21
a
b
c
d
e
f
g
5 mm
22A
a
d
b
c
e
3 mm
22B
a
b
c
d
3 mm
22C
2 mm
a
b
c
d
e
f

Plate VI

Figure 23 A. *Tichodroma* †*capeki* nova sp. – humerus dext. (Polgárdi, V.11.68.1; V29143), cranial view, a. *caput humeri*; b. *tuberculum dorsale*; c. *sulcus lig. transversus*; d. *crista bicipitalis.*

Figure 23 B. *Tichodroma* †*capeki* nova sp. – humerus dext. (Polgárdi, V.11.68.1; V29143), caudal view, e. *tuberculum ventrale*; f. *crus fossae*; g. *fossae pneumotricipitalis*.

Figure 24. *Muscicapa* † *miklosi* nova sp.– –femur sin. (Polgárdi, MÁFI V.11.67.1; V.29142), caudal view, a. *trochlea fibularis*; b. *condylus lateralis*; c. *incisura intercondylaris*; d. *condylus medialis*; e. *epicondylus medialis.*

Figure 25. *Muscicapa* † *petényii* nova sp. – carpometacarpus dext. (Beremend, BKA), ventral view: a. *trochlea carpalis*; b. *proc. extensorius*; c. *processus alularis*; d. *fovea subalularis*; e. *protuberantia metacarpalis;* f. basis of *metacarpus majus;* g. end of *os metacarpi minus.*

Figure 26. *Luscinia* † *denesi* nova sp. – humerus dext. (Polgárdi, MÁFI V.11.72.1; V.29147), cranial view, a. *epicondylus ventralis*; b. *processus flexorius*; c. *condylus ventralis*; d. *incisura intercondylaris*; e. *condylus dorsalis*; f. *epicondylus dorsalis*; g. *processus supracondylaris dorsalis.*

Figure 27A. *Luscinia* † *pliocaenica* nova sp. – humerus dext. (Beremend, BKA), cranial view: a. *tuberculum supracondylare ventrale*; b. *epicondylus ventralis*; c. *processus flexorius*; d. *condylus ventralis*; e. *incisura intercondylaris*; f. *condylus dorsalis*; g. *epicondylus dorsalis*; h. *processus supracondylaris dorsalis.*

Figure 27 B. *Luscinia* † *pliocaenica* nova sp. – carpometacarpus sin. (Beremend, BKA), ventral view: a. *trochlea carpalis*; b. *fovea subalularis*; c. *protuberantia metacarpalis;* d. end of *os metacarpi minus.*

Figure 28 A. *Erithacus* † *minor* nova sp. – humerus dext. (Beremend, BKA), cranial view: a. *tuberculum supracondylare ventrale*; b. *epicondylus ventralis*; c. *processus flexorius*; d. *condylus ventralis*; e. *incisura intercondylaris*; f. *condylus dorsalis*; g. *epicondylus dorsalis*; h. *processus supracondylaris dorsalis.*

Figure 28 B. *Erithacus* † *minor* nova sp. – carpometacarpus dext. (Beremend, BKA), ventral view: a. *trochlea carpalis*; b. *proc. extensorius*; c. *processus alularis*; d. *fovea subalularis*; e. *protuberantia metacarpalis;* f. basis of *metacarpus majus;* g. end of *os metacarpi minus.*

Plate VI

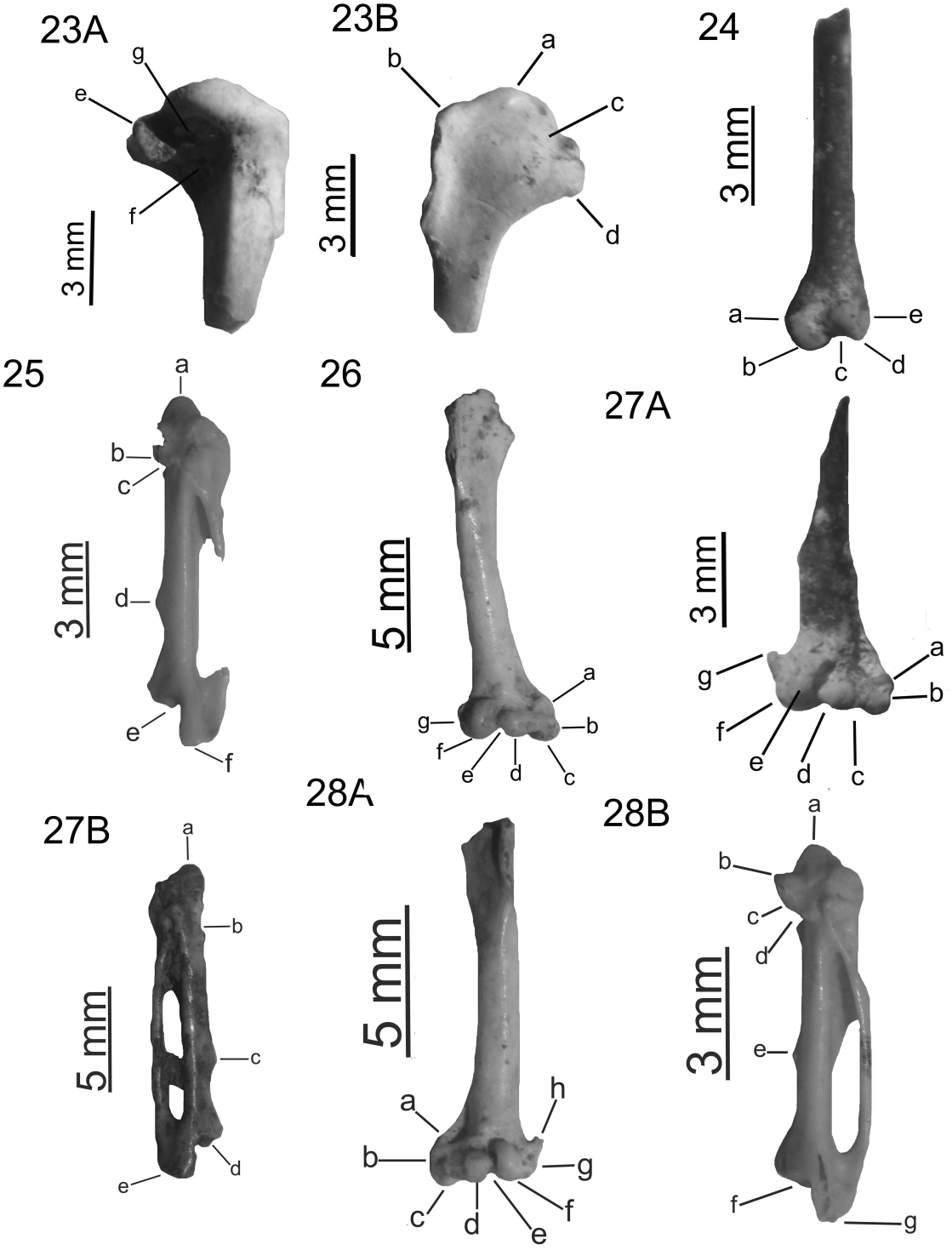
23A
g
e
f
3 mm
23B
a
b
c
d
3 mm
24
3 mm
a
e
b
c
d
25
a
b
c
d
e
f
3 mm
26
5 mm
a
g
b
f
e
d
c
27A
3 mm
a
g
b
f
e
d
c
27B
a
b
c
d
e
5 mm
28A
5 mm
a
h
b
g
c
d
e
f
28B
a
b
c
d
e
3 mm
f
g

Plate VII

Figure 29. *Phoenicurus* † *erikai* nova sp. – ulna dext. (MÁFI V.11.25.1; V.29100), medial view, a. *condylus dorsalis*; b. *sulcus intercondylaris*; c. *condylus ventralis*; d. *tuberculum carpale.*

Figure 30. *Phoenicurus* † *baranensis* nova sp. – humerus dext. (Beremend, BKA), cranial view: a. *tuberculum supracondylare ventrale*; b. *epicondylus ventralis*; c. *processus flexorius*; d. *condylus ventralis*; e. *incisura intercondylaris*; f. *condylus dorsalis*; g. *epicondylus dorsalis*; h. *processus supracondylaris dorsalis.*

Figure 31. *Monticola* † *pongraczi* nova sp. – humerus sin. (Beremend, BKA), cranial view: a. *tuberculum supracondylare ventrale*; b. *epicondylus ventralis*; c. *processus flexorius*; d. *condylus ventralis*; e. *incisura intercondylaris*; f. *condylus dorsalis*; g. *epicondylus dorsalis*; h. *processus supracondylaris dorsalis.*

Figure 32 A. *Saxicola* †*lambrechti* nova sp. – humerus sin. (Polgárdi, MÁFI V.11.106.1; V.29181), caudal view, a. *tuberculum dorsale*; b. *caput humeri*; c. *tuberculum ventrale*; d. *crista bicipitalis*; e. *crus fossae*; f. *fossae pneumotricipitalis*.

Figure 32 B. *Saxicola* †*lambrechti* nova sp. – humerus sin. (Polgárdi, MÁFI V.11.106.1; V.29181), cranial view, g. *tuberculum supracondylare ventrale*; h. *epicondylus* vedntralis; i. *processus flexorius*; j. *condylus ventralis*; k. *incisura intercondylaris*; l. *condylus dorsalis*; m. *epicondylus dorsalis*; n. *processus supracondylaris dorsalis.*

Figure 32 C. *Saxicola* †*lambrechti* nova sp. – ulna sin. (Polgárdi, MÁFI V.11.110.3, V.11.128.2), cranial view, a. *oleocranon*; b. *cotyla dorsalis*; c. *cotyla ventralis*; d. *tuberculum lig. colat. ventralis*; e. *depressio m. brachialis*.

Figure 32 D. *Saxicola* †*lambrechti* nova sp. – tibiotarsus sin. (Polgárdi, MÁFI V.29185, V.29203), cranial view, a. *tuberositas retinaculi m. fibularis*; b. *sulcus extensorius*; c. *pons supratendineus*; d. *condylus lateralis*; e. *incisura intercondylaris*; f. *condylus medialis.*

Figure 33 A. *Saxicola* † *baranensis* nova sp.– humerus dext. (Beremend, BKA), cranial view: a. *tuberculum supracondylare ventrale*; b. *epicondylus ventralis*; c. *processus flexorius*; d. *condylus ventralis*; e. *incisura intercondylaris*; f. *condylus dorsalis*; g. *epicondylus dorsalis*; h. *processus supracondylaris dorsalis.*

Figure 33 B. *Saxicola* † *baranensis* nova sp. – ulna dext. (Csarnóta, MÁFI V.11.18.1; V.29093), cranial view, a. *oleocranon*; b. *cotyla dorsalis*; c. *cotyla ventralis*; d. *tuberculum lig. colat. ventralis*; e. *depressio m. brachialis*.

Figure 33 C. *Saxicola* † *baranensis* nova sp.– ulna dext. (Beremend, BKA), caudal view, a. *condylus dorsalis*; b. *sulcus intercondylaris*; c. *condylus ventralis*; d. *tuberculum carpale.*

Plate VII

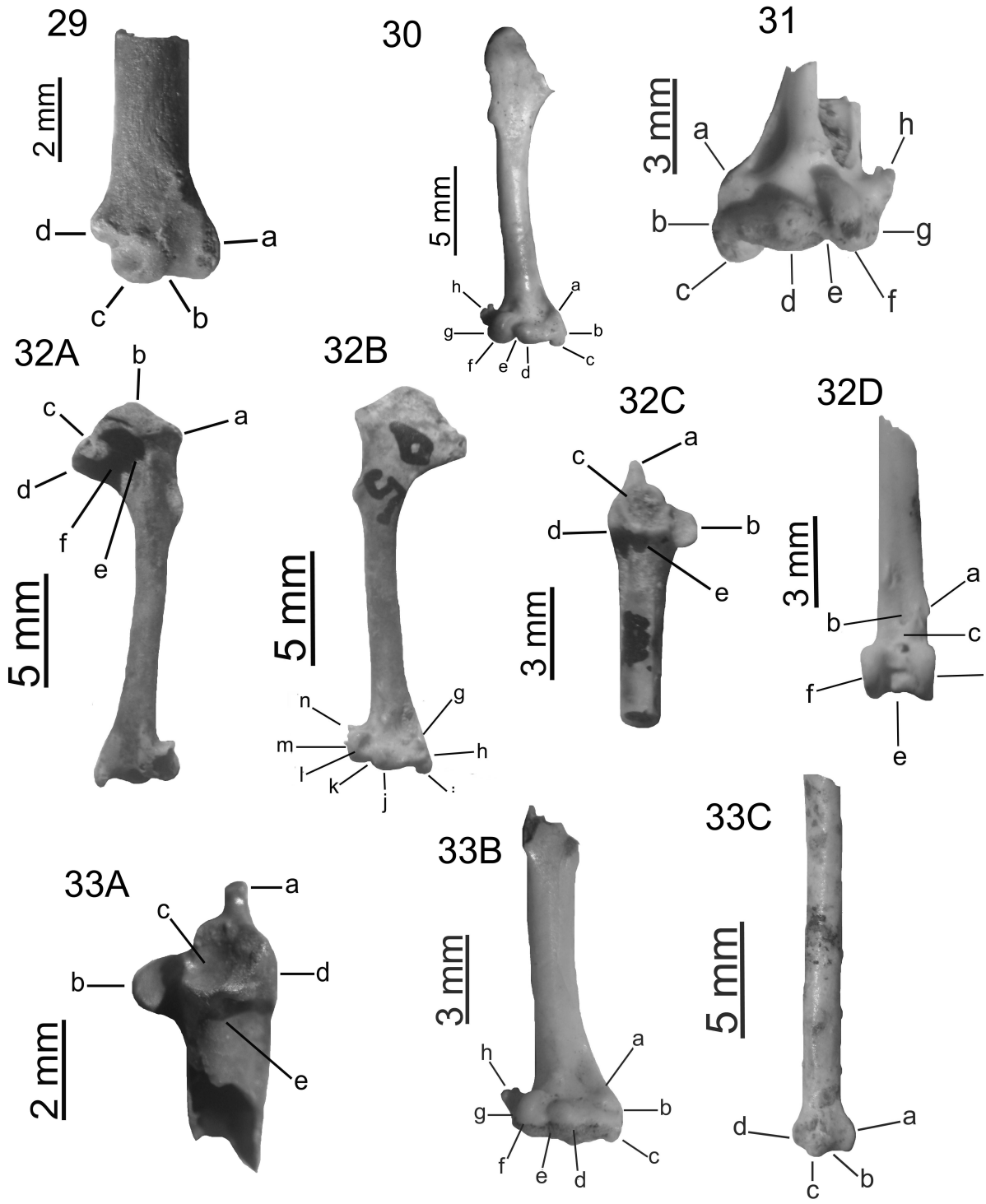
29
2 mm
d
a
c
b
30
5 mm
h
a
g
b
f
e
d
c
31
3 mm
a
h
b
g
c
d
e
f
32A
b
c
a
d
f
e
5 mm
32B
5 mm
n
g
m
h
l
k
j
32C
c
a
d
b
e
3 mm
32D
3 mm
a
b
c
f
e
33A
a
c
b
d
e
2 mm
33B
3 mm
h
a
g
b
f
e
d
c
33C
5 mm
d
a
c
b

Plate VIII

Figure 34. *Saxicola* †*parva* nova sp. – ulna dext. (Csarnóta, MÁFI V.11.24.1; V.29099), cranial view, a. *oleocranon*; b. *cotyla dorsalis*; c. *cotyla ventralis*; d. *tuberculum lig. colat. ventralis*; e. *depressio m. brachialis*.

Figure 35. *Saxicola* † *magna* Nova sp.– humerus sin. (Beremend, BKA), cranial view: a. *tuberculum supracondylare ventrale*; b. *epicondylus ventralis*; c. *processus flexorius*; d. *condylus ventralis*; e. *incisura intercondylaris*; f. *condylus dorsalis*; g. *epicondylus dorsalis*; h. *processus supracondylaris dorsalis.*

Figure 36 A. *Oenanthe* †*kormosi* nova sp. – carpometacarpus dext. (Polgárdi, MÁFI V.11.125.3; V.29200/1), ventral view, a. *trochlea carpalis*; b. *proc. extensorius*; c. *processus alularis*; d. *fovea subalularis*.

Figure 36 B. *Oenanthe* †*kormosi* nova sp. – femur dext. (Polgárdi, MÁFI V.11.103.1; V.29178), caudal view, a. *trochanter femoris*; b. *fossa trochanteris*; c. *facies articularis acetabularis*; d. *impressiones obturatoriae*; e. *trochlea fibularis*; f. *crista tibiofibularis*; g. *condylus lateralis*; h. *incisura intercondylaris*; i. *condylus medialis*; j. *epicondylus medialis.*

Figure 36 C. *Oenanthe* †*kormosi* nova sp. – tibiotarsus dext. (Polgárdi, MÁFI V.11.125.3; V.29200/2), cranial view, a. *tuberositas retinaculi m. fibularis*; b. *sulcus extensorius*; c. *pons supratendineus*; d. *condylus lateralis*; e. *incisura intercondylaris*; f. *condylus medialis.*

Figure 36 D. *Oenanthe* †*kormosi* nova sp. – tarsometatarsus sin. (Polgárdi, MÁFI V.11.125.3; V.29200/3), dorsal view, a. *trochlea metatarsi* II.; b. *incisura intertrochlearis medialis*; c. *trochlea metatarsi* III.; d. *incisura intertrochlearis lateralis*; e. *trochlea* metatarsi IV.

Figure 37A. *Oenanthe* † *pongraczi* nova sp.– humerus sin. (Beremend, BKA), cranial view: a. *tuberculum supracondylare ventrale*; b. *epicondylus ventralis*; c. *processus flexorius*; d. *condylus ventralis*; e. *incisura intercondylaris*; f. *condylus dorsalis*; g. *epicondylus dorsalis*; h. *processus supracondylaris dorsalis.*

Figure 37 B. *Oenanthe* † *pongraczi* nova sp. – ulna dext. (Csarnóta, MÁFI V.11.23.1; V.29098), medial view, a. *condylus dorsalis*; b. *sulcus intercondylaris*; c. *condylus ventralis*; d. *tuberculum carpale.*

Figure 37 C. *Oenanthe* † *pongraczi* nova sp.– carpometacarpus sin. (Beremend, BKA), ventral view: a. *trochlea carpalis*; b. *processus extensorius;* c. *fovea subalularis*; d. *protuberantia metacarpalis;* e. basis of the *facies articularis digiti major* f. end of the *os metacarpi minus.*

Figure 37 D. *Oenanthe* † *pongraczi* nova sp.– phalanga alae 1. dig.II. (Beremend, BKA), a. ventral point; b. dorsal point; c. proximal edge; d. dorsal edge; e. distal edge.

Plate VIII

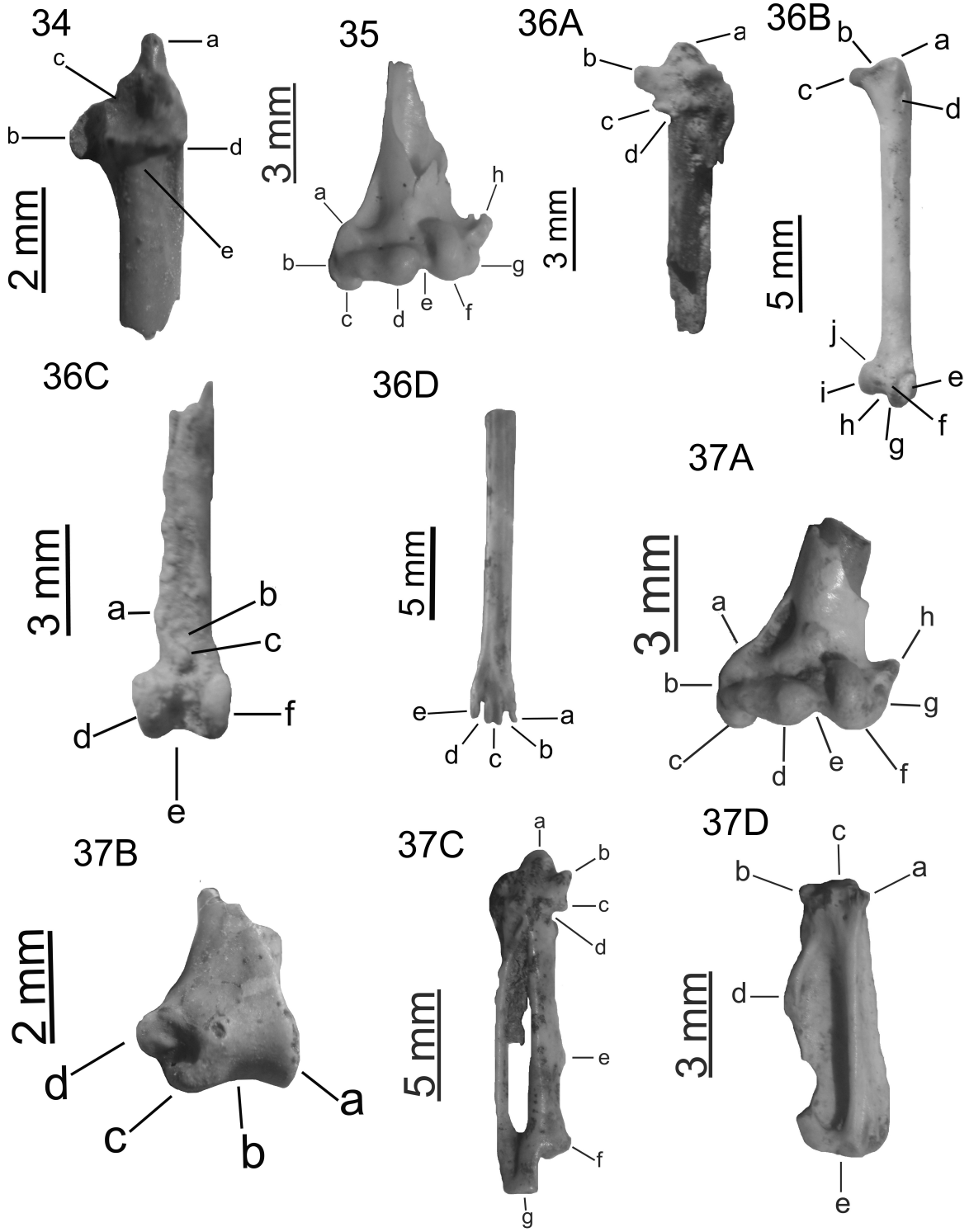

Plate IX

Figure 38 A. †*Turdicus pannonicus* n. sp. – ulna sin. (Polgárdi, MÁFI V.11.105.1; V.29180), medial view, a. *condylus dorsalis*; b. *sulcus intercondylaris*; c. *condylus ventralis*; d. *tuberculum carpale.*

Figure 38 B. †*Turdicus pannonicus* nova sp. – tibiotarsus dext. (Polgárdi, MÁFI V.11.85.1; V.29160), cranial view, craniális nézet, a. *tuberositas retinaculi m. fibularis*; b. *sulcus extensorius*; c. *pons supratendineus*; d. *condylus lateralis*; e. *incisura intercondylaris*; f. *condylus medialis.*

Figure 39 A. *Turdus* †*miocaenicus* nova sp. – coracoid sin. (Polgárdi, MÁFI V.11.124.1; V.29199), dorsal view, a. *acrocoracoid*; b. *facies aricularis humerális*; c. *sulcus m. supracoracoidei*; d. *processus procoracoidei*.

Figure 39 B. *Turdus* †*miocaenicus* nova sp. – ulna sin. (Polgárdi, MÁFI V.11.102.1; V.29177), medial view, a. *condylus dorsalis*; b. *sulcus intercondylaris*; c. *condylus ventralis*; d. *tuberculum carpale.*

Figure 40 A. *Turdus* †*polgardiensis* nova sp. – ulna dext. (Polgárdi, MÁFI V.11.100.1; V.29175), cranial view, a. *cotyla dorsalis;* b. *cotyla ventralis*; c. *tuberculum lig. colat. ventralis*; d. *depressio m. brachialis*.

Figure 40 B. *Turdus* †*polgardiensis* nova sp. – ulna dext. (Polgárdi, MÁFI V.11.100.1; V.29175), medial view, e. *condylus dorsalis*; f. *sulcus intercondylaris*; g. *condylus ventralis*; h. *tuberculum carpale.*

Figure 41A. Turdus † major nova sp.– humerus dext. (Beremend, BKA), caudal view: a. tuberculum dorsale; b. caput humeri; c. tuberculum ventrale; d. crista bicipitalis; e. crus fossae; f. fossae pneumotricipitalis.

Figure 41 B. *Turdus* † *major* nova sp.– humerus sin. (Csarnóta, MÁFI V.11.19.1; V.29094), cranial view, a. *tuberculum supracondylare ventrale*; b. *epicondylus* vedntralis; c. *processus flexorius*; d. *condylus ventralis*; e. *incisura intercondylaris*; f. *condylus dorsalis*; g. *epicondylus dorsalis*; h. *processus supracondylaris dorsalis.*

Figure 41 C. *Turdus* † *major* nova sp. – carpometacarpus sin. (Beremend, BKA), ventral view: a. *trochlea carpalis*; b. *processus extensorius;* c. *processus alularis*; d. *fovea subalularis*; e. *protuberantia metacarpalis;* f. basis of the *facies articularis digiti major*; g. end of the *os metacarpi minus.*

Figure 41 D. *Turdus* † *major* nova sp. – phalanga alae 1. dig.II. (Beremend, BKA), a. ventral point; b. dorsal point; c. proximal edge; d. dorsal edge; e. distal edge.

Figure 41 E. *Turdus* † *major* nova sp. – tarsometatarsus sin. (Beremend, BKA), dorsal view: a. *trochlea metatarsi* II.; b. *incisura intertrochlearis medialis*; c. *trochlea metatarsi* III.; d. *incisura intertrochlearis lateralis*; e. *trochlea metatarsi* IV.

Plate IX

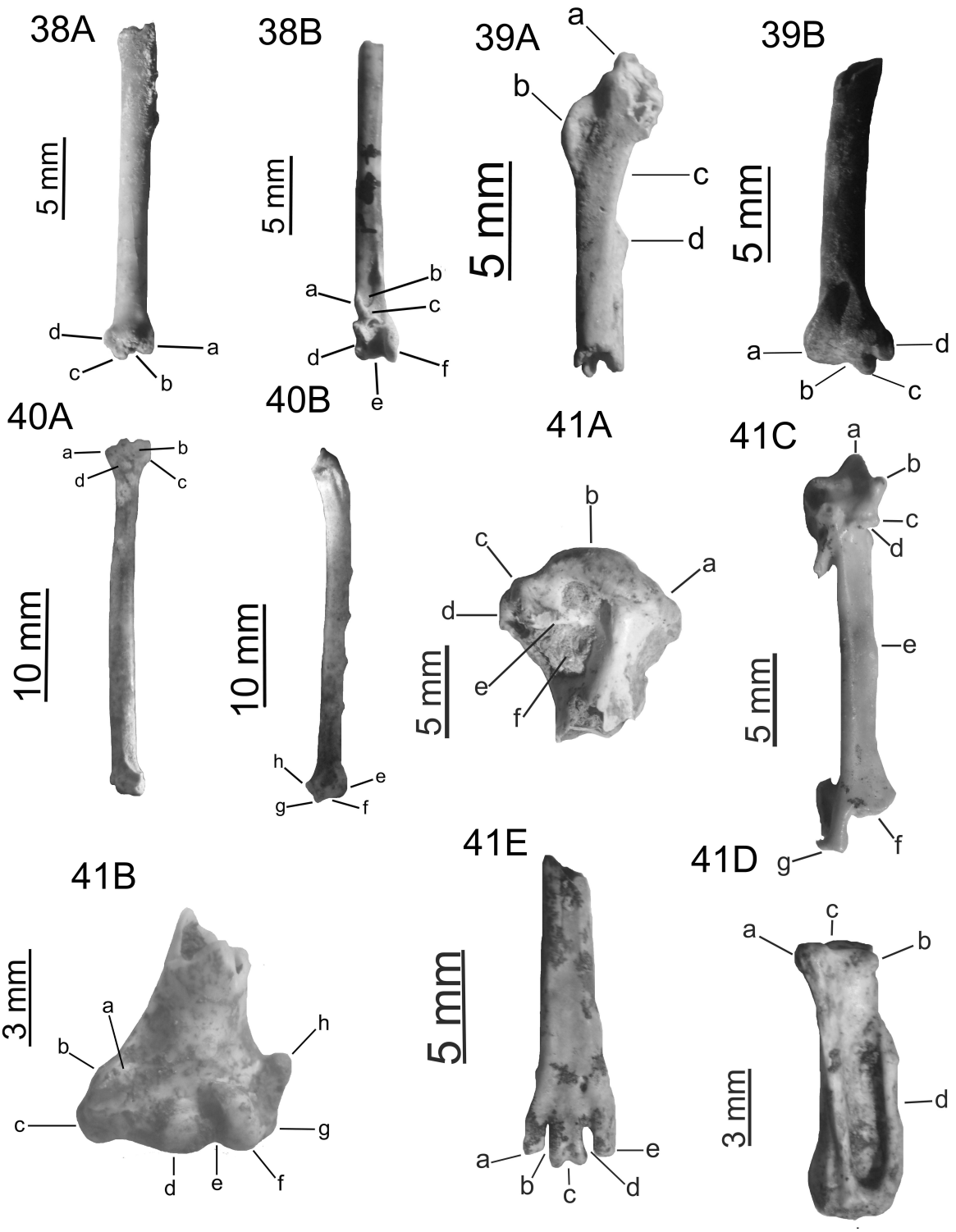
38A
5 mm
d
a
c
b
38B
5 mm
a
b
c
d
f
e
39A
a
b
c
d
5 mm
39B
5 mm
a
d
b
c
40A
a
b
d
c
10 mm
40B
10 mm
h
e
g
f
41A
b
c
a
d
e
f
5 mm
41C
a
b
c
d
e
5 mm
f
g
41B
3 mm
a
b
h
c
g
d
e
f
41E
5 mm
a
e
b
c
d
41D
c
a
b
3 mm
d

Plate X

Figure 42 A. *Turdus* † *medius* nova sp. – humerus sin. (Beremend, BKA), caudal view: a. *tuberculum dorsale*; b. *caput humeri*; c. *tuberculum ventrale*; d. *crista bicipitalis*; e. *crus fossae*; f. *fossae pneumotricipitalis*.

Figure 42 B. *Turdus* † *medius* nova sp. – humerus dext. (Csarnóta, MÁFI V.11.26.1; V.29101), cranial view, a. *tuberculum supracondylare ventrale*; b. *epicondylus* vedntralis; c. *processus flexorius*; d. *condylus ventralis*; e. *incisura intercondylaris*; f. *condylus dorsalis*; g. *epicondylus dorsalis*; h. *processus supracondylaris dorsalis.*

Figure 42 C. *Turdus* † *medius* nova sp. – ulna dext. (Csarnóta, MÁFI V.11.44.2; V.29119), medial view, a. *condylus dorsalis*; b. *sulcus intercondylaris*; c. *condylus ventralis*; d. *tuberculum carpale.*

Figure 42 D. *Turdus* † *medius* nova sp. – carpometacarpus dext. (Beremend, BKA), ventral view: a. *trochlea carpalis*; b. *processus extensorius;* c. *processus alularis*; d. *fovea subalularis*; e. *protuberantia metacarpalis;* f. basis of *facies articularis digiti major*; g. end of *os metacarpi minus*.

Figure 42 E. *Turdus* † *medius* nova sp. – tibiotarsusus dext. (Csarnóta, MÁFI V.11.44.3; V.29119), cranial view, a. *tuberositas retinaculi m. fibularis*; b. *sulcus extensorius*; c. *pons supratendineus*; d. *condylus lateralis*; e. *incisura intercondylaris*; f. *condylus medialis.*

Figure 42 F. *Turdus* † *medius* nova sp. – tarsometatarsus dext. (Beremend, BKA), dorsal view: a. *trochlea metatarsi* II.; b. *incisura intertrochlearis medialis*; c. *trochlea metatarsi* III.; d. *incisura intertrochlearis lateralis*; e. *trochlea metatarsi* IV.

Figure 43 A. Turdus † minor nova sp. – humerus sin. (Beremend, BKA), caudal view: a. caput humeri; b. tuberculum ventrale; c. crista bicipitalis; d. crus fossae; e. fossae pneumotricipitalis.

Figure 43 B. *Turdus* † *minor* nova sp. – humerus sin. (Csarnóta, MÁFI V.11.27.1; V.29102), cranial view, a. *tuberculum supracondylare ventrale*; b. *epicondylus* vedntralis; c. *processus flexorius*; d. *condylus ventralis*; e. *incisura intercondylaris*; f. *condylus dorsalis*; g. *epicondylus dorsalis*; h. *processus supracondylaris dorsalis.*

Figure 43 C. *Turdus* † *minor* nova sp. – carpometacarpus dext. (Csarnóta, MÁFI V.11.45.2; V.29120), ventral view, a. *trochlea carpalis*; b. *proc. extensorius*; c. *processus alularis*; d. *fovea subalularis*; e. *protuberantia metacarpalis.*

Figure 43 D. *Turdus* † *minor* nova sp. – tarsometatarsusdext. (Csarnóta, MÁFI V.11.45.3; V.29120), dorsal view, a. *trochlea metatarsi* II.; b. *incisura intertrochlearis medialis*; c. *trochlea metatarsi* III.; d. *incisura intertrochlearis lateralis*; e. *trochlea* metatarsi IV.

Plate X

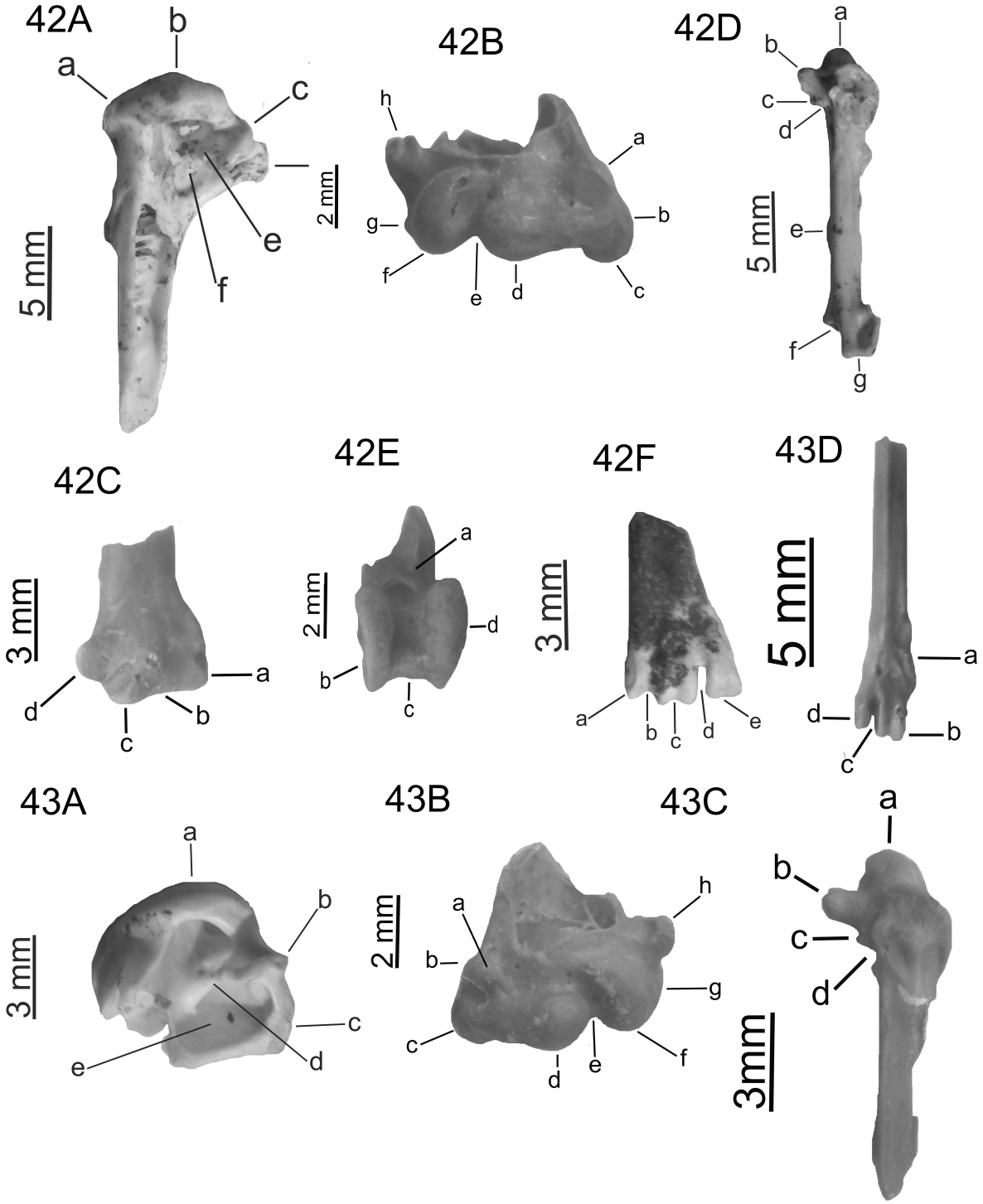

Plate XI

Figure 44 A. *Oriolus* † *beremendensis* nova sp. – humerus sin. (Beremend, BKA), cranial view: a. *tuberculum supracondylare ventrale*; b. *epicondylus ventralis*; c. *processus flexorius*; d. *condylus ventralis*; e. *incisura intercondylaris*; f. *condylus dorsalis*; g. *epicondylus dorsalis*; h. *processus supracondylaris dorsalis.*

Figure 44 B. *Oriolus* †*beremendensis* nova sp. – ulna sin. (Beremend, BKA), cranial view, a. *oleocranon*; b. *cotyla dorsalis*; c. *cotyla ventralis*; d. *tuberculum lig. colat. ventralis*; e. *depressio m. brachialis*.

Figure 44 C. *Oriolus* † *beremendensis* nova sp. – ulna sin. (Beremend, BKA), medial view, f. *condylus dorsalis*; g. *sulcus intercondylaris*; h. *condylus ventralis*; i. *tuberculum carpale.*

Figure 44 D. *Oriolus* † *beremendensis* nova sp. – carpometacarpus dext. (Beremend, BKA), ventral view: a. *trochlea carpalis*; b. *processus extensorius;* c. *processus alularis*; d. *fovea subalularis*; e. *protuberantia metacarpalis;* f. basis of the *facies articularis digiti major*; g. end of the *os metacarpi minus.*

Figure 44 E. *Oriolus* †*beremendensis* nova sp. – tibiotarsus sin. (Beremend, BKA). cranial view, a. *tuberositas retinaculi m. fibularis*; b. *sulcus extensorius*; c. *pons supratendineus*; d. *condylus lateralis*; e. *incisura intercondylaris*; f. *condylus medialis.*

Figure 45 A. *Acrocephalus* † *major* nova sp. – humerus sin. (Polgárdi, MÁFI V.11.87.26; V.29162/1), caudal view, a. *tuberculum dorsale*; b. *caput humeri*; c. *tuberculum ventrale*; d. *crista bicipitalis*; e. *crus fossae*; f. *fossae pneumotricipitalis*.

Figure 45 B. *Acrocephalus* † *major* nova sp. – humerus dext. (Polgárdi, MÁFI V.11.87.26; V.29162/2), cranial view, g. *epicondylus ventralis*; h. *processus flexorius*; i. *condylus ventralis*; j. *incisura intercondylaris*; k. *condylus dorsalis*; l. *epicondylus dorsalis*; m. *processus supracondylaris dorsalis.*

Figure 45 C. *Acrocephalus* † *major* nova sp. – ulna dext. (Polgárdi, MÁFI V.11.107.1; V.29182), cranial view, a. *oleocranon*; b. *cotyla dorsalis* c. *cotyla ventralis*; d. *tuberculum lig. colat. ventralis*.

Figure 45 D. *Acrocephalus* † *major* nova sp. – ulna dext. (Polgárdi, MÁFI V.11.107.1; V.29182), medial view, e. *condylus dorsalis*; f. *sulcus intercondylaris*; g. *condylus ventralis*; h. *tuberculum carpale.*

Figure 45 E. *Acrocephalus* † *major* nova sp. – tibiotarsus dext. (Polgárdi, MÁFI V.11.87.26; V.29162/3), cranial view, a. *tuberositas retinaculi m. fibularis*; b. *sulcus extensorius*; c. *pons supratendineus*; d. *condylus lateralis*; e. *incisura intercondylaris*; f. *condylus medialis.*

Plate XI

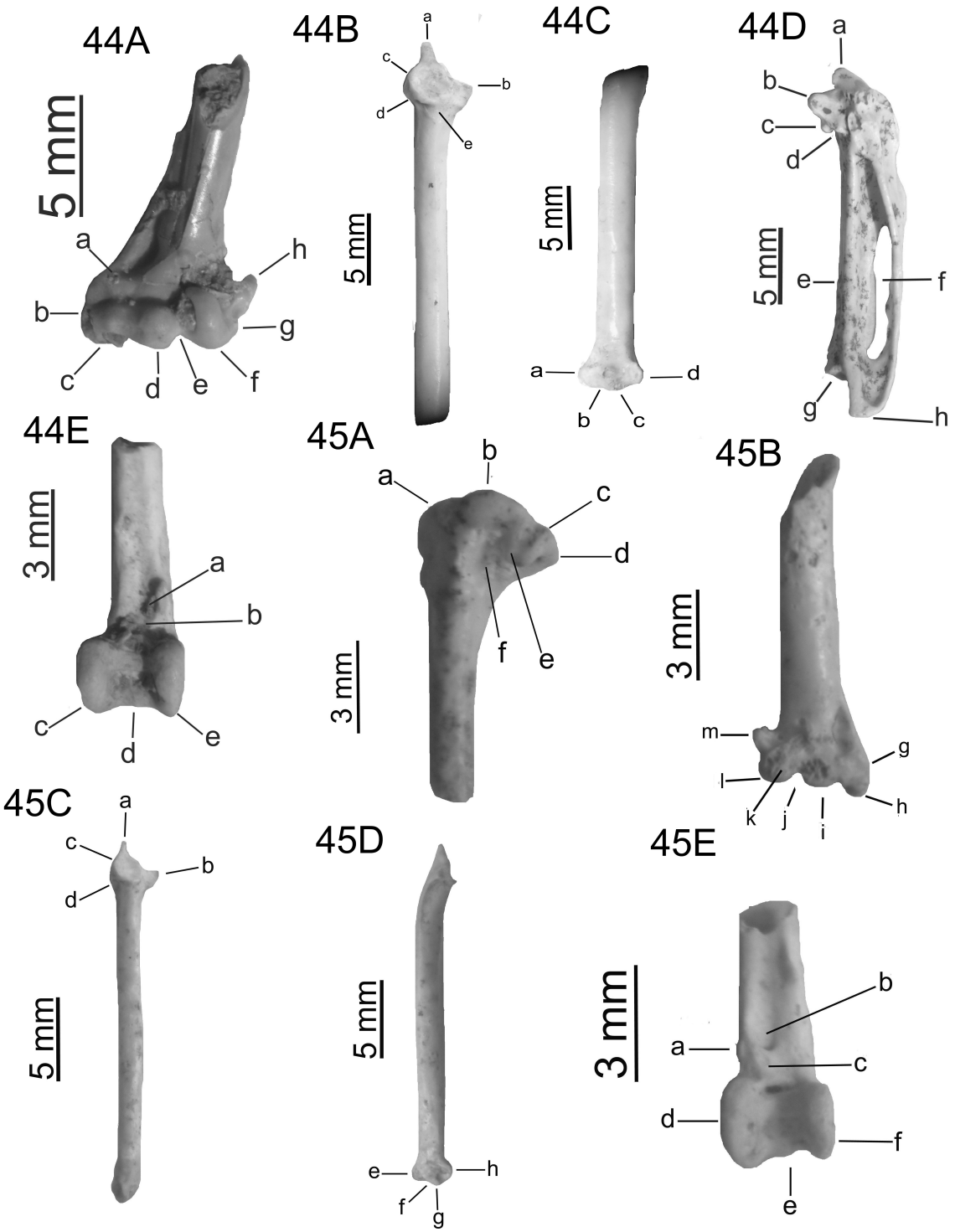
44A
5 mm
a
b
c
d
e
f
g
h
44B
5 mm
a
b
c
d
e
44C
5 mm
a
b
c
d
44D
5 mm
a
b
c
d
e
f
g
h
44E
3 mm
a
b
c
d
e
45A
3 mm
a
b
c
d
e
f
45B
3 mm
g
h
i
j
k
l
m
45C
5 mm
a
b
c
d
45D
5 mm
e
f
g
h
45E
3 mm
a
b
c
d
e
f

Plate XII

Figure 46 A. *Acrocephalus* † *minor* nova sp. – humerus sin. (Polgárdi, MÁFI V.11.71.1; V.29146), caudal view, a. *tuberculum dorsale*; b. *caput humeri*; c. *tuberculum ventrale*; d. *crista bicipitalis*; e. *crus fossae*; f. *fossae pneumotricipitalis*.

Figure 46 B. *Acrocephalus* † *minor* nova sp. – humerus dext. (Polgárdi, MÁFI V.11.88.10; V.29163/1), cranial view, g. *epicondylus ventralis*; h. *processus flexorius*; i. *condylus ventralis*; j. *incisura intercondylaris*; k. *condylus dorsalis*; l. *epicondylus dorsalis*; m. *processus supracondylaris dorsalis.*

Figure 46 C. *Acrocephalus* † *minor* nova sp. – ulna sin. (Polgárdi, MÁFI V.11.88.10; V.29163/2), cranial view, a. *oleocranon*; b. *cotyla dorsalis*; c. *cotyla ventralis*; d. *tuberculum lig. colat. ventralis*.

Figure 46 D. *Acrocephalus* † *minor* nova sp. – ulna sin. (Polgárdi, MÁFI V.11.88.10; V.29163/3), medial view, e. *condylus dorsalis*; f. *sulcus intercondylaris*; g. *condylus ventralis*; h. *tuberculum carpale.*

Figure 46 E. *Acrocephalus* † *minor* nova sp. – tibiotarsus dext. (Polgárdi, MÁFI V.11.88.10; V.29163/4), cranial view, a. *tuberositas retinaculi m. fibularis*; b. *sulcus extensorius*; c. *pons supratendineus*; d. *condylus lateralis*; e. *incisura intercondylaris*; f. *condylus medialis.*

Figure 47 A. *Acrocephalus* † *kretzoii* nova sp. – carpometacarpus sin. (Csarnóta, MÁFI V.11.1.1; V.29076), ventral view, a. *trochlea carpalis*; b. *proc. extensorius*; c. *processus alularis*; d. *fovea subalularis*; e. *protuberantia metacarpalis.*

Figure 47 B. *Acrocephalus* † *kretzoii* nova sp. – tarsometatarsus dext. (Csarnóta, MÁFI V.11.39.3; V.29144), dorsal view, a. *trochlea metatarsi* II.; b. *incisura intertrochlearis medialis*; c. *trochlea metatarsi* III.; d. *incisura intertrochlearis lateralis*; e. *trochlea* metatarsi IV.

Figure 47 C. *Acrocephalus* † *kretzoii* nova sp. – tarsometatarsus dext. (Beremend, BKA), dorsal view: a. *trochlea metatarsi* II.; b. *incisura intertrochlearis medialis*; c. *trochlea metatarsi* III.; d. *incisura intertrochlearis lateralis*; e. *trochlea metatarsi* IV.

Figure 48. *Acrocephalus* † *kordosi* nova sp. – carpometacarpus dext. (Csarnóta, MÁFI V.11.2.1; V.29077), ventral view, a. *trochlea carpalis*; b. *proc. extensorius*; c. *processus alularis*; d. *fovea subalularis*; e. *protuberantia metacarpalis.*

Figure 49. *Cettia* † *janossyi* nova sp. – humerus dext. (Polgárdi, MÁFI V.11.100.2; V.29176), cranial view, a. *tuberculum dorsale*; b. *caput humeri*; c. *epicondylus ventralis*; d. *processus flexorius*; e. *condylus ventralis*; f. *incisura intercondylaris*; g. *condylus dorsalis*; h. *epicondylus dorsalis*; i. *processus supracondylaris dorsalis.*

Figure 50. *Cettia* † *kalmani* nova sp. – humerus dext. (Csarnóta, MÁFI V.11.28.1; V.29103), cranial view, a. *tuberculum supracondylare ventrale*; b. *epicondylus* vedntralis; c. *processus flexorius*; d. *condylus ventralis*; e. *incisura intercondylaris*; f. *condylus dorsalis*; g. *epicondylus dorsalis*; h. *processus supracondylaris dorsalis.*

Plate XII

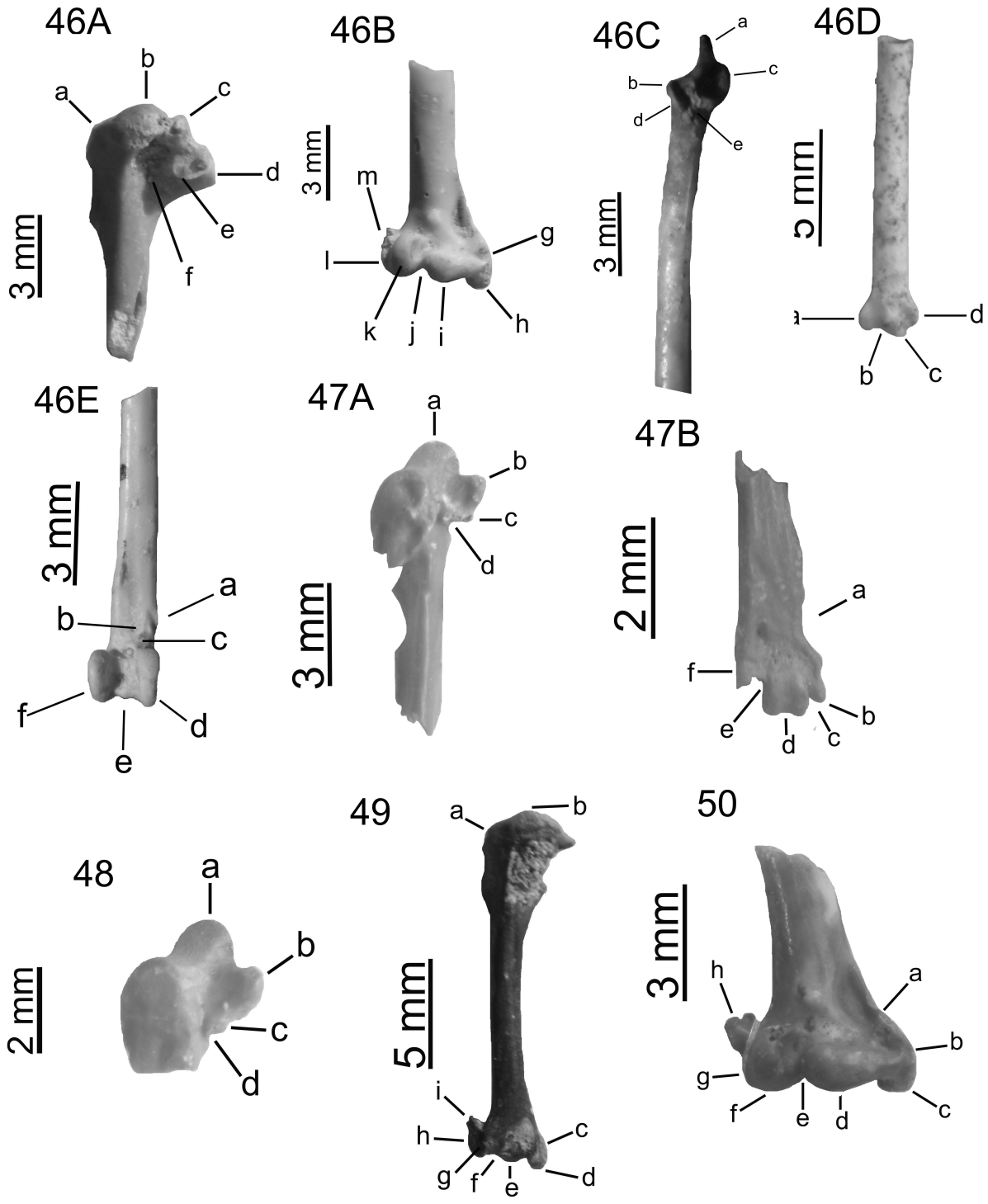

Plate XIII

Figure 51 A. *Hippolais* †*veterior* nova sp. – humerus dext. (Polgárdi, MÁFI V.11.84.5; V.29159/1), cranial view, a. *tuberculum supracondylare ventrale* b. *epicondylus ventralis*; c. *processus flexorius*; d. *condylus ventralis*; e. *incisura intercondylaris*; f *condylus dorsalis*; g *epicondylus dorsalis*; h. *processus supracondylaris dorsalis.*

Figure 51 B. *Hippolais* †*veterior* nova sp. – carpometacarpus sin. (Polgárdi, MÁFI V.11.70.1; V.29145), ventral view, a. *trochlea carpalis*; b. *proc. extensorius*; c. *processus alularis*; d. *fovea subalularis*; e. *protuberantia metacarpalis.*

Figure 51 C. *Hippolais* †*veterior* nova sp. – tibiotarsus dext. (Polgárdi, MÁFI V.11.84.5; V.29159/2), cranial view, a. *tuberositas retinaculi m. fibularis*; b. *sulcus extensorius*; c. *pons supratendineus*; d. *condylus lateralis*; e. *incisura intercondylaris*; f. *condylus medialis.*

Figure 52 A. *Sylvia* †*intermedia* nova sp. – humerus dext. (Polgárdi, MÁFI V.11.86.9; V.29161/1), caudal view, a. *caput humeri*; b. *tuberculum ventrale*; c. *crista bicipitalis*; d. *cruss fossae*; e. *fossae pneumotricipitalis;* f. *tuberculum dorsale.*

Figure 52 B. *Sylvia* †*intermedia* nova sp. – humerus dext. (Polgárdi, MÁFI V.11.86.9; V.29161/2), cranial view, g. *tuberculum supracondylare ventrale* h. *epicondylus ventralis*; i. *processus flexorius*; j. *condylus ventralis*; k. *incisura intercondylaris*; l *condylus dorsalis*; m. *epicondylus dorsalis*; n. *processus supracondylaris dorsalis.*

Figure 52 C. *Sylvia* †*intermedia* nova sp. – carpometacarpus dext. (Polgárdi, MÁFI V.11.69.1; V.29144), ventral view, a. *trochlea carpalis*; b. *proc. extensorius*; c. *processus alularis*; d. *fovea subalularis*; e. *protuberantia metacarpalis.*

Figure 52 D. *Sylvia* †*intermedia* nova sp. – tibiotarsus dext. (Polgárdi, MÁFI V.11.86.9; V.29161/3), cranial view, a. *tuberositas retinaculi m. fibularis*; b. *sulcus extensorius*; c. *pons supratendineus*; d. *condylus lateralis*; e. *incisura intercondylaris*; f. *condylus medialis.*

Figure 52 E. *Sylvia* †*intermedia* nova sp. – tarsometatarsus sin. (Polgárdi, MÁFI V.11.86.9; V.29161/4), dorsal view, a. *fossa metatarsi* I.; b. edge betwen *fossa metatarsi* I. and *trochlea metatarsi* II.; c. *trochlea metatarsi* II.; d. *incisura intertrochlearis medialis*; e. *trochlea metatarsi* III.; f. *incisura intertrochlearis lateralis*; g. *trochlea* metatarsi IV.

Figure 53 A. *Sylvia* †v*pusilla* nova sp. – humerus dext. (Beremend, BKA), caudal view: a. tuberculum dorsale; b. caput humeri; c. tuberculum ventrale; d. crista bicipitalis; e. crus fossae; f. fossae pneumotricipitalis.

Figure 53 B. *Sylvia* † *pusilla* nova sp. – carpometacarpus sin. (Csarnóta, MÁFI V.11.7.1; V.29082), ventral view, a. *trochlea carpalis*; b. *proc. extensorius*; c. *processus alularis*; d. *fovea subalularis*; e. *protuberantia metacarpalis.*

Figure 53 C. *Sylvia* † *pusilla* nova sp. – tarsometatarsus sin. (Csarnóta, MÁFI V.11.108.3; V.29183), dorsal view, a. *trochlea metatarsi* II.; b. *incisura intertrochlearis medialis*; c. *trochlea metatarsi* III.; d. *incisura intertrochlearis lateralis*; e. *trochlea* metatarsi IV.

Plate XIII

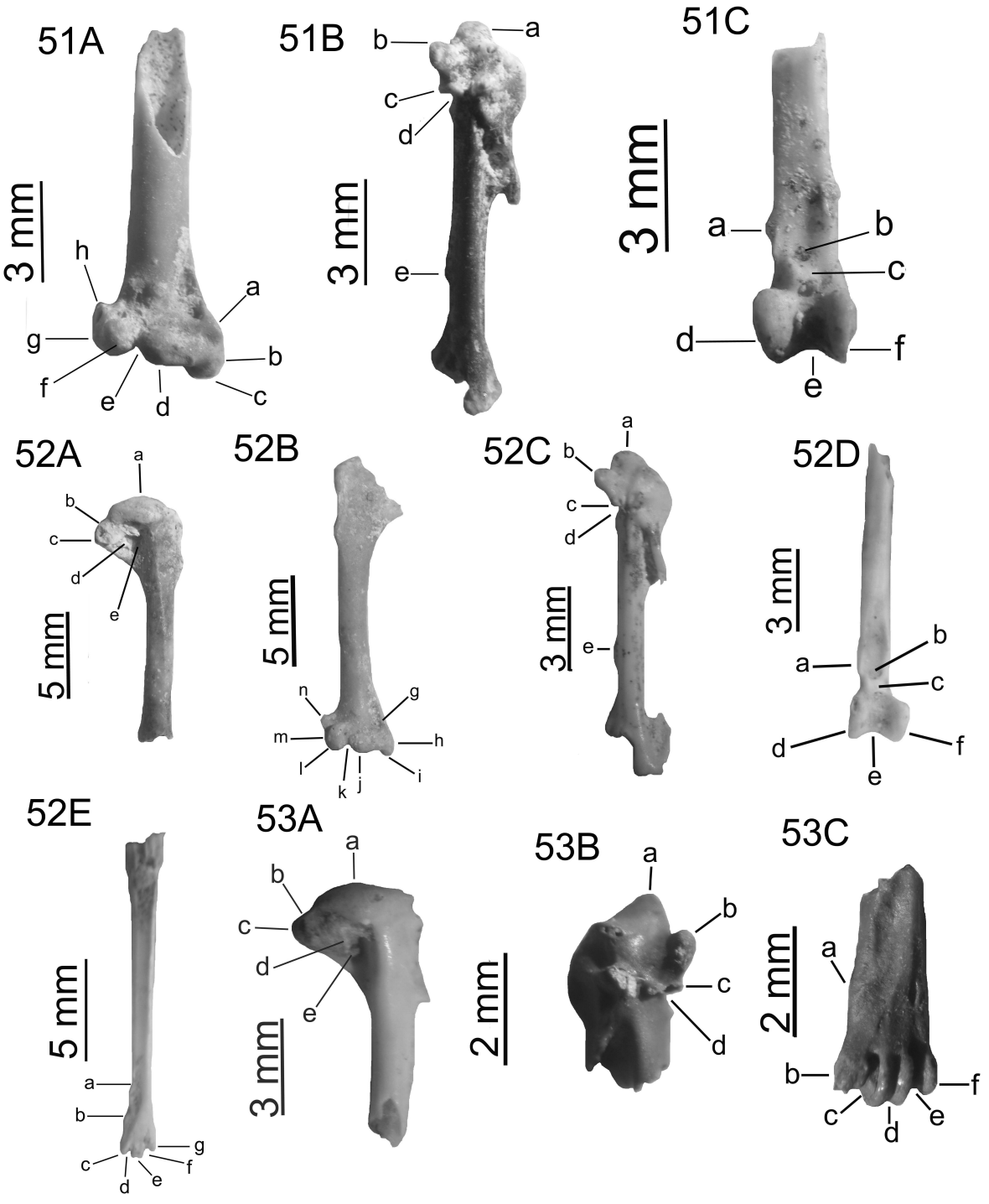
51A
3 mm
h
a
g
b
f
e
d
c
51B
b
a
c
d
3 mm
e
51C
3 mm
a
b
c
d
f
e
52A
a
b
c
d
e
5 mm
52B
5 mm
n
g
m
h
l
k
j
i
52C
a
b
c
d
3 mm
e
52D
3 mm
b
a
c
d
f
e
52E
5 mm
a
b
g
c
f
d
e
53A
a
b
c
d
e
3 mm
53B
a
b
2 mm
c
d
53C
2 mm
a
b
f
c
e
d

Plate XIV

Figure 54 A. *Locustella* † *kordosi* nova sp. – humerus dext. (Polgárdi, MÁFI V.11.104.1; V.29179), caudal view, a. *tuberculum dorsale*; b. *caput humeri*; c. *tuberculum ventrale*; e. *crus fossae*; f. *fossae pneumotricipitalis*.

Figure 54 B. *Locustella* † *kordosi* nova sp. – humerus dext. (Polgárdi, MÁFI V.11.104.1; V.29179), cranial view, d. *crista bicipitalis.*

Figure 54 C. *Locustella* † *kordosi* nova sp. – ulna sin. (Polgárdi, MÁFI V.11.111.1, V.29186), medial view, a. *condylus dorsalis*; b. *sulcus intercondylaris*; c. *condylus ventralis*; d. *tuberculum carpale.*

Figure 54 D. *Locustella* † *kordosi* nova sp. – tibiotarsus dext. (Polgárdi, MÁFI V.11.126.9; V.29201), cranial view, a. *tuberositas retinaculi m. fibularis*; b. *sulcus extensorius*; c. *pons supratendineus*; d. *condylus lateralis*; e. *incisura intercondylaris*; f. *condylus medialis.*

Figure 55 A. *Locustella* † *janossyi* nova sp. – humerus sin. (Beremend, BKA), cranial view: a. *tuberculum supracondylare ventrale*; b. *epicondylus ventralis*; c. *processus flexorius*; d. *condylus ventralis*; e. *incisura intercondylaris*; f. *condylus dorsalis*; g. *epicondylus dorsalis*; h. *processus supracondylaris dorsalis.*

Figure 55 B. *Locustella* † *janossyi* nova sp. – tibiotarsus dext. (Csarnóta, MÁFI V.11.35.1; V.29110), cranial view, a. *tuberositas retinaculi m. fibularis*; b. *sulcus extensorius*; c. *pons supratendineus*; d. *condylus lateralis*; e. *incisura intercondylaris*; f. *condylus medialis.*

Figure 56 A. *Locustella* † *magna* nova sp. – humerus sin. (Beremend, BKA), caudal view: a. *tuberculum dorsale*; b. *caput humeri*; c. *tuberculum ventrale*; d. *crista bicipitalis*; e. *crus fossae*; f. *fossae pneumotricipitalis*.

Figure 56 B. *Locustella* † *magna* nova sp. – humerus sin. (Beremend, BKA), cranial view: g. *tuberculum supracondylare ventrale*; h. *epicondylus ventralis*; i. *processus flexorius*; j. *condylus ventralis*; k. *incisura intercondylaris*; l. *condylus dorsalis*; m. *epicondylus dorsalis*; n. *processus supracondylaris dorsalis.*

Figure 57. *Regulus pliocaenicus* nova sp. – humerus sin. (Beremend, BKA), caudal view: a. *tuberculum dorsale*; b. *caput humeri*; c. *tuberculum ventrale*; d. *crista bicipitalis*; e. *crus fossae*; f. *fossae pneumotricipitalis*; g. *processus supracondylaris dorsalis.*

Plate XIV

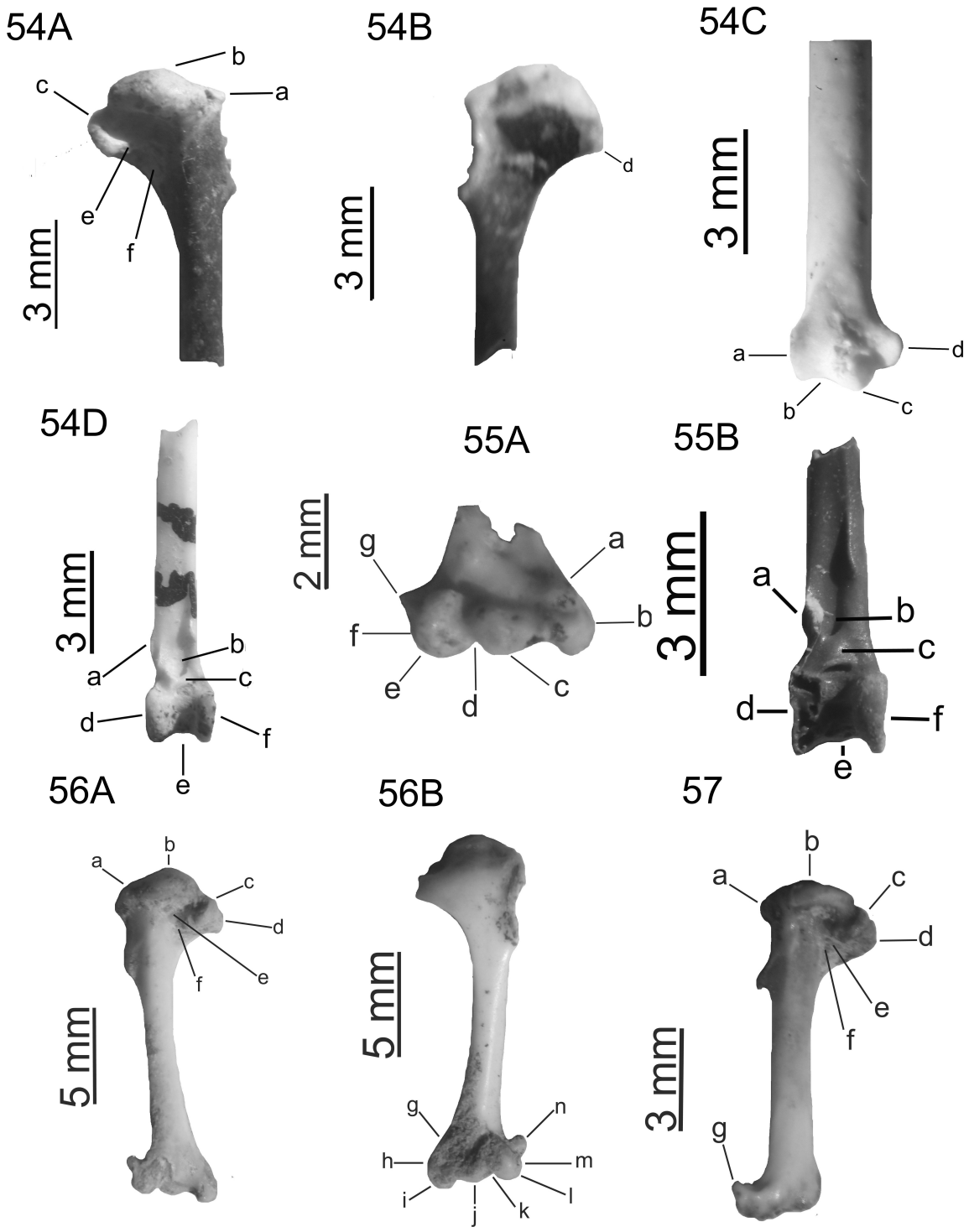
54A
b
c
a
e
f
3 mm
54B
d
3 mm
54C
3 mm
a
d
b
c
54D
3 mm
b
a
c
d
f
e
55A
2 mm
g
a
f
b
e
d
c
55B
3 mm
a
b
c
d
f
e
56A
b
a
c
d
f
e
5 mm
56B
5 mm
g
n
h
m
i
l
j
k
57
b
a
c
d
e
f
3 mm
g

Plate XV

Figure 58 A. *Phylloscopus* †*venczeli* nova sp. – ulna sin. (Polgárdi, MÁFI V.11.89.4; V.29164/1), cranial view, a. *oleocranon*; b. *cotyla dorsalis* c. *cotyla ventralis*; d. *tuberculum lig. colat. ventralis,* e. *depressio m. brachialis.*

Figure 58 B. *Phylloscopus* †*venczeli* nova sp. – ulna sin. (Polgárdi, MÁFI V.11.89.4; V.29164/1), medial view, f. *condylus dorsalis*; g. *sulcus intercondylaris*; h. *condylus ventralis*; i. *tuberculum carpale.*

Figure 58 C. *Phylloscopus* †*venczeli* nova sp. – carpometacarpus dext. (Polgárdi, MÁFI V.11.74.1; V.29149), ventral view, a. *trochlea carpalis*; b. *proc. extensorius*; c. *processus alularis;* d. *fovea subalularis.*

Figure 59. *Phylloscopus* † *pliocaenicus* nova sp. – humerus dext. (Csarnóta, MÁFI V.11.3.1; V.29078), cranial view, a. *tuberculum supracondylare ventrale*; b. *epicondylus* vedntralis; c. *processus flexorius*; d. *condylus ventralis*; e. *incisura intercondylaris*; f. *condylus dorsalis*; g. *epicondylus dorsalis*; h. *processus supracondylaris dorsalis.*

Figure 60 A. *Anthus* †*hiri* nova sp. – carpometacarpus dext. (Polgárdi, MÁFI V.11.98.1; V.29173), ventral view, a. *trochlea carpalis*; b. *proc. extensorius*; c. *processus alularis*; e. *protuberantia metacarpalis.*

Figure 60 B. *Anthus* † *hiri* nova sp. – carpometacarpus dext. (Polgárdi, MÁFI V.11.98.1; V.29173), dorsal view, d. *fovea subalularis.*

Figure 60 C. *Anthus* † *hiri* nova sp. – tarsometatarsus sin. (Polgárdi, MÁFI V.11.122.3; V.29197), dorsal view, a. *trochlea metatarsi* II.; b. *incisura intertrochlearis medialis*; c. *trochlea metatarsi* III.; d. *incisura intertrochlearis lateralis*; e. *trochlea* metatarsi IV.

Figure 61 A. *Anthus* † *baranensis* nova sp. – coracoideum dext. (Csarnóta, MÁFI V.11.8.1; V.29083). dorsal view, a. *acrocoracoideum*; b. *processus accesorius*; c. *sulcus m. supracoracoidei*; d. *processus procoracoidei*.

Figure 61 B. *Anthus* † *baranensis* nova sp. – ulna sin. (Csarnóta, MÁFI V.11.36.1; V.29111). caudal view, a. *condylus dorsalis*; b. *sulcus intercondylaris*; c. *condylus ventralis*; d. *tuberculum carpale.*

Plate XV

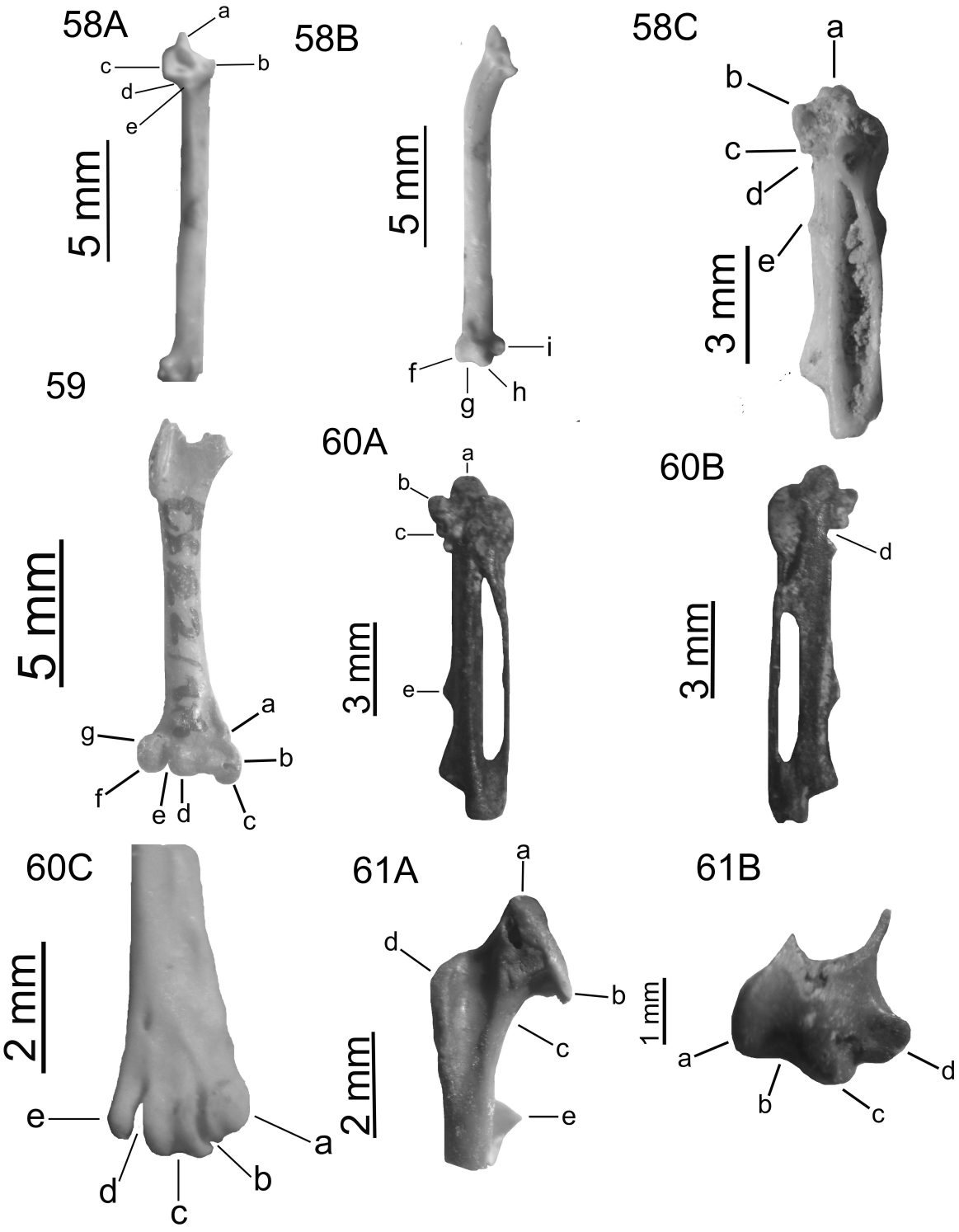
58A
a
b
c
d
e
5 mm
58B
5 mm
i
f
g
h
58C
a
b
c
d
e
3 mm
59
5 mm
a
g
b
f
e
d
c
60A
a
b
c
3 mm
e
60B
d
3 mm
60C
2 mm
e
a
d
b
c
61A
a
d
b
c
2 mm
e
61B
1 mm
a
d
b
c

Plate XVI

Figure 62 A. *Motacilla* †*intermedia* nova sp. – humerus dext. (Polgárdi, MÁFI V.11.114.7, V.29189/1), caudal view, a. *tuberculum dorsale*; b. *caput humeri*; c. *tuberculum ventrale*; d. *crista biccipitalis;* e. *fossae pneumotricipitalis*.

Figure 62 B. *Motacilla* †*intermedia* nova sp. – humerus dext. (Polgárdi, MÁFI V.11.114.7, V.29189/2), cranial view, f. *epicondylus ventralis*; g. *processus flexorius*; h. *condylus ventralis*; i. *incisura intercondylaris*; j *condylus dorsalis*; k. *epicondylus dorsalis*; l. *processus supracondylaris dorsalis.*

Figure 62 C. *Motacilla* †*intermedia* nova sp. – ulna sin. (Polgárdi, MÁFI V.11.114.7, V.29189/3), medial view, a. *condylus dorsalis*; b. *sulcus intercondylaris*; c. *condylus ventralis*; d. *tuberculum carpale.*

Figure 62 D. *Motacilla* †*intermedia* nova sp. – carpometacarpus sin. (Polgárdi, MÁFI V.11.119.9; V.29154/1), ventral view, a. *trochlea carpalis*; b. *proc. extensorius*; c. *processus alularis*; d. *fovea subalularis*; e. *protuberantia metacarpalis.*

Figure 62 E. *Motacilla* †*intermedia* nova sp. – femur sin. (Polgárdi, MÁFI V.11.119.9; V.29154/2), caudal view, a. *trochlea fibularis*; b. *condylus lateralis*; c. *incisura intercondylaris*; d. *condylus medialis*; e. *epicondylus medialis.*

Figure 62 F. *Motacilla* †*intermedia* nova sp. – tibiotarsus dext. (Polgárdi, MÁFI V.11.119.9; V.29154/3), cranial view, a. *tuberositas retinaculi m. fibularis*; b. *sulcus extensorius*; c. *pons supratendineus*; d. *condylus lateralis*; e. *incisura intercondylaris*; f. *condylus medialis.*

Figure 62 G. *Motacilla* †*intermedia* nova sp. – tarsometatarsus sin. (Polgárdi, MÁFI V.11.119.9; V.29154/4), dorsal view, a. *trochlea metatarsi* II.; b. *incisura intertrochlearis medialis*; c. *trochlea metatarsi* III.; d. *incisura intertrochlearis lateralis*; e. *trochlea* metatarsi IV.

Figure 63. *Motacilla minor* nova sp. – carpometacarpus dext. (Beremend, BKA), ventral view: a. *trochlea carpalis*; b. *processus extensorius;* c. *processus alularis*; d. *fovea subalularis*; e. *protuberantia metacarpalis.*

Figure 64. *Motacilla robusta* nova sp. – humerus sin. (Beremend, BKA), caudal view: a. *tuberculum dorsale*; b. *caput humeri*; c. *tuberculum ventrale*; d. *crista bicipitalis*; e. *crus fossae*; f. *fossae pneumotricipitalis*.

Plate XVI

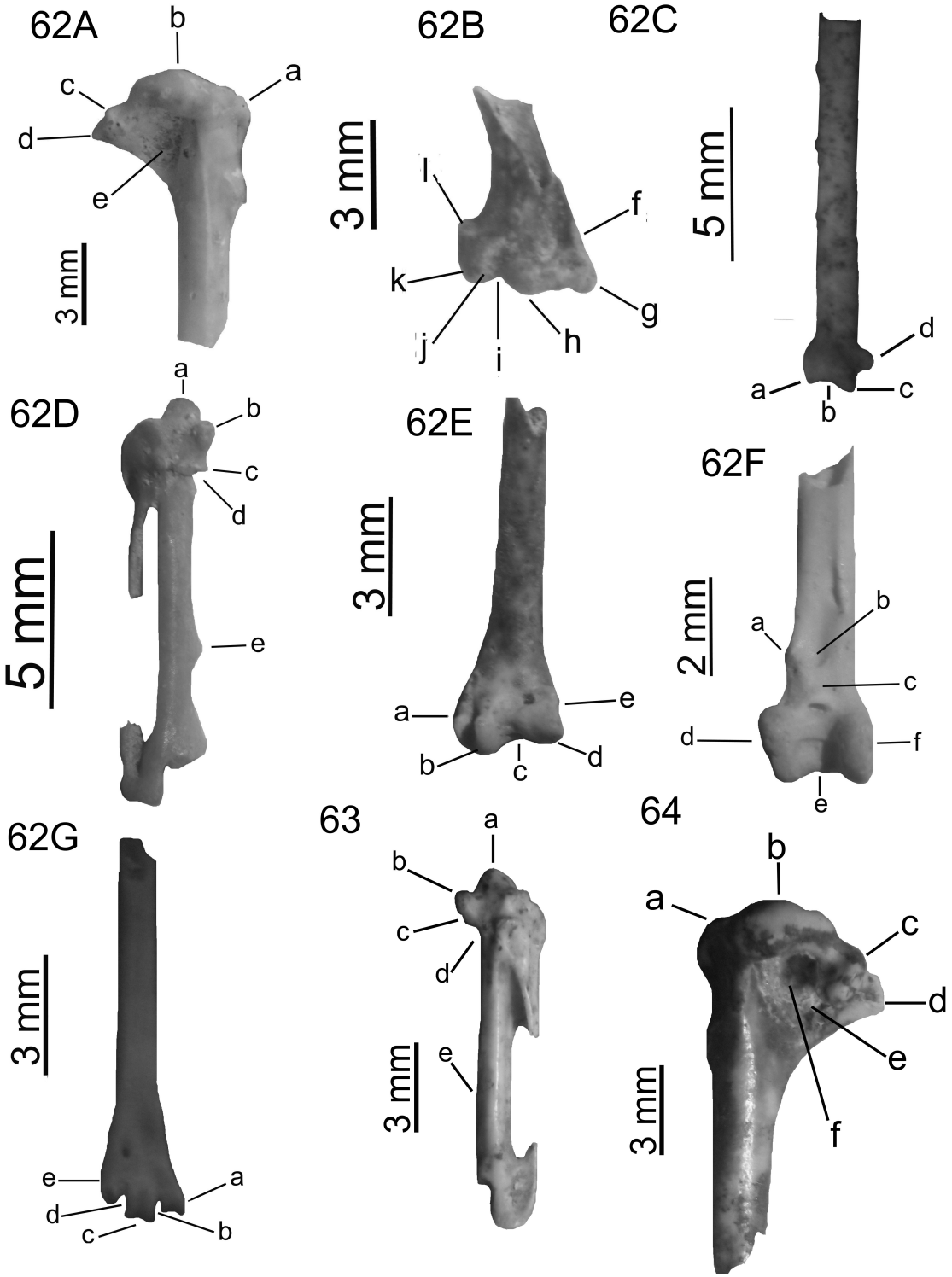
62A
b
a
c
d
e
3 mm
62B
3 mm
l
f
k
g
j
i
h
62C
5 mm
d
a
c
b
62D
a
b
c
d
5 mm
e
62E
3 mm
a
e
b
c
d
62F
2 mm
a
b
c
d
f
e
62G
3 mm
e
a
d
c
b
63
a
b
c
d
3 mm
e
64
b
a
c
d
e
f
3 mm

Plate XVII

Figure 65 A. *Bombycilla* † *brevia* nova sp. – coracoid dext. (Polgárdi, MÁFI V.11.96.1; V.29171), dorsal view, a. *acrocoracoid*; b. *processus accesorius*; c. *sulcus m. supracoracoidei*; d. *processus procoracoidei*; e. *facies articularis humeralis.*

Figure 65 B. *Bombycilla* † *brevia* nova sp. – humerus dext. (Polgárdi, MÁFI V.11.120.2; V.29195/1), cranial view, a. *epicondylus ventralis*; b. *processus flexorius*; c. *condylus ventralis*; d. *incisura intercondylaris*; e *condylus dorsalis*; f. *epicondylus dorsalis*; g. *processus supracondylaris dorsalis.*

Figure 65 C. *Bombycilla* † *brevia* nova sp. – tibiotarsus sin. (Polgárdi, MÁFI V.11.120.2; V.29195/2), cranial view, a. *tuberositas retinaculi m. fibularis*; b. *sulcus extensorius*; c. *pons supratendineus*; d. *condylus lateralis*; e. *incisura intercondylaris*; f. *condylus medialis.*

Figure 66 A. *Bombycilla* † *kubinyii* nova sp. – humerus sin. (Beremend, BKA), cranial view: a. *tuberculum supracondylare ventrale*; b. *epicondylus ventralis*; c. *processus flexorius*; d. *condylus ventralis*; e. *incisura intercondylaris*; f. *condylus dorsalis*; g. *epicondylus dorsalis*; h. *processus supracondylaris dorsalis.*

Figure 66 B. *Bombycilla* † *kubinyii* nova sp. – tibiotarsus sin. (Beremend, BKA). cranial view, a. *tuberositas retinaculi m. fibularis*; b. *sulcus extensorius*; c. *pons supratendineus*; d. *condylus lateralis*; e. *incisura intercondylaris*; f. *condylus medialis.*

Figure 67 A. *Troglodytes* †*robustus* nova sp. – humerus sin. (Polgárdi, MÁFI V.11.64.1; V.29139), caudal view, a. *tuberculum dorsale*; b. *caput humeri*; c. *tuberculum ventrale*; d. *crista bicipitalis*; e. *crus fossae*; f. *fossae pneumotricipitalis*; g. *margo caudalis.*

Figure 67 B. *Troglodytes* † *robustus* nova sp. – humerus sin. (Polgárdi, MÁFI V.11.64.1; V.29139), cranial view, h. *epicondylus ventralis*; i. *processus flexorius*; j. *condylus ventralis*; k. *incisura intercondylaris*; l. *condylus dorsalis*; m. *epicondylus dorsalis*; n. *processus supracondylaris dorsalis.*

Figure 67 C. *Troglodytes* † *robustus* nova sp.– ulna dext. (Polgárdi, MÁFI V.11.121.3; V.29196/1), cranial view, a. *oleocranon* b. *cotyla dorsalis*; c. *cotyla ventralis*; d. *tuberculum lig. colat. ventralis*; e. *depressio m. brachialis*.

Figure 67 D. *Troglodytes* † *robustus* nova sp. – carpometacarpus dext. (Polgárdi, MÁFI V.11.121.3; V.29196/2), ventral view, a. *trochlea carpalis*; b. *proc. extensorius*; c. *processus alularis*; d. *fovea subalularis*; e. *protuberantia metacarpalis.*

Figure 67 E. *Troglodytes* † *robustus* nova sp. – tibiotarsus sin. (Polgárdi, MÁFI V.11.121.3; V.29196/3), cranial view, a. *tuberositas retinaculi m. fibularis*; b. *sulcus extensorius*; c. *pons supratendineus*; d. *condylus lateralis*; e. *incisura intercondylaris*; f. *condylus medialis*; g. *arrow transverses*.

Plate XVII

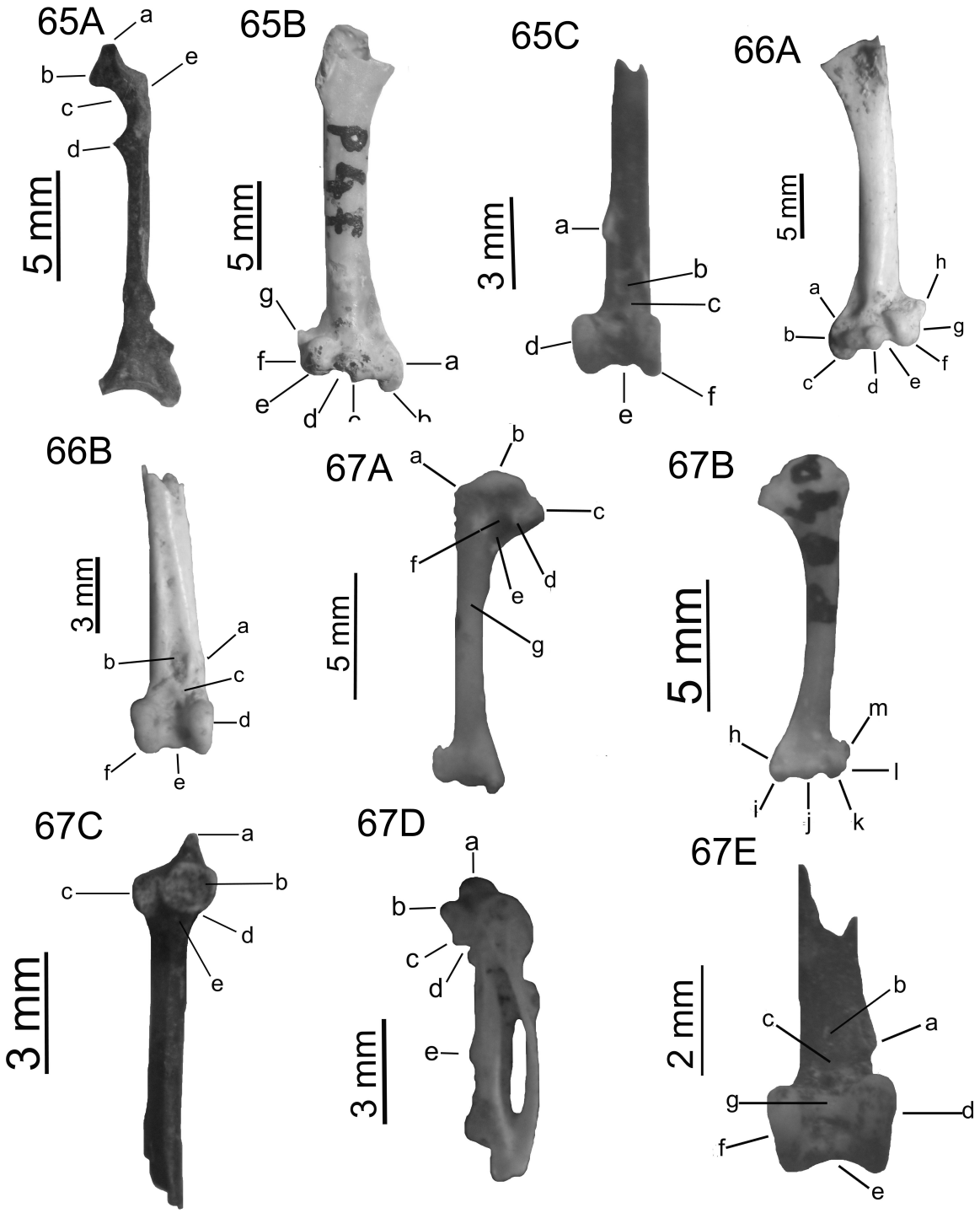
65A
a
b
c
d
e
5 mm
65B
5 mm
g
f
a
e
d
65C
3 mm
a
b
c
d
e
f
66A
5 mm
h
a
b
g
c
d
e
f
66B
3 mm
a
b
c
d
f
e
67A
b
a
c
f
d
e
g
5 mm
67B
5 mm
m
h
l
i
j
k
67C
a
c
b
d
e
3 mm
67D
a
b
c
d
e
3 mm
67E
2 mm
b
c
a
g
d
f
e

Plate XVIII

Figure 68. *Cinclus* † *gaspariki* nova sp. – carpometacarpus sin. (Polgárdi, MÁFI V.11.99.1; V.29174), ventral view, a. *trochlea carpalis*; b. *proc. extensorius*; c. *processus alularis*; d. *fovea subalularis.*

Figure 69. *Cinclus* †*minor* nova sp. – ulna dext. (Csarnóta, MÁFI V.11.9.1, V.29084), caudal view, a. *condylus dorsalis*; b. *sulcus intercondylaris*; c. *condylus ventralis*; d. *tuberculum carpale.*
Figure 70 A. *Prunella* †*freudenthali* nova sp. – humerus sin. (Polgárdi, MÁFI V.11.101.1, V.29176), caudal view, a. *tuberculum dorsale*; b. *caput humeri*; c. *tuberculum ventrale*; d. *crista bicipitalis*; e. *crus fossae*; f. *fossae pneumotricipitalis.*

Figure 70 B. *Prunella* †*freudenthali* nova sp. – ulna sin. (Polgárdi, MÁFI V.11.123.5; V.29198/1), medial view, a. *condylus dorsalis*; b. *sulcus intercondylaris*; c. *condylus ventralis*; d. *tuberculum carpale.*

Figure 70 C. *Prunella* †*freudenthali* nova sp. – femur dext. (Polgárdi, MÁFI V.11.123.5; V.29198/2), caudal view, a. *trochlea fibularis*; b. *condylus lateralis*; c. *incisura intercondylaris*; d. *condylus medialis*; e. *epicondylus medialis.*

Figure 71 A. *Prunella* †*kormosi* nova sp. – coracoideum sin. (Csarnóta, MÁFI V.11.4.1; V.29079), dorsal view, a. *acrocoracoideum*; b. *processus accesorius*; c. *sulcus m. supracoracoidei*; d. *processus procoracoidei*.

Figure 71 B. *Prunella* †*kormosi* nova sp. – humerus dext. (Csarnóta, MÁFI V.11.40.5; V.29155), caudal view, a. *tuberculum dorsale*; b. *caput humeri*; c. *tuberculum ventrale*; d. *crista bicipitalis*; e. *crus fossae*; f. *fossae pneumotricipitalis*.

Figure 71 C. *Prunella* †*kormosi* nova sp. – ulna sin. (Csarnóta, MÁFI V.11.40.6; V.29155), medial view, a. *condylus dorsalis*; b. *sulcus intercondylaris*; c. *condylus ventralis*; d. *tuberculum carpale.*

Figure 71 D. *Prunella* †*kormosi* nova sp. – tarsometatarsus dext. (Beremend, BKA), dorsal view: a. edge between *metatarsus* I. and *trochlea metatarsi* II.; b. *trochlea metatarsi* II.; c. *incisura intertrochlearis medialis*; d. *trochlea metatarsi* III.; e. *incisura intertrochlearis lateralis*; f. *trochlea metatarsi* IV.

Plate XVIII

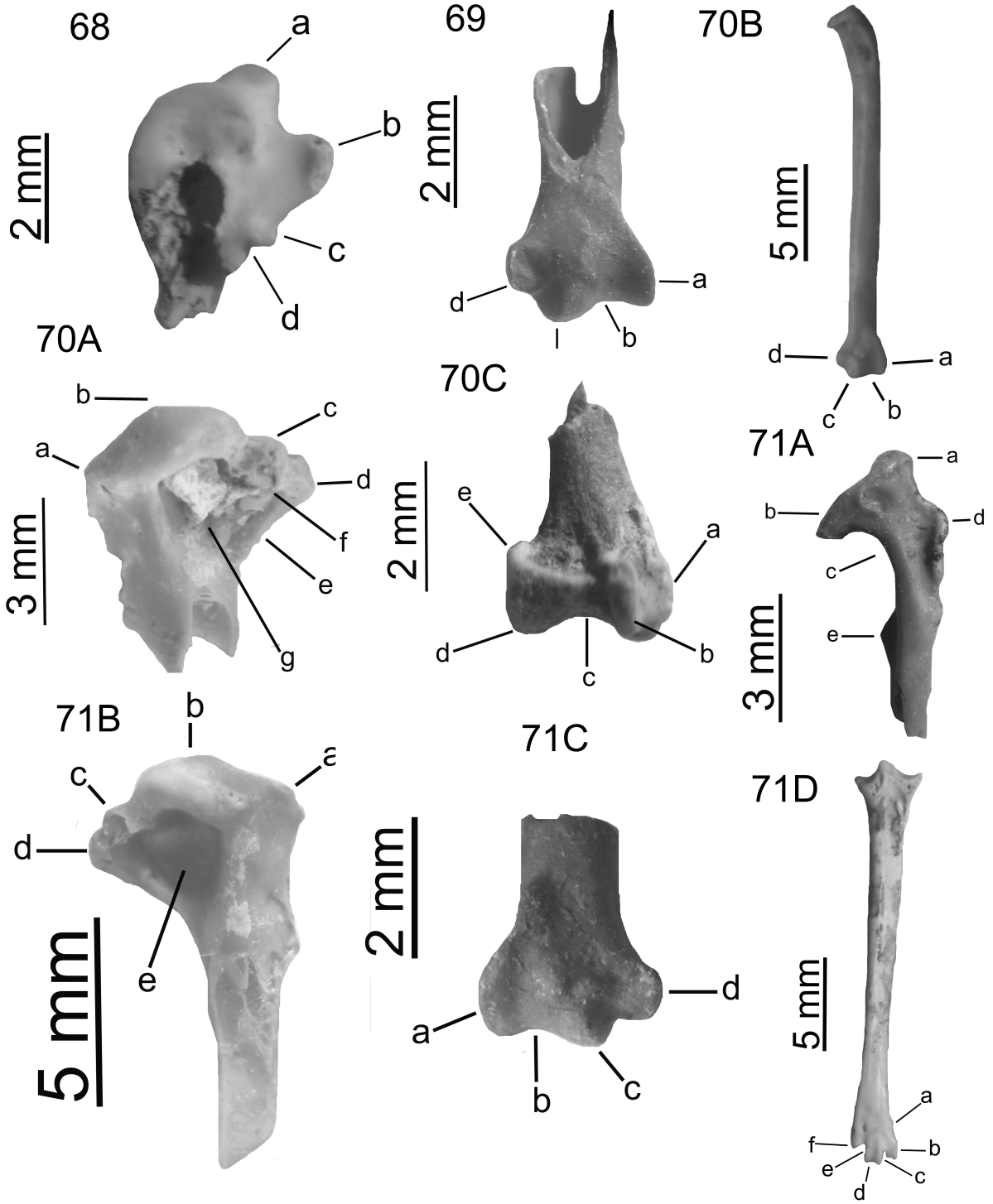
68
a
b
c
d
2 mm
69
2 mm
a
d
b
70B
5 mm
d
a
c
b
70A
b
c
a
d
f
e
g
3 mm
70C
e
a
2 mm
d
c
b
71A
a
b
d
c
e
3 mm
71B
b
c
a
d
e
5 mm
71C
2 mm
d
a
b
c
71D
5 mm
a
f
b
e
c
d

Plate XIX

Figure 72. *Lanius* †*capeki* nova sp. – coracoid dext. (Polgárdi, MÁFI V.11.54.1; V.29129), dorsal view, a. *acrocoracoid*; b. *processus acessorius*; c. *sulcus m. supracoracoidei*; d. *facies aricularis humeralis*; e. *processus procoracoidei*.

Figure 73 A. *Lanius* † *hungaricus* nova sp. – coracoideum sin. (Csarnóta, MÁFI V.11.5.1; V.29080), dorsal view, a. *acrocoracoideum*; b. *processus accesorius*; c. *sulcus m. supracoracoidei*;

Figure 73 B. *Lanius* † *hungaricus* nova sp. – coracoideum sin. (Csarnóta, MÁFI V.11.5.1; V.29080), ventral view. d. *processus procoracoidei*.

Figure 73 C. *Lanius* † *hungaricus* nova sp. – scapula sin. (Csarnóta, MÁFI V.1.41.2; V.29116), lateral view. a. *acromion – costal branch*; b. edge between branches; c. *acromion – lateral branch*; d. *facies atricularis humeralis.*

Figure 73 D. *Lanius* † *hungaricus* nova sp. – carpometacarpus sin. (Csarnóta, MÁFI V.1.41.3; V.29116), ventral view, a. *trochlea carpalis*; b. *proc. extensorius*; c. *processus alularis.*
Figure 73 E. *Lanius* † *hungaricus* nova sp. – carpometacarpus sin. (Csarnóta, MÁFI V.1.41.3; V.29116). dorsal view, d. *fovea subalularis.*

Figure 74 A. *Lanius* † *major* nova sp. – humerus dext. (Beremend, BKA), caudal view: a. *tuberculum dorsale*; b. *caput humeri*; c. *tuberculum ventrale*; d. *crista bicipitalis*; e. *fossae pneumotricipitalis*.

Figure 74 B. *Lanius* † *major* nova sp. – humerus dext. (Beremend, BKA), cranial view: f. *tuberculum supracondylare ventrale*; g. *epicondylus ventralis*; h. *processus flexorius*; i. *condylus ventralis*; j. *incisura intercondylaris*; k. *condylus dorsalis*; l. *epicondylus dorsalis*; m. *processus supracondylaris dorsalis.*

Figure 74 C. *Lanius* † *major* nova sp. – carpometacarpus sin. (Beremend, BKA), ventral view: a. *trochlea carpalis*; b. *processus extensorius;* c. *processus alularis*; d. *fovea subalularis*; e. *protuberantia metacarpalis.*

Figure 74 D. *Lanius* † *major* nova sp. – tarsometatarsus dext. (Beremend, BKA), dorsal view: a. edge between *metatarsus* I. and *trochlea metatarsi* II.; b. *trochlea metatarsi* II.; c. *incisura intertrochlearis medialis*; d. *trochlea metatarsi* III.; e. *incisura intertrochlearis lateralis*; f. *trochlea metatarsi* IV.

Plate XIX

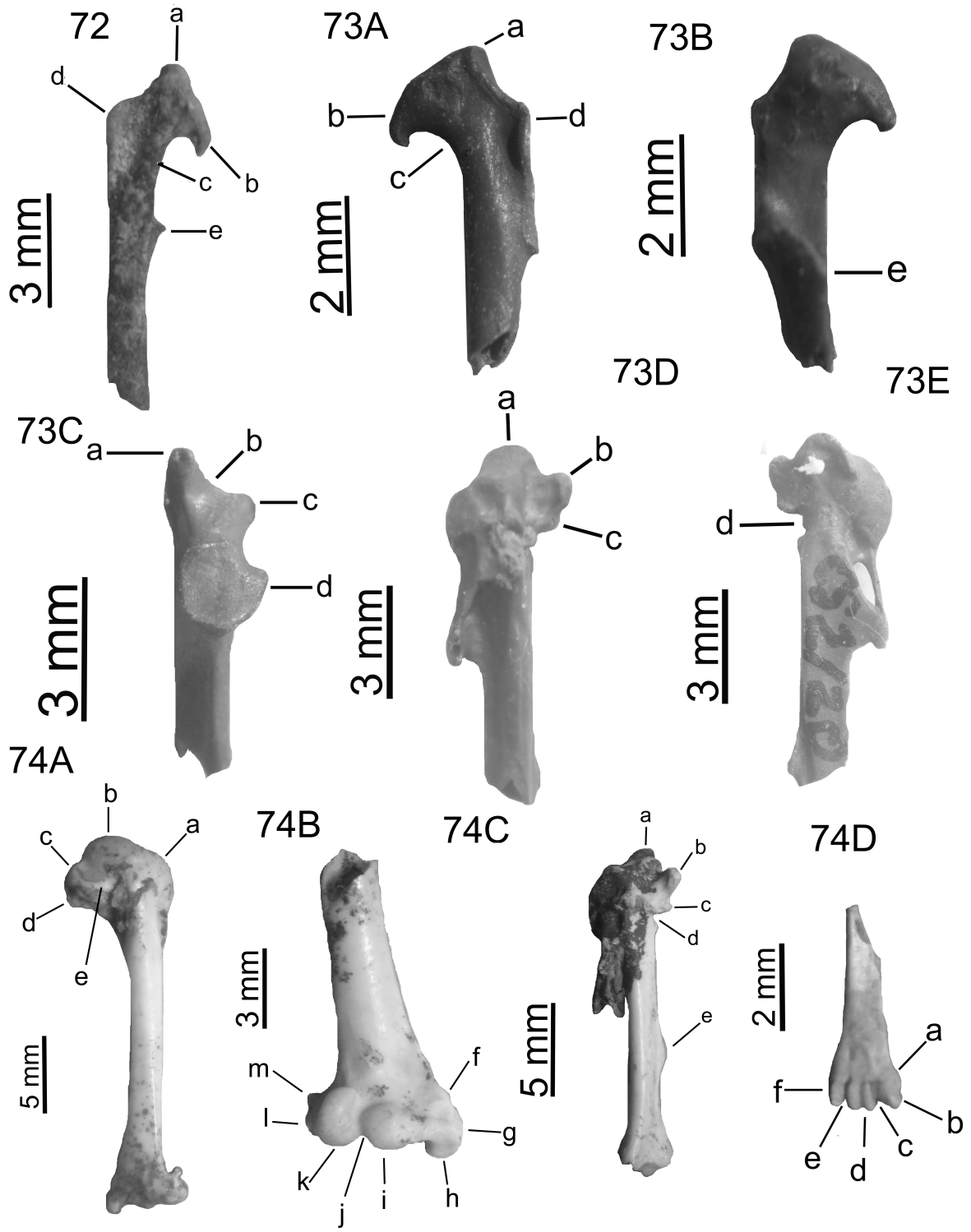
72
a
d
c
b
e
3 mm
73A
a
b
d
c
2 mm
73B
2 mm
e
73D
73E
73C
a
b
c
d
3 mm
a
b
c
3 mm
d
3 mm
74A
b
c
a
d
e
5 mm
74B
3 mm
m
f
l
g
k
j
i
h
74C
a
b
c
d
e
5 mm
74D
2 mm
a
f
b
e
d
c

Plate XX

Figure 75 A. *Lanius* † *intermedius* nova sp. – humerus dext. (Beremend, BKA), caudal view: a. *tuberculum dorsale*; b. *caput humeri*; c. *tuberculum ventrale*; d. *crista bicipitalis*; e. *crus fossae*; f. *fossae pneumotricipitalis*.

Figure 75 B. *Lanius* † *intermedius* nova sp. – carpometacarpus dext. (Beremend, BKA), ventral view: a. *trochlea carpalis*; b. *processus extensorius;* c. *processus alularis*; d. *fovea subalularis*; e. *protuberantia metacarpalis.*

Figure 76 A. *Sturnus* † *brevis* nova sp. – coracoid dext. (Polgárdi, MÁFI V.11.55.1, V.29130), dorsal view, a. *acrocoracoid*; b. *processus acessorius*; c. *sulcus m. supracoracoidei*; d. *facies aricularis humerális*; e. *processus procoracoidei*.

Figure 76 B. *Sturnus* † *brevis* nova sp. – humerus dext. (Polgárdi, MÁFI V.11.115.2; V.29190/1), cranial view, a. *tuberculum supracondylare ventrale*; b. *epicondylus ventralis*; c. *processus flexorius*; d. *condylus ventralis*; e. *incisura intercondylaris*; f. *condylus dorsalis*; g. *epicondylus dorsalis*; h. *processus supracondylaris dorsalis.*

Figure 76 C. *Sturnus* † *brevis* nova sp. – tibiotarsus dext. (Polgárdi, MÁFI V.11.115.2; V.29190/2), cranial view, a. *tuberositas retinaculi m. fibularis*; b. *sulcus extensorius*; c. *pons supratendineus*; d. *condylus lateralis*; e. *incisura intercondylaris*; f. *condylus medialis.*

Figure 77 A. *Sturnus* † *pliocaenicus* nova sp. – humerus dext. (Beremend, BKA), caudal view: a. *tuberculum dorsale*; b. *caput humeri*; c. *tuberculum ventrale*; d. *crista bicipitalis*; e. *crus fossae*; f. *fossae pneumotricipitalis*.

Figure 77 B. *Sturnus* † *pliocaenicus* nova sp. – humerus dext. (Beremend, BKA), cranial view: g. *tuberculum supracondylare ventrale*; h. *epicondylus ventralis*; i. *processus flexorius*; j. *condylus ventralis*; k. *incisura intercondylaris*; l. *condylus dorsalis*; m. *epicondylus dorsalis*; n. *processus supracondylaris dorsalis.*

Figure 77 C. *Sturnus* † *pliocaenicus* nova sp. – tarsometatarsus dext. (Beremend, BKA), dorsal view: a. edge between *metatarsus* I. and *trochlea metatarsi* II.; b. *trochlea metatarsi* II.; c. *incisura intertrochlearis medialis*; d. *trochlea metatarsi* III.; e. *incisura intertrochlearis lateralis*; f. *trochlea metatarsi* IV.

Figure 78 A. *Sturnus* † *baranensis* nova sp. – humerus dext. (Beremend, BKA), caudal view: a. *tuberculum ventrale*; b. *crista bicipitalis*; c. *crus fossae*; d. *fossae pneumotricipitalis*.

Figure 78 B. *Sturnus* † *baranensis* nova sp. – humerus dext. (Beremend, BKA), cranial view: e. *tuberculum supracondylare ventrale*; f. *condylus ventralis*; g. *incisura intercondylaris*; h. *condylus dorsalis*; i. *epicondylus dorsalis*; j. *processus supracondylaris dorsalis.*

Plate XX

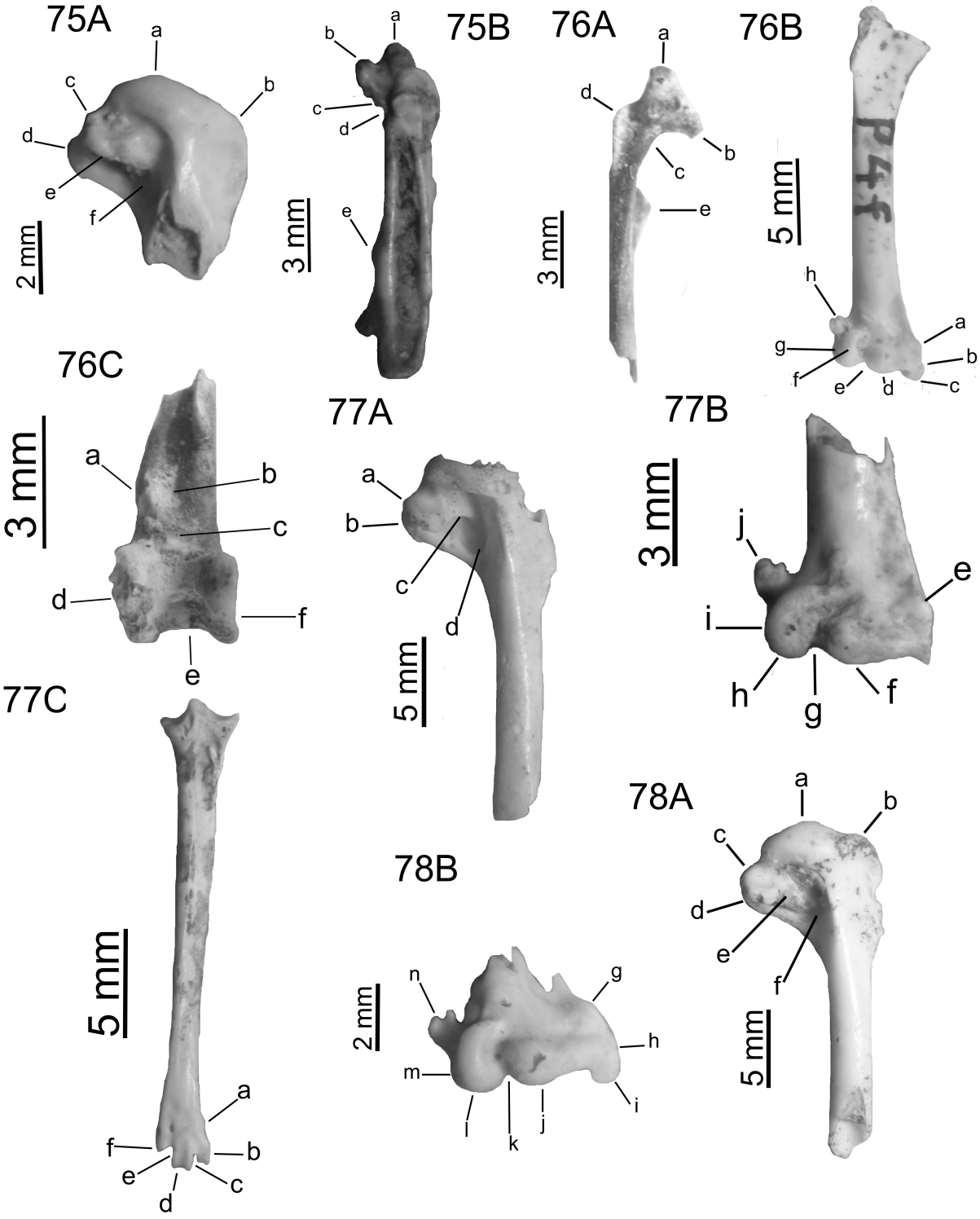
75A
a
b
c
d
e
f
2 mm
75B
a
b
c
d
e
3 mm
76A
a
b
c
d
e
3 mm
76B
P4f
5 mm
h
g
f
e
d
c
b
a
76C
3 mm
a
b
c
d
e
f
77A
a
b
c
d
5 mm
77B
3 mm
j
i
e
h
g
f
77C
5 mm
a
b
c
d
e
f
78A
a
b
c
d
e
f
5 mm
78B
2 mm
n
g
h
m
i
l
k
j

Plate XXI

Figure 79 A. *Passer* † *hiri* nova sp. – ulna sin. (Polgárdi, MÁFI V.11.61.1, V.29136); cranial view, a. *oleocranon* b. *cotyla dorsalis*; c. *cotyla ventralis*; d. *tuberculum lig. colat. ventralis*; e. *depressio m. brachialis*.

Figure 79 B. *Passer* † *hiri* nova sp. – carpometacarpus sin. (Polgárdi, MÁFI V.11.78.4; V.29153/1), ventral view, a. *trochlea carpalis*; b. *proc. extensorius*; c. *processus alularis*; d. *fovea subalularis*; e. *protuberantia metacarpalis.*

Figure 79 C. *Passer* † *hiri* nova sp. – tibiotarsus sin. (Polgárdi, MÁFI V.11.78.4; V.29153/2), cranial view, a. *tuberositas retinaculi m. fibularis*; b. *sulcus extensorius*; c. *pons supratendineus*; d. *condylus lateralis*; e. *incisura intercondylaris*; f. *condylus medialis.*

Figure 80. *Passer* † *minusculus* nova sp. – coracoideum dext. (Csarnóta, MÁFI V.11.6.1; V.29081), dorsal view, a. *acrocoracoideum*; b. *processus accesorius*; c. *sulcus m. supracoracoidei*; d. *processus procoracoidei*.

Figure 81. *Passer* † *pannonicus* nova sp. – carpometacarpus sin. (Beremend, BKA), ventral view: a. *trochlea carpalis*; b. *processus alularis*; c. *fovea subalularis*; d. *protuberantia metacarpalis;* e. basis of the *facies articularis digiti major*; f. end of the *os metacarpi minus.*

Figure 82 A. *Fringilla* †*kormosi* nova sp. – coracoid sin. (Polgárdi, MÁFI V.11.75.1; V.29150), dorsal view, a. *acrocoracoid*; b. *processus acessorius*; c. *sulcus m. supracoracoidei*; d. *facies aricularis humerális*; e. *processus procoracoidei*.

Figure 82 B. *Fringilla* †*kormosi* nova sp. – humerus dext. (Polgárdi, MÁFI V.11.56.1; V.29131),), cranial view, a. *tuberculum dorsale*; b. *caput humeri*; c. *tuberculum ventrale*; d. *crista bicipitalis*; f. *tuberculum supracondylare ventrale*; g. *epicondylus ventralis*; h. *processus flexorius*; i. *condylus ventralis*; j. *incisura intercondylaris*; k. *condylus dorsalis*; l. *epicondylus dorsalis*; m. *processus supracondylaris dorsalis.*

Figure 82 C. *Fringilla* †*kormosi* nova sp. – humerus dext. (Polgárdi, MÁFI V.11.56.1; V.29131), caudal view, e. *fossae pneumotricipitalis.*

Figure 83 A. *Fringilla* † *petenyii* nova sp. – tibiotarsusus dext. (Csarnóta, MÁFI 11.49.1; V.29124), cranial view, a. *tuberositas retinaculi m. fibularis*; b. *sulcus extensorius*; c. *pons supratendineus*; d. *condylus lateralis*; e. *incisura intercondylaris*; f. *condylus medialis.*

Figure 83 B. *Fringilla* † *petenyii* nova sp. – tarsometatarsus dext. (Csarnóta, MÁFI V.11.29.1; V.29104), dorsal view, a. *trochlea metatarsi* II.; b. *incisura intertrochlearis medialis*; c. *trochlea metatarsi* III.; d. *incisura intertrochlearis lateralis*; e. *trochlea* metatarsi IV.

Plate XXI

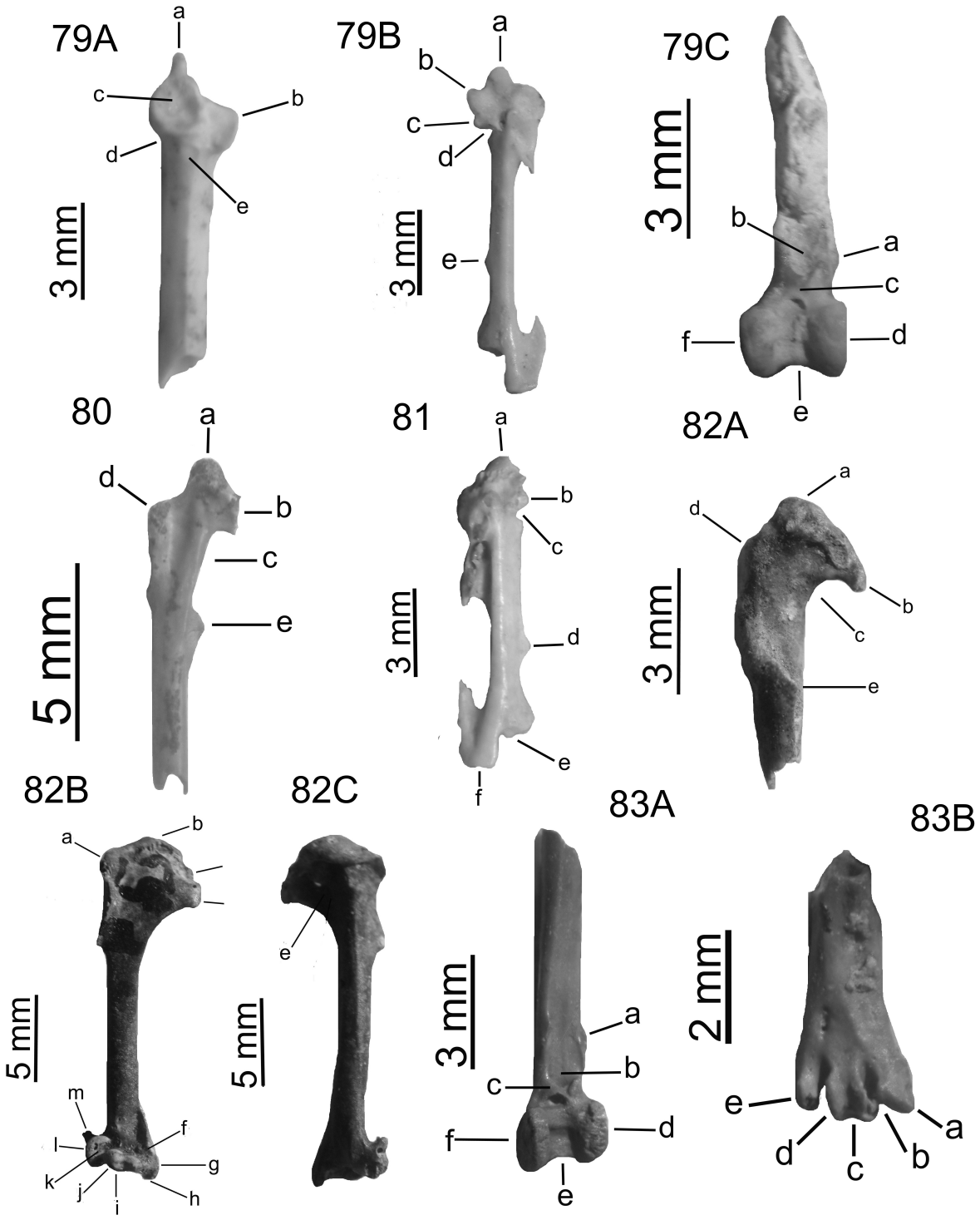

Plate XXII

Figure 84 A. *Carduelis* †*kretzoii* nova sp. – coracoid sin. (Polgárdi, MÁFI V.11.112.9; V.29187/1), dorsal view, a. *acrocoracoid*; b. *processus acessorius*; c. *sulcus m. supracoracoidei*; d. *facies aricularis humeralis*; e. *processus procoracoidei*.

Figure 84 B. *Carduelis* †*kretzoii* nova sp. – humerus dext. (Polgárdi, MÁFI V.V.11.91.1; V.29166), caudal view, a. *tuberculum dorsale*; b. *caput humeri*; c. *tuberculum ventrale*; d. *crista bicipitalis*; e. *fossae pneumotricipitalis.*

Figure 84 C. *Carduelis* †*kretzoii* nova sp. – humerus dext. (Polgárdi, MÁFI V.V.11.91.1; V.29166), cranial view, f. *tuberculum supracondylare ventrale*; g. *epicondylus ventralis*; h. *processus flexorius*; i. *condylus ventralis*; j. *incisura intercondylaris*; k. *condylus dorsalis*; l. *epicondylus dorsalis*; m. *processus supracondylaris dorsalis.*

Figure 84 D. *Carduelis* †*kretzoii* nova sp. – carpometacarpus dext. (Polgárdi, MÁFI V.11.112.9; V.29187/2), ventral view, a. *trochlea carpalis*; b. *proc. extensorius*; c. *processus alularis*; d. *fovea subalularis*; e. *protuberantia metacarpalis.*

Figure 84 E. *Carduelis* †*kretzoii* nova sp. – femur dext. (Polgárdi, MÁFI V.11.116.7; V.29191/1), caudal view, a. *trochlea fibularis*; b. *condylus lateralis*; c. *incisura intercondylaris*; d. *condylus medialis*; e. *epicondylus medialis.*

Figure 84 F. *Carduelis* †*kretzoii* nova sp. – tibiotarsus sin. (Polgárdi, MÁFI V.11.116.7; V.29191/2), cranial view, a. *tuberositas retinaculi m. fibularis*; b. *sulcus extensorius*; c. *pons supratendineus*; d. *condylus lateralis*; e. *incisura intercondylaris*; f. *condylus medialis.*

Figure 85 A. *Carduelis* †*lambrechti* nova sp. – coracoid dext. (Polgárdi, MÁFI V.11.77.4; V.29152), dorsal view, a. *acrocoracoid*; b. *processus acessorius*; c. *sulcus m. supracoracoidei*; d. *facies aricularis humerális*; e. *processus procoracoidei*.

Figure 85 B. *Carduelis* †*lambrechti* nova sp. – humerus sin. (Polgárdi, MÁFI V.11.58.1; V.29133), caudal view, a. *tuberculum dorsale*; b. *caput humeri*; c. *tuberculum ventrale*; d. *crista bicipitalis*; e. *fossae pneumotricipitalis.*

Figure 85 C. *Carduelis* †*lambrechti* nova sp. – humerus sin. (Polgárdi, MÁFI V.11.58.1; V.29133),), cranial view, f. *tuberculum supracondylare ventrale*; g. *epicondylus ventralis*; h. *processus flexorius*; i. *condylus ventralis*; j. *incisura intercondylaris*; k. *condylus dorsalis*; l. *epicondylus dorsalis*; m. *processus supracondylaris dorsalis.*

Plate XXII

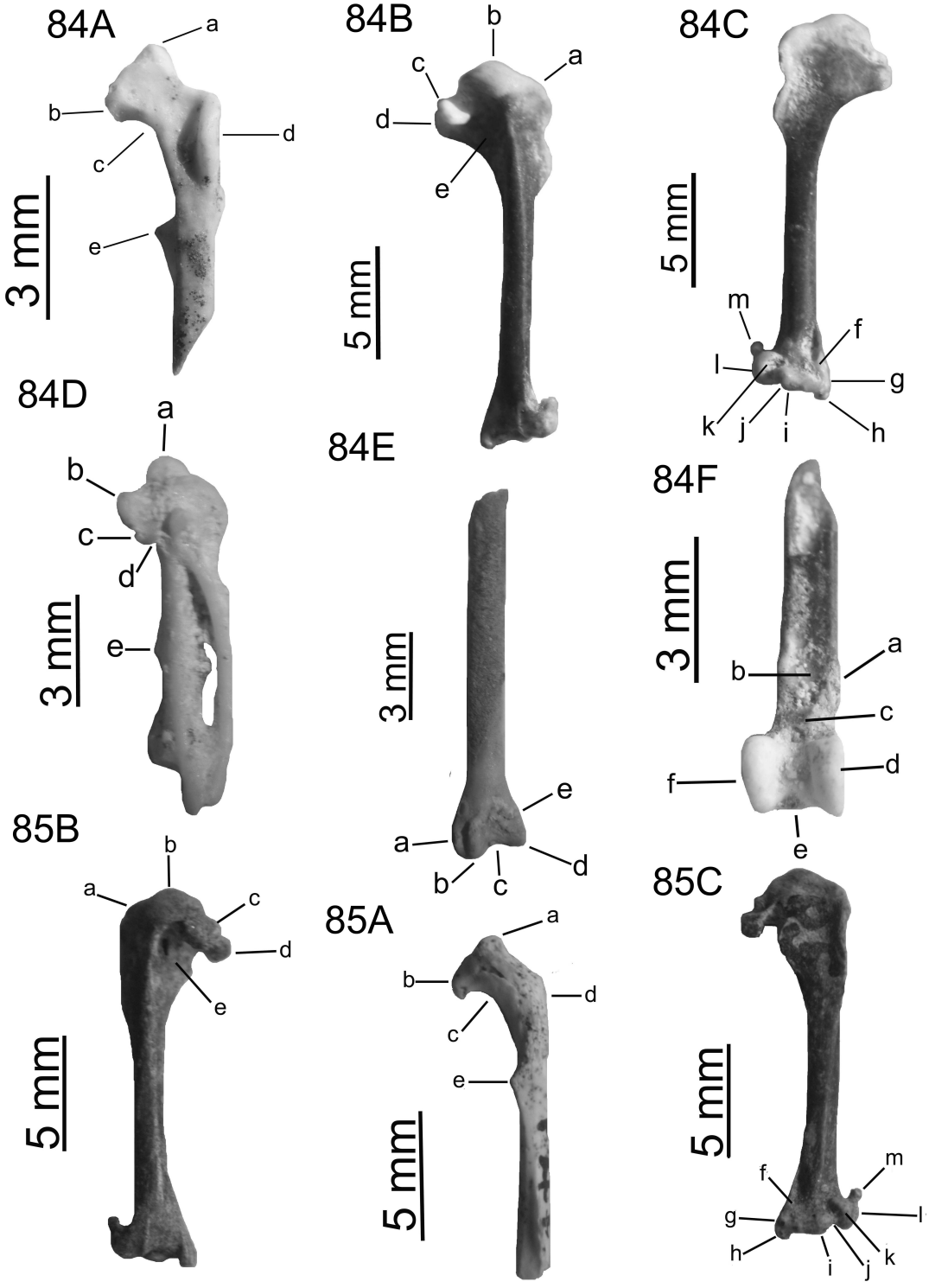
84A
a
b
c
d
e
3 mm
84B
b
c
a
d
e
5 mm
84C
5 mm
m
f
l
g
k
j
i
h
84D
a
b
c
d
e
3 mm
84E
3 mm
e
a
d
b
c
84F
3 mm
a
b
c
d
f
e
85B
b
a
c
d
e
5 mm
85A
a
b
d
c
e
5 mm
85C
5 mm
f
m
g
l
h
i
j
k

Plate XXIII

Figure 86 A. *Carduelis* †*parvulus* nova sp. – coracoideum dext. (Csarnóta, MÁFI V.11.10.1; V.29085), dorsal view, a. *acrocoracoideum*; b. *processus accesorius*; c. *sulcus m. supracoracoidei*; d. *processus procoracoidei*.

Figure 86 B. *Carduelis* †*parvulus* nova sp. – ulna sin. (Csarnóta, MÁFI V.11.37.1; V.29112), medial view, a. *condylus dorsalis*; b. *sulcus intercondylaris*; c. *condylus ventralis*; d. *tuberculum carpale.*

Figure 87. *Carduelis* † *medius* nova sp. – coracoideum sin. (Csarnóta, MÁFI V.11.11.1, V.29086). dorsal view, a. *acrocoracoideum*; b. *processus accesorius*; c. *sulcus m. supracoracoidei*; d. *processus procoracoidei*.

Figure 88 A. *Pyrrhula* † *gali* nova sp. – humerus sin. (Polgárdi, MÁFI V.11.129.1; V.29204), caudal view, a. *tuberculum dorsale*; b. *caput humeri*; c. *tuberculum ventrale*; d. *crista bicipitalis*; e. *fossae pneumotricipitalis.*

Figure 88 B. *Pyrrhula* † *gali* nova sp. – humerus sin. (Polgárdi, MÁFI V.11.129.1; V.29204), cranial view, f. *tuberculum supracondylare ventrale*; g. *epicondylus ventralis*; h. *processus flexorius*; i. *condylus ventralis*; j. *incisura intercondylaris*; k. *condylus dorsalis*; l. *epicondylus dorsalis*; m. *processus supracondylaris dorsalis.*

Figure 88 C. *Pyrrhula* † *gali* nova sp. – ulna sin. (Polgárdi, MÁFI V.11.129.1; V.29204/3), cranial view, a. *oleocranon* b. *cotyla dorsalis*; c. *cotyla ventralis*; d. *tuberculum lig. colat. ventralis*; e. *depressio m. brachialis*.

Figure 89 A. *Pyrrhula* † *minor* nova sp. – coracoideum sin. (Csarnóta, MÁFI V.11.48.2; V.29123), dorsal view, a. *acrocoracoideum*; b. *processus accesorius*; c. *sulcus m. supracoracoidei*; d. *processus procoracoidei*.

Figure 89 B. *Pyrrhula* † *minor* nova sp. – humerus sin. (Csarnóta, MÁFI V.11.12.1, V.29087), cranial view, a. *tuberculum supracondylare ventrale*; b. *epicondylus* vedntralis; c. *processus flexorius*; d. *condylus ventralis*; e. *incisura intercondylaris*; f. *condylus dorsalis*; g. *epicondylus dorsalis*; h. *processus supracondylaris dorsalis.*

Figure 89 C. *Pyrrhula* † *minor* nova sp. – ulna dext. (Csarnóta, MÁFI V.11.48.3; V.29123), medial view, a. *condylus dorsalis*; b. *sulcus intercondylaris*; c. *condylus ventralis*; d. *tuberculum carpale.*

Plate XXIII

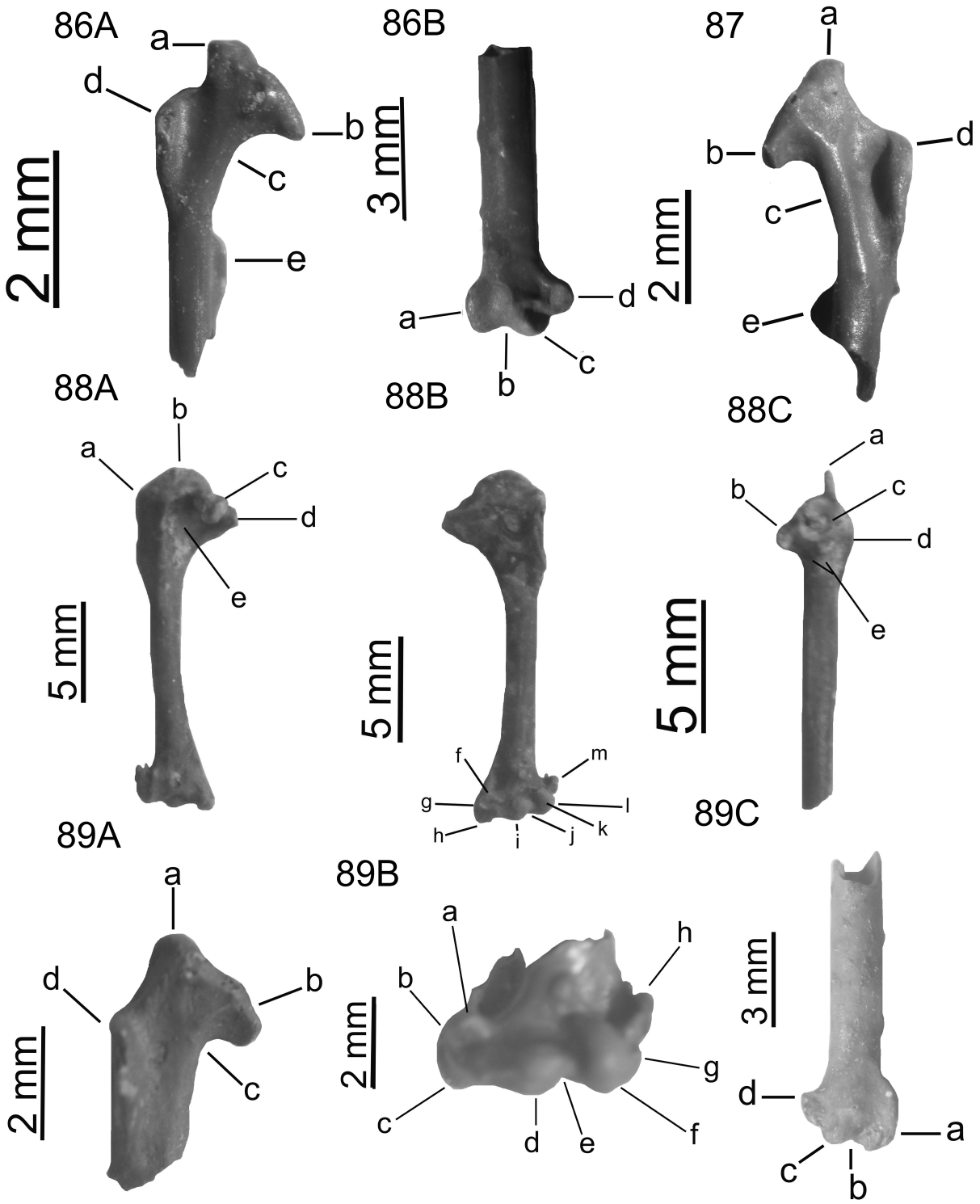
86A
a
d
b
c
e
2 mm
86B
3 mm
a
d
b
c
87
a
b
d
c
e
2 mm
88A
b
a
c
d
e
5 mm
88B
5 mm
f
m
g
l
h
i
j
k
88C
a
b
c
d
e
5 mm
89A
a
d
b
c
2 mm
89B
a
h
b
g
c
d
e
f
2 mm
3 mm
d
a
c
b
89C

Plate XXIV

Figure 90 A. *Loxia* † *csarnotanus* nova sp. – humerus dext. (Csarnóta, MÁFI V.11.30.1; V.29105), cranial view, a. *tuberculum supracondylare ventrale*; b. *epicondylus* vedntralis; c. *processus flexorius*; d. *condylus ventralis*; e. *incisura intercondylaris*; f. *condylus dorsalis*; g. *epicondylus dorsalis*; h. *processus supracondylaris dorsalis.*

Figure 90 B. *Loxia* † *csarnotanus* nova sp. – ulna sin. (Csarnóta, MÁFI V.11.50.1, V.29125). medial view, a. *condylus dorsalis*; b. *sulcus intercondylaris*; c. *condylus ventralis*; d. *tuberculum carpale.*

Figure 90 C. *Loxia* † c*sarnotanus* nova sp. – tibiotarsus dext. (Beremend, BKA), cranial view, a. *tuberositas retinaculi m. fibularis*; b. *sulcus extensorius*; c. *pons supratendineus*; d. *condylus lateralis*; e. *incisura intercondylaris*; f. *condylus medialis.*

Figure 91. *Pinicola* † *kubinyii* nova sp. – scapula sin. (Csarnóta, MÁFI V.11.31.1; V.29106), lateral view. a. *acromion – costal branch*; b. edge between branches; c. *acromion – lateral branch*; d. *facies atricularis humeralis.*

Figure 92 A. *Coccothraustes* † *major* nova sp. – maxilla (Beremend, BKA), dorsal view.

Figure 92 B. *Coccothraustes* † *major* nova sp. – mandibula (Beremend, BKA), ventral view.

Figure 92 C. *Coccothraustes* † *major* nova sp. – mandibula (Beremend, BKA), dorsal view.

Figure 92 D. *Coccothraustes* † *major* nova sp. – humerus sin. (Beremend, BKA), caudal view: a. *caput humeri*; b. *tuberculum dorsale*; c. *tuberculum ventrale*; d. *crista bicipitalis*; e. *fossae pneumotricipitalis*.

Figure 92 E. *Coccothraustes* † *major* nova sp. – humerus dext. (Beremend, BKA), cranial view: f. *tuberculum supracondylare ventrale*; g. *epicondylus ventralis*; h. *processus flexorius*; i. *condylus ventralis*; j. *incisura intercondylaris*; k. *condylus dorsalis*; l. *epicondylus dorsalis*; m. *processus supracondylaris dorsalis.*

Figure 92 F. *Coccothraustes* † *major* nova sp. – tarsometatarsus sin. (Beremend, BKA), dorsal view: a. *trochlea metatarsi* II.; b. *incisura intertrochlearis medialis*; c. *trochlea metatarsi* III.; d. *incisura intertrochlearis lateralis*; e. *trochlea metatarsi* IV.

Plate XXIV

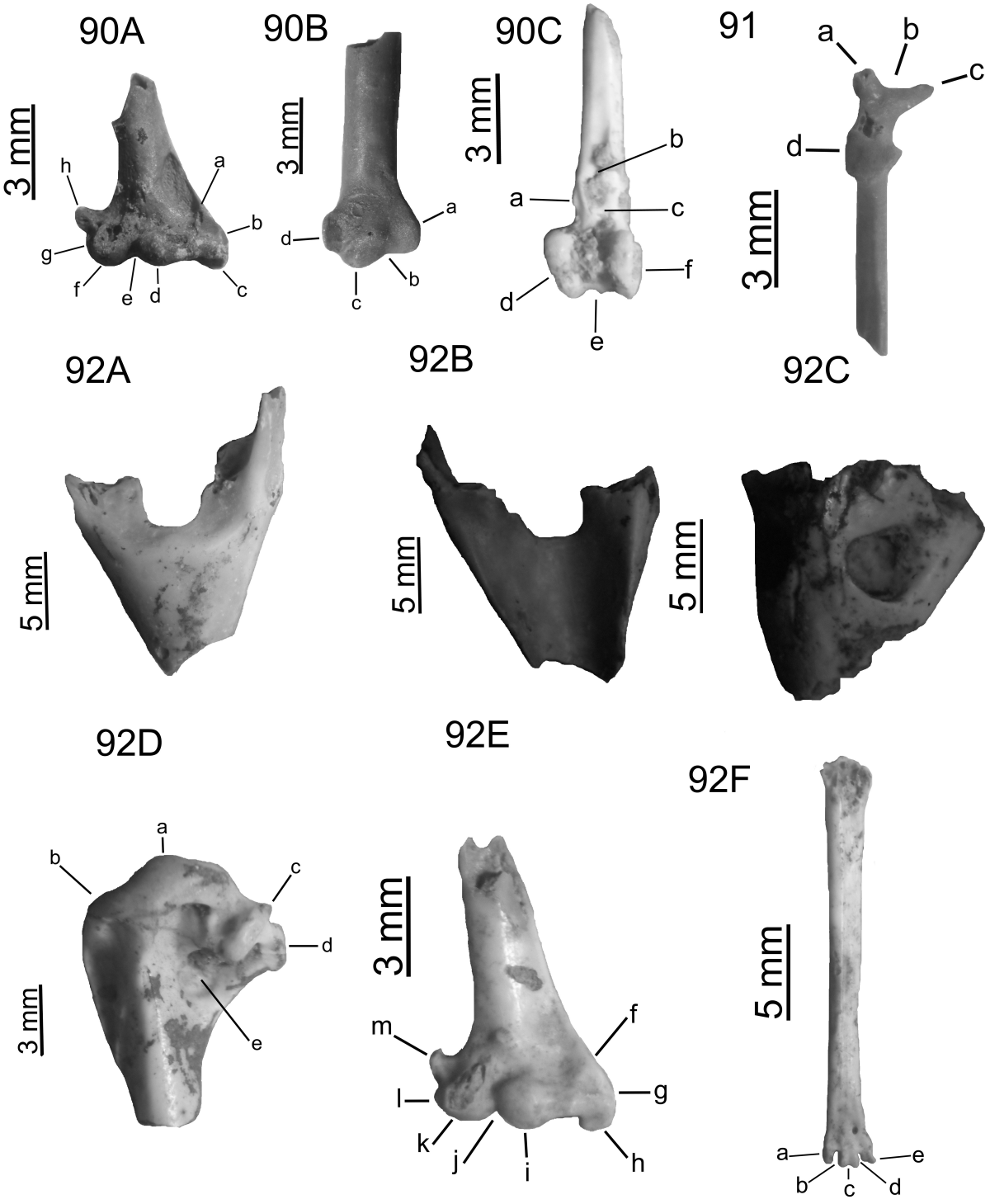
90A
3 mm
h
a
b
g
f
e
d
c
90B
3 mm
a
d
b
c
90C
3 mm
b
a
c
f
d
e
91
a
b
c
d
3 mm
92A
5 mm
92B
5 mm
92C
5 mm
92D
3 mm
a
b
c
d
e
92E
3 mm
m
f
l
g
k
j
i
h
92F
5 mm
a
e
b
c
d

Plate XXV

Figure 93 A. *Emberiza* † *pannonica* nova sp. – humerus dext. (Polgárdi, MÁFI V.11.92.1; V.29167), caudal view, a. *tuberculum dorsale*; b. *caput humeri*; c. *tuberculum ventrale*; d. *crista bicipitalis*; e. *crus fossae*; f. *fossae pneumotricipitalis.*

Figure 93 B. *Emberiza* † *pannonica* nova sp. – ulna sin. (Polgárdi, MÁFI V.11.113.3, V.29188 /1), cranial view, a. *oleocranon* b. *cotyla dorsalis*; c. *cotyla ventralis*; d. *tuberculum lig. colat. ventralis*; e. *depressio m. brachialis*.

Figure 93 C. *Emberiza* † *pannonica* nova sp. – carpometacarpus dext. (Polgárdi, MÁFI V.11.113.3, V.29188 /2), ventral view, a. *trochlea carpalis*; b. *proc. extensorius*; c. *processus alularis*; d. *fovea subalularis*; e. *protuberantia metacarpalis.*

Figure 93 D. *Emberiza* † *pannonica* nova sp. – tibiotarsus sin. (Polgárdi, MÁFI V.11.117.1; V.29192), cranial view, a. *tuberositas retinaculi m. fibularis*; b. *sulcus extensorius*; c. *pons supratendineus*; d. *condylus lateralis*; e. *incisura intercondylaris*; f. *condylus medialis.*

Figure 94 A. *Emberiza* †*polgardiensis* nova sp. – humerus dext. (Polgárdi, MÁFI V.11.79.19; V.29154/1), caudal view, a. *tuberculum dorsale*; b. *caput humeri*; c. *tuberculum ventrale*; d. *crista bicipitalis*; e. *crus fossae*; f. *fossae pneumotricipitalis.*

Figure 94 B. *Emberiza* †*polgardiensis* nova sp. – humerus dext. (Polgárdi, MÁFI V.11.79.19; V.29154/1), cranial view, g. *tuberculum supracondylare ventrale*; h. *epicondylus ventralis*; i. *processus flexorius*; j. *condylus ventralis*; k. *incisura intercondylaris*; l. *condylus dorsalis*; m. *epicondylus dorsalis*; n. *processus supracondylaris dorsalis.*

Figure 94 C. *Emberiza* †*polgardiensis* nova sp. – ulna sin. (Polgárdi, MÁFI V.11.79.19; V.29154/2), cranial view, a. *oleocranon* b. *cotyla dorsalis*; c. *cotyla ventralis*; d. *tuberculum lig. colat. ventralis*; e. *depressio m. brachialis*.

Figure 94 D. *Emberiza* †*polgardiensis* nova sp. – ulna dext. (Polgárdi, MÁFI V.11.79.19; V.29154/3), medial view, f. *condylus dorsalis*; g. *sulcus intercondylaris*; h. *condylus ventralis*; i. *tuberculum carpale.*

Figure 94 E. *Emberiza* †*polgardiensis* nova sp. – tibiotarsus dext. (Polgárdi, MÁFI V.11.61.1; 29137), cranial view, a. *tuberositas retinaculi m. fibularis*; b. *sulcus extensorius*; c. *pons supratendineus*; d. *condylus lateralis*; e. *incisura intercondylaris*; f. *condylus medialis.*

Figure 94 F. *Emberiza* †*polgardiensis* nova sp. – tarsometatarsus sin. (Polgárdi, MÁFI V.11.79.19; V.29154/3), dorsal view, a. *trochlea metatarsi* II.; b. *incisura intertrochlearis medialis*; c. *trochlea metatarsi* III.; d *incisura intertrochlearis lateralis*; e. *trochlea* metatarsi IV.

Plate XXV

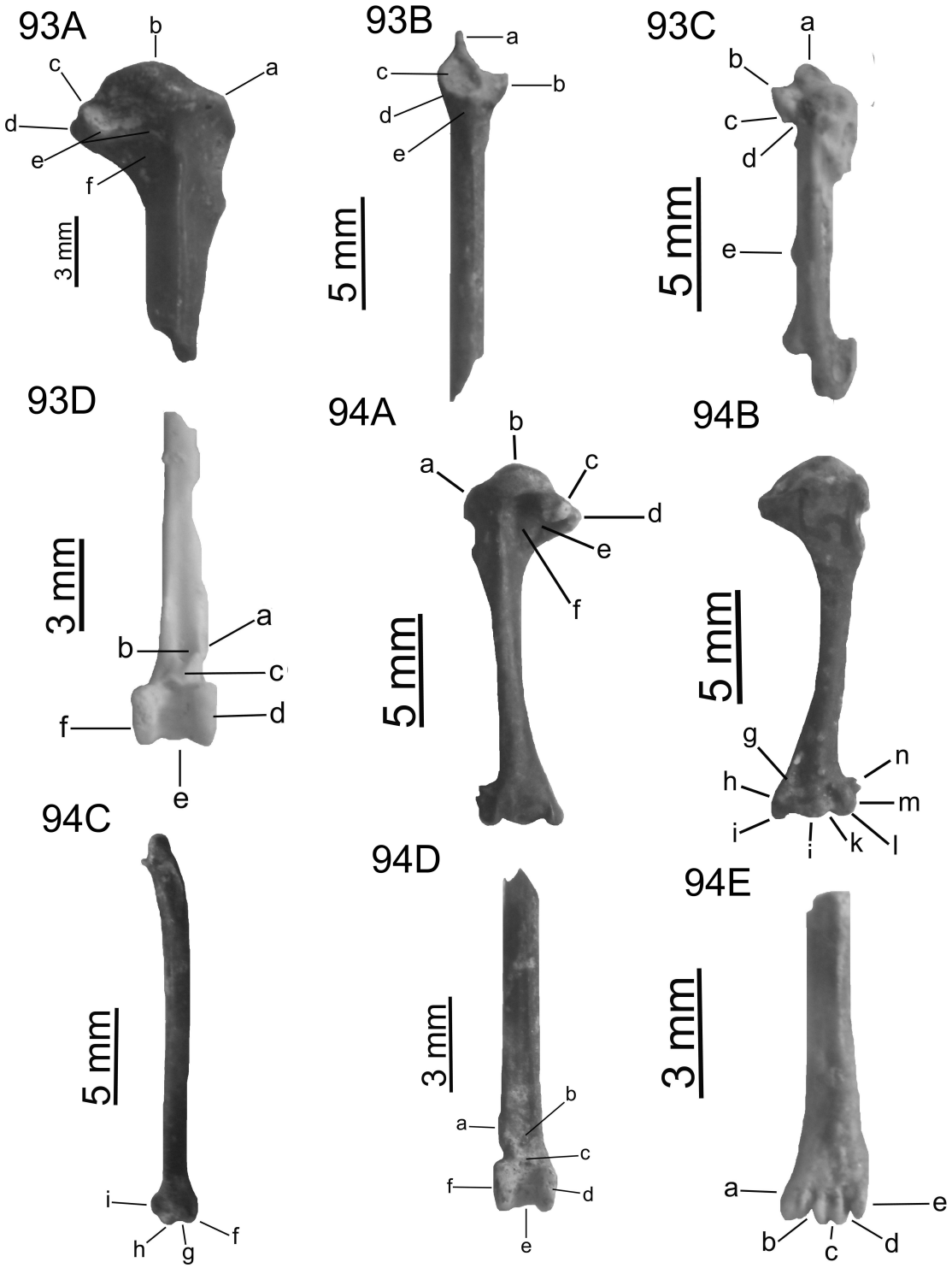
93A
b
c
a
d
e
f
3 mm
93B
a
c
b
d
e
5 mm
93C
a
b
c
d
e
5 mm
93D
3 mm
a
b
c
f
d
e
94A
b
a
c
d
e
f
5 mm
94B
5 mm
g
n
h
m
i
k
l
94C
5 mm
i
h
g
f
94D
3 mm
b
a
c
f
d
e
94E
3 mm
a
e
b
c
d

Plate XXVI

Figure 95 A. *Emberiza* † *media* nova sp. – humerus sin. (Csarnóta, MÁFI V.11.33.1; V.29108), caudal view, a. *tuberculum dorsale*; b. *caput humeri*; c. *tuberculum ventrale*; d. *crista bicipitalis*; e. *crus fossae*; f. *fossae pneumotricipitalis*.

Figure 95 B. *Emberiza* † *media* nova sp. – humerus sin. (Csarnóta, MÁFI V.11.33.1; V.29108), cranial view, g. *tuberculum supracondylare ventrale*; h. *epicondylus ventralis*; i. *processus flexorius*; j. *condylus ventralis*; k. *incisura intercondylaris*; l. *condylus dorsalis*; m. *epicondylus dorsalis*; n. *processus supracondylaris dorsalis.*

Figure 95 C. *Emberiza* † *media* nova sp. – ulna dext. (Csarnóta, MÁFI V.11.51.1; V.29126), medial view, a. *condylus dorsalis*; b. *sulcus intercondylaris*; c. *condylus ventralis*; d. *tuberculum carpale.*

Figure 96 A. *Emberiza* † *parva* nova sp. – coracoideum dext. (Csarnóta, MÁFI V.11.32.1; V.29107), dorsal view, a. *acrocoracoideum*; b. *processus accesorius*; c. *sulcus m. supracoracoidei*; d. *processus procoracoidei*.

Figure 96 B. *Emberiza* † *parva* nova sp. – humerus sin. (Csarnóta, MÁFI V.11.52.6, V.29127). cranial view, g. *tuberculum supracondylare ventrale*; h. *epicondylus ventralis*; i. *processus flexorius*; j. *condylus ventralis*; k. *incisura intercondylaris*; l. *condylus dorsalis*; m. *epicondylus dorsalis*; n. *processus supracondylaris dorsalis.*

Figure 96 C. *Emberiza* † *parva* nova sp. – ulna sin. (Csarnóta, MÁFI V.11.52.7; V.29127), medial view, a. *condylus dorsalis*; b. *sulcus intercondylaris*; c. *condylus ventralis*; d. *tuberculum carpale.*

Figure 97 A. *Emberiza* † *gaspariki* nova sp. – humerus sin. (Beremend, BKA), caudal view: a. *tuberculum dorsale*; b. *caput humeri*; c. *tuberculum ventrale*; d. *crista bicipitalis*; e. *fossae pneumotricipitalis*.

Figure 97 B. *Emberiza* † *gaspariki* nova sp. – humerus sin. (Beremend, BKA), cranial view: f. *tuberculum supracondylare ventrale*; g. *epicondylus ventralis*; h. *processus flexorius*; i. *condylus ventralis*; j. *incisura intercondylaris*; k. *condylus dorsalis*; l. *epicondylus dorsalis*; m. *processus supracondylaris dorsalis.*

Figure 97 C. *Emberiza* † *gaspariki* nova sp. – carpometacarpus dext. (Beremend, BKA), ventral view: a. *trochlea carpalis*; b. *processus flexorius*; c. *processus alularis*; d. *fovea subalularis*; e. *protuberantia metacarpalis.*

Figure 98. *Plectrophenax* †*veterior* nova sp. – tibiotarsus sin. (Polgárdi MÁFI V.11.59.1; V.29134), cranial view, a. *tuberositas retinaculi m. fibularis*; b. *sulcus extensorius*; c. *pons supratendineus*; d. *canalis extensorius*; e. *condylus lateralis*; f. *incisura intercondylaris*; g. *condylus medialis.*

Plate XXVI

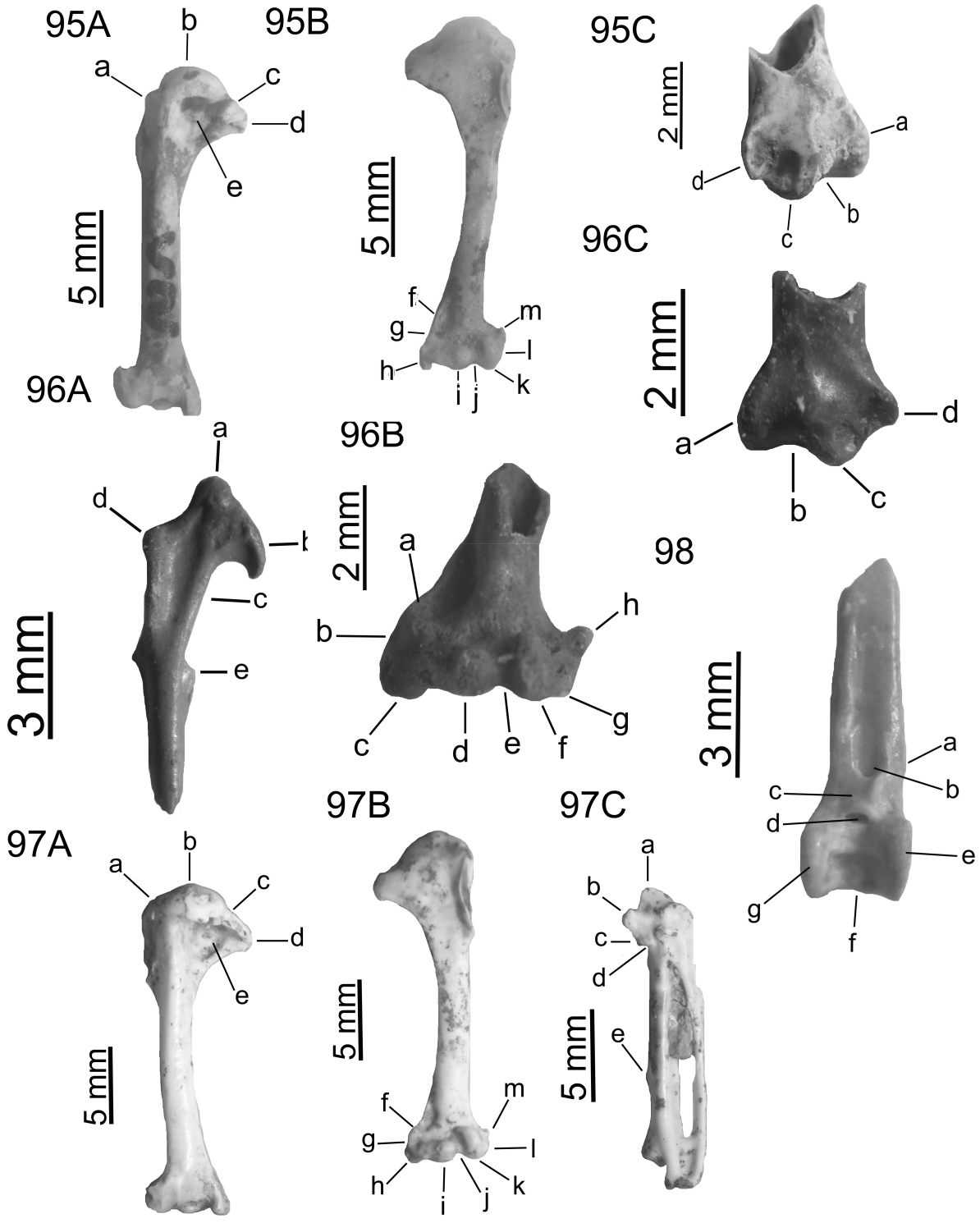

Hantkeniana 8, 151—161, Budapest, 2013

The Late Pleistocene microvertebrate fauna of the Vaskapu Cave (North Hungary) and its taphonomical, biostratigraphical and palaeoecological implications

Attila VIRÁG[1,2,3], Zoltán SZENTESI[1,2,3], Tünde CSÉFÁN[1], Lilla M. KELLNER[1]

(with 1 figure and 2 plates)

Numerous well-preserved plant-remains were discovered at the Upper Cretaceous Iharkút vertebrate fossil site (Csehbánya Formation, Bakony Mts., Hungary). A well determinable, but rare mesofossil form belongs to the Sabiaceae family. The internationally excellent Cenozoic fossil record makes the family of special phytogeographical and palaebotanical interest. Based on endocarp morphology we assigned the Iharkút specimens to *Sabia menispermoides*. These characters are also typical for the recent *Sabia* genus. KNOBLOCH and MAI described *Sabia menispermoides* from the Cretaceous of České Budějovice in 1986 as *Sabia* because of the high similarity to the recent forms. The now living Sabiaceae plants are trees, shrubs and lianas. The known representatives of the family are members of the subtropical and tropical vegetations in Asia and America. Their presence at Iharkút indicates subtropical climatic conditions of the vertebrate locality.

Introduction

The Vaskapu Cave (Fig. 1.) is a rock shelter, situated approximately 4 km NW from Felsőtárkány on the west side of the Lök Valley (Bükk Mountains, North Hungary) close to the Eger-Miskolc highway. Rich Late Pleistocene microvertebrate fauna and a few larger remains were described by KADIĆ and MOTTL (1938) and later by MOTTL (1941) from the original locality (mentioned here as Vaskapu I). In the summer of 1994 Dr. János HÍR (director of the Museum of Pásztó) identified a previously unexplored fissure (mentioned here as Vaskapu II) near the original site, with a microvertebrate-rich infilling. Additional sites were numbered later with a bottom-up approach. Vaskapu VI and VII (which provided similar fauna) are most plausibly connected to the same fissure as Vaskapu II, while Vaskapu III, IV and V (which yielded a recent assemblage) are connected to an other fissure closer to the Eger-Miskolc highway. Present study aimed to make the revision of the vertebrate fauna (paying particular attention to the previously poorly studied herpetofauna) of the fossil localities, to summarize the complex taphonomic situation of the fissure system, and to draw biostratigraphical and palaeoecological consequences.

Material and Methods

KADIĆ and MOTTL (1938) described 4 layers from the Cave (Vaskapu I locality) which are the following:

1. reddish-brown clay with limestone fragments near the entrance of the main rock shelter
2. greenish-gray sandy clay (plausibly a stream sediment) with a few limestone fragments
3. light gray clay with limestone fragments situated above layer 2.
4. dark brown or black humus at the top of the sequence

The fauna originated from layer 1-3 of the original site is also discussed here, although the material (a total of about 220 kg) studied in the present article was collected during several different field surveys from 1994 to 2009 from the reddish-brown clay infilling of the approximately 15 m high fissure (with the Vaskapu II locality at the bottom and the Vaskapu

[1] Eötvös University, Department of Palaeontology, H-1117 Budapest, Pázmány Péter sétány 1/c.
[2] Hungarian Natural History Museum, Department of Paleontology and Geology, H-1083 Budapest, Ludovika tér 2.
[3] MTA-MTM-ELTE Research Group for Paleontology, H-1051 Budapest, Nádor utca 7.

VII at the top) closest to the 6 m wide and 5 m high rock shelter (namely the Vaskapu I site). This sediment is plausibly the same as layer 1 of the first excavation in 1933 (described by KADIĆ and MOTTL, 1938, see above). Most of the samples (approximately 180 kg) are originated from the Vaskapu II site, and additional 20 kg samples were removed from the Vaskapu VI and VII localities.

The material was washed through a 0.5 mm sieve and in several cases was pre-treated with hydrogen-peroxide to remove the high organic content. The studied fossils were emplaced to the Stratigraphical Collection of The Department of Paleontology and Geology at the Hungarian Natural History Museum.

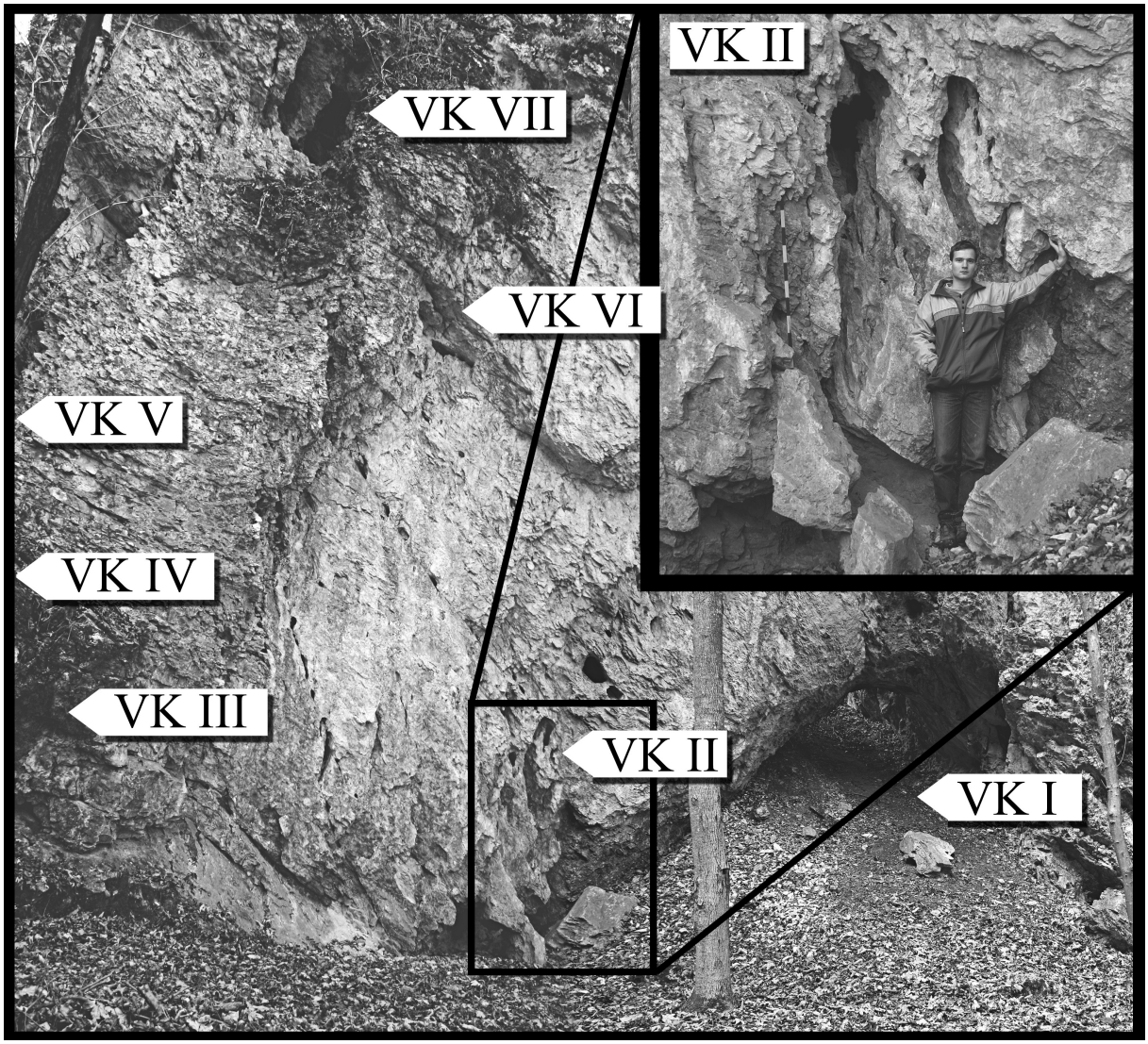

Fig. 1. The Vaskapu Cave (Vaskapu I site) and its surrounding fissure system (with Vaskapu II – Vaskapu VII localities). *Abbreviations:* VK = Vaskapu.

The fauna

Fish

The group Osteichthyes is represented in the studied material only with 4 amphicoelous vertebral centra from the Vaskapu II site. No such remains were found from the surrounding localities so far.

Amphibians

Approximately 100 anuran skeletal elements (including cranial remains, vertebrae, limb bones, pectoral and pelvic girdles) was found in the material studied in the present paper of which 8 ilium and an angulospleniale was securely identifiable on a species level from the Vaskapu II site. Most of the other

remains are attributable to the genus *Bufo* or *Rana*. The identification of the anuran remains was carried out by T. CSÉFÁN and Z. SZENTESI.

The most distinctive skeletal element of the Pleistocene anurans is the ilium. The genus *Bufo* and *Rana* were identified on the basis of the ilia from the Vaskapu II locality.

The ilium of a bufonid toad usually lacking dorsal crest (or vexillum), but have a pronounced dorsal prominence (also called tuber superior). According to HOLMAN (1998) three species belongs to the genus *Bufo* are detectable in the European Pleistocene record, which are *B. bufo*, *B. viridis*, and *B. calamita*.

B. calamita has a triangular dorsal prominence and a noticeable ridge and/or groove (often called calamita ridge, see Pl. 1, Fig. 2b) on the posteroventral side of the ilial shaft just anterior to the ventral acetabular expansion (or pars descendens ilii). The other species lack this ridge and/or groove. *B. bufo* has a low, rounded (or occasionally blade-like) dorsal prominence sometimes with a rough dorsal surface, while *B. viridis* has a two-lobed dorsal prominence (see Pl. 1, Fig. 5b).

All the three species were detected in the case of the Vaskapu II locality. Specimen VK2.18 (Pl. 1, Fig. 3) and VK2.19 shows typical characteristics of a *B. bufo*. VK2.20 and VK2.21 have a more pronounced tuber superior, similar to *B. calamita*, however the distinctive ridge of the latter taxon is not present, therefore these specimens were identified here as *B. bufo* as well. VK2.15 (Pl. 1, Fig. 5a,b) and VK2.16 (Pl. 1, Fig. 4) have a bilobate dorsal prominence, characteristic to *B. viridis*. VK2.17 (Pl. 1, Fig. 2a,b) is a typical *B. calamita* with triangular tuber superior and a well-developed ridge and groove on the posteroventral side of the ilial shaft just anterior to the ventral acetabular expansion.

Rana is a diverse genus usually with a pronounced dorsal crest and an elongate, compressed dorsal prominence. Specific identification could be difficult in closely related species, but the VK2.14 specimen (Pl. 1, Fig. 1) has a smooth, elongated tuber superior and a well-developed vexillum, therefore identified here as a member of the aforementioned genus. Compared with the European Pleistocene *Rana* species, it has a more pronounced and anteriorly downward sloping dorsal crest, broadly similar to *R. arvalis*. In contrast, according to HOLMAN (1998), the other common Pleistocene brown frog, namely *R. temporaria* have noticeably less-developed vexillum and a tuber superior with often not smooth but slightly roughened dorsal surface.

An additional angulospleniale (VK2.22, Pl. 1, Fig. 6) was identified in the present study as *R. temporaria*. The shaft of the bone is only moderately curved, or almost straight, and the processus coronoideus have a steep posterior surface in lateral view. In contrast, the angulospleniale of a bufonid toad (such as VK2.23 on Pl. 1, Fig. 7 and VK 2.24 on Pl. 1, Fig. 8) is obviously curved, the processus coronoideus is less prominent, while the Meckelian canal is more pronounced (BAILÓN, 1999).

Based on the above described observations, the following anuran taxa were indentified from the Vaskapu II locality:

Bufo bufo
Bufo viridis
Bufo calamita
Rana temporaria
Rana cf. *R. arvalis*

Reptiles

Among the relatively few snake and lizard material studied in the present paper, postcranial elements (ribs and anteriorly concave but posteriorly convex procoelous vertebrae) were the most abundant. 13 tooth-bearing skeletal remains were also found from the Vaskapu II site, which were identified here as lacertids. The identification of these remains was carried out by L. M. KELLNER.

Lacertidae is a widespread lizard group (PIANKA & VITT 2003, BAILÓN 2004, VITT & CALDWELL 2008), of which generic and/or specific identification is problematic in many respects. There is a remarkable osteological homogeneity between the different members of the clade and in addition the intraspecific variability of each taxon is significant. The most easily recognizable, but not always diagnostic skeletal elements are the tooth-bearing maxillary, praemaxillary and dentary bones with the following main characteristics:

1. The teeth are pleurodont, usually have two (bicuspid), but occasionally only one (unicuspid) or even three (tricuspid) cusps, and their shafts are approximately cylindrical. The number of teeth should not always be taken into a reliable taxonomic allocation, since it depends on the age of the individual (DELFINO & BAILÓN, 2000) (see e.g. Pl. 2, Fig. 1b and 2b).
2. The subdental shelf, of which outline could be diagnostic in several cases extends medially below the tooth row (ESTES et al. 1988).
3. The Meckelian canal is widely open medially (RAGE & BAILÓN, 2005), as in most scincomorphs (ESTES et al. 1988).
4. An intramandibular septum is located in the Meckelian canal between the descending inner wall of the dentary bone and the subdental shelf (ESTES et al. 1988).

VK2.1 (Pl. 2, Fig. 1a-d) is a left dentary bone with

space for 19 teeth and with a broadly similar overall morphology to *L. agilis*. According to KOSMA (2004) unicuspidity is restricted to the two anteriormost teeth in the case of the most representatives of the latter species, as in the case of the VK2.1 specimen. In contrast, the other two abundant Pleistocene European small lacertid species, *Podarcis muralis* and *Lacerta vivipara* have 1-5 and 4 anterior unicuspid teeth, respectively. The following teeth are bicuspid with a distally situated main cusp and a smaller mesial accessory cusp, while tricuspid morphology lacks in the case of the VK2.1 specimen. Teeth become more robust in the distal portion of the tooth row. The length of the tooth row is 7.2 mm. On the basis of the data presented by HOLMAN (1998), the length of the tooth raw is approximately 5-6 mm in the case of an adult *L. agilis*, which is a bit more than *Podarcis muralis* and *Lacerta vivipara*, but noticeably less than in the case of *L. viridis*. The teeth are slightly worn, but obviously striated lingually and labially, which feature is arguing against the genus *Podarcis* (KOSMA, 2004). The posterior border of the intramandibular septum (which is located approximately below the 5th or 6th tooth positions counted from posterior to anterior direction) is parabolic in ventromedial view (Pl. 2, Fig. 1d). Based on the aforementioned observations specimen VK2.1 is identified here as *Lacerta* cf. *L. agilis*.

VK2.4 is a smaller left dentary bone with space for 20 or 21 teeth. The length of the tooth row is 5.1 mm. The parabolic posterior border of the intramandibular septum is located under the 5th or 6th tooth positions counted from posterior to anterior direction. The existence or the number of anterior unicuspid teeth can not be determined, since the fragmentary nature of the specimen. In contrast to the above described VK2.1 specimen, this dentary has tricuspid teeth posteriorly. Despite the differences in the size and tooth morphology, the specimen is plausibly assignable to the same morphotype as VK2.1.

VK2.8 (Pl. 2, Fig. 2a-d) is a right dentary bone with space for 21 or 22 teeth. The teeth are striated with the striae restricted to the lingual surface of the crown which is characteristic for *L. viridis* according to KOSMA (2004). The adult specimens of the latter species have usually 21 to 26 tooth positions. The first 4 teeth of the VK2.8 specimen are unicuspid, while the next 3 are rather unrecognizable as a result of damage. The following teeth are bicuspid. Teeth are more or less equally robust along the entire length of the tooth row, which is 7.2 mm. The posterior border of the intramandibular septum is located below the 7th and 8th tooth positions (counted from posterior to anterior direction) and is not parabolic but sigmoid in outline with an anteriorly descending ventral edge (Pl. 2, Fig. 2d). Based on the previous observations this specimen is referred here to an other morphotype, which is plausibly closely related to *L. viridis*.

VK2.9 is a fragment of a left dentary bone with at least 21 tooth places of which the most are apparently bicuspid starting from the 3rd tooth position. Teeth are more or less equally robust along the entire length of the tooth row, which is 7.5 mm. The tooth crowns are striated lingually. The posterior border of the intramandibular septum is located below the 7th and 8th tooth positions (counted from posterior to anterior direction) and similar to the VK2.8 specimen. Asides from some uncertain striation on the labial side of the tooth crown, this dentary plausibly belongs to the same morphotype as VK2.8.

Specimen VK2.6, VK2.10 and VK2.12 are dentary bones, which show lacertid characteristics, however the fragmentary preservation does not allow even generic level identification.

VK2.2 (see on Pl. 2, Fig. 3a,b), VK2.3, VK2.7 (see on Pl. 2, Fig. 4a,b), VK2.11, and VK2.13 are maxillary fragments with a broadly similar morphology with a space for a relatively reduced number of tooth positions (16 or 17). The total length of the tooth row is 6-6.5 mm. The opening of the canalis alveolaris superior is usually placed at the border of the middle and the posterior third of the dental lamina above the 6th or 7th tooth position (counted from posterior to anterior direction). According to DELFINO & BAILÓN (2000) the latter morphology is similar to the genus *Podarcis*. However, on the basis of KOSMA (2004), *Podarcis* lacks striated tooth crowns, which is clearly present in the case of the aforementioned specimens. HOLMAN (1998) stated that tricuspid teeth are absent in the case of the *L. agilis* maxillae, while often present in the case of *L. viridis*. On the basis of the tricuspid tooth morphology observed on the VK2.2 and VK2.7 specimen, this morphogroup was identified here as *Lacerta* cf. *L. viridis*.

VK2.5. is a significantly fragmentary maxillary bone, which shows lacertid characteristics, however the preservation does not allow generic level identification.

Based on the above described observations, the following reptiles were indentified from the Vaskapu II locality:

Serpentes indet.
Lacerta cf. *L. agilis*
Lacerta cf. *L. viridis*

Birds

Birds are mainly represented by a few praemaxillary bones, carpometacarpi and tarsometatarsi from both the Vaskapu II and Vaskapu VII site. Based on the revision of the list presented by KADIĆ & MOTTL (1938), the following taxa can be found at the Vaskapu I site:

Lagopus albus
Lagopus mutus
Tetrao (or *Lyrurus*) *tetrix*
Pyrrhocorax alpinus
Falco tinnunculus

Mammals

The most abundant and most frequently studied part of the material is the mammalian fauna. KADIĆ and MOTTL (1938) described small and large mammals from the Vaskapu I locality, MÉSZÁROS (1999, 2003, 2004 and 2013) paid particular attention to the shrew remains from the Vaskapu II site, while SÓRON & VIRÁG (2009) focused mainly on the rodent assemblage of the latter locality.

Based on the revised list of KADIĆ and MOTTL (1938), the data published in the above mentioned articles, and the present observations of A. VIRÁG, the following other mammalian remains can be found at the Vaskapu I, II, VI, and VII sites:

Chiroptera indet. (Vaskapu II and VII)
Talpa europaea (mentioned from the Vaskapu I locality)
Sorex alpinus (Vaskapu II and VII) [4]
Sorex minutus (Vaskapu II and VII)[4]
Sorex araneus (Vaskapu II and VII)[4]
Crocidura russula (Vaskapu VII)[4]
Crocidura suaveolens (Vaskapu II and VII)[4]
Lepus sp. (Vaskapu I and II)
Ochotona pusilla (Vaskapu I and II)
Spermophilus (formerly *Citellus*) *rufescens* (mentioned from the Vaskapu I locality)
Glis glis (Vaskapu I, II, and VII)
Apodemus cf. *sylvaticus* (Vaskapu I, II, and VII)
Cricetus cricetus (Vaskapu I and II)
Myodes (formerly *Clethrionomys*) *glareolus* (Vaskapu I, II, and VII)
Arvicola terrestris (Vaskapu I, II, and VII)
Microtus arvalis-agrestis gr. (Vaskapu I, II, and VII)
Microtus (*Alexandromys*) *oeconomus* (mentioned from the Vaskapu I locality)
Microtus (*Stenocranius*) *gregalis* (Vaskapu I, II, and VII)
Chionomys (formerly *Microtus*) *nivalis* (mentioned from the Vaskapu I locality)
Canis lupus (mentioned from the Vaskapu I locality)
Vulpes vulpes (mentioned from the Vaskapu I locality)
Ursus arctos (mentioned from the Vaskapu I locality)
Martes martes (mentioned from the Vaskapu I locality)
Mustela erminea (mentioned from the Vaskapu I locality)
Mustela nivalis (mentioned from the Vaskapu I locality)
Rangifer tarandus (Vaskapu I; represented by a molar at Vaskapu VI?)
Rupicapra rupicapra (Vaskapu I; represented by a molar at Vaskapu VII?)
Bison priscus (mentioned from the Vaskapu I locality)

Taphonomy of the Vaskapu localities

The fauna most likely represent a mixture of a more or less contemporaneous but mosaic environment (forest and grassland within a small area) or could also be the result of a repeated redeposition of successively changing habitats[5]. The remains were transported to the Vaskapu site by water (probably by a stream) from the original biocoenoses. It is possible, that layer 2 of Vaskapu I represent the sediment of the aforementioned stream. Nevertheless, the smaller or occasionally greater limestone fragments embedded in the clayey layers are indicative for some gravitational movement.

Similar or the same material was washed later from the plateau at top of the Vaskapu VII locality into the fissure system by the spring snowmelt and the repeated rainfalls. This model is in agreement with the results of the taphonomic study carried out by SÓRON & VIRÁG (2009), according to which splitting and flaking resulting from weathering and drying of the bones are common modifications at the locality. The material under the influence of gravity as well as the infiltrating water moved downwards in the fissure system (i.e. towards Vaskapu II locality). During the latter transportation the remains were further damaged and size selective processes were occurred. It is in agreement with the fact that the material is more fragmented and contains less relatively long (more than 10 mm) bones at the Vaskapu II site compared with the Vaskapu VII locality. It is also in agreement with the observations of SÓRON & VIRÁG (2009), according to which the most common fractures of the limb bones are perpendicular to the main axis of the bone and the broken surface is smooth or stepped, which means that the damage occurred after the loss of the collagen fibers (i.e. the remains was most likely at least partly mineralized at that time). The abundance of bone fragments, isolated molars and empty alveolar spaces suggest a relatively significant transportation of the material.

[4] See the article published in the present volume by MÉSZÁROS (2013) for details.

[5] In order to decide the contemporaneity of each site and the entire VK II-VI-VII fissure system as a whole, a radiocarbon study is in progress at the moment.

Although the Vaskapu II locality has a natural sediment refill from the fissure system situated above the site, it was almost deserted due to the repeated sediment extraction from 1994 to 2009. As the airspace of the cavity gradually increased it became more often inhabited by recent faunal elements. As a consequence, the sediment collected in 2009 contains some recent remains as well, but those bones obviously differ from the fossil ones which are more fragmented and have darker (yellow or yellowish-brown) colour.

Biostratigraphical and palaeoecological conclusions

According to BÖHME (1996) the development of the herpetofauna reflects the major phases of the Central European climatic cycles during the Pleistocene epoch:

1. *Rana temporaria* tends to be the only species present in ice-free areas during full cold stages.
2. *Bufo bufo, Rana arvalis,* and *Vipera berus* are early pioneers during the latter part of a cold stage.
3. *Rana dalmatina*, *Rana lessonae*, *Triturus cristatus*, *Triturus vulgaris*, *Anguis fragilis*, *Lacerta agilis*, *Coronella austriaca,* and *Natrix natrix* appears mainly during the early part of a warm stage.
4. *Salamandra salamandra, Bombina bombina, Hyla arborea, Pelobates fuscus, Rana ridibunda, Lacerta viridis, Elaphe longissima,* and *Emys orbicularis* are typical species of a climatic optimum.
5. *Bufo calamita* and *Bufo viridis* appears during the latter part of a warm stage.
6. *Rana temporaria, Bufo viridis, Lacerta vivipara and Vipera berus* are characteristic taxa of an outgoing warm stage and a developing cold stage.

Based on the observations of HOLMAN (1998), the model seems broadly applicable to the northern part of the continent as well, especially for e.g. *Rana temporaria, Hyla arborea, Elaphe longissima,* and *Emys orbicularis*. RAGE & ROČEK (2003) also stated that *Rana* is often the only genus present in the herpetofauna during the glaciation periods, while *Bufo* is more often associated with interglacial conditions.

In the case of the Vaskapu fauna, the occurrence of *Bufo bufo*, *Rana arvalis* and *Lacerta agilis* suggest phase 2 or 3 (i.e. postglacial and developing interglacial) of BÖHME (1996) which is in agreement with the mammalian fauna (described below). In contrast, *Bufo viridis*, *Bufo calamita*, and *Lacerta viridis* could suggest even warmer climate, however it is important to take into account the following considerations:

The fact that the herpetological species compared with the homoiotherms lack complex physiological mechanisms which are able to regulate the body temperature often led to the assumption that the amphibians and reptiles have greater sensitivity to temperature changes, therefore these taxa are much better indicators of local thermal conditions than are birds and mammals. HOLMAN (1998) stated, that some European herpetological species are indeed restricted to relatively warm habitats, but on the contrary, several taxa (e.g. *Rana arvalis*, *Rana temporaria*, *Lacerta vivipara* and *Vipera berus*) have very broad ranges and are able to exist in warm as well as significantly cold environments, therefore the ability to draw palaeoecological consequences on the basis of the herpetofauna is limited.

The mammalian material from the Vaskapu I site and the surrounding fissure system (including the Vaskapu II, VI and VII localities) is similar to the Late Würm faunas of Hungary (e.g. Pilisszántó I Rock Shelter, Bivak Cave, Peskő Cave, Jankovich Cave, Remetehegy Rock Shelter and Remete Cave) (see JÁNOSSY et al., 1957 and JÁNOSSY, 1986 for details). The aforementioned localities belong to the Pilisszántóian substage of the local biochronological system, which is characterised by the abundance of reindeers (*Rangifer tarandus*) as well as arctic-alpine vole species (such as *M. gregalis* and *C. nivalis*) and the occurrence of the arctic lemming (*Dicrostonyx torquatus*). Ptarmigans (such as *L. albus* and *L. mutus*) were dominant among the birds, and *Rana mehelyi*[6] was dominant among the amphibians. However, in the case of the material studied in the present article the absence of the collared lemmings (genus *Dicrostonyx*) and the abundance (but obviously not dominance) of the forest elements, as well as the relatively rich herpetofauna (without *Rana mehelyi*) suggest a slightly younger date and a slightly warmer and more humid climate (i.e. the locality shows a transition to the Palánkian substage).

The same conclusions can be drawn from the shrew fauna. The exclusive occurrence of the genus *Sorex* within the shrew fauna is marking a cold episode, however the sporadic presence of genus *Crocidura* (see MÉSZÁROS 2013 for details) suggest slightly warmer climate.

[6] *Rana mehelyi* differs from *Rana temporaria* only in its larger size and it is presently often synonymized with the latter (see e.g. HOLMAN, 1998).

The co-occurrence of the faunal elements of the forest habitat (e.g. *Glis glis*, *Apodemus sylvaticus-flavicollis* gr., *Myodes glareolus*) and the open environment (e.g. *Microtus arvalis-agrestis* gr.) could be explained by a mosaic or quickly shifting environment left behind a retractive glaciation. The presence (but not abundance in the case of the Vaskapu site) of the *Rangifer tarandus* indicates that the boundary zone of the taiga and the tundra were still close to the locality at that time.

Similar postglacial fauna was mentioned by BÁCSKAY & KORDOS (1984) from the layer 9-6 of the Jankovich Cave, which is transitional between the older *Dicrostonyx* and *M. gregalis* dominated sediments of the Würm-3 glaciation (layer 11-10) and the younger Holocene deposits with *Apodemus* as well as abundant lizard and snake material (layer 5-1). PAZONYI (2006, in press) dated layer 7 and 8 of the Jankovich Cave to approximately 12000 uncal B.P. (which is ca. 13-15000 cal B.P.). According to her, the age of the Bivak Cave (which is close to a glacial fauna with even *Dicrostonyx*) is slightly older (approximately 15000 uncal B.P., which means ca. 19000 cal B.P.). Although the age estimation of the locality remains uncertain without an exact radiocarbon date, the above mentioned observations suggest a 15-14 kya age for the Vaskapu locality.

Acknowledgements

We would like to express our thanks to János HÍR, Miklós KÁZMÉR, Lukács MÉSZÁROS and István SZENTE for their assistance on the field. We are grateful to László MAKÁDI and Piroska PAZONYI for the useful suggestions. Sincere thanks to Zsófia HAJDU and András Szabolcs SÓRON for their previous contributions to the present study. This work was supported by the TÁMOP 4.2.2/B-10/1-2010-0030 project and the Hantken Miksa Foundation. This is MTA-MTM-ELTE Paleo contribution No. 178.

References

BAILON, S. (1999): Différenciation ostéologique des Anoures (Amphibia, Anura) de France. – In.: DESSE, J. & DESSE-BERSET, N. (eds.): Fiches d'ostéologie animale pour l'archéologie, Série C., pp. 1-38.

BAILÓN, S. (2004): Fossil records of Lacertidae in Mediterranean islands: The state of the art. – In: PÉREZ-MELLADO, V., RIERA, N. & PERERA, A. (eds.): The Biology of Lacertid Lizards. Evolutionary and Ecological Perspectives. – Institut Menorquí d'Estudis, Recerca, pp. 37-62.

BÁCSKAY, E. & KORDOS, L. (1984): Fontosabb szórványleletek a MÁFI gerinces-gyűjteményében (9. közlemény). - Annual Report of the Hungarian Geological Institute of 1982, pp. 356-361.

BÖHME, G. (1996): Zur historischen Entwicklung der Herpetofaunen Mitteleuropas im Eiszeitalter (Quartär). – In: GÜNTHER, R. (ed.): Die Amphibien und Reptilien Deutschlands. – Gustav Fischer, Jena, pp. 30-39.

DELFINO, M. & BAILÓN, S. (2000): Early Pleistocene herpetofauna from Cava Dell'Erba and Cava Pirro (Apulia, southern Italy). – Herpetological Journal 10, pp. 95-110.

ESTES, R., de QUEIROZ, K. & GAUTHIER, J. (1988): Phylogenetic relationships within Squamata. – In: ESTES, R. & PREGILL, G.: Phylogenetic Relationships of the Lizard Families. – Stanford University Press, Stanford, pp. 119-281.

HOLMAN, J.A. (1998): Pleistocene Amphibians and Reptiles in Britain and Europe. – Oxford Monographs on Geology and Geophysics 38, 254 pp.

JÁNOSSY, D. (1986): Pleistocene Vertebrate Faunas of Hungary. – Akadémiai Kiadó, Budapest, 208 pp.

JÁNOSSY, D., KRETZOI-VARRÓK, S., HERRMANN, M. & VÉRTES, L. (1957): Forschungen in der Bivakhöhle, Ungarn. – Eiszeitalter und Gegenwart 8, pp. 18-36.

KADIĆ, O. & MOTTL, M. (1938): Felsőtárkány vidékének barlangjai – Barlangkutatás 16(1), pp. 56-70.

KOSMA, R. (2004): The dentitions of recent and fossil scincomorphan lizards (Lacertilia, Squamata). Systematics, Functional Morphology, Palecology. – Doctoral dissertation, Vom Fachbereich Geowissenschaften und Geographie der Universität Hannover, Hannover, 187 pp.

MÉSZÁROS, L. GY. (1999): Uppermost Pleistocene shrews (Mammalia, Soricidae) from Vaskapu Cave, Northern Hungary. – Annales Universitatis Scientiarum Budapestinensis, Sectio Geologica 32, pp. 43-50.

MÉSZÁROS, L. (2003): Felső würm "alpesi" fauna a bükki Vaskapu-barlangból. – Abstracts of the 6th Annual Meeting of the Hungarian Palaeontologists, pp. 21.

MÉSZÁROS, L. GY. (2004): Taxonomical revision of the Upper Würm Sorex (Mammalia, Insectivora) remains of Hungary, for proving the presence of an alpine ecotype in the Pilisszántó Horizon. – Annales Universitatis Scientiarum Budapestinensis, Sectio Geologica 37, pp. 5-25.

MÉSZÁROS. L. (2013): Review of the Late Pleistocene Soricidae (Mammalia) fauna of the Vaskapu Cave (North Hungary). – Hantkeniana 8, pp. 163-169.

MOTTL, M. (1941): Die Interglazial und Interstadialzeiten im Lichte der ungarischen Säugetierefauna. – Annals of the Geological Institute of Hungary 35(3), pp. 1-40.

PAZONYI, P. (2006): A Kárpát-medence kvarter emlősfauna közösségeinek paleoökológiai és rétegtani vizsgálata. – Doctoral dissertation, Eötvös Loránd University, Department of Palaeontology, 114 pp.

PAZONYI, P. (in press): Pleistocene vertebrate faunas of the Süttő Travertine Complex (Hungary). – Quaternary International, DOI: 10.1016/j.quaint.2013.02.031.

PIANKA, E.R. & VITT, L.J. (2003): Lizards. Windows to the Evolution of Diversity. – University of California Press, California, 333 pp.

RAGE, J-C. & BAILÓN, S. (2005): Amphibians and squamate reptiles from the late Early Miocene (MN4) of Béon 1 (Montréal-du-Gers, southwestern France). – Geodiversitas 27(3), pp. 413-441.

RAGE, J.C., ROČEK, Z. (2003): Evolution of anuran assemblages on the Tertiary and Quaternary of Europe, in the context of palaeoclimate and palaeogeography. – Amphibia-Reptilia 24(2) pp. 133-167.

SÓRON, A.SZ. & VIRÁG, A. (2009): Detailed quantitative method in microvertebrate taphonomy int he case of Pleistocene filling of the Vaskapu II rock shelter. – Central European Geology 52(2), pp. 185-198.

VITT, L.J. & CALDWELL, J.P. (2008): Herpetology. An Introductory Biology of Amphibians and Reptiles. - Academic Press, San Diego, 697 pp.

Plate 1

Frogs

1. *Rana* cf. *R. arvalis* (VK2.14) left ilium in lateral view from the Vaskapu II site.

2. *Bufo calamita* (VK2.17) left ilium (a) in lateral view from the Vaskapu II site. The characteristic calamita ridge is shown in ventral view (b).

3. *Bufo bufo* (VK2.18) left ilium in lateral view from the Vaskapu II site.

4. *Bufo viridis* (VK2.16) left ilium in lateral view from the Vaskapu II site.

5. *Bufo viridis* (VK2.15) right ilium fragment (a) in lateral view from the Vaskapu II site. The bilobate dorsal prominence is shown in lateral view (b).

6. *Rana temporaria* (VK2.22) right angulospleniale in lateral view from the Vaskapu II site.

7. *Bufo* sp. (VK2.23) right angulospleniale in lateral view from the Vaskapu II site.

8. *Bufo* sp. (VK2.24) right angulospleniale in lateral view from the Vaskapu II site.

Abbreviations:
a = acetabulum;
cr = calamita ridge and/or groove
dae = dorsal acetabular expansion or pars ascendens ilii
dc = dorsal crest or vexillum
dp = dorsal prominence or tuber superior
is = ilial shaft
Mc = Meckelian canal
paf = preacetabular fossa
pc = processus coronoideus
saf = supraacetabular fossa
vae = ventral acetabular expansion or pars descendens iliI

Plate 1

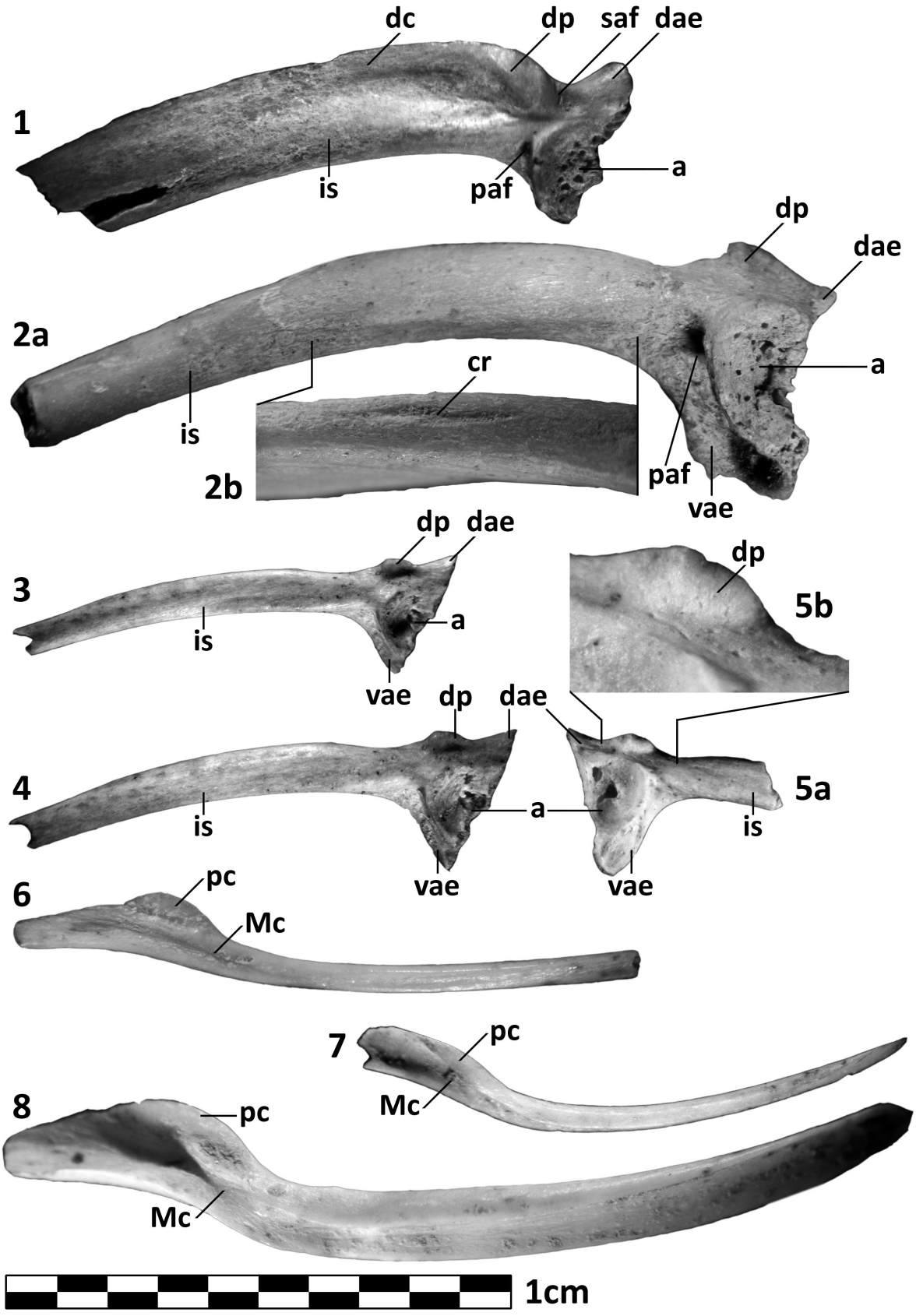
dc
dp
saf
dae
1
is
paf
a
dp
dae
2a
cr
a
is
2b
paf
vae
dp
dae
3
a
is
vae
dp
5b
dp
dae
4
a
5a
is
is
vae
vae
pc
6
Mc
pc
7
Mc
8
pc
Mc
1cm

Plate 2

Lizards

1. *Lacerta* cf. *L. agilis* (VK2.1.) left dentale in lateral (a) and in medial view (b,c) from the Vaskapu II site. The posterior border of the intramandibular septum is shown in ventromedial view (d).

2. *Lacerta* cf. *L. viridis* (VK2.8.) right dentale in lateral (a) and in medial view (b,c) from the Vaskapu II site. The posterior border of the intramandibular septum is shown in ventromedial view (d).

3. *Lacerta* cf. *L. viridis* (VK2.2.) right maxilla in medial (a) and in lateral (b) view from the Vaskapu II site.

4. *Lacerta* cf. *L. viridis* (VK2.7.) right maxilla in medial (a) and in lateral (b) view from the Vaskapu II site.

Abbreviations:
ac = accessory cusp;
dl = dental lamina;
is = intramandibular septum;
mc = main cusp;
Mc = Meckelian canal;
ocas = opening of the canalis alveolaris superior;
pis = posterior border of the intramandibular septum;
rp = resorption pit;
sds = subdental shelf;
uni = unicuspid tooth.

Plate 2

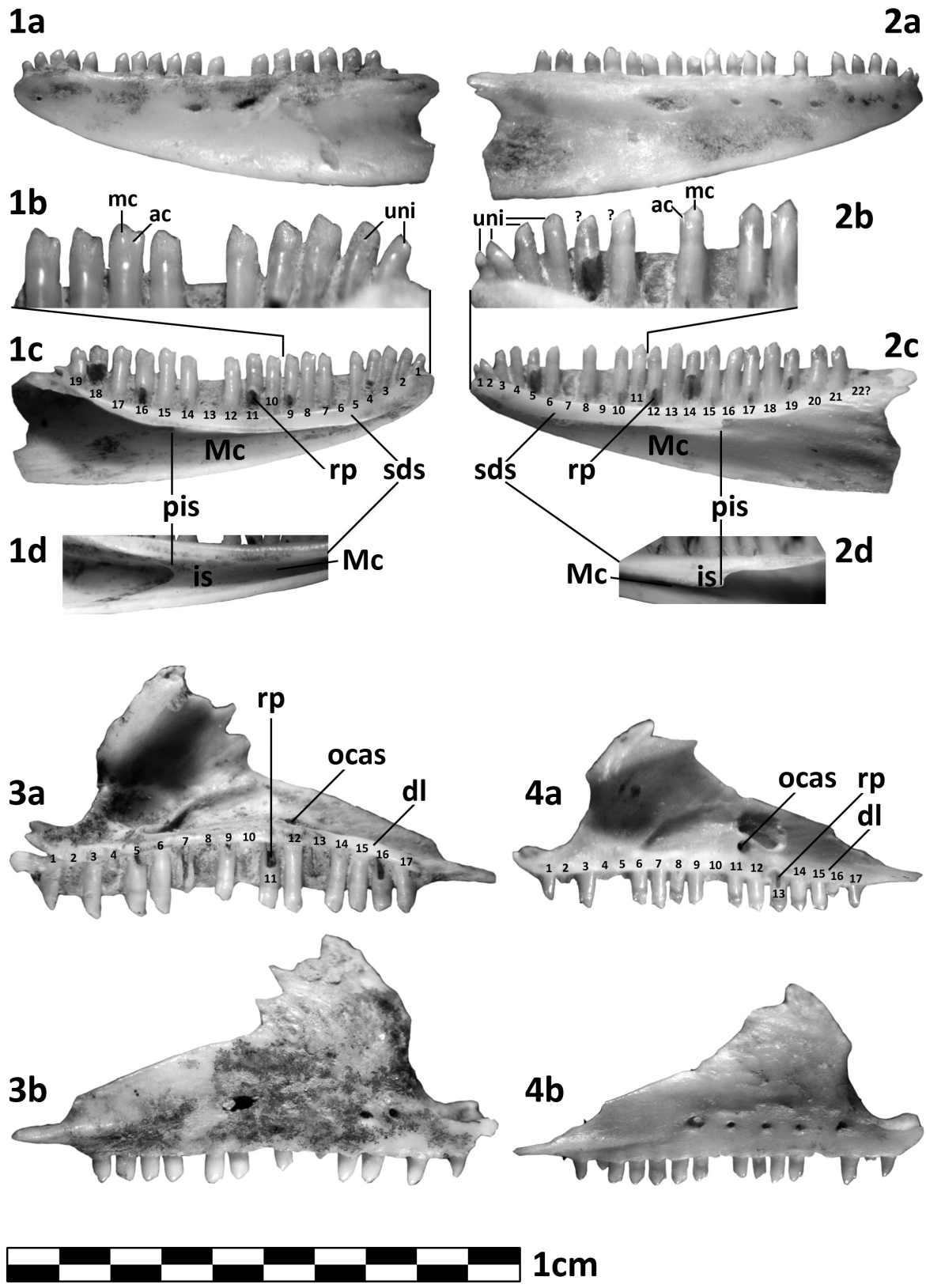
1a
2a
1b
mc
ac
uni
2b
uni
?
?
ac
mc
1c
2c
Mc
rp
sds
pis
1d
is
Mc
2d
sds
rp
Mc
pis
Mc
is
3a
rp
ocas
dl
4a
ocas
rp
dl
3b
4b
1cm

Hantkeniana 8, 163—169, Budapest, 2013

Review of the Late Pleistocene Soricidae (Mammalia) fauna of the Vaskapu Cave (North Hungary)

Lukács MÉSZÁROS[1]

(with 2 figures, 2 tables and 1 plate)

The summary of the Late Pleistocene Soricidae remains of the North Hungarian Vaskapu Cave II and VII localities is given in the present paper. Five species (*Sorex alpinus* SHINZ, 1837, *Sorex minutus* LINNAEUS, 1766, *Sorex araneus* LINNAEUS 1758, *Crocidura russula* HERMANN, 1780 and *Crocidura suaveolens* PALLAS, 1811) were identified in the fauna. The species composition of the shrew assemblage indicates cold climate with diversified ecotypes in the mountain surroundings, with forests and open grasslands as well. Also the new location (in the Stratigraphical Collection of the Department of Paleontology and Geology at the Hungarian Natural History Museum) with definitive inventory numbers of the formerly published Vaskapu fossils is present here.
.

Introduction

The first report of the Late Pleistocene fauna of the Vaskapu Cave was given by Kadič and Mottl (1938). János Hír and Lukács Mészáros collected another fossil sample from Vaskapu II locality, of which Soricid species were published by MÉSZÁROS (1999). The further excavations carried out by L. Mészáros, M. Kázmér, I. Szente, A. Virág and A. Sóron yielded more shrew remains, with new species. A review of the shrew assemblage, with its palaeoecological implications, was required, because of the new results (Fig. 1).

MÉSZÁROS (1999) mentioned 3 *Sorex* species (*S. alpinus*, *S. minutus*, and *S. araneus*) from the Vaskapu II site. In contrast, two additional taxa (namely *Crocidura russula* and *Crocidura suaveolens*) are reported here. Only the soricid elements of the fauna are present in this paper. For the complete presentation of the Vaskapu fissure system and its microvertebrate assemblage see the article published in the present volume by VIRÁG et al. (2013).

Material and method

Because of the not definitive inventory, the material described and figured by MÉSZÁROS (1999) was mentioned only with "working numbers". At present all the Vaskapu findings are stored in the Stratigraphical Collection of the Department of Palaeontology and Geology at the Hungarian Natural History Museum, Budapest. The detailed data and the catalogue numbers of the old and the new Soricidae material are given in Tabs 1-2. Morphological terms in Pl. 1 are used after REUMER (1984).

[1] Eötvös University, Department of Palaeontology, H-1117 Budapest, Pázmány Péter sétány 1/C, Hungary. E-mail: salpin@freemail.hu

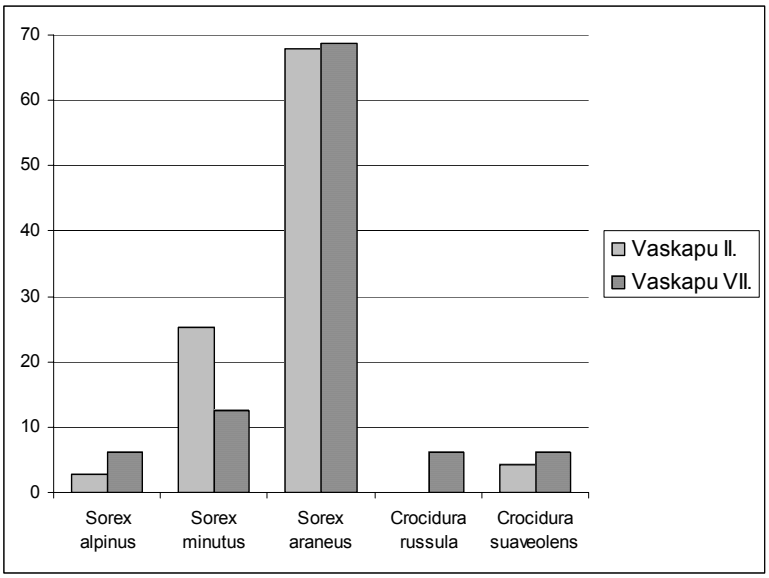

Figure 1. Species composition of the Vaskapu Soricidae faunas (% of the specimens)

Systematic review

Shrews have dilambdodont molars and elongated lower incisors, usually with a variable number of low cusplets along the edge of the latter. A dark red pigmentation is often present on the top of the dental cusps in the case of the group Soricinae (see on Pl. 1, Fig. 1-3), while Crocidurinae have white teeth, because they lack the aforementioned pigment. In the case of the latter group, the dorsal edge of the lower incisor is rather smooth, with traces of cusplets only (see on Pl. 1, Fig. 4 and 5).

Subfamily Soricinae

According to RZEBIK-KOWALSKA (1995), the Soricinae forms (pigmented toothed shrews), especially genus *Sorex* are adapted colder environment, than the Crocidurinae. They prefer wet, wooded environments to the open grasslands. Since they live in cold regions, they are characterized higher metabolic levels and average body temperature, than Crocidurinae.

Genus *Sorex* LINNAEUS, 1758

Sorex alpinus SHINZ, 1837

- 4 specimens from the Vaskapu II and 1 from the Vaskapu VII site.

Sorex minutus LINNAEUS, 1766

- 36 specimens from the Vaskapu II and 2 from the Vaskapu VII site (Pl. 1 Figs 1-2)

Sorex araneus LINNAEUS, 1758

- 96 specimens from the Vaskapu II and 11 from the Vaskapu VII site (Pl. 1 Fig. 3)

Subfamily Crocidurinae

This subfamily (Crocidurinae or white-toothed shrews) contains mainly tropical forms. They differ from Soricinae mainly in their preferences, concerning humidity. They are adapted to more arid conditions than are Soricinae (RZEBIK-KOWALSKA 1995).

Genus *Crocidura* WAGLER, 1862

Crocidura russula HERMANN, 1780

- 1 specimen from the Vaskapu VII site (Pl. 1 Fig. 4)

Crocidura suaveolens PALLAS, 1811

- 6 specimens from the Vaskapu II and 1 from the Vaskapu VII site (Pl. 1 Fig. 5)

Palaeoecological conclusions

On the basis of the shrew fauna (with many *Sorex araneus* and *Sorex minutus* findings, and the occurrence of the Alpine shrew, *Sorex alpinus* in the sample), MÉSZÁROS (2003) raised the idea of the presence of an "Alpine ecotope" in the higher areas of the Bükk Mountains during the time of the

sedimentation of the Vaskapu Cave layers. This ecological change could be caused by the cold climate in the Pilisszántó Horizon (Late Würm). He supposed that there could be occurred open mountain vegetation in the Bükk Plateau, somewhat higher than the studied locality, which could be situated in the pine forest zone. The model is in agreement with the taphonomical observations of SÓRON & VIRÁG (2009), according to which the remains were transported to the plateau at the top of the Vaskapu VII locality by a stream from a somewhat higher area with both forest and open vegetation. The fossil ecosystem, which was determined in the Bükk Mountains, was very similar to the recent communities of the European high mountains (MÉSZÁROS 2004). This view is not refuted by the new *Crocidura* findings in the locality (Fig. 2). MÉSZÁROS (2011) studied recent sedimentations of similar samples to the fossil ones in the high mountain ecosystems (Eastern Austria, Rax Alps.) Comparison of the fossil and recent samples supported the hypotheses, that the Vaskapu localities actually represent an Alpine ecosystem. Although *Crocidura* species usually indicate some warmer and more arid climate than *Sorex* ones, however, the forms mentioned here rarely occur in the open mountain vegetation of the Rax Plateau.

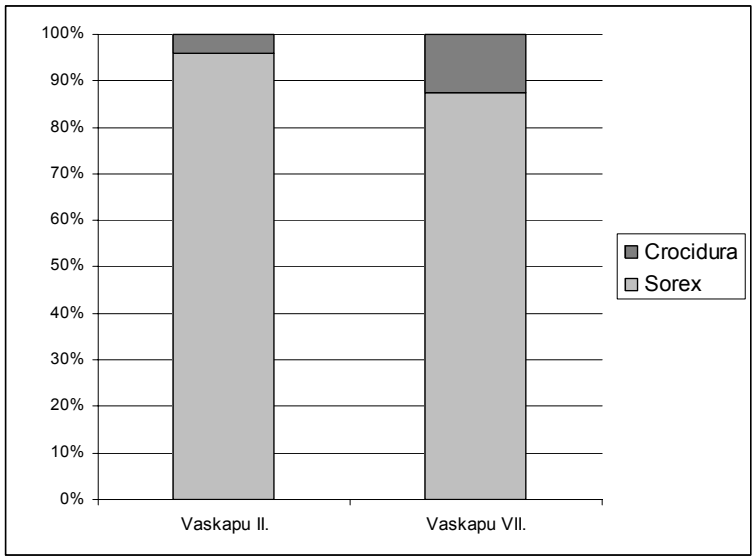

Figure 2. Generic composition of the Vaskapu Soricidae faunas (% of the specimens)

.

Acknowledgements

The author would like to express his thanks to János Hír, András Szabolcs Sóron and Attila Virág for the chance of studying the material collected by them. He is indebted to Miklós Kázmér and István Szente for their assistance on the field. Special thanks to Attila Virág for his help in making the photo plate.

References

MÉSZÁROS, L. GY. (1999): Uppermost Pleistocene shrews (Mammalia, Soricidae) from Vaskapu Cave, Northern Hungary. – Annales Universitatis Scientiarum Budapestinensis, Sectio Geologica 32, pp. 43-50.

MÉSZÁROS, L. (2003): Felső würm "alpesi" fauna a bükki Vaskapu-barlangból. – Abstracts of the 6th Annual Meeting of the Hungarian Palaeontologists, pp. 21.

MÉSZÁROS, L. GY. (2004): Taxonomical revision of the Upper Würm Sorex (Mammalia, Insectivora) remains of Hungary, for proving the presence of an alpine ecotype in the Pilisszántó Horizon. – Annales Universitatis Scientiarum Budapestinensis, Sectio Geologica 37, pp. 9-25.

MÉSZÁROS, L. (2011): Aktuopaleontológiai vizsgálatok a kelet-ausztriai Rax-hegységben. (Actuo-palaeontological studies in the Rax Alps, Austria). – In: KÁZMÉR M. (ed.): Környezettörténet 2. Környezeti események a honfoglalástól napjainkig történeti és természettudományi források tükrében. – Hantken Kiadó, Budapest, pp. 253-263.

REUMER, J. W. F. (1984): Ruscinian and Early Pleistocene Soricidae from Tegelen (The

Netherlands) and Hungary. – Scripta Geologica, 73, pp. 1–173.

RZEBIK-KOWALSKA B. (1995): Climate and history of European shrews (Family Soricidae). – Acta Zoologica Cracoviensa 38, pp. 95-107.

SÓRON, A.SZ. & VIRÁG, A. (2009): Detailed quantitative method in microvertebrate taphonomy in the case of Pleistocene filling of the Vaskapu II rock shelter. – Central European Geology 52(2), pp. 185-198.

VIRÁG, A., SZENTESI, Z., CSÉFÁN, T. & KELLNER, L. M. (2013): The Late Pleistocene microvertebrate fauna of the Vaskapu Cave (North Hungary) and its taphonomical, biostratigraphical and palaeoecological implications. – Hantkeniana 8, pp. 151-161.

Table 1. New location of the Vaskapu II. Soricidae material in the Stratigraphical Collection of the Department of Palaeontology and Geology at the Hungarian Natural History Museum.

Catalogue number	Material	Collected by	First report in	Figured in
VK2.S.1.	*Sorex alpinus* left mandible fragment	Hír and Mészáros (1994)	Mészáros 1999	Mészáros 1999, fig. 4
VK2.S.2.	*Sorex minutus* right mandible	Hír and Mészáros (1994)	Mészáros 1999	Mészáros 1999, fig. 3
VK2.S.3.	*Sorex minutus* left mabdible	Hír and Mészáros (1994)	Mészáros 1999	This paper
VK2.S.4.	*Sorex minutus* right maxillary fragment	Hír and Mészáros (1994)	Mészáros 1999	-
VK2.S.5.	*Sorex minutus* 16 mandible fragments and lower teeth	Hír and Mészáros (1994)	Mészáros 1999	-
VK2.S.6.	*Sorex araneus* left mandible	Hír and Mészáros (1994)	Mészáros 1999	Mészáros 1999, fig. 1
VK2.S.7.	*Sorex araneus* right maxillary fragment	Hír and Mészáros (1994)	Mészáros 1999	Mészáros 1999, fig. 2
VK2.S.8.	*Sorex araneus* 45 mandible fragments and lower teeth	Hír and Mészáros (1994)	Mészáros 1999	-
VK2.S.9.	*Sorex araneus* 20 maxillary fragments and upper teeth	Hír and Mészáros (1994)	Mészáros 1999	-
VK2.S.10.	*Sorex alpinus* 3 mandible fragments	Kázmér, Mészáros and Szente (2002)	This paper	-
VK2.S.11.	*Sorex minutus* 12 mandible fragments and lower teeth	Kázmér, Mészáros and Szente (2002)	This paper	-
VK2.S.12.	*Sorex minutus* 3 maxillary fragments and upper teeth	Kázmér, Mészáros and Szente (2002)	This paper	-
VK2.S.13.	*Sorex araneus* 13 mandible fragments	Kázmér, Mészáros and Szente (2002)	This paper	-
VK2.S.14.	*Sorex araneus* 1 maxillary fragment and 1 upper tooth	Kázmér, Mészáros and Szente (2002)	This paper	-
VK2.S.15.	*Crocidura suaveolens* 5 mandible fragments and lower teeth	Kázmér, Mészáros and Szente (2002)	This paper	-
VK2.S.16.	*Crocidura suaveolens* right maxillary fragment	Kázmér, Mészáros and Szente (2002)	This paper	-
VK2.S.17.	*Sorex minutus* right mandible fragment	Sóron and Virág 2005-2009	This paper	-
VK2.S.18.	*Sorex minutus* right maxillary fragment	Sóron and Virág 2005-2009	This paper	-
VK2.S.19.	*Sorex araneus* 15 mandible fragments and lower teeth	Sóron and Virág 2005-2009	This paper	-
VK2.S.20.	*Crocidura suaveolens* left mandible fragment	Sóron and Virág 2005-2009	This paper	-

Table 2. New location of the Vaskapu VII. Soricidae material in the Stratigraphical Collection of the Department of Paleontology and Geology at the Hungarian Natural History Museum.

Catalogue number	Material	Collected by	First report in	Figured in
VK7.S.21.	*Sorex alpinus* right mandible fragment	Kázmér, Mészáros and Szente (2002)	This paper	-
VK7.S.22.	*Sorex minutus* left mandible	Kázmér, Mészáros and Szente (2002)	This paper	This paper
VK7.S.23.	*Sorex minutus* right mandible fragment	Kázmér, Mészáros and Szente (2002)	This paper	-
VK7.S.24.	*Sorex araneus* left mandible	Kázmér, Mészáros and Szente (2002)	This paper	This paper
VK7.S.25.	*Sorex araneus* 10 mandible fragments and teeth	Kázmér, Mészáros and Szente (2002)	This paper	-
VK7.S.26.	*Crocidura russula* left mandible	Kázmér, Mészáros and Szente (2002)	This paper	This paper
VK7.S.27.	*Crocidura suaveolens* right mandible	Kázmér, Mészáros and Szente (2002)	This paper	This paper

Plate 1

1. *Sorex minutus* (VK2.S.3.) left mandible in lingual view from the Vaskapu II site.
2. *Sorex minutus* (VK7.S.22.) left mandible in buccal view from the Vaskapu VII site.
3. *Sorex araneus* (VK7.S.24.) left mandible in buccal view from the Vaskapu VII site.
4. *Crocidura russula* (VK7.S.26.) left mandible in buccal view from the Vaskapu VII site.
5. *Crocidura suaveolens* (VK7.S.27.) right mandible in buccal view from the Vaskapu VII site.

Abbreviations:

c = caninus;
i = incisivus**;**
m = molaris;
maf = mandibular foramen;
mef = mental foramen;
p = praemolaris;
pang = processus angularis;
pcond = processus condyloideus;
pcor = processus coronoideus.

Plate 1

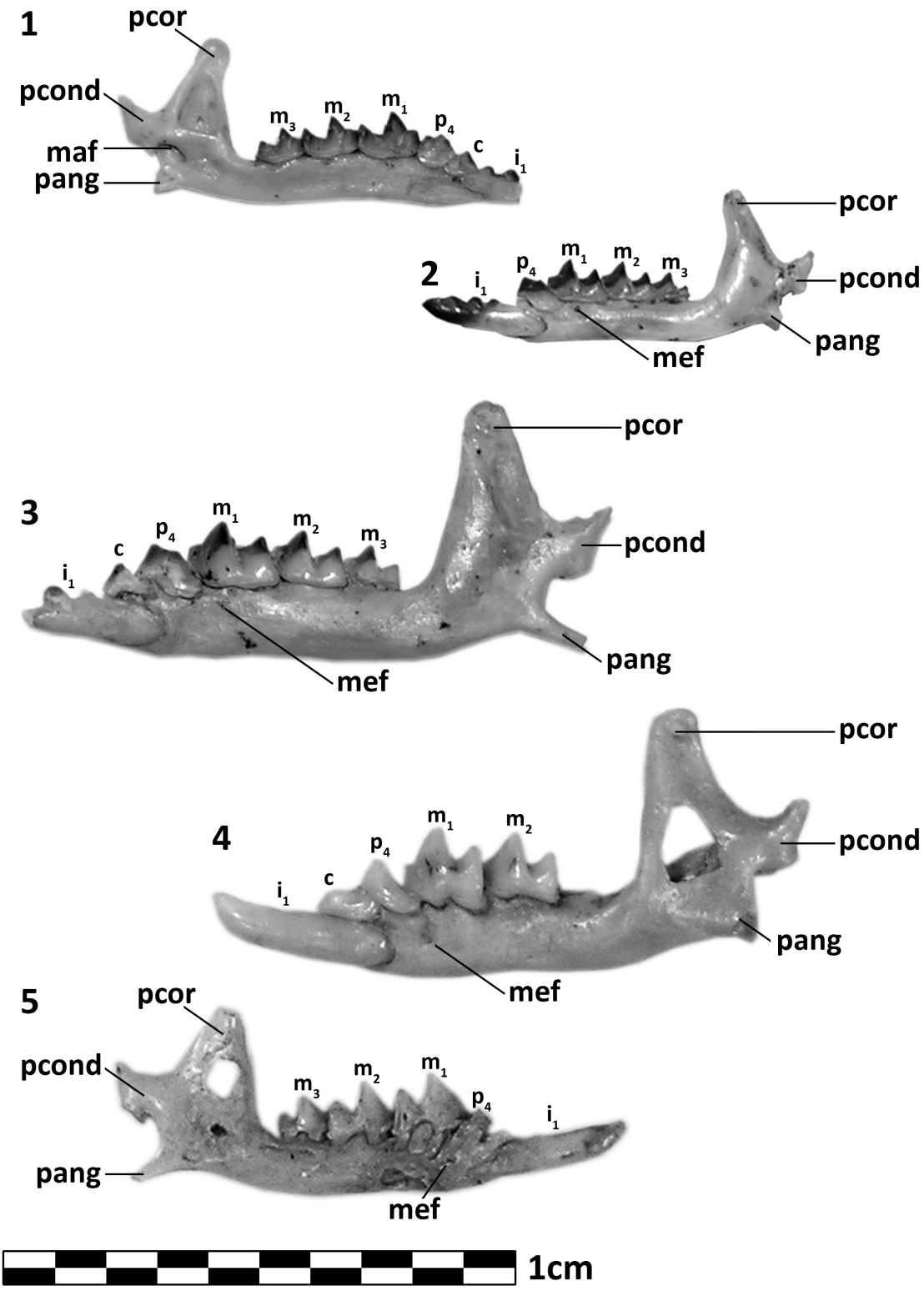
1
pcor
pcond
maf
pang
m3
m2
m1
p4
c
i1
2
pcor
pcond
pang
mef
p4
m1
m2
m3
i1
3
pcor
pcond
pang
mef
c
p4
m1
m2
m3
i1
4
pcor
pcond
pang
mef
m1
m2
p4
c
i1
5
pcor
pcond
pang
mef
m3
m2
m1
p4
i1
1cm